Functional dissection of the Smc5/6 complex: roles of the SUMO ligase Nse2/Mms21 in the maintenance of genome stability

Maciej Kliszczak

Chromosome Biology Laboratory,
School of Natural Sciences,
NUI Galway, Ireland

A thesis submitted to the National University of Ireland Galway for the degree of Doctor of Philosophy

June 2011

Supervisor: Dr. Ciaran Morrison

TABLE OF CONTENTS

LIST OF FIGURES

LIST OF TABLES

ABBREVIATIONS

APS	ammonium persulphate
ATP	adenosine-5’-triphosphate
BER	base excision repair
BLAST	basic local alignment search tool
bp	base pair(s)
BSA	bovine serum albumin
cDNA	complementary DNA
CLAP	chymostatin, leupeptin, antipain, pepstatin A
C-terminus	carboxy terminus
DABCO	1,4-diazabicyclo[2.2.2]octane
DAPI	4’,6-diamidino-2-phenylindole
DDR	DNA damage response
DEPC	diethylpyrocarbonate
dH_2O	de-ionised water
DMSO	dimethylsulfoxide
DNA	deoxyribonucleic acid
dsDNA	double-stranded DNA
ssDNA	single-stranded DNA
dNTP	deoxyribonucleotide-5’-triphosphate
DSB	double-strand break
DTT	dithiothreitol
ECL	enhanced chemiluminesence
EDTA	ethylenediaminetetraacetic acid
FBS	fetal bovine serum
FITC	fluorescein isothiocyanate
g	gravity
GFP	green fluorescent protein
GST	glutathione S transferase
HR	homologous recombination
HRP	horseradish peroxidase
ICL	inter- or intrastrand DNA cross-link

IF	immunofluorescence microscopy
IP	immunoprecipitation
IPTG	isopropyl ß-D-thiogalactopyranoside
IR	ionising radiation
kb	kilobase pair(s)
kDa	kilodaltons
LB	Luria-Bertani medium
mRNA	messenger RNA
N-terminus	amino terminus
NHEJ	non-homologous end joining
NER	nucleotide excision repair
OD	optical density
PBS	phosphate buffered saline
PCR	polymerase chain reaction
PMSF	phenylmethylsulfonyl fluoride
RNA	ribonucleic acid
RNase	ribonuclease
RT-PCR	reverse transcription PCR
PVDF	polyvinylidene difluoride
SDS	sodium dodecyl sulphate
SDS-PAGE	SDS polyacrylamide gel electrophoresis
TAE	tris acetate EDTA
TEMED	N,N,N’,N’-tetramethylethylenediamine
Tris	Tris (hydroxymethyl) aminomethane
TRIzol	Total RNA Isolation reagent
UV	ultraviolet
WT	wild-type

ACKNOWLEDGEMENTS

I would like to thank my supervisor Dr. Ciaran Morrison for his constant support while working on my project and writing the thesis. Thank you Ciaran, you are a really good mentor.

Many, many, many thanks to my wife Anna, who has to put up with me on a daily basis and for all her support and love. Without you, this thesis would be a complete mess.

I would also like to thank to all the members of Chromosome Biology Laboratory: my dear friend Anna, Helen, Carol, Tiago, Burçu, Pauline, Loretta, Sinead, Yi-fan and David. Thank you for your help and laughs.

Many thanks to all my colleagues from the Chromosome Biology Centre and NCBES for all your help and advice.

To my family, thank you, you always watch my back.

And finally to ***GGS*** for the strength and confidence that comes with it.

I dedicate this thesis to my wife and soulmate

Anna Kliszczak

ABSTRACT

The eukaryotic Structural Maintenance of Chromosomes (SMC) family comprises six members; Smc1 to Smc6. Smc proteins contain five characteristic domains: Walker A and B motifs at N- and C-terminus, respectively, two coiled-coil regions and a hinge motif situated in the centre of the polypeptide. Smc1-Smc3 heterodimer (cohesin) and Smc2-Smc4 (condensin) are required for sister chromatid cohesion and mitotic DNA condensation, respectivel. The Smc5-Smc6 heterodimer is crucial for proper DNA repair and response to DNA damage through homologous recombination (HR). The Smc5-Smc6 scaffold binds six non-Smc elements (Nse1 to Nse6) which supplement the structure. Each subunit of the yeast Smc5-Smc6 complex is essential for viability and their mutants are sensitive to DNA damage.

We generated *Smc5*$^{-}$, *Nse2*$^{-/-/-}$ (SUMO E3 ligase) and *Nse2*$^{-/-/-}$*Smc5*$^{-}$ chicken DT40 cells. All three cell lines are viable, but differ in their phenotypes. *Smc5* cells show increased mitotic index and number of aberrant mitotics compared to wild type and *Nse2* mutants. Additionally, *Smc5* mutants are sensitive to ionizing radiation (IR) and methyl methanesulfonate (MMS), whereas *Nse2* show decreased survival and elevated chromosomal aberrations only after MMS treatment. Both cell lines have decreased break induced sister chromatid recombination activities but additionally, *Nse2* show slightly elevated gene targeting efficiencies. Nse2-, Smc5-deficient and *Nse2*$^{-/-/-}$*Smc5*$^{-}$ cells showed increased levels of sister chromatid exchanges, compared to wild type. Moreover, loss of Smc5 protein but not Nse2, results in impaired sister chromatid cohesion as measured by distances between a tet repressor GFP bound to chromosomally integrated tet operator arrays.

The different phenotypes of *Smc5* and *Nse2* cells suggest possible separate functions of Smc5 and Nse2 proteins. This was supported by the epistatis analysis of the doubly targeted clones *Nse2*$^{-/-/-}$*Smc5*$^{-}$. Additionally, the observed discrepancies can be explained by distinct levels of Smc5-Smc6 complex destabilization in *Smc5* and *Nse2* backgrounds. Taken together, our

results suggest that the Smc5-Smc6 complex does not play a direct role in HR but that it is possibly a part of the HR regulatory machinery. We conclude that Smc5 and Nse2 proteins are required for proper regulation of DNA repair and recombination after DNA damage.

Chapter 1 Introduction

1.1 DNA and genome stability

Deoxyribonucleic acid (DNA) was discovered in 1869 by Johann Friedrich Miescher, a Swiss biochemist working in Tübingen, Germany (Brown, 2002). Almost a century later, experiments with bacteria performed by Avery and co-workers, gave evidence for DNA being the bearer of genetic information (Avery et al., 1944). In 1952, Hershey and Chase used viral particles to demonstrate that during bacterial cell infection, DNA is transferred from virus to bacterial host, not proteins as previously believed (Hershey and Chase, 1952). A year later Watson and Crick, using X-ray differentiation patterns, elucidated the DNA helix structure (Watson, 1953).

DNA is a bio-polymer built up of two anti-parallel strands of deoxyribonucleotides linked by phosphodiester bonds. Each deoxyribonucleotide consists of a sugar ring (deoxyribose), and a negatively charged phosphate group, which together form the backbone of the strand and one of four highly hydrophobic nitrogenous bases (pyrimidines-like adenine (A) and guanine (G) or pyridines-like thymine (T) and cytosine (C), Figure 1.1A). The water-soluble backbone of DNA interacts with the solvent molecules, shielding hydrophobic bases stacked between the two strands (Figure 1.1B). Individual DNA strands contain two different ends with either a 3’ hydroxy group (3’ end) or a 5’ phosphate moiety (5’ end) (Watson, 1953) (Figure 1.1B). The anti-parallel strands interact through non-covalent hydrogen bonds of A-T and C-G base pairs. The genetic information is embedded in the sequence of deoxyribonucleotides. The DNA molecule contains many chemical moieties that can easily undergo chemical modifications and it is pivotal for any living entity to ensure DNA stability and the correctness of its sequence. The maintenance of genomic integrity is essential for the survival and prosperity of each single species. It has been estimated that tens of thousands of lesions per day are being introduced into the DNA of a single cell (Lindahl and Barnes, 2000).

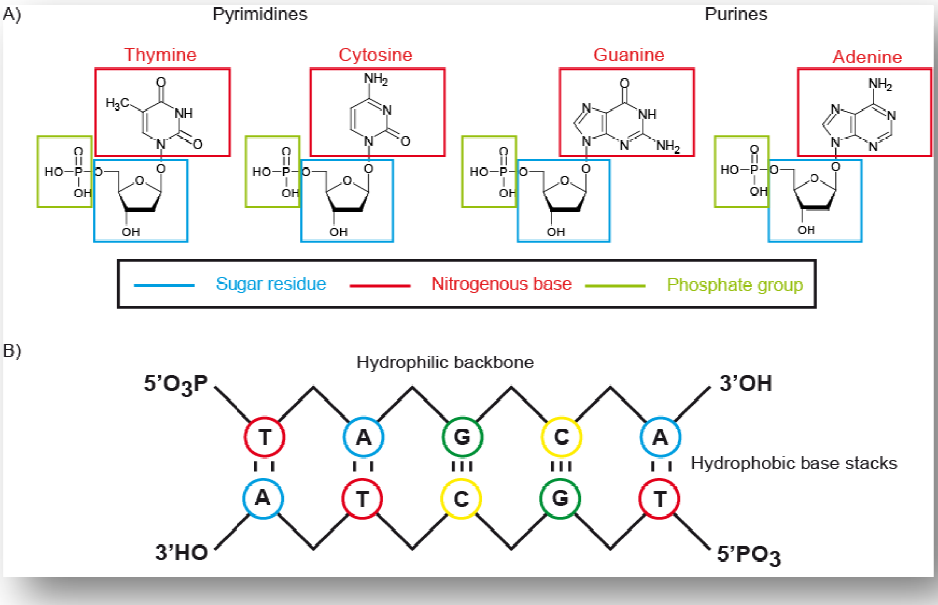

Figure 1.1 DNA composition.

Graphical representation of A) chemical structure of the DNA bases, B) linear structure of the DNA double helix.

All of these DNA alterations have to be removed before they become fixed as permanent mutations. The accumulation of such changes may threaten cell and organism viability or result in different pathological conditions, such as cancer, tri-nucleotide repeat disorders (fragile X syndrome, Huntington's disease, Friedrich's ataxia etc.) and heart disease. Cells have evolved specific mechanisms to deal with and remove various DNA lesions and prevent dramatic changes in their genetic material. These include cell cycle checkpoints, DNA repair and cell death pathways.

1.2 Cell cycle

Every cell grows and divides, giving rise to new progeny. Somatic cells go through repetitive changes called the cell cycle. The cell cycle comprises four different stages: M, G_1, S and G_2 (Figure 1.2). In the DNA synthesis phase (S phase), the genetic material is duplicated and later it is divided between two new cells during mitosis (M phase). The G_1 and G_2 phases (G for gap) separate DNA synthesis and mitosis stages of the cell cycle. During G_1 and G_2, cells continue to

grow and synthesise proteins essential for execution of S and M phases, respectively. This includes enzymes required for DNA synthesis, microtubules and membrane components.

The cell cycle is regulated through a class of enzymes called cyclin dependent kinases (CDKs). CDK activities are determined by cyclin levels and vary across the cell cycle, corresponding with crucial events in each of the phases.

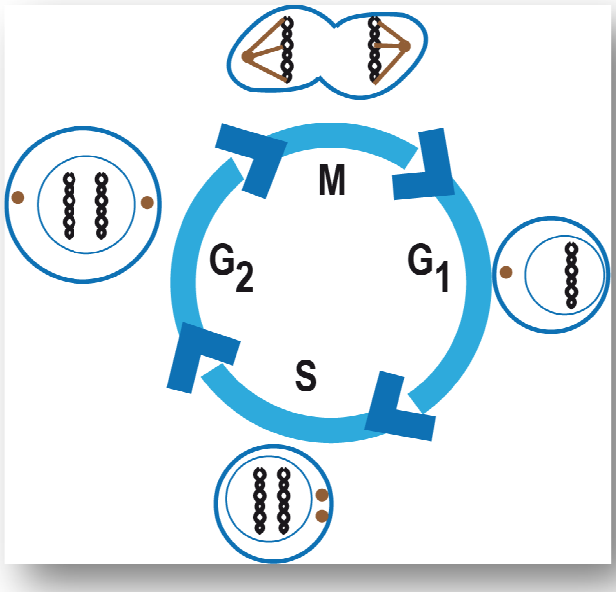

Figure 1.2 Cell cycle.

Graphical representation of the cell cycle phase: M – mitosis, G_1 and G_2 – gap phases 1 and 2, S – DNA synthesis phase. Black helices represents DNA, brown spots and fibers show centrosomes and microtubules, respectively.

There is a single cyclin dependent kinase gene in *Saccharomyces cerevisiae* (*Cdc2*), three in *Schizosaccharomyces pombe* (*CDC28*, *PHO85* and *KIN28*) and at least 13 (*CDK1-13*) in human (Morgan, 1995, 1997; Sullivan and Morgan, 2007). These kinases can bind to at least 15 different cyclin families (A-L, O, T and Y) (reviewed in (Murray, 2004)). Each stage of cell cycle has its specific CDK and cyclin complexes that drive activation of processes essential for that stage. Activation of CDKs is an essential requirement for any cell to progress into next cell cycle phase, and for such catalytical competency binding of cyclin subunit and subsequent post-translational modifications (PTM) of CDK is

required (reviewed in (Nurse, 2002)). For example, Cdk1 activation is mandatory for mitotic progression. Cdk1 is activated by binding to its cyclin B partner (reviewed in (Sanchez and Dynlacht, 2005)). Availability of the cyclin B is balanced through its constant expression and degradation. In addition, to cyclin binding, Cdk1 has to be phosphorylated at the activating T160 site by cyclin activating kinase (CAK) (reviewed in (Sanchez and Dynlacht, 2005)). Another regulatory site of Cdk1, T14 is phosphorylated by Wee1 kinase (reviewed in (Niida and Nakanishi, 2006)), but this modification has to be removed to fully activate Cdk1. This is achieved by phosphatase activity of the Cdc25 family of proteins. Once Cdk1 is bound to cyclin B and phosphorylated at T160, it can modify specific substrates, such as anaphase promoting complex (APC), that are essential for progression through the M phase (reviewed in (Rudner and Murray, 2000)). Similar regulatory events are required for the activation of other cyclin dependent kinases. Figure 1.3 shows how the expression of specific cyclins and activity of CDKs changes during the cell cycle.

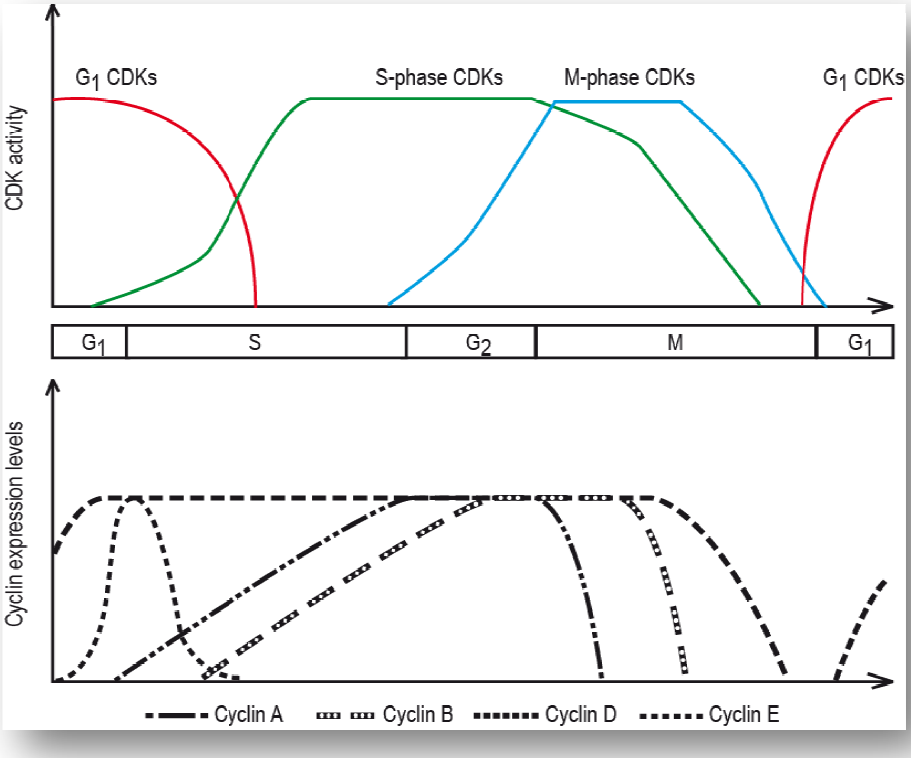

Figure 1.3 Cell cycle regulation by CDK-cyclin complexes.

Cartoon represents cyclin levels and CDs activities through the stages of the cell cycle.

Cyclin D is constitutively expressed through the cell cycle, whereas cyclin E, A and B are specific for G_1 to S phase, S phase to G_2 and G_2 to M phase transitions, respectively (reviewed in (Sanchez and Dynlacht, 2005)). CDK2,-4,-5 and -6 are activated during G_1 phase (G_1 CDKs), CDK1 and -2 control S and M phase progression (S and M phase CDKs) (reviewed in (Murray, 2004)).

1.3 DNA damage

As mentioned earlier, DNA is a very unstable molecule that is constantly being physically and chemically modified. Depending on the source of the DNA damaging agent we can distinguish two types of DNA damage: endogenous and exogenous (reviewed in (Friedberg, 2003)).

Endogenous DNA damage is the result of the metabolic activity of the cell and it is caused by reactive oxygen species (ROS), nitrogen compounds produced by cell metabolism and during the inflammatory response by the immune system, alkylating agents (like S-adenosylmethionine) and replication errors (reviewed in (Lindahl and Barnes, 2000)).

Exogenous DNA damage is a result of exposure to UV-light, gamma and X-rays, thermal factors, toxins (for example food toxins like aflatoxins or heterocyclic amines present and in over-cooked meats), chemicals like those present in a cigarette smoke (benzopyrene) and many more environmental challenges (reviewed in (Harper and Elledge, 2007)).

Both endogenous and exogenous DNA damage cause different DNA modifications. Those are base (deaminations, oxidations and alkylations) and strand alterations (single and double strand breaks, intra- and inter-strand cross-links). Each of these DNA lesions triggers a specific response to restore the integrity of the genetic information. Depending on the level of DNA damage the cell can either stall the cell cycle and repair the lesions or undergo controlled death (apoptosis). In the next few sections the responses to DNA damage and specific DNA repair pathways will be described in detail.

1.4 DNA damage response (DDR)

The DNA damage response is a complicated network of protein-protein interactions whose ultimate goal is to restore DNA integrity. The vast network of proteins comprises three main classes of DDR components, namely DNA damage sensors, signal mediators and effectors (Figure 1.4).

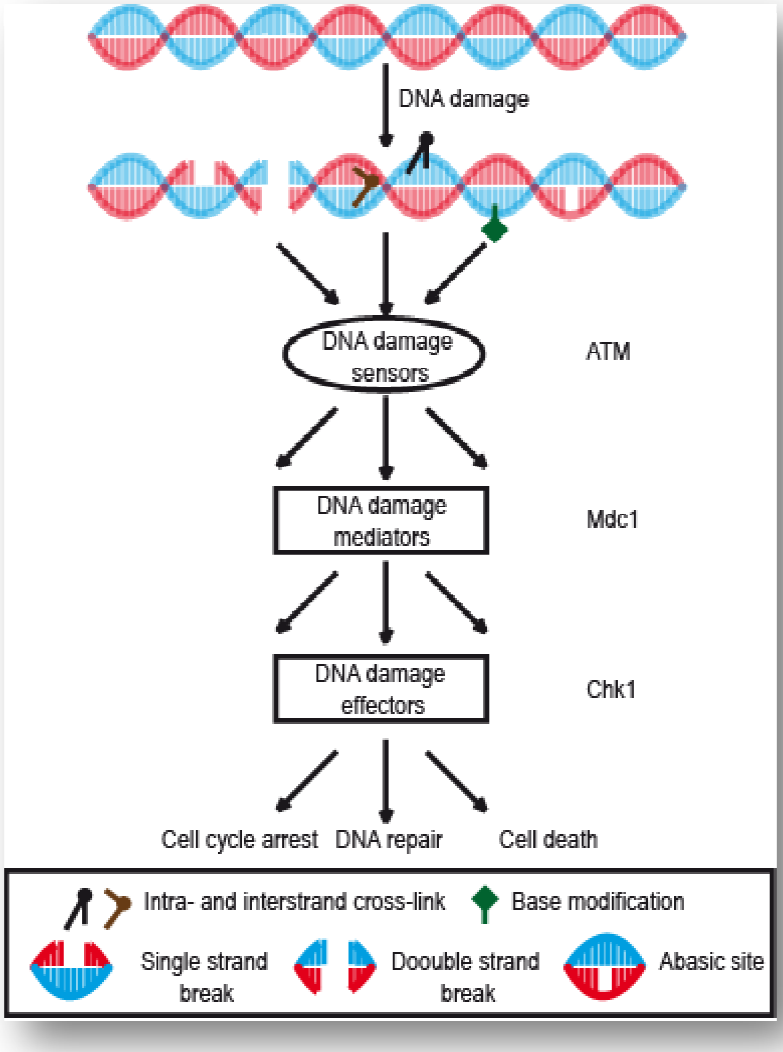

Figure 1.4 DNA damage response pathways.

Graphical representation of DNA damage response pathways. After DNA damage, specialised proteins (DNA sensors) sense the lesions and activate the mediator proteins (signal transducers). The function of the mediator proteins is to mobilise the DNA damage effectors which then trigger specific cellular responses, such as cell cycle arrest, DNA repair or cell death.

The DDR is regulated at many different levels by protein-protein interactions and a plethora of protein modifications (reviewed in (Bergink and Jentsch, 2009; Harper and Elledge, 2007; Misteli and Soutoglou, 2009)). It is crucial for cell survival that these happen in the right place in the right time. Many different proteins are required for the proper response to DNA damage (reviewed in (Ciccia and Elledge, 2010)). Another layer of DDR control comes from up- and down-regulation of specific genes required for cellular responses to stressful conditions.

After introduction of DNA damage, specific DDR pathways are activated to stall the cell cycle progression and repair introduced lesions or trigger controlled cell death (reviewed in (Niida and Nakanishi, 2006)). The decision is mainly made according to the severity of the DNA damage and cell cycle stage. Depending on the DNA damage timing, cell cycle arrest is achieved by activation of specific surveillance pathways, including degradation of Cdc25 phosphatases, degradation of cyclins and finally, inhibition of CDKs (discussed in Section 1.5 and reviewed in (Nurse, 2002)). These cellular mechanisms, termed cell cycle checkpoints, prevent cell proliferation under DNA damage and stress conditions.

Parallel to checkpoint establishment, the DNA damage is being repaired by specialised protein complexes. Two families of sensor proteins play a central role in the DNA damage response, the phosphatidylinositol 3-kinase like protein kinases (PIKKs) family which include the ATM (ataxia telangiectasia mutated), ATR (ataxia telangiectasia related) and DNA-PK (DNA dependent protein kinase) kinases and a group of poly(ADP)ribose polymerases (PARP) proteins (Harper and Elledge, 2007; Meek et al., 2008). The ATM and DNA-PK kinases are principally involved in responses to DNA double strand breaks (DSB), whereas ATR functions to ensure the integrity of DNA replication forks in response to DNA damage (reviewed in (Cimprich and Cortez, 2008)). The PARP family of proteins is mainly required for base excision repair (BER) and single strand break (SSB) repair pathways. However, it also has been shown to play a regulatory role in DSB repair (reviewed in (Schreiber et al., 2006)). The ATM/ATR/DNA-PK proteins regulate the DDR outcome by protein phosphorylation, whereas PARPs function by attachment of ADP-ribose residues

to their targets. Once activated, the sensor proteins recruit the mediator factors to the site of the damage. The mediator proteins, such as mediator of DNA checkpoint 1 (Mdc1), breast cancer type susceptibility protein 1 (BRCA1) and 53 binding protein 1 (53BP1) migrates to site of DNA damage (reviewed in (Ciccia and Elledge, 2010; Harper and Elledge, 2007). Many of the mediator proteins contain the BRCA1 C-terminus (BRCT) domains necessary for transduction of DNA damage signals. These domains are required for protein-protein interactions through binding to phospho-proteins (reviewed in (Canman, 2003)).

Each sensor interacts and modifies many different mediator molecules in order to amplify the signal. Subsequently, the mediator factors such as Mdc1, BRCA1, 53BP1 regulate the activity of effector proteins, such as Chk1 (checkpoint 1) and Chk2 (checkpoint 2) kinases, which activate a specific response to the stress conditions. For example, phosphorylation of the target effector proteins, such as the Cdc25 family of phosphatases and cyclin dependent kinases by ATM-Chk2 and ATR-Chk1 pathways is required for slowing cell cycle progression after DNA damage (reviewed in (Ciccia and Elledge, 2010)). Activation of another protein, the p53 transcription factor plays important role in the DDR. Its activation by ATM-Chk2 and ATR-Chk1 dependent phosphorylation up-regulates gene expression. These genes activate cell cycle inhibitory pathways, control DNA damage repair or induce apoptosis.

1.5 Cell cycle checkpoints

Control of cell cycle progression is important for cell survival. Specific pathways have evolved to precisely monitor the advance of the cell through stages of the cell cycle. These pathways, called checkpoints, are present in G_1, S, G_2 and M phases and ensure the order of cell cycle events to preserve genomic integrity. These mechanisms prevent cell cycle progression and allow for DNA repair before the cell can enter the next stage of the cell cycle (Hartwell and Weinert, 1989).

The G_1 checkpoint ensures that cells do not enter S phase with damaged DNA (reviewed in (Zhou and Elledge, 2000)). It is mainly controlled by the tumour suppressor protein p53 which accumulates post-DNA damage in order to stall the cell cycle. ATM and ATR phosphorylate p53 at S15 and S20 in order to

activate it (Banin et al., 1998). The p53 protein can also be phosphorylated at the same sites by the ATM/ATR target kinases Chk1 and Chk2 (Canman and Kastan, 1998; Canman et al., 1998). Normally p53 protein forms a complex with the ubiquitin ligase MDM2, which ensures the rapid turnover of the p53 protein (Wahl and Carr, 2001). The phosphorylated form of p53 does not interact with MDM2 and therefore is no longer targeted for degradation (Chehab et al., 1999). This results in the accumulation of active p53 protein (Chehab et al., 1999). In addition, post-DNA damage MDM2 is also modified by the ATM/ATR kinases and targeted for proteasomal degradation, which further amplifies the signal for p53 protein release and accumulation (Maya et al., 2001). These events lead to increased levels of p53 protein, which is then translocated to the nucleus (Maya et al., 2001). The transcriptional activity of p53 stimulates the expression of genes involved in the control of cell cycle progression. Genes regulated by p53 are the growth arrest genes $p21^{CIP1/WAF1}$, Gadd45, DNA repair genes, such as p53R2 and apoptosis genes Bax, Apaf-1, PUMA and NoxaA (Kastan et al., 1992; Lowe et al., 1993; Vogelstein et al., 2000). $p21^{CIP1/WAF}$ is a CDK inhibitor that negatively regulates Cdk2/cyclin E activity leading to G_1 cell cycle arrest (Lowe et al., 1993). In addition, ATR and ATM kinases control CDK phosphorylation status through the regulation of Cdc25A phosphatase activity (reviewed in (Morgan, 1997)). Upon modification by ATM/ATR, Cdc25A protein is targeted for degradation (Bartek et al., 2004). Without the activity of Cdc25A, the Cdk2/cyclin E complex cannot be activated by dephosphorylation to promote cell progression through G_1 to S transition.

The G_1 phase contains another checkpoint-like pathway. Each cell has to pass through the G_1 phase 'restriction point', after which cell commits to finish DNA duplication and division. This is regulated by the RB (retinoblastoma protein)/E2F (transcription factor) complex. Phosphorylation of pRB by the G_1 CDK complex (Cdk4/6-cyclin D) releases the E2F protein. The E2F transcription factor then regulates expression of genes required for progression from G_1 to S phase (including Cdc25A, Cdk2, PCNA, DNA polymerase α/β, cyclin A/D) (Bartek et al., 1997; Sherr and McCormick, 2002).

The S phase checkpoint induces DNA replication stalling upon DNA damage and controls origin firing (Costanzo et al., 2003). When S phase cells are

exposed to DNA damage, ATM and ATR kinases are activated in order to decrease the rate of DNA synthesis or to stop it until DNA lesions are removed (reviewed in (Bartek et al., 2004; Osborn et al., 2002)). It is important to protect replication fork integrity as collapsed forks are highly toxic (reviewed in (Bartek et al., 2004)). There are two different pathways ensuring for such an outcome. The first of the pathways inhibits origin firing by regulation of the Cdc25A phosphatase levels in manner similar to that described for the G_1 checkpoint. ATR/Chk1 is activated and ensures low levels of Cdc25A through activation of the Skp1–Cullin–F-box (SCF) ubiquitin ligase βTrCP which targets Cdc25A for proteasome-mediated hydrolysis (Busino et al., 2003a). This keeps Cdk2 in its inactive hyperphosphorylated state and inhibits Cdc45 protein (Bartek et al., 2004; Busino et al., 2003b; Jin et al., 2003). Cdc45 is an essential component of the CMG complex (Cdc45-Mcm2-7-GINS) required for initiation of DNA replication (Moyer et al., 2006). In addition, in the absence of Cdc45, the DNA polymerase δ cannot be loaded onto DNA and start DNA synthesis (reviewed in (Bell and Dutta, 2002)).

In the second branch, ATM phosphorylates several proteins, such as structural maintenance of chromosomes 1 (Smc1), Nbs1 and BRCA1 to activate an S phase checkpoint (Kitagawa et al., 2004; Olson et al., 2007; Yazdi et al., 2002). Smc1 modification is required for the activation of the S phase checkpoint in response to IR and this activation is Nbs1 dependent (Yazdi et al., 2002). BRCA1 mediates activation of the S phase checkpoint through interaction with checkpoint proteins, such as ATR, Nbs1 and Mdc1 (Cortez et al., 1999; Stewart et al., 2003; Tibbetts et al., 2000; Xu et al., 2002). The mechanism of the ATM-Nbs1-BRCA1-Smc1 branch is not well understood but it is necessary for the full activation of the S phase checkpoint and inhibition of DNA synthesis upon DNA damage.

The G_2 checkpoint protects cells from entering mitosis with unrepaired DNA. ATM-Chk2 and ATR-Chk1 activate Cdc25C phosphatase in response to genotoxic stress (Capasso et al., 2002; Falck et al., 2001). The 14-3-3 complex interacts with the phosphorylated form of Cdc25C and relocates it from the nucleus where it is targeted for proteasome-mediated degradation (Mailand et al., 2000). Loss of Cdc25C activity impedes the full activation of the mitosis-specific

Cdk1/cyclin B complex (reviewed in (Sancar et al., 2004)). In addition, activated Chk1 stabilises Wee1, leading to Cdk1 deactivation by its phosphorylation at the inhibitory site T14 (Raleigh and O'Connell, 2000). Inactive Cdk1/cyclin B complex cannot drive the cell to enter the mitosis. In addition, Chk2 kinase phosphorylates p53, which is followed by increased expression of $p21^{CIP1/WAF1}$ and 14-3-3σ proteins (Bunz et al., 1998; Chan et al., 1999). $p21^{CIP1/WAF1}$ inhibits the activity of Cdk1/cyclin B directly and 14-3-3σ proteins indirectly by sequestering the Cdk1/cyclin B complex activator the Cdc25C phosphatase.

The spindle assembly checkpoint (SAC) ensures proper attachment of microtubules to chromosomes. This pathway operates early in mitosis and is conserved from yeast to human. Defects in this mechanism result in abnormal anaphase and aneuploidy (Vallee et al., 2006). Its principal components in yeast, Aurora B (aurora kinase B), Bub1 (budding uninhibited by benzimidazole), Mps1 (monopolar spindle 1), Bub3, Mad1 (mitotic arrest deficient) and BubR1 localize to kinetochores (reviewed in (Przewloka and Glover, 2009)). In metazoan cells, SAC proteins also include Zwint-1, CENP-E/I/F (Mehta et al., 2010; Starr et al., 2000). The central function of this checkpoint is to monitor spindle health, its proper tension and microtubule attachment to chromosomes at the kinetochores. In response to conditions of abnormal spindle attachment to chromosomes, Bub1 phosphorylates Mad1 in a Bub3-dependent manner (Hardwick and Murray, 1995; Hardwick et al., 1996). This is required for formation of the mitotic checkpoint complex (MCC) which inhibits activity of the anaphase promoting complex/cyclosome (APC/C) and degradation of cyclin B and Pds1/Securin (precocious dissociation of sisters). Activation of the MCC complex is not clear but it may occur through two different mechanisms. In the first mechanism, abnormal interaction between microtubules and kinetochores is sensed and signals for the formation of the MCC complex. In the second pathway, the MCC complex is thought to be a part of the kinetochore and it is activated when unattached microtubules are present (reviewed in (Lu et al., 2009)). Normally, the APC/C complex is required for removal of residual kinetochore-localised sister chromatid cohesin through degradation of Securin. MCC activation leads to prolonged mitosis through negative regulation of sister chromatid separation (reviewed in (Nezi and Musacchio, 2009)). If the spindle

forces and kinetochore attachment are restored cell is promoted to enter mitosis and finish the cell cycle.

1.6 DNA repair

There are many different DNA repair pathways that can deal with various types of DNA lesions. These pathways are highly conserved throughout evolution, confirming the importance of genomic maintenance and DNA repair activity. DNA damage that can occur includes base modifications (deaminations, alkylations, oxidations), sugar modifications, mismatches, intra- and inter-strand cross-links, single and double strand breaks (reviewed in (Ciccia and Elledge, 2010)). Sections 1.6.1 – 1.6.4 describe the various mechanisms involved in DNA repair.

1.6.1 DNA alkylation and oxidation repair

DNA alkylation is a process in which an alkyl group (-R) is transferred onto a nitrogen or oxygen atom in the DNA helix. The alkyl groups can be as simple as methyl ($-CH_3$) or ethyl ($-CH_2CH_3$) groups, or more complicated like those found in the antineoplastic agents nitrogen mustard, nitrosoureas and alkyl sulphonates. The main responses to DNA alkylation are direct demethylation pathways and base excision repair (BER).

In the direct demethylation process, methyl transferase proteins, such as methylguanine-DNA methyltransferase (MGMT) or alkylguanine-DNA transferase (AGT) remove the DNA alkylation by coupling the damaging alkyl group with its active site cysteine (reviewed in (Lindahl et al., 1988; Sedgwick, 2004)). O^6-alkylguanine and O^4-alkylthymine adducts are repaired through a direct reversal mechanism. In this process a cysteine residue attacks the alkyl adduct and receives it in a S_N2 (nucleophilic substitution bimolecular) reaction. This leads to irreversible inactivation of the enzyme which is then targeted for degradation. Other types of DNA adducts such as N^1-methyladenine and N^3-methylcytosine are removed by *Escherichia coli* AlkB protein and its human orthologues. These lesions are reversed through an oxidative dealkylation

reaction in which the oxidised product decomposes to give a repaired base (Falnes et al., 2002; Trewick et al., 2002).

The BER pathway is required for removal of single DNA bases that have been modified. The lesions removed by BER are alkylations, oxidations, DNA base mismatches, cytosine deaminations (uracil) and 5-methylcytosines (reviewed in (Lindahl, 1997; Lindahl and Barnes, 2000)). The modified base is first recognised and excised from the DNA strand (Figure 1.5 (1)).

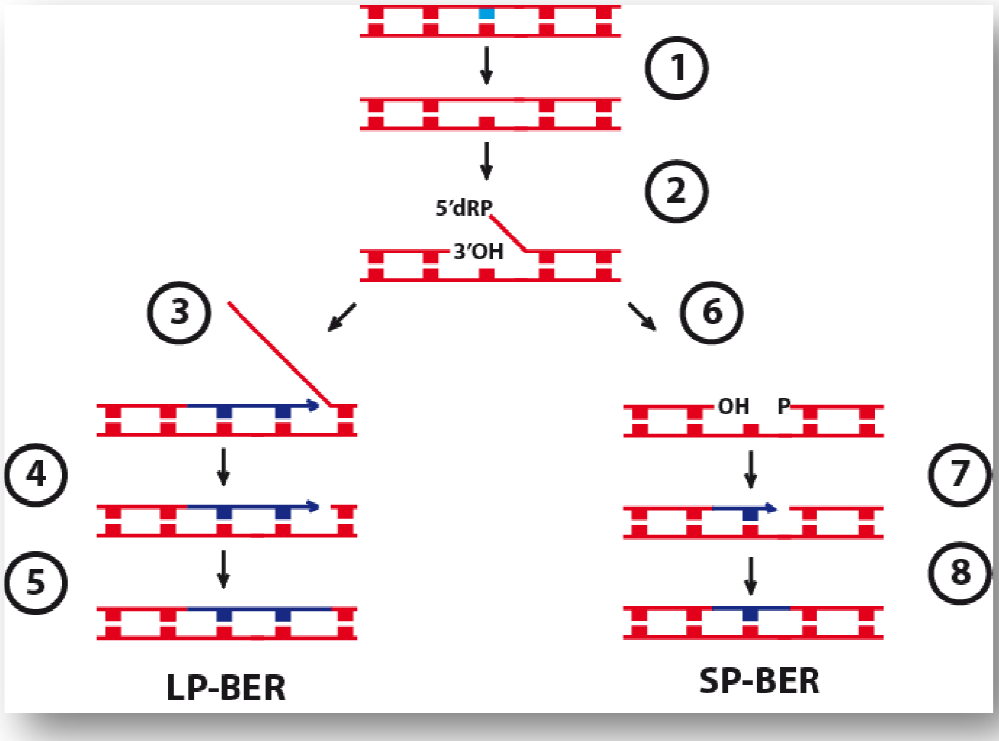

Figure 1.5 Base excision repair pathway.

Cartoon shows mechanisms of long and short patch BER with the enzymes involved in each step: (1) DNA glycosylase removes damaged base, (2) APE-1 cleaves the AP site, (3,7) DNA polymerase fills the resulting gap, (4) FEN1 removes the 5' flap, (5,8) DNA ligase,seals the DNA gap (6) 5'-deoxyribosephosphate (5'dRP) lyase removes the 5'-deoxyribose.

Depending on the modified base or the type of alteration, a specific DNA glycosylase is recruited to remove the damaged base (reviewed in (Lindahl and Barnes, 2000)). There are two different types of DNA glycosylases, monofunctional and bifunctional (reviewed in (Lindahl and Barnes, 2000)). A monofunctional glycosylase has only a glycosylase activity, whereas a bifunctional one has additional apurinic/apyrimidinic (AP) lyase activity

(reviewed in (Lindahl and Barnes, 2000)). For example the thymine-DNA glycosylase (TDG) is required for removal of thymine from G/T mismatches, and uracil-DNA glycosylase removes mis-incorporated uracil from DNA (reviewed in (Lindahl, 1982)). The *E.coli* DNA glycosylase AlkA and its human orthologue MPG (DNA-3-methyladenine glycosylase) process 3-methyladenine (3mA) (reviewed in (Seeberg 1995)). Other proteins including *E.coli* and human endonuclease III and 8-oxoguanine glycosylase repair thymine glycols, hydroxycytosine and 8-oxoguanine, respectively (reviewed in (Seeberg et al., 1995)).

After removal of the base, the AP site is left behind (Figure 1.5 (1)). This site is then cleaved by the activity of either a bifunctional DNA glycosylase or by a specialised AP endonuclease. AP endonuclease 1 (APE-1) cleaves the phosphodiester backbone immediately 5' to the AP site leaving a single strand break with 3'-hydroxyl and 5'-deoxyribose phosphate termini (Figure 1.5 (2)) (Demple et al., 1991). The DNA single strand break (SSB) with or without the remaining 5'-deoxyribose phosphate can be processed by two different pathways termed long patch BER (LP-BER) or short patch BER (SP-BER) (Figure 1.5 (3-5) or (6-8)). In LP-BER, DNA polymerase β synthesises a short oligonucleotide using the 3'-hydroxyl terminus as a primer (Matsumoto and Kim, 1995; Sobol et al., 1996). In this reaction, the 5' part of the same strand is displaced forming a flap that is later removed by flap endonuclease 1 (FEN1) (Li et al., 1995a). In SP-BER, the 5'-deoxyribose phosphate moiety is first removed by 5' dRP lyase and then a single nucleotide is added by DNA polymerase β to fill the gap. The backbone in either of the pathways is sealed by DNA ligase III/XRCC1 complex activity (reviewed in (Frosina et al., 1996)).

In addition to base removal, the BER pathway is the main route for SSB repair. The SSBs are mainly formed by ionizing radiation, topoisomerase I inhibition, UV, oxidative stress (H_2O_2) and indirectly during the above-described base excision repair (BER) pathway (reviewed in (Caldecott, 2008)). An SSB is sensed by PARPs which catalyse poly(ADP-ribosyl)ation of many acceptor proteins involved in SSB repair, including histones H1 and H2B and PARP-1 (Schreiber et al., 2002; Schreiber et al., 2006). Such modification of the histone proteins is believed to be required for the recruitment and assembly of further

chromatin modifiers (polycomb and histone deacetylase complexes) and SSB repair factors (Chou et al., 2010; Schreiber et al., 2006). Once the SSB sensed it is processed similarly to an AP site in the BER pathway.

Loss of the base excision repair activity results in many diseases, such as cancer, neurodegenerative pathologies (ataxia-oculomtor apraxia 1 (AOA1) and spinocereballar ataxia with axonal neuropathy 1 (SCAN1). The oxidative stress caused by reactive oxygen species (ROS) has been associated with increased rates of carcinogenesis. Exposure of cells to high levels of ROS can lead to cellular transformation (Zimmerman and Cerutti, 1984). Mouse knockouts of the antioxidant superoxide dismutase enzyme develop cancer or die early after birth (Elchuri et al., 2005; Li et al., 1995b). In addition, it has been shown that oxidative stress and antioxidant defences affect life span. Experiments with caloric restricted diet (reduced radical production) in mice, found significantly increased life span in these animals (Kregel and Zhang, 2007). Recently, a huge effort is being made to develop small molecule inhibitors of BER as potential anticancer drugs. Promising results have been observed in BRCA1/BRCA2-deficient tumours, where inhibition of PARP-1 specifically induces tumour death, leaving normal cells untouched (reviewed in (Cipak and Jantova, 2010)).

1.6.2 Nucleotide excision repair

During nucleotide excision repair (NER), bulky DNA adducts or helix-distorting DNA modifications are repaired (reviewed in (Lindahl et al., 1995)). Members of a family of proteins mutated in rare recessive disease Xeroderma Pigmentosum (XP) are required for proper repair of these DNA adducts. The XPA gene encodes for the DNA binding protein and XPC for a highly hydrophobic protein (Tanaka et al., 1990). The XPB/D are the DNA helicases and XPG/F encode for DNA nucleases (Flejter et al., 1992; Scherly et al., 1993; Weeda et al., 1990a; Weeda et al., 1990b). The most common lesions repaired by NER are UV photoproducts (thymidine dimmers and 6-4 photoproducts), DNA alkylation and intra- and interstrand DNA cross-links such as those caused by chemotherapeutics cis-platin and psoralen (Moggs et al., 1996). In the first steps, the DNA damage is sensed by HR23B (UV excision repair protein Rad23

homologue B)-XPC complex what is accompanied by UV-DDB (damage-specific DNA binding protein 1) (reviewed in (Rastogi et al., 2010) (Figure 1.6 (1)).

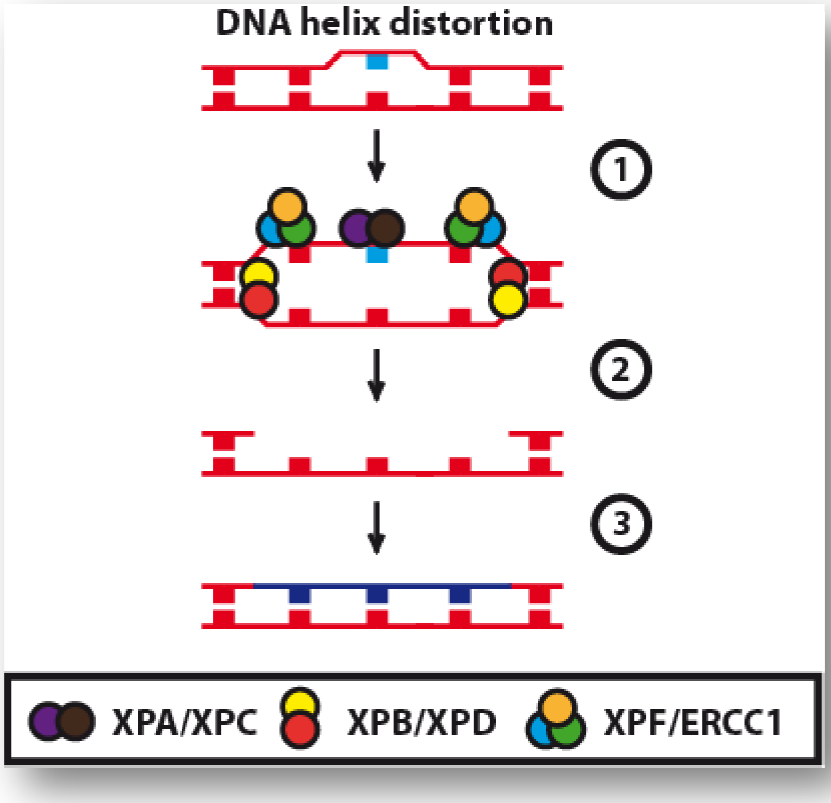

Figure 1.6 Nucleotide excision repair pathway.

Cartoon shows mechanism of nucleotide excision repair with enzymes involved in each step: (1) DNA damage is recognised by XPA/C, and DNA helix unwinding by XPB/D. (2) DNA damage is excised by XPF/ERCC1, (3) and resulting gap is filled and sealed by DNA polymerase δ or ε and DNA ligase.

The mechanism by which XPC recognises the DNA lesion is not clear but some data suggests that it may bind to stretches of ssDNA that occur on the strand opposite to the lesion (Maillard et al., 2007). Then the TFIIH complex which contains the XPB and XPD DNA helicases, locally unwinds the DNA, allowing access of repair factors to the lesion (Schultz et al., 2000). After DNA unwinding step, three proteins RPA, XPA and XPG bind to the DNA damage site (Jones and Wood, 1993; Matsuda et al., 1995). These are required for efficient excision of DNA lesion catalysed by activity of XPG and ERCC1-XPF DNA specific

nucleases (Figure 1.6 (1) and (2)). The DNA fragment of 24-32 oligonucleotides is removed by strand cleavage up- and downstream of the lesion (Figure 1.6 (2), (reviewed in (Wood, 1996)). The resulting gap is then filled by PCNA-dependent DNA polymerase δ or ε activity and sealed by DNA ligase (Figure 1.6 (3), (reviewed in (Robins and Lindahl, 1996)).

In addition to the removal of bulky DNA adducts, NER is also involved in repair of DNA intra- and inter-strand cross-links (ICL). Both of these lesions are severely toxic for the cell during DNA replication. Intra-strand cross-links are replication fork barriers and inter-strand cross-links inhibit the DNA unwinding step. Intra-strand cross-links are mainly repaired by similar mechanism as UV photoproducts. This include sensing of the inter-strand crosslink, local unwinding of DNA, adduct excision and gap filling (reviewed in (Naegeli, 1995)). Inter-strand cross-links are more challenging to remove as they cannot be simply excised from the DNA. However, cleavage of both strands and double strand break induction during inter-strand cross-link repair has been reported (Jones and Yeung, 1990; Ramaswamy and Yeung, 1994). In *E.coli,* the UvrABC heterotrimeric endonuclease is able to excise inter-strand psoralen DNA adducts in an ATP-dependent reaction (Hearst et al., 1984; Kanne et al., 1984). In the first steps, one of the DNA strands is cleaved at adduct flanking 5’ and 3’ sites. The other strand is left undigested (Van Houten et al., 1986). One DNA end adjacent to the DNA adduct is a potential substrate for the RecA protein which can catalyse further repair by recombination (Sladek et al., 1989). This mechanism is reflected by studies in eukarytotic systems where homologous recombination deficiency is associated with hypersensitivity towards inter-strand cross-links (reviewed in (Hinz, 2010)). After RecA induced recombination the resulting gap in the DNA can be filled by DNA polymerase and further excision of the adduct can be then performed (Cheng et al., 1988).

In mammalian cells, mutations in ERCC1 or XPF genes result in hypersensitivity towards inter-strand crosslink agents, whereas mutations in XPB/D/G show only moderate effects, suggesting a significant difference in repair of regular NER substrates and ICLs (Andersson et al., 1996; Clingen et al., 2005; De Silva et al., 2000; Niedernhofer et al., 2004). In higher eukaryotes, similarly to *E. coli,* cells, the ICLs are repaired by combined action of NER and

recombination pathways (reviewed in (Hinz, 2010)). In eukaryotic models, when the replication machinery encounters the ICL, the lesion is first unhooked on one end by the activity of the Mus81/Eme1 endonuclease (cuts 3' to the lesion) followed by an ERCC1/XPF cut 5' to the lesion (Figure 1.7, (1) and (2)) (Hanada et al., 2006; Niedernhofer et al., 2004).

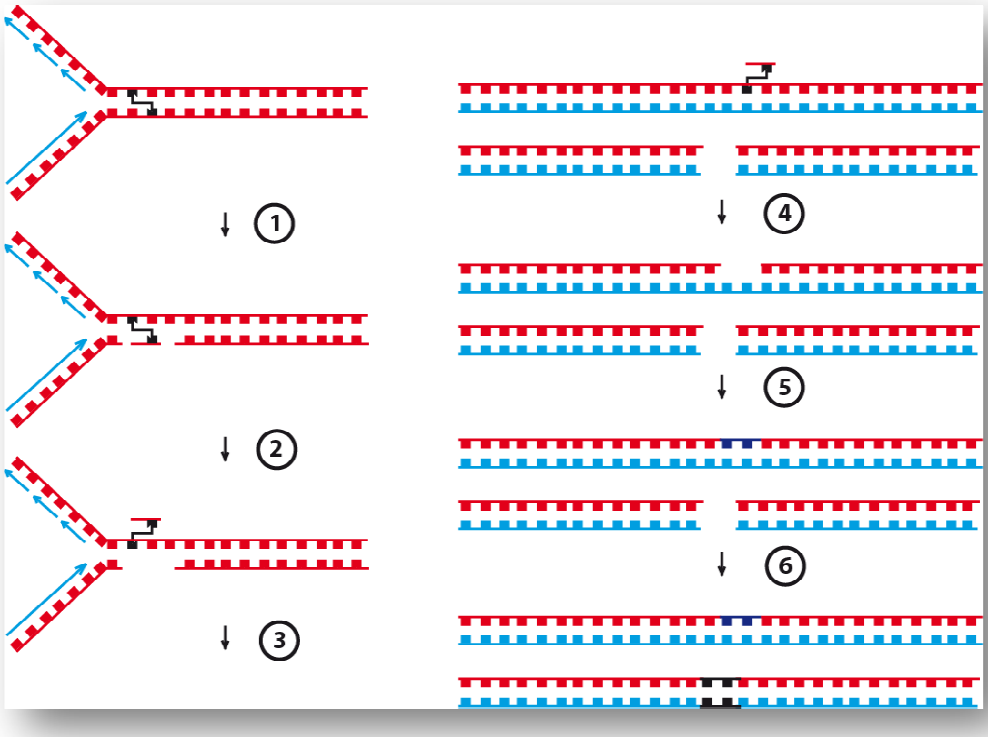

Figure 1.7 Inter-strand DNA crosslink repair.

Cartoon shows a mechanism of DNA inter-strand cross-link repair with the enzymes involved at each step: (1) DNA excision 5' and 3' of the DNA adduct is catalysed by ERCC1/XPF and Mus81/Eme1, respectively. (2) DNA adduct flip, (3) TLS at the site of an adduct, (4, 5) excision of an adduct by NER, (6) DSB repair by homologous recombination.

This generates one sided DSB. In one of the possible scenarios the strand containing the unhooked adduct is then synthesised by translesion synthesis (TLS) polymerases (Figure 1.7, (3)) (Rahn et al., 2010). The second strand is duplicated by the converging replication fork what leads to formation of a DSB break (Figure 1.7 (3)). In the next step, ICL is removed by NER (Figure 1.7 (4)), the gap is filled and sealed by DNA polymerase and ligase activities (Figure 1.7 (5)). The resulting DSB is then repaired by Rad51 dependent homologous recombination (Figure 1.7 (6)) (described in section 1.6.3).

In an alternative scenario, induction of the one sided DSB, recruits FANCD2 and Rad51 proteins in order to initiate recombination at the stalled replication fork (Al-Minawi et al., 2009; Bhagwat et al., 2009; McCabe et al., 2008). The Rad51 coated 3' end of the one sided DSB is then invading the homologous sequence (if available) or non-homologous chromosome with extensive sequence homology (reviewed in (Rahn et al., 2010)). The non-homologous sequence is then removed by ERCC1/XPF (end trimming) and the recombination intermediate is resolved (reviewed in (Rahn et al., 2010)).

XP is an autosomal recessive genetic disorder. XP patients have defective NER and cannot properly repair UV-induced DNA damage. Mutations in eight of NER genes, including XPA-G and Polymerase η result in XP (reviewed in (Kannouche and Stary, 2003)). Mutations in the XP genes are often associated with skin cancer predisposition (reviewed in (Lindahl et al., 1995; Wood, 1996)). Inability to properly repair the NER substrates results in increased mutation rate and tumourgenesis in XP individuals. Mutations of NER genes result in two other genetic diseases, Cockayne's syndrome (CS) and Trichothiodystrophy (TTD) (reviewed in (Bergoglio and Magnaldo, 2006)). Patients with these syndromes show UV light sensitivity and premature aging, but do not have increased cancer predisposition. CS and TTD are caused by mutations in CSA/B and XPB/D, and are defective in removal of DNA damage in transcribed sequences of the genome, namely transcription coupled DNA repair (reviewed in (Bergoglio and Magnaldo, 2006)).

1.6.3 DNA double strand break repair

DNA double strand breaks (DSB), if not repaired, are the most mutagenic and potentially lethal of all DNA lesions. DSB causes discontinuity of the genetic information. Such a situation is dangerous for the cell as the fragmented chromosome may be lost, duplicated or fused with inappropriate parts of the genome. This can potentially lead to tumourgenesis if the deleted chromosomal sequence encodes a protein that normally prevents tumour formation (tumour suppressor gene) or if the amplified region contains genes promoting cell proliferation (oncogene).

DNA double strand breaks are mainly processed by two distinct mechanisms error-free homologous recombination pathway (HR) and the error-prone non-homologous end joining process (NHEJ). Both pathways compete for access to the DSB (Ciccia and Elledge, 2010; Hochegger et al., 2006; Rapp, 2004). The HR pathway normally requires a sister chromatid as a template for repair and because of that, its activity peaks in late S and G_2 phase of the cell cycle. In the non-homologous end joining or alternative-NHEJ, broken DNA ends are directly re-joined without or with the help of a short homology sequence, respectively. The NHEJ pathway operates mainly in G_1 and early S phase, when a second copy of the DNA is not yet available for repair. However, recent data suggest that NHEJ is far more accurate and is engaged in the repair of a greater number of DSB during the cell cycle than was previously believed (Beucher et al., 2009a).

1.6.3.1 Homologous recombinational repair

After induction of DSB, they are sensed within few seconds and bound by many proteins, such as PARP-1, Ku70/Ku80, and MRN (reviewed in (Ciccia and Elledge, 2010)). In the HR, DSBs are processed by Mre11 (meiotic recombination 11), Rad50 (radiation sensitive 50) and Nbs1 (Nijmegen breakage syndrome 1) complex (MRN) together with Sgs1 helicase and Dna2/Exo1 nucleases (Figure 1.8) (Mimitou and Symington, 2008; Williams and Tainer, 2007; Zhu et al., 2008). The MRN complex then recruits the ATM kinase via the C-terminal region of the Ns1 protein in order to activate DNA damage response cascade (Jazayeri et al., 2008; Lee and Paull, 2005; Paull and Lee, 2005) (Figure 1.8). The MRN heterotrimer then activates ATM/ATR which phosphorylate the BRCA1, Nbs1, H2AX histone (γ-H2AX) and Smc1 proteins (Ciccia and Elledge, 2010). The γ-H2AX modification is introduced up to 1-2 Mb around the actual DSB site in an ATM-dependent manner (Pilch et al., 2003). Phosphorylation of histone H2AX around the DSB site has been shown to be required for recruitment and assembly of DNA damage repair proteins (Rogakou et al., 1998). This is believed to be an essential platform for factors, such as replication protein A (RPA), BRCA1, BRCA2 and Rad51/52/54/55/57/59 (reviewed in (Ciccia and Elledge, 2010; Symington, 2002).

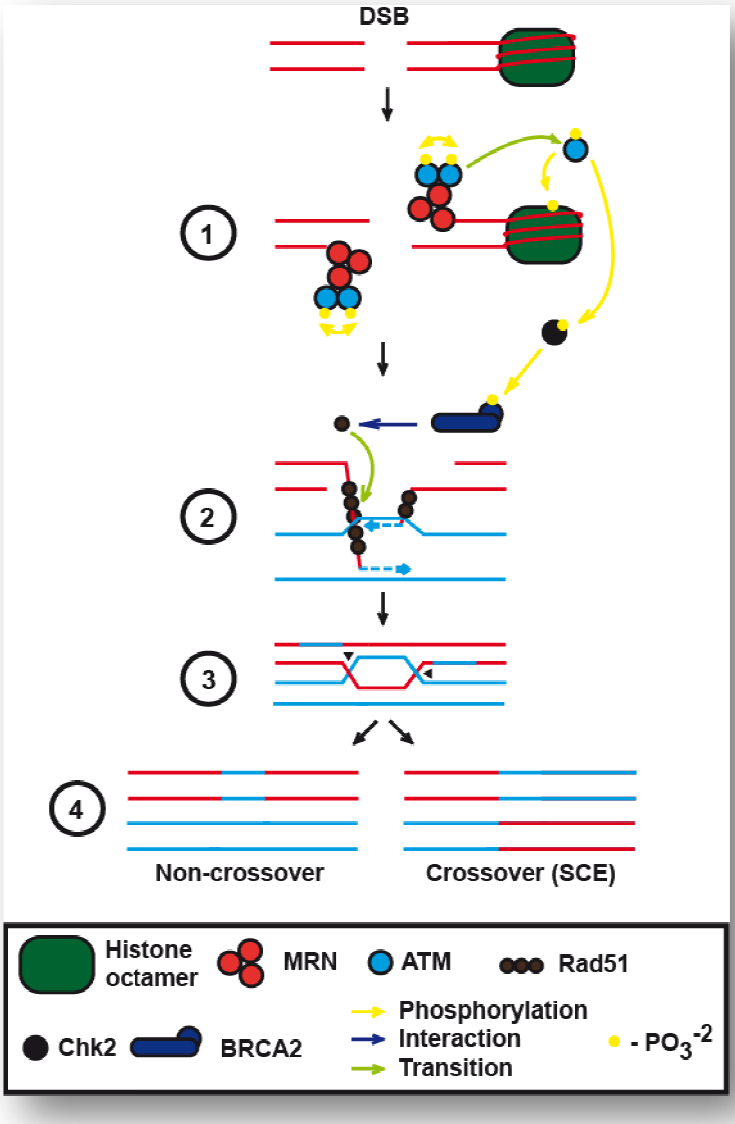

Figure 1.8 Model of double strand break repair through double Holliday junction (dHJ).
Cartoon show a mechanism of DSB repair through formatin of double Holliday junction, with the principal enzymes involved in each step. (1) In the HR pathway the 5' ends of the DSB are recessed by the MRN complex, which activates the DNA damage response through ATM kinase. ATM phosphorylates many cellular targets including histone γ-H2AX, Chk2 and itself. (2) A nucleoprotein Rad51 filament is formed at the 3' overhangs in a BRCA2-dependent manner, and then invades the homologous sequence. (3) A double Holliday junction (dHJ) is formed after strand invasion and DNA synthesis, (4) HJs are resolved to give cross- or non-crossover products.

Enzymes with chromatin remodelling activities like INO80 (putative DNA helicase INO80 complex homologue 1) and SWI/SNF (SWI/SNF-related, matrix associated, actin dependent regulator of chromatin) are also recruited to the DSB

and are believed to facilitate regulation of the local chromatin conformation (Lee et al., 2010; van Attikum et al., 2004). Recently, ubiquitylation and SUMOylation have been shown to regulate protein recruitment and repair at the DSB. For example ubiquitylation of lysine 63 of histone H2A by RNF8 ubiquitin ligase is essential for recruitment of the RAP80 (receptor associated protein 80) and BRCA1 proteins to the damage site (Huen et al., 2007; Kolas et al., 2007; Wang and Elledge, 2007). Localisation of the BRCA1 protein is dependent on PIAS1- and PIAS4-mediated (protein inhibitory of activated STAT 1 and 4) BRCA1 SUMOylation (Galanty et al., 2009; Morris et al., 2009).

In the early steps of HR, the endonuclease activity of the MRN complex together with Exo1/Dna2 resects the 5' ends of the DSB to facilitate strand invasion (Figure 1.8 (1), reviewed in (Huen and Chen, 2010)). DNA end processing is controlled by the ATM, CtIP (CtBP-interacting protein), BRCA1, EXO1 (Exonuclease 1), BLM (Bloom helicase) and ARTEMIS (DNA cross-link repair 1C protein) proteins (Beucher et al., 2009b; Bolderson et al., 2010; Huen and Chen, 2010). In order to protect single-stranded 3' ends from degradation, overhangs are coated with RPA, which binds tightly to single stranded DNA (Wold, 1997). The RPA-DNA complex is then displaced by Rad51 recombinase in a process dependent on BRCA2 (breast cancer type 2 susceptibility protein) and Chk2-dependent BRCA2 phosphorylation (Figure 1.8 (2), (Esashi et al., 2005; West, 2003). Additionally, SUMOylation of the RPA subunit RPA1 and phosphorylation of Rad51 by Chk1 are required for assembly of the Rad51 protein on 3' overhangs (Dou et al., 2010; Sorensen et al., 2005). In the next step Rad51-coated DNA invades the sister chromatid in search for a homologous DNA sequence (Figure 1.8 (2), reviewed in (West, 2003). This process is stimulated by Rad52/54/55/57 proteins (reviewed in (Symington, 2002)). Rad55 and Rad57 are important in formation and stabilisation of the Rad51 filament (Mozlin et al., 2008). Rad54 protein interacts with Rad51 and stimulates the strand exchange reaction catalysed by Rad51 (Alexeev et al., 2003). Rad52 is also required for formation of the Rad51 nucleoprotein filament but additionally Rad52 promotes annealing of the 3' overhang with homologous DNA sequence (Nimonkar et al., 2009). When the search is finished, the DNA is then synthesised to restore the lost genomic information at the site of DSB, using the

sister chromatid as a template (Figure 1.8 (2)). The Holliday junctions are formed after the DNA strand synthesis and ligation (Figure 1.8 (3)). These structures are often moved by specialised DNA helicases (BLM, WRN**)** and cleaved by the action of Holliday junction dissoluting complexes (BLM/TOPOIII) or resolving conplexes, such as, nucleases GEN1, MUS81/EME1, SLX1/SLX4 (Figure 1.8 (3), (Andersen et al., 2009; Ciccia et al., 2008; Fekairi et al., 2009; Ip et al., 2008; Muñoz et al., 2009; Svendsen et al., 2009). Depending on Holliday junction resolution pathway cross-over (GEN1, MUS81/EME1 or SLX1/SLX4) or non cross-over (BLM/TOPOIII) products are formed (Figure 1.8 (4), (Heyer, 2004; Hollingsworth and Brill, 2004; Yamada et al., 2004).

Additional homologous recombinational repair pathways exist in eukaryotic cells. In one of them, termed synthesis dependent strand annealing (SDSA), the initial steps are identical to those in the double Holliday junction model (Figure 1.9). The 5' resected ends coated with Rad51 the invade sister chromatid to search for homologous sequence (Figure 1.9 (1) and (2)). After synthesis of DNA using the sister chromatid as a template, the DNA duplex between sister chromatids is displaced by the activity of RecQ helicases (Sgs1/Rqh1/BLM) and offers the possibility of re-annealing DSB ends (Figure 1.9 (3) and (4)) (Ira et al., 2003; Robert et al., 2006; Wu and Hickson, 2003). It has been shown that BLM is able to dismantle Rad51 nucleofilaments (Bugreev et al., 2007) and DSB ends can be then annealed. Repair is completed by gap filling and ligation. The SDSA pathway leads exclusively to non-crossover products suggesting that it may be a major pathway for DSBs repair in somatic cells.

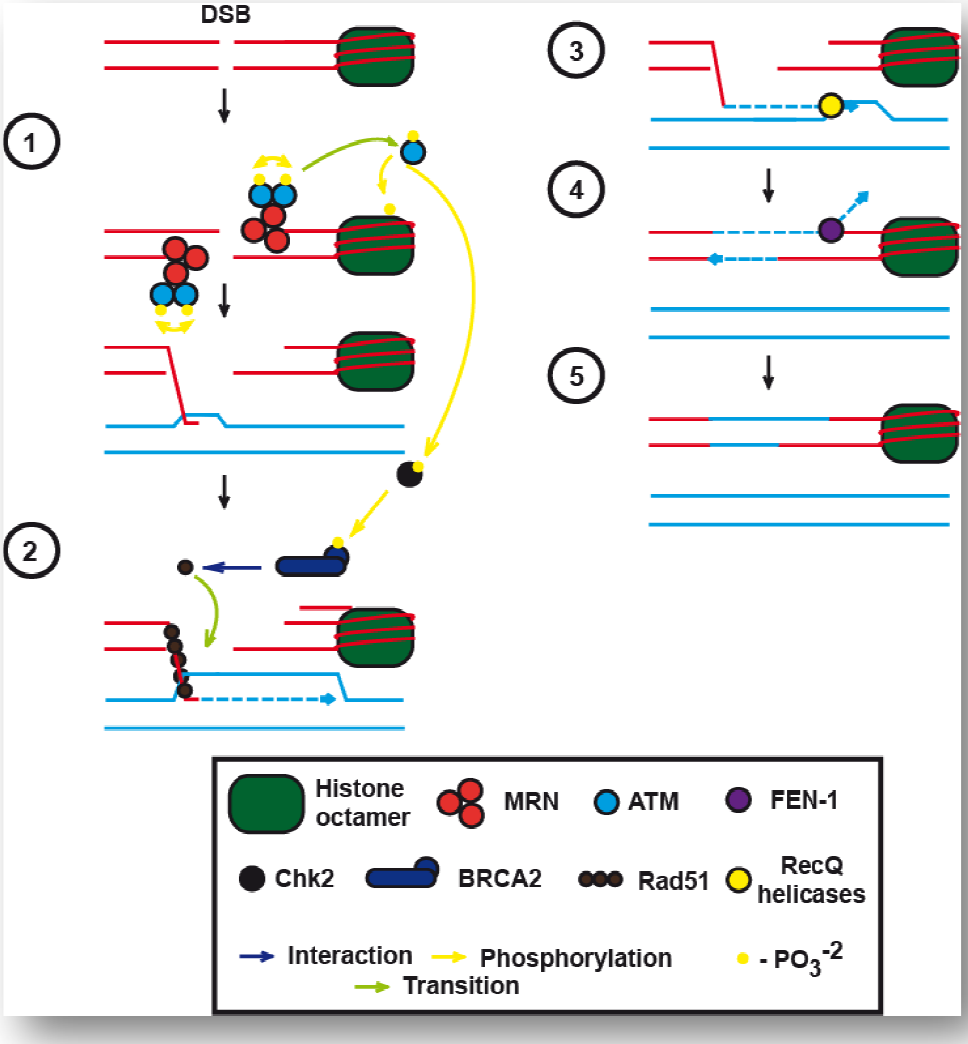

Figure 1.9 Double strand break repair through synthesis-dependent strand annealing (SDSA). *Cartoon shows a model for the mechanism of synthesis dependent strand annealing (SDSA), a DSB repair process, with the principal enzymes involved in each step. (1) Similarly to double the Holliday junction model, the 5' ends of the DSB are recessed by the MRN complex, which activates the DNA damage response through ATM kinase. ATM phosphorylates many cellular targets including histone γ-H2AX, Chk2 and itself. (2) A Rad51 nucleoprotein filament is formed at the 3' overhangs in a BRCA2-dependent manner, and then invades the homologous sequence, which is used as a template to synthesise DNA at the site of DSB. (3) The Rad51 nucleoprotein filament is dismantled by displacement of Rad51 through activity of RecQ helicases. (4) DSB ends anneal and terminal sequences are removed by FEN-1 endonuclease. (5) SDSA leads to only non-crossover products.*

In the second pathway, termed single strand annealing (SSA), DSBs are repaired using a homologous sequence within the same sister chromatid (Figure

1.10). The SSA pathway repairs DSBs which have occurred between two direct repeats. First, 5' end resection uncovers the direct repeat sequences (Figure 1.10 (1)), which can then anneal together to repair the break (Figure 1.10 (2)). The annealing step is mediated by Rad52 but not Rad51, which is recruited to ssDNA by RPA (Hays et al., 1998). The terminal sequences (flaps) not involved in annealing are removed by specific endonucleases, such as Rad1-Rad10 (Fishman-Lobell and Haber, 1992; Saparbaev et al., 1996) (Figure 1.10 (2)).

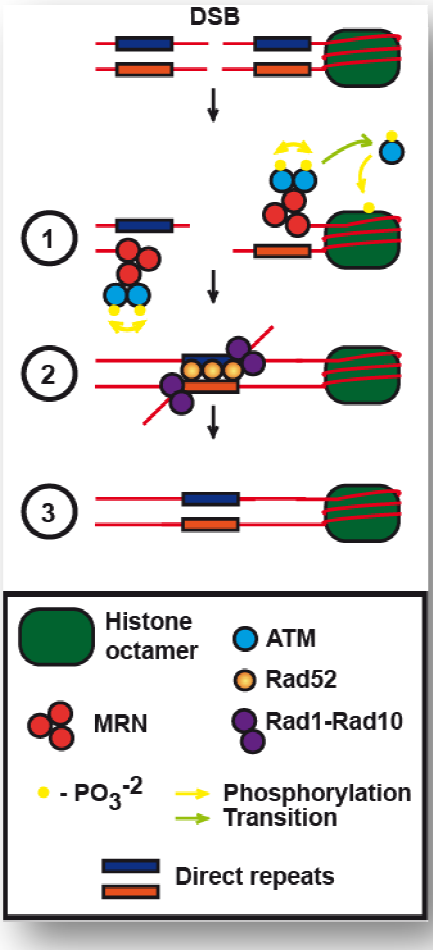

Figure 1.10 Double strand break repair through single strand annealing (SSA).

Graphical representation of the single strand anneling (SSA) mechanism and principal enzymes involved in each step. (1) First, 5' ends of the DSB are recessed by the MRN complex, which activates the DNA damage response through ATM kinase. Resection of the 5' ends uncovers direct repeat sequences (2) Homologous sequences can then anneal through a Rad52-dependent single strand annealing process. (3) Terminal sequences are removed by the activity of the specific endonuclease Rad1-Rad10 (5) SSA leads to loss of one of the repeats and the region located between the direct repeat sequences.

Similarly to other HR pathways, repair is completed by gap filling and ligation (Figure 1.10 (3)). SSA leads to deletion of one of the DNA repeats and a region located between the repeats, therefore it is considered as mutagenic. However, eukaryotic genomes contain a significant amount of repeated sequences which are likely repaired this way if the sister chromatid is not available for repair.

1.6.3.2 Non-homologous recombinational repair

In the non-homologous end joining (NHEJ) process no homology or just a few nucleotides of microhomology is required for the repair of the DSB (Figure 1.8). During NHEJ the broken DNA ends are rapidly bound by the Ku70/Ku80 heterodimer which recruits the DNA-PK (Figure 1.11 (1), reviewed in (Mahaney et al., 2009). DNA-PK prevents DNA end resection, regulates chromatin structure and facilitates DSB repair by protein phosphorylation (Figure 1.11 (2), reviewed in (Meek et al., 2008)). After loading of the DNA-PK, DNA ligase IV/XRCC4 complex is recruited to the site of the damage (reviewed in (Mahaney et al., 2009)). Additional end regulation may be performed before ligation by ARTEMIS, APLF (aprataxin-and PNK-like factor) nucleases and PNK (polynucleotide phosphatase/kinase) kinase/phosphatase (Figure 1.11 (2), reviewed in (Mahaney et al., 2009). Processed DNA ends are brought together and rejoined by activity of the DNA ligase IV/XRCC4 protein complex (reviewed in (Mahaney et al., 2009)) (Figure 1.11 (3)).

In the alternative NHEJ pathway the double strand break is sensed by the PARP-1/2 proteins (Wang et al., 2006). Experiments in DT40 cells lacking *PARP-1* have shown that PARP-1 and Ku70 compete for the binding of the DSB ends (Hochegger et al., 2006). In addition, PARP-1 has been shown to be required for ATM activation post-DSB induction (Haince et al., 2007; Haince et al., 2008). In this process, PARP-1 mediates the recruitment of the DSB repair protein CtIP and the MRN complex to the sites of damage (Haince et al., 2007; Haince et al., 2008; Yun and Hiom, 2009). Short stretches of homology are required for rejoining of the broken ends by the DNA ligase III/XRCC1 complex (You and Bailis, 2010; Yun and Hiom, 2009).

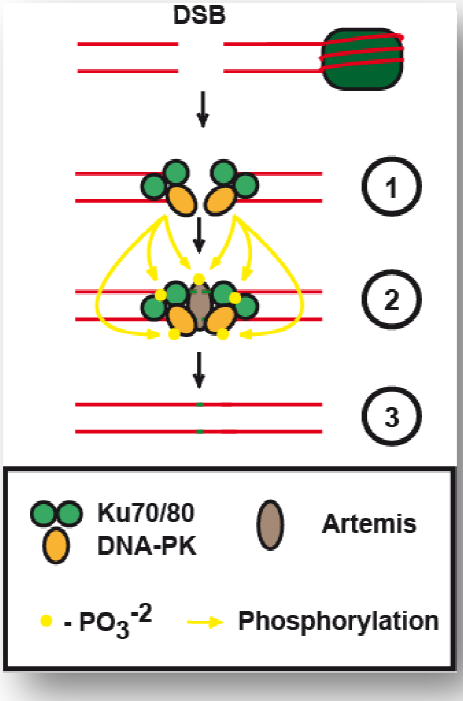

Figure 1.11 Double strand break repair through non-homologous end joining.
Cartoon shows mechanism of non-homologous end joining (NHEJ), a DSB repair process, with the principal enzymes involved in each step. (1) During NHEJ, DSB ends are bind by the Ku70/Ku80/DNA-PK complex (2) DNA-PK is activated when bound to DSB ends. DNA-PK phosphorylates target proteins, such as Ku70/Ku80 heterodimer, Artemis and itself. (3) This leads to rejoining of broken DNA ends by the DNA ligase IV/XRCC4 complex. (A double arrow head shows autophosphorylation events and DNA sequence in green represents short stretches of homology or processed DNA ends).

Deficiency in DSB repair is a hallmark of broad spectrum of physiological defects, such as pathologies of the nervous, reproductive and immune systems. Inefficient DSB repair leads to increased rates of tumourgenesis and aging (reviewed in (Ciccia and Elledge, 2010)). Well-studied mutations in the *ATM* gene result in the genetic disease, ataxia telangiectasia, a disorder characterised by severe movement impairment caused by progressive neuronal degradation (reviewed in (Biton et al., 2008)). A similar phenotype has been reported in individuals with mutations in the *MRE11* gene, the product of which is required for ATM activation *in vivo* (Limbo et al., 2011). Different types of microcephalies are associated with loss of function of genes such as *ATR*, *MCPH1* (microcephalin 1) which are also involved in DSB repair

(reviewed in (Kerzendorfer and O'Driscoll, 2009; O'Driscoll and Jeggo, 2008)). The Bloom and Werner syndromes, both of which are associated with a broad spectrum of malignancies, show hyperrecombination phenotypes. The products of the *BLM* and *WRN* genes, Bloom and Werner helicases, respectively, are involved in the resolution of HR intermediates (reviewed in (Chu and Hickson, 2009)). Mutations in the *BRCA1* and *BRCA2* genes are detected in 10% of patients diagnosed with breast and ovarian cancers (reviewed in (Fackenthal and Olopade, 2007)). These mutations are hereditary and their early detection increases the possibility of efficiently treating breast and ovarian cancer (reviewed in (Jackson and Bartek, 2009)).

1.6.4 Mismatch repair

Mismatch repair is a DNA repair mechanism activated during DNA synthesis. During replication of the genomic material, mis-incorporation of the wrong base happens with a rate of 10^{-7} to 10^{-9} (reviewed in (Kunkel and Bebenek, 2000)). Base mismatches are sensed by the DNA sliding clamp, MSH2/MSH6 heterodimer (also known as MutSα). MutSα is able to travel along the DNA in an ATP-dependent manner in search of wrongly-incorporated bases (Blackwell et al., 1998; Gradia et al., 1999; Iaccarino et al., 2000). Another heterodimer MLH1/PMS2 accompanies the MutSα mismatch recognition complex (Li and Modrich, 1995). In bacterial cells, the MutSα homologue can distinguish between old and newly-synthesised DNA strands by sensing their methylation status (Glickman, 1982). The human MutSα/MLH1/PMS2 complex recognises the newly synthesised strand by the presence of Okazaki fragments on the lagging strand or a 3' terminus on the leading strand (Genschel and Modrich, 2003). After mismatch detection, the MMR complex removes the erroneous base by recruitment of the exonuclease NEO1 (5' – 3' activity), which digests the new strand containing the wrong base (Dzantiev et al., 2004; Genschel and Modrich, 2003, 2009). The resulting single stranded DNA is bound by RPA to protect it from further digestion and the gap is then filled by the activity of DNA polymerase in a PCNA-dependent manner (reviewed in (Kolodner, 1996)).

In addition, MMR proteins have been implicated in the repair of other DNA lesions such as single and double strand breaks, DNA methylations and DNA cross-links (Stojic et al., 2004a; Stojic et al., 2004b). Yan et al. showed a moderate sensitivity of hMSH1 and hMSH2 deficient cells and a G_2 checkpoint defect after IR treatment (Yan et al., 2001). In cells treated with methylating agents such as MNU or MNNG, the 6-methylguanine can be mismatched during replication with a T nucleotide. Such structures have been shown to be bound by MutSα (Duckett et al., 1996). Analogously, the 1,2GpG cis-platin adducts are bound by the same MMR heterodimer *in vitro* (Duckett et al., 1996).

Hereditary nonpolyposis colorectal cancer (HNPCC, Lynch syndrome) is a result of heterozygous mutation in mismatch repair genes (*MLH1*, *MSH2*, *MSH6* and *PMS2*) (Spry et al., 2007). HNPCC is a most prevalent cancer type in developed countries. Most of the cases (approximately 20%) have a familial background (Lynch et al., 2004). Mutations in the MMR genes have been also involved in other types of diseases such as microsatellite instability and trinucleotide repeat disorders (reviewed in (Iacopetta et al., 2010; La Spada, 1997)).

1.7 Structural maintenance of chromosome (Smc) proteins

The structural maintenance of chromosome (Smc) family is a group of well conserved proteins involved in many aspects of DNA metabolism. Smc proteins are relatively large (around 100-150 kDa) and contain extensive coiled-coil regions (Hirano, 2002). Each Smc protein consists of three characteristic domains: the ATP binding and hydrolysis domains (Walker A and B) at the N- and C-terminal ends, with long coiled-coil arms separated by the flexible hinge (Hirano and Hirano, 2002) (Figure 1.9). The hinge domain allows the coiled-coil arms to fold back on themselves. Interaction between hydrophobic coiled-coil arms brings the ATP binding and hydrolysis domains together in order to form a functional ATPase unit, called the Smc head (Figure 1.9). The eukaryotic Smc proteins form heterodimers through hinge-hinge interactions (homodimers are observed in prokaryotes). The consensus glycine motifs GX_6GX_3GG and

GX_5GGX_3GG have been identified at the hinge domain of the eukaryotic and prokaryotic Smc proteins, respectively (reviewed in (Chiu et al., 2004)). Mutation of 4 of the 5 glycine residues in the *Bacillus subtilis* Smc protein hinge domain results in the inability of the protein to form a homodimer and bind DNA (Hirano and Hirano, 2002).

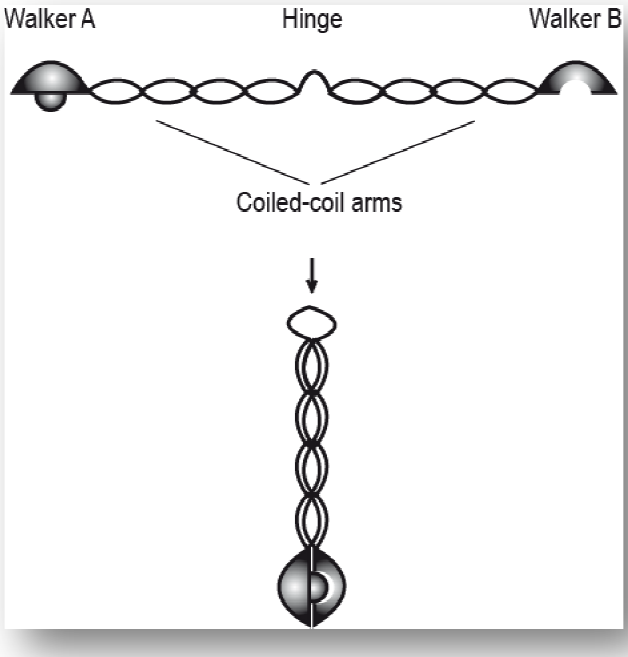

Figure 1.12 Structure of the Smc proteins.
Graphical representation of Smc protein structure showing characteristic domains: Walker A and B, coiled-coil arms and hinges (adapted from (Hirano, 2006)).

Similar experiments on eukaryotic Smc hinges revealed that mutation of a single Smc1 or Smc3 hinge motif did not abolish heterodimer formation and DNA binding *in vitro*. But when both hinges were mutated the interaction was no longer detected, suggesting a difference in the mechanism involved in the formation of prokaryotic and eukaryotic Smc dimers (reviewed in (Chiu et al., 2004)). Similarly, mutation of the ATP binding and hydrolysis sites in cohesin and condensin proteins, abolishes ATP nucleotide binding and hydrolysis, respectively (reviewed in (Hirano, 2002)).

In eukaryotes there are seven Smc proteins identified to date. Smc1/2/3/4/5/6 and Rad50 proteins share a similar structure but play very different cellular roles (reviewed in (Hirano, 2005; Losada and Hirano, 2005)).

On the other hand, there is only a single Smc gene in bacterial cells. Within the eukaryotic cell, three distinct heterodimers are formed: Smc1-Smc3 (cohesin), Smc2-Smc4 (condensin) and Smc5-Smc6 (reviewed in (Losada and Hirano, 2005)). The seventh member of the eukaryotic Smc family, Rad50, similarly to bacterial Smc, homodimerises to became an assembly platform for the Mre11 and Nbs1 proteins. This MRN complex is essential for DSB repair (reviewed in (Paull, 2001)). Smc heterodimers adopt a V shaped structure but their conformations are slightly different (Anderson et al., 2002; Anderson et al., 2001) (Figure 1.10).

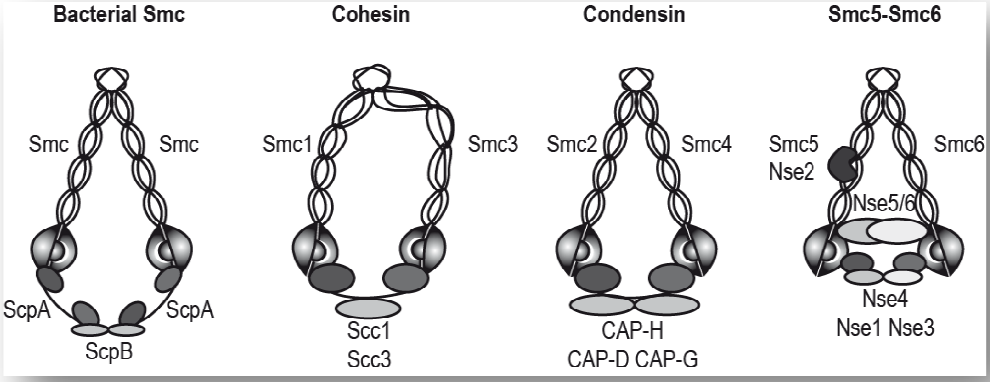

Figure 1.13 Structure of the bacterial and eukaryotic Smc complexes.
Graphical representation of Smc complexes found in bacterial and eukaryotic cells (protein sizes are not to scale).

The condensin arms are close together, whereas the cohesin hinge is more open, allowing significant separation of the arms. This is consistent with the different functions of these complexes.

Besides the Smc proteins, other factors are required for full functionality of these complexes. These non-Smc elements can bind to heads or arms of the Smc proteins, regulating their function (reviewed in (Hirano, 2005)). One of them, called the kleisin element (ScpA in *B.subtitlis* Smc, Scc1 in cohesin, CAP-H in condensin and Nse4 in the Smc5-Smc6 complex), closes the V shaped structure by binding to the Smc heads (Dervyn et al., 2004; Palecek et al., 2006; Schleiffer et al., 2003). The other non-Smc elements regulate various functions of the complex and serve as protein-protein interaction domains.

As previously mentioned, when two ends of Smc protein come together a functional ATPase is formed (reviewed in (Hirano, 2005)). It has been proposed that ATP binding and hydrolysis promotes the closing and opening of the Smc arms, respectively (Arumugam et al., 2003; Hirano et al., 2001). Work of Hirano and co-workers suggests that intra– and inter-molecular interactions between the heads of different Smc complexes may occur in the presence of DNA (reviewed in (Hirano and Hirano, 2004; Hirano et al., 2001)). Analysis of the bacterial Smc protein ATPase cycle revealed a three step mechanism. This involves ATP binding, the so called transition-state and ATP hydrolysis steps (reviewed in (Hirano and Hirano, 2004; Hirano, 2005)). Mutations in the Smc sequence which affect any of these steps had no or only moderate effects on interactions with DNA. However, the same study showed that the conformation of the Smc heads in the transition state strongly favours DNA binding (reviewed in (Hirano and Hirano, 2004)). From these results, a simple model of action emerged. In the first step, ATP binding induces opening of the Smc arms in order to accommodate and bind DNA. Interaction with nucleic acid stimulates ATP hydrolysis and closing of the arms, inducing intra- or inter-molecular head-to-head interactions (reviewed in (Hirano and Hirano, 2004; Hirano, 2005)).

1.7.1 Smc1-Smc3 complex (cohesin)

All Smc complexes interact with DNA and play important roles in DNA metabolism. The Smc1-Smc3 (cohesin) heterodimer was first identified in *Saccharomyces cerevisiae* (Michaelis et al., 1997). The Smc1-Smc3 binds to Scc1/Mcd1/Rad21 and Scc3/SAs subunits to form a functional complex required for sister chromatid cohesion. Mutation of the cohesin complex results in premature sister chromatid separation (Michaelis et al., 1997). The cohesin complex was later identified in other organisms including *Xenopus laevis*, *Saccharomyces pombe* and humans (Losada et al., 1998; Losada et al., 2000; Sumara et al., 2000; Tomonaga et al., 2000). In humans, three different isotypes of cohesin have been identified so far and, depending on the Scc3 subunit have been termed cohesin^{SA1}, cohesin^{SA2} (observed in somatic cells) and cohesin^{SA3} mainly found in cells undergoing meiosis (Losada et al., 2000; Sumara et al., 2000). The cohesin complex is loaded onto chromatin in early G_1 phase by the

action of the Scc2/Scc4 complex (Ciosk et al., 2000). Sister chromatid cohesion is established during S-phase by modification of Smc3 through the activity of Ctf7/Eco1 acetyltransferase (Skibbens, 2009). During S phase, the Smc1-Smc3 complex interacts with the DNA sliding clamp PCNA providing direct evidence for a link between sister chromatid cohesion and DNA replication (Tóth et al., 1999). The inter-molecular DNA tethering lasts from S phase to mitosis, when the cohesin complex is removed from the DNA allowing sister chromatids to separate (Hirano et al., 1997; Michaelis et al., 1997). Differences in this process exist between lower and higher eukaryotes. Whereas in *S. cerevisiae* most of the cohesin is removed by proteolytic cleavage of the Scc1 subunit in anaphase by the Separase protease, in humans the bulk of the Smc1-Smc3 complex dissociates from chromatin in prometaphase after phosphorylation mediated by polo like kinase 1 (Plk-1) (Amon, 2001; Hornig and Uhlmann, 2004; Sumara et al., 2002). Residual cohesion is left behind in the centromeric region where it is protected from cleavage and phosphorylation until anaphase by shugoshin and protein phosphatase 2A, respectively (Rivera and Losada, 2006; Waizenegger et al., 2000; Warren et al., 2000). Chromatin immunoprecipitation studies identified the centromeres, chromosome arms and recently, replication origins, as the primary cohesin binding sites (Blat and Kleckner, 1999; Guillou et al., 2010).

In addition, the cohesin complex is believed to facilitate DSB repair by keeping the sister chromatids together in close proximity around the damage site. Smc1-Smc3 is also required for G_2 checkpoint activation (Bauerschmidt et al., 2010; Bauerschmidt et al., 2011; Dodson and Morrison, 2009b; Ellermeier and Smith, 2005; Kim et al., 2002; Watrin and Peters, 2009).

1.7.2 Smc2-Smc4 complex (condensin)

The Smc2-Smc4 complex (together with CAP-D2/G/H) was first identified in *Xenopus laevis* (Hirano et al., 1997). Temperature-sensitive *S. cerevisiae* mutants *smc2-1* and *smc2-6* show premature chromosome segregation and anaphase bridges formed by non-segregated chromosomes (Strunnikov et al., 1995). Similarly to Smc1-Smc3, the condensin complex is loaded onto DNA by the Scc2/Scc4 heterodimer (Gartenberg and Merkenschlager, 2008). *In vitro* experiments showed that condensin is able to introduce positive supercoils in the

presence of topoisomerase I (TopoI) and knots in the presence of topoisomerase II (TopoII) (Kimura et al., 1998; Kimura and Hirano, 1997). This suggests that similar activities may play a role in chromosome condensation *in vivo*. In addition to the mitotic functions of the Smc2-Smc4 heterodimer, a condensin subcomplex is involved in non-mitotic events such as dosage compensation in *Caenorhabditis elegans* (Lieb et al., 2000). The dosage compensation complex is specifically recruited to both X chromosomes in order to reduce gene expression by half (Lieb et al., 1998; Lieb et al., 2000). Condensin has also been implicated in gene silencing in *Drosophila melanogaster* or rDNA gene cluster organisation in humans and *S. cerevisiae* (Cabello et al., 2001; Freeman et al., 2000; Lupo et al., 2001).

1.7.3 The Smc5-Smc6 complex

The third of the Smc complexes, Smc5-Smc6, was first identified in *Schizosaccharomyces pombe* (Lehmann et al., 1995). The as yet unnamed Smc5-Smc6 complex, together with six non-Smc elements (Nse1 to Nse6), is mainly required for DNA damage repair and G_2 checkpoint maintenance (Verkade et al., 1999) after treatment with a broad range of DNA damaging agents, including UV, IR, MMS and cis-platin (Fousteri and Lehmann, 2000; Lehmann et al., 1995; Taylor et al., 2001). All genes of the Smc5-Smc6 complex are essential for viability in *S. cerevisiae.* On the contrary, the *S. pombe Nse5* and *Nse6* are not required for viability. Surprisingly, the human (Potts et al., 2006; Potts and Yu, 2005), *Arabidopsis thaliana* (Watanabe et al., 2009) and chicken (Stephan et al., 2011a) Smc5-Smc6 complexes are not essential for cell proliferation.

Similarly to the cohesin and condensin complexes, the Smc5 and Smc6 proteins heterodimerise through hinge interactions to form a scaffold for a high molecular weight complex. The non-Smc elements bind to this scaffold to form a functional Smc5-Smc6 complex. Among the non-Smc elements of the Smc5-Smc6 complex, the Nse1 protein contains a zing finger domain similar to E3 ubiquitin ligases but no activity has yet been observed *in vivo* (McDonald et al., 2003). Recent work by Pebernard et al. revealed no ubiquitin ligase activity for Nse1 *in vitro.* The authors suggested that the zinc finger domain is required for formation of the Nse1-Nse3-Nse4 subcomplex (Pebernard et al., 2008b).

However, Nse1 showed a robust activity in the presence of Nse3, indicating that Nse1 is a functional E3 ubiquitin ligase (Doyle et al., 2010). Nse2/MMS21 is an active Siz/PIAS E3 SUMO ligase that SUMOylates many cellular targets (see section 1.10.4). Nse3 is a member of the MAGE (melanoma associated antigen) family of unknown function (Pebernard et al., 2004). Nse4 has been identified as the kleisin element of the Smc5-Smc6 complex, whose function is to bridge the Smc5-Smc6 heterodimer heads (Palecek et al., 2006). It contains the kleisin-like domain composed of a helix-turn-helix motif, which is also found in other members of the family, including Scc1 and CAP-H (Palecek et al., 2006; Pebernard et al., 2004). Nse5 does not contain any known domains and Nse6 has been identified as HEAT (Huntingtin, elongation factor 3 (EF3), protein phosphatase 2A (PP2A), and the yeast PI3-kinase TOR1) repeat protein (Palecek et al., 2006; Pebernard et al., 2006). The Nse5 and Nse6 proteins form another subcomplex and like the Nse1-Nse3-Nse4 heterotrimer, bind to the heads or arms of the Smc5-Smc6 complex in *S. pombe* (Palecek et al., 2006; Pebernard et al., 2006) and to hinges in *S. cerevisiae* (Duan et al., 2009b).

Chromatin immunoprecipitation (ChiP) experiments in budding and fission yeast revealed different chromosomal localisations of the Smc5-Smc6 complex, with enrichment at telomeres, centromeres and rDNA gene clusters (Ampatzidou et al., 2006; Lindroos et al., 2006; Pebernard et al., 2008c; Torres-Rosell et al., 2005a). Defective HR at the repetitive DNA sequences can result in gross chromosomal rearrangements such as deletions and insertions at these loci. It has been proposed that the localisation of the Smc5-Smc6 complex on these sequences regulates their status through recombination (Torres-Rosell et al., 2005b; Zhao and Blobel, 2005). In addition, yeast Smc5-Smc6 mutants show increased telomere shortening and in human cells, the Smc5-Smc6 is required for recombination-dependent alternative telomere lengthening (ALT) process (Chavez et al., 2010b; Potts and Yu, 2007). DNA repair and segregation at ribosomal loci is also mediated by the Smc5-Smc6 complex (Torres-Rosell et al., 2005a; Torres-Rosell et al., 2005b; Torres-Rosell et al., 2007).

The functions of the Smc5-Smc6 complex are considered to be in DNA repair. The *S. pombe Rad18/Smc6* gene is required for maintenance of G_2 checkpoint and repair after DNA damage (Lehmann et al., 1995; Verkade et al.,

1999). The Smc5-Smc6 complex plays a role in the restart of the stalled replication forks by regulating recombination (Ampatzidou et al., 2006; Irmisch et al., 2009). Studies in yeast, chicken and human cells have revealed that the Smc5-Smc6 complex is required for efficient homologous recombinational repair (Lehmann et al., 1995; Potts et al., 2006; Stephan et al., 2011a; Verkade et al., 1999). In epistasis analyses experiments, combined mutation of *Smc5* and HR genes, such as *Rad51 or Rad54* does not enhance sensitivity towards IR, UV or MMS, further confirming a HR role for the complex (Ampatzidou et al., 2006; Bermúdez-López et al., 2010; Lehmann et al., 1995; McDonald et al., 2003; Stephan et al., 2011a). Consistent with such a role for Smc5-Smc6, depletion of the NHEJ gene *Ku70* in chicken Smc5-deficient cells caused further sensitisation of *Smc5* mutants to IR-induced DNA damage (Stephan et al., 2011a). Recruitment of the Rad51 and Rad54 proteins to DSB is unaffected in chicken and fission yeast mutants of the Smc5-Smc6 complex, suggesting its activity in late stages of HR (Ampatzidou et al., 2006; Stephan et al., 2011a). Extensive studies in budding and fission yeast using 2D gel electrophoresis revealed a significant increase in the X-shaped molecules in the absence of functional Smc5-Smc6 complex before and after MMS or HU treatment (Ampatzidou et al., 2006; Branzei et al., 2006; Chavez et al., 2010a; Chavez et al., 2010b; Chen et al., 2009; Choi et al., 2010). The nature of these X-shaped molecules has not been confirmed yet but a large body of data suggests that this are recombination intermediates (Ampatzidou et al., 2006; Bermúdez-López et al., 2010; Branzei et al., 2006; Choi et al., 2010). This is also associated with aberrant mitosis as defined by chromosome mis-segregation, premature septation in the presence of unrepaired or not completely replicated DNA (‘cut’ phenotype), nuclear segregation and unequal DNA mass separation between mother and daughter cells (Ampatzidou et al., 2006; Chavez et al., 2010a; Chavez et al., 2010b; Chen et al., 2009; Choi et al., 2010; Lehmann et al., 1995; Verkade et al., 1999). Together, these observations indicate that the Smc5-Smc6 complex acts in the late stages of HR. The loss of Smc5-Smc6 complex leads to impaired HR and the accumulation of lethal DNA repair intermediates. The X-shaped DNA molecules arising in *smc6-1* and *mms21-sp* can be removed and the mitotic aberrations reversed by restoration of the Smc5-Smc6 complex through expression of either

wild-type Smc6 or Nse2 in these mutants (Bermúdez-López et al., 2010; Branzei et al., 2006; Chavez et al., 2010b). Additional evidence for a HR function of the Smc5-Smc6 complex comes from experiments where deletion of HR factors such as MphI/FANCM helicase in *smc6-9* and *mms21-sp*, Shu complex in *smc6-P4* and *smc6-56*, the post replicative repair protein MMS2 in *smc6-P4* and *smc6-56* or overexpression of the 6-BRCT containing protein Brc1 in *smc6-74*, reverse hypersensitivity towards DNA damaging agents such as MMS, HU and UV (Ampatzidou et al., 2006; Chavez et al., 2010a; Choi et al., 2010; Lee et al., 2007; Sheedy et al., 2005). These findings clearly indicate that the Smc5-Smc6 complex is required for resolution of specific HR intermediates which can be removed by other HR factors acting upstream of the Smc5-Smc6 complex or by shifting the repair balance towards alternative HR repair pathways.

In HeLa cells but not in budding and fission yeast, cohesin recruitment to DSB is mediated by the Smc5-Smc6 complex (De Piccoli et al., 2006; Outwin et al., 2009; Potts et al., 2006). As the Smc1-Smc3 complex is required for local sister chromatid cohesion around the double strand break, these data suggest that Smc5-Smc6 complex may regulate cohesion to facilitate DSB repair (Ström et al., 2004). Another group reported that upon Nse2 and Smc5 siRNA mediated knockdown, HeLa cells showed severe loss of sister chromatid cohesion (Behlke-Steinert et al., 2009). Our group found that depletion of chicken *Smc5* in DT40 cells results in increased inter-sister chromatid distances before and after DSB induction. We also observed no further cohesion loss in double $Scc1^{-/-}$ $Smc5^{-}$ mutants, what demonstrates that Smc5-Smc6 complex is epistatic to cohesin in cohesion maintenance (Stephan et al., 2011a). Another group found that in fission yeast, in the absence of functional Smc5-Smc6 complex, the cohesin complex is retained at chromosome arms resulting in chromosome segregation defects (Outwin et al., 2009). Recruitment of cohesin to DSB by Smc5-Smc6 is recognised as a very early event in the HR process. Similarly, the localisation of the 'early' HR factor Rad52, which is required for recombination at stalled replication forks is Smc5-Smc6 dependent (Irmisch et al., 2009). We found that Smc5-deficient cells efficiently mobilise Rad51 to IR-induced DNA repair foci (Stephan et al., 2011a). These findings indicate dual functions of the Smc5-Smc6 complex at different stages of the HR pathway. It is hard to explain

how a single complex could be involved at various steps of DNA repair where different activities are required. Therefore many groups have proposed that the Smc5-Smc6 complex is involved in the regulation of global chromatin conformation, like other Smc complexes rather than acting at specific steps of DNA repair (Ampatzidou et al., 2006; Torres-Rosell et al., 2007).

1.8 SUMO modification

Protein modification by small like ubiquitin modifiers (SUMOs), unlike ubiquitin, does not target the protein for proteosome-mediated degradation. SUMOylation regulates many cellular processes including protein trafficking (nuclear targeting), cell signalling, chromosome segregation, DNA synthesis and repair (reviewed in (Johnson, 2004)). SUMO family members are small, approximately 100 amino acid long, proteins that are attached to ε-amino group of lysines in the substrate that meet the minimal requirements of the consensus site (ψKXE, where ψ is a large hydrophobic amino acid, K is the target lysine, X any amino acid and E glutamic acid). Non-consensus site lysines have also been found to be modified (for example AKCP, TKET, TKED, VKYC, VKFT, GKVDGKVE) (reviewed in (Johnson, 2004)). The SUMO peptide sequences are very different from the ubiquitin protein (76 amino acids) but almost identical in their folding pattern (Bayer et al., 1998). The extra amino acids found in the SUMO peptides code for an extended N-terminal tail which is relatively flexible in solution (Bayer et al., 1998; Johnson, 2004). The SUMO gene is essential for budding but not fission yeast viability. There is a single SUMO gene (Smt3/Pmt3/SUMO-1) in yeasts, four in higher eukaryotes (SUMO-1/2/3/4) and eight SUMO genes in *Arabidopsis* (Johnson, 2004; Kamitani et al., 1998; Lois et al., 2003). The higher eukaryotic SUMO-2/3 proteins are almost identical with approximately 95% homology but are only 50% identical to SUMO-1. It has been observed that SUMO-1 conjugation is a constitutive modification, where SUMO-2/3 attachment is induced by different stimuli (Saitoh and Hinchey, 2000). In addition, SUMO-2/3 can be automodified to form poly-SUMO conjugates as they contain the ψKXE consensus site within their sequence. This is absent in the SUMO-1 protein (Tatham et al., 2001). Mutation of the

SUMO2/3 SUMOylation consensus site abolishes poly-SUMO chain formation as observed for histone deacetylase HDAC4 protein (Tatham et al., 2001).

1.9 SUMOylation pathway

For a protein modification to occur, a specific enzyme that transfers the chemical moiety and a source of such a group are required. In the SUMO modification pathway, three distinct enzymes work sequentially to transfer the SUMO peptide onto a target protein. The SUMO E1 activating enzyme (SAE1) is the first enzyme that interacts with the SUMO peptide. SAE1 is a heterodimer formed of Aos1/Uba2 subunits (Johnson and Blobel, 1997). The second enzyme in the pathway is the SUMO conjugating enzyme E2 (Ubc9) which directly binds to the substrate consensus site and the E3 ligase (Bernier-Villamor et al., 2002; Tatham et al., 2003). The E2 conjugating enzyme Ubc9 is sufficient to modify around 90% of the target proteins *in vitro* but it is believed that within the cell, the activity of the third enzyme, the E3 ligase, is essential for substrate specificity. The E3 SUMO ligase can directly interact with E2 enzyme and activated SUMO peptide to catalyse SUMO peptide transfer (Bernier-Villamor et al., 2002). Cells produce the SUMO peptide in an inactive form and it has to be processed before it can be transferred onto a target protein (Figure 1.11, (1)). The mature form of the SUMO peptide lacks several C-terminal amino acids. The SUMO-specific proteases (SENPs) mediate cleavage of the C-terminal end to reveal a C-terminal di-glycine motif (Figure 1.11. (1)) (Matunis et al., 1996). First, the carbonyl group of the C-terminal glycine of SUMO protein attacks the ATP molecule to form a SUMO adenylate derivative. Then the AMP group is replaced by SAE1 in a reaction which involves the nucleophilic attack of its active site cysteine and formation of high energy thioester bond (Figure 1.11, (2)). In the next step, the activated SUMO peptide is passed to the Ubc9 enzyme (Figure 1.11, (3)). The Ubc9-SUMO intermediate forms an identical covalent link (the thiolester bond) with SUMO as the SAE1 enzyme. The final step of SUMOylation is catalysed by E3 SUMO ligase which, together with Ubc9, directs the SUMO peptide onto a specific site of the target protein (Figure 1.11, (4)). SUMOylation is a reversible protein modification. The SUMO peptide can

be recovered by isopeptidase activity of the SENP proteases and reused in the next cycle of the SUMOylation process (Figure 1.11, (5)) (reviewed in (Yeh et al., 2000)).

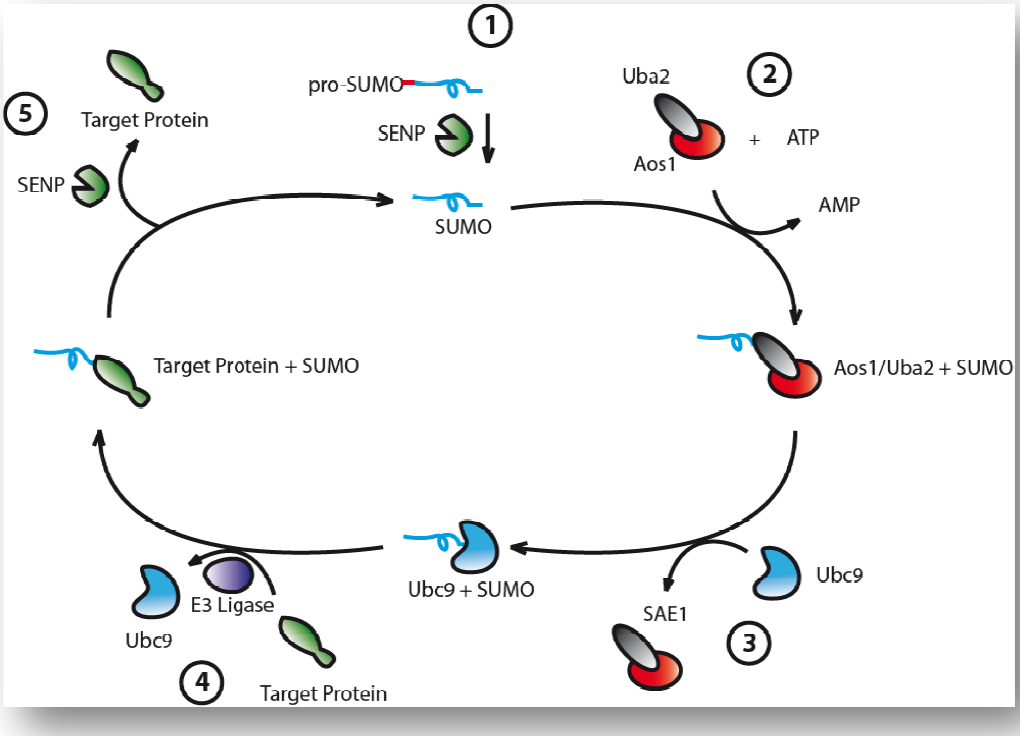

Figure 1.14 SUMOylation pathway.

Cartoon shows mechanism of protein modification by SUMO. (1) The pro-SUMO peptide is first cleaved by SENP proteases and (2) then activated by SAE1 (3) Activated SUMO is next transferred to SUMO conjugating enzyme Ubc9. (4) Co-operative activity of Ubc9 and target-specific E3 ligase is required for transfer of the SUMO peptide onto protein. (5) The SUMO peptide can be recycled by SENP protease-mediated cleavage.

1.10 Characterisation of E3 ligases

There are three distinct families of SUMO ligases identified to date: PIAS, RanBP2 and PC2 (Jackson, 2001b; Jackson and Bartek, 2009; Kagey et al., 2003; Pichler et al., 2002). All of the above mentioned SUMO ligases interact with the E2 conjugating enzyme Ubc9 and SUMO, and bind to a set of substrates to enhance their modification by SUMO attachment. The function of the E3 ligases is to bridge a specific substrate with the Ubc9-SUMO intermediate.

1.10.1 Siz/PIAS

The PIAS type of SUMO ligases were first identified in *S. cerevisiae* (Jackson and Bartek, 2009). The Siz/PIAS ligases contain the SP-RING (Siz/Pias-RING) that resembles the RING finger domain of the ubiquitin ligases and a characteristic N-terminal domain SAP (SAR, Acinus, PIAS ~400 residues) that binds DNA (Jackson, 2001a). The SP-RING is a catalytic domain and also Ubc9 interaction motif (Kahyo et al., 2001; Sachdev et al., 2001; Takahashi et al., 2001). The PIAS SUMO ligases possess a short sequence called SXS domain. The SXS sequence is made up of hydrophobic amino acids followed by a string of acidic residues (Minty et al., 2000). This is a SUMO interacting motif that binds to SUMO proteins and it has been proven to be required for proper ligases localisation (Kotaja et al., 2002). The C-terminal domain of the PIAS proteins is the least well-characterised and the most variable between the ligases in this family. It is speculated that various C-terminal ends play a role in substrate specificity (reviewed in (Johnson, 2004)). As mentioned before, the SP-RING of PIAS proteins resembles the one found in the ubiquitin ligases. The major difference between these two classes of proteins lies in number of cysteines found in the catalytic domain (six for ubiquitin ligases and four for Siz/PIAS SUMO ligases) (Jackson, 2001a). Two main members of this family, the *S. cerevisiae* Siz1 and Siz2 proteins SUMOylate cytoskeletal proteins (septins), the replication factor PCNA and the sister chromaitd cohesion protein Pds5 (Hoege et al., 2002; Stead et al., 2003). Neither protein is essential for *S. cerevisiae* viability, nor are the *S. pombe* homologues (Johnson and Gupta, 2001; Takahashi et al., 2001; Takahashi et al., 2003; Xhemalce et al., 2004). The mammalian PIAS family consist of four ligases, PIAS1, 3, x and y (reviewed in (Chung et al., 1997; Shuai, 2000)). PIASx and -y are mainly expressed in testis, suggesting a role in meiosis and sperm production, whereas PIAS1 and PIAS3 are found in all cell types (reviewed in (Chung et al., 1997; Moilanen et al., 1999)).

1.10.2 RanBP2

Another class of SUMO ligase are the homologues of the nuclear pore protein RanBP2/Nup358 (RNA binding protein 2/Nuclear pore complex protein 358). RanBP2 proteins contain a specific E3 domain called the internal repeat domain (IR) which consists of two repeats of 50 amino acids. The IR domain does not share significant similarity with other known E3 ligases (reviewed in (Avis and Clarke, 1996)). The RanBP2 protein localises to the nuclear pore where it is part of a high weight molecular complex that regulates protein transport by SUMOylation (Pichler et al., 2002). RanBP2 SUMOylates RanGap1 (Ran GTPase activating protein 1) protein and this SUMOylation is required for RanGap1 nuclear pore localisation (Matunis et al., 1998; Saitoh et al., 1997). *In vitro* studies revealed that SUMOylation of HDAC4, Sp100 and RanGap1 is enhanced by RanBP2, but only RanGap1 has been confirmed as an *in vivo* substrate thus far (Kirsh et al., 2002; Pichler et al., 2002).

1.10.3 PC2

The third subgroup of SUMO ligases are the polycomb group proteins (PcG). The PcG are nuclear proteins first identified in *D. melanogaster* (reviewed in (Lewis, 1978)). PcG proteins form complexes with histone methylation activity and function in gene silencing through modification of chromatin structure (Kagey et al., 2003). They do so by post translational modification of histone proteins. The PcG SUMO ligases such as Pc2 (polycomb 2 homologue) are part of the nuclear polycomb bodies, where Pc2-mediated SUMOylation is believed to occur. At least two different polycomb-repressive complexes (PCRs) exist in cells, PRC1 and PRC2 (Levine et al., 2004). PRC1/2 bind to DNA and maintain gene expression of genes required for cell differentiation and organism development. The PRCs have been also implicated in embryonic stem (ES) cell self-renewal and pluripotency (Rajasekhar and Begemann, 2007). One of the identified Pc2 substrates is the transcriptional co-repressor CtBP1 (C-terminal binding protein 1), which localises to PcG bodies (Kagey et al., 2003). Recently, two SUMO interacting motifs have been

described in Pc2 protein and one of them (SIM2) is essential for Pc2 autoSUMOylation and modification of CtBP1 (Yang and Sharrocks, 2010).

1.10.4 Nse2/MMS21 SUMO ligase

Mms21/Nse2 is a SUMO ligase and a member of the Siz/PIAS family of proteins (hereafter Nse2). The *Nse2* gene was first identified in *S. cerevisae* (as Mms21) in a screen for DNA damage sensitive mutants (Prakash and Prakash, 1977). It is a small (~30 kDa) globular protein with the SP-RING domain at the C-terminal end (Andrews et al., 2005; McDonald et al., 2003; Pebernard et al., 2004; Potts and Yu, 2005). The N-terminal SAP domain specific for the PIAS proteins required for DNA localisation is absent in the Nse2 protein. However, Nse2 is still targeted to DNA via its interaction with the Smc5-Smc6 complex (Andrews et al., 2005; Lindroos et al., 2006; Potts and Yu, 2005; Zhao and Blobel, 2005). The N-terminal domain (NTD) of the Nse2 SUMO ligase is responsible for interaction with Smc5, allowing the C-terminal SP-RING free access to potential substrates (Figure 1.12) (Duan et al., 2009a; Sergeant et al., 2005). The interaction between Smc5 and Nse2 is mediated by set of non-covalent interactions such as hydrogen bonds, hydrophobic interactions and salt bridges (Duan et al., 2009a). Two distinct helices (P16 to S52 and D60 to A100) in the Nse2 NTD motif have been identified as essential for binding to Smc5 (Duan et al., 2009a). These helices wrap around the Smc5 arms, anchoring the Nse2 protein as shown in Figure 1.15 (Duan et al., 2009a). In contrast to the *Siz1* and *Siz2* genes, *Nse2* is essential for budding and fission yeast viability (Andrews et al., 2005; Zhao and Blobel, 2005). Hypomorphic *Nse2* alleles resulting in SUMO ligase dead forms of Nse2 show sensitivity to a broad range of DNA-damaging agents, including cis-platin, IR, MMS, HU and UV (Andrews et al., 2005; Pebernard et al., 2004; Potts and Yu, 2005; Sergeant et al., 2005; Zhao and Blobel, 2005). Therefore, the SUMO ligase activity of Nse2 is not essential for cell survival but required for DNA damage responses and DNA repair (Andrews et al., 2005). *Nse2* mutations in *S. pombe* are epistatic with $Rhp51^{Rad51}$ in response to IR and UV (Andrews et al., 2005). Surprisingly, the hypomorphic *nse2-21* allele is not epistatic with *Rad18/Smc6* in response to UV and double mutants of *smc6* and *nse2* show greater growth retardation than either single

mutant, suggesting the existence of some non-overlapping functions of Nse2 and Smc6 (Andrews et al., 2005; Chavez et al., 2010b). Similarly to *smc6-9* mutants, *mms21-sp* cells accumulate X-shaped molecules and chromosomal linkages after DNA damage (Bermúdez-López et al., 2010; Branzei et al., 2006; Chavez et al., 2010a).

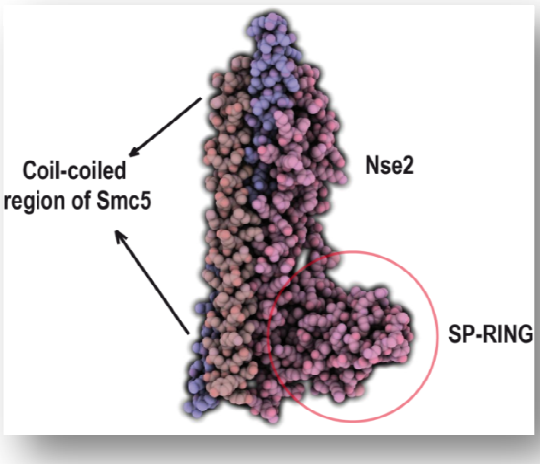

Figure 1.15 Crystal structures of the Nse2 protein and Smc5 coiled-coil region.
Graphical representation of the crystal structure of the coiled-coil region of S. cerevisiae Smc5 and Nse2 (Duan et al., 2009a).

As mentioned earlier, siRNA-mediated depletion of Nse2 in HeLa cells results in increased gene targeting and decreased sister chromatid exchanges. The same group found that cohesin recruitment to *I-SceI* induced DSB was impeded in the cells lacking Nse2 (Potts et al., 2006), suggesting that cohesin may be regulated through Nse2-dependent SUMOylation. This is indeed the case in human cells where the Scc1 subunit of cohesion is modified by Nse2 (Potts et al., 2006). A different group observed a severe loss of metaphase sister chromatid cohesion after siRNA-mediated depletion of Smc5 and Nse2 but not Smc6. This surprising observation led to the detection of two distinct complexes containing Nse2-Smc5-Smc6 in interphase and Nse2-Smc5 in mitosis (Behlke-Steinert et al., 2009). These data suggest the existence of two separate complexes (Smc5-Smc6-Nse2 and Smc5-Nse2) with potentially distinct functions in DNA metabolism. Additionally, two different complexes have been described by Hazbun et al. in budding yeast (Hazbun et al., 2003).

Nse2 SUMO ligase has been also implicated in telomere maintenance. In the *S. cerevisiae mms21-sp* mutants an increased rate of senescence has been observed (Chavez et al., 2010b). In human cells, Nse2-dependent SUMOylation of the telomere sheltering proteins Trf1, Trf2, Tin1 and Rap1 is required for telomere integrity and extension through the ALT process (Potts and Yu, 2007). Depletion of the Nse2 SUMO ligase activity in budding and fission yeast causes fragmentation of nucleoli and an increased number of repair foci in this nuclear organelle, confirming a function for Nse2 in the maintenance of repetitive DNA sequences (Torres-Rosell et al., 2005a; Torres-Rosell et al., 2007; Zhao and Blobel, 2005).

Other known substrates of Nse2 SUMO ligase are listed in Table 1.1 Nse3, Nse4, Smc5, Smc6 and Nse2 itself are SUMOylated by Nse2 (Andrews et al., 2005; Potts et al., 2006; Zhao and Blobel, 2005). Modification of multiple subunits of the Smc5-Smc6 complex by Nse2 indicates a potential role in the regulation of the activity of the complex. It is possible that SUMO-interacting motifs are present within the sequence of Smc5-Smc6 complex subunits, but their existence awaits discovery. Zhao and Blobel showed that the NHEJ protein Ku70 is also modified by Nse2, indicating a multiple roles in the DNA damage response of the Smc5-Smc6 complex-associated SUMO ligase (Zhao and Blobel, 2005).

Table 1.1 Nse2 substrates.

Protein	Organism	Function	Reference
Ku70	*S. cerevisiae*	NHEJ	(Zhao and Blobel, 2005)
Nse2	*H. sapiens, S. cerevisiae* and *S. pombe*	HR	(Andrews et al., 2005; Potts et al., 2006; Zhao and Blobel, 2005)
Nse3	*S. pombe*	HR	(Andrews et al., 2005)
Nse4	*S. pombe*	HR	(Pebernard et al., 2008c)
Rap1	*H. sapiens*	Telomere maintenance	(Potts and Yu, 2007)
SA2	*H. sapiens*	Sister chromatid cohesion	(Potts et al., 2006)
Scc1	*H. sapiens*	Sister chromatid	(Potts et al., 2006)

		cohesion	
Smc5	*S. cerevisiae*	HR	(Zhao and Blobel, 2005)
Smc6	*H. sapiens* and *S. pombe*	HR	(Andrews et al., 2005; Potts et al., 2006)
Tin2	*H. sapiens*	Telomere maintenance	(Potts and Yu, 2007)
Trax	*H. sapiens*	Unknown	(Potts and Yu, 2005)
Trf1	*H. sapiens*	Telomere maintenance	(Potts and Yu, 2007)
Trf2	*H. sapiens*	Telomere maintenance	(Potts and Yu, 2007)

1.11 SUMOylation in DNA repair

As previously mentioned, protein SUMOylation can lead to significant changes in protein biochemical properties (section 1.8). It has been well established that many proteins in the DNA damage response are modified by SUMOylation **(**reviewed in (Jackson and Bartek, 2009)). During DNA synthesis, the DNA polymerase occasionally encounters a lesion which can be by-passed by the activity of Y-family DNA polymerases (reviewed in (Ho and Schärer, 2010)). In this process, a polymerase switch has to occur in order to continue DNA replication over the lesion. The heterotrimeric PCNA sliding clamp is required for maintenance of polymerase fidelity. The PCNA sliding clamp is a heterotrimeric protein that binds different polymerases (reviewed in (Hubscher, 2009)). SUMO modification of PCNA is required for error-free DNA translesion synthesis pathway (TLS). PCNA ubiquitinylation on K164 is essential for for that process (Vanoli et al., 2010). Steller and co-workers showed that SUMOylation competes with ubiquitylation for modification of that site. SUMOylation at the PCNA K164 residue prevents unwanted TLS and inhibits mutagenesis (Stelter and Ulrich, 2003). In addition, SUMOylation of K164 leads to recruitment of the Srs2 helicase through its SUMO interacing motif (SIM). Notably, Srs2 helicase binds SUMOylated PCNA with a higher affinity than unmodified PCNA. The active Srs2 helicase is able to remove filaments of Rad51 protein from chromatin, leading to inhibition of recombination (Pfander et

al., 2005). Another lysine 127, located at the PIP-box, the main PCNA interacting domain, can also be modified by SUMO attachment (Moldovan et al., 2007). PCNA modification at K127 abrogates binding of Eco1 acetyl transferase required for cohesin recruitment to newly-synthesised DNA and sister chromaitd cohesion establishment (Moldovan et al., 2006).

Another example comes from studies on the base excision repair protein TDG. TDG is a DNA glycosylase that removes thymine or uracil bases from T-G or U-G mismatches, producing an AP site (Hardeland et al., 2002). TDG shows high binding affinity to damaged DNA. After removal of the lesion, TDG has to be dissociated from DNA in order to allow access of downstream BER factors to the AP site. This is stimulated by the downstream enzyme APE1 and SUMO modification of the TDG protein by an as-yet unidentified E3 ligase (Hardeland et al., 2002). Interestingly the TDG protein contains the SIM motif which binds to SUMO peptide upon TDG SUMOylation, forming an intra-molecular bridge. This radically changes the conformation of the TDG protein and affects TDG affinity to DNA. Later SUMO peptide is cleaved off, allowing TDG to participate in the next cycle of DNA repair.

SUMOylation is also required for proper repair of DSBs. The SUMO modification of many targets including BRCA1 and RNF8/UBC13 proteins is essential for this DNA repair pathway (Galanty et al., 2009). Two SUMO ligases, PIAS1 and PIAS4, localise to the DSB and PIAS4 is required for modification of the RNF8/UBC13 ubiquitin ligase (Morris et al., 2009). This stimulates recruitment of BRCA1 and RNF168 to the DSB (Galanty et al., 2009; Morris et al., 2009). Additionally, PIAS1 is responsible for BRCA1 SUMOylation *in vivo* (Galanty et al., 2009). These results indicate that SUMOylation enhances ubiquitin ligase activity of the BRCA1 and RNF8 proteins. With the new technologies used to study protein modifications, many novel substrates of SUMO pathway will be identified in the near future, permitting improved understanding of the function of this elusive protein PTM.

1.12 Gene targeting

Gene targeting is defined as the controlled and artificial introduction of a specific DNA sequence into a desired position in the genome of a cell (reviewed in (Hudson et al., 2002)). Gene targeting is a designed modification of a cell allowing for introduction of a desirable change in cell's genotype. It has been successfully used to genetically modify plants to obtain abundant harvests and protect them from environmental conditions. For decades, gene targeting has been used to study mouse genetics. This has allowed understanding of different cellular mechanisms involved in pathologies and diseases. Additionally, gene targeting in mouse has led to the development of human disease models, facilitating their analysis and drug development. Gene targeting is also used in reverse genetics, a method which allows the study of gene functions by their mutation or disruption and analysis of this gene product deficit on the biological system of interest. Reverse genetics has become routine for analysis of vertebrate genes. Many strategies have been developed for gene targeting in order to study gene functions in various systems, including bacteria, yeast, mouse, hamster, pig, chicken, plants and humans (Capecchi, 1989; Cost et al., 2010; Geurts et al., 2009; Liu et al., 2010; Rémy et al., 2010; Watanabe et al., 2010).

1.12.1 Gene disruption in vertebrate cells

Extensive knowledge of the gene of interest is the most important information required to design a targeting strategy. To disrupt or introduce mutation(s) in the specific gene, a set of targeting vectors is generated. The targeted region can be the whole coding sequence, domains essential for protein function or single nucleotides. Each targeting vector must contain at least one homology arm (two are recommended) and a selective marker (Figure 1.13A). The homology arm(s) specify the targeted region and marker which allows for subsequent isolation of cells containing the desire mutation.

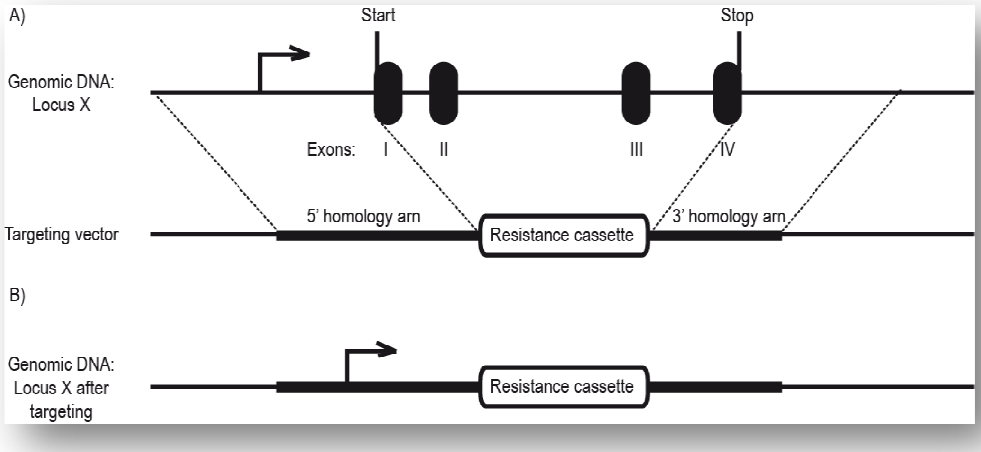

Figure 1.16 General strategy for gene disruption.

A) Alignment of gene X locus with a targeting vector showing a disrupted region between the two homology arms. B) Genomic locus X after targeting event showing replacement of gene X exon and intron sequences by the resistance cassette from the targeting vector.

To study the function of vertebrate genes mouse and chicken model systems are widely used. In the mouse model, the targeting vector with the mutation(s) is first introduced into embryonic stem (ES) cells by electroporation or microinjection. Then, the clones positive for the selective marker are screened in search for a designed mutation. The majority of the cells that take up the foreign DNA will randomly insert this sequence into their genome. In a small population of the cells the arms of the targeting vector will pair with homologous sequence in the genome and transfer the mutation by homologous recombination. After identification of the cell clones in which the targeting event has occurred successfully, the cells are grown and later injected *in vitro* into the blastocoel cavity of a pre-implantation mouse embryo. The resulting blastocyst is then transferred into mouse uterus and allowed to develop. The result of such manipulation is a mouse chimera which carries modified genes from the donor stem cells and host blastocyst (Capecchi, 1989). In the last steps the mouse chimeras are first bred with wild-type animals to give heterozygote progeny (+/- for desired mutation). The +/- animals are bred together and the progeny of such crosses are screened to search for the designed mutation in both alleles of interest. Phenotypes of the knockout mice are then analysed and the functions of the gene under study can be defined. This technique has allowed the

determination of the role of many genes involved in cellular functions. Mouse knockout technology paved the way to establish animal models for studying human diseases such as different types of cancer, skin disorders, bone marrow and metabolic pathologies, muscular dysthrophies, immunodeficiencies and others (reviewed in (Bedell et al., 1997)).

The chicken system mentioned earlier is also useful to study vertebrate gene function. Chicken DT40 cells are a transformed B lymphoblast cell line originally derived from an avian leukosis virus (ALV)-induced bursal lymphoma (Baba et al., 1985; Baba and Humphries, 1984). Characteristics of DT40 cells include cell surface IgM, increased expression of *c-myc* and continuous Ig light chain gene conversion (Baba et al., 1985). Studies in DT40 allowed for understanding mechanisms of gene conversion and vertebrate DNA repair (Kim et al., 1990; Morrison and Takeda, 2000). Whereas in human cell lines, the average ratio of random DNA integration to targeted integration is between 1:10000 – 1:100000, in the DT40 cells it is between 1:100 -1:1000 (Buerstedde and Takeda, 1991). As in the mouse model, chicken DT40 cells are transfected with targeting vectors designed for the locus of interest. Heterozygotes and later homozygotes are selected and screened for the desired mutation. Multiple knockout clones can be obtained and easily analysed using the DT40 model.

Gene disruption has also been reported in humans, rat, hamster and pig cells (Dai et al., 2002; Kragh et al., 2009; Lai et al., 2001; Rogers et al., 2008). Recently, new technology based on DNA sequence specific zinc-finger nucleases has been developed and successfully used to target rat, pig and hamster genes (Geurts et al., 2009; Mashimo et al., 2010; Watanabe et al., 2010).

1.12.2 Mechanism of gene disruption

The mechanism of gene disruption by homologous recombination has been extensively studied in mouse embryonic stem cells (Capecchi, 1989). Gene targeting by homologous recombination requires active replication as shown by experiments with synchronised cells. Cells transfected during S phase had the highest gene targeting frequencies (Wong and Capecchi, 1986). Additionally, linear DNA molecules are the most favourable substrates for efficient gene targeting (Thomas and Capecchi, 1986). Correlation between the size of

homology arms and number of positive clones has been also reported. Targeting vectors with arm sizes between 10-14 kb had the highest frequencies observed in these experiments (Capecchi, 1989). In one of the models proposed for a gene targeting mechanism, the linearised targeting vector is first processed at 5' ends to expose single stranded DNA. These 3' overhangs then invade the homologous sequence on the chromosome through RPA- and Rad51-dependent reactions. In the last steps the heteroduplex between episomal and genomic DNA is resolved and the original sequence is removed leaving the synthetic sequence behind (Niedernhofer et al., 2001).

In the novel zinc-finger nucleases (ZNFs) technology, artificial chimeras between the DNA binding zinc-finger proteins and unspecific DNA endonucleases such as an isolated active site of the *FokI* restriction enzyme are used (Rémy et al., 2010). The DNA binding part of the ZNF can be carefully designed to recognise a specific DNA sequence. The zinc-finger domain then binds to sequence of interest and brings the nuclease into close proximity to the DNA. This results in the cleavage of the desired DNA sequence. The double strand break induced this way has to be repaired. The cleavage of the sequence is then induced again and again. Inevitably, this cycle leads to loss of the genetic information at the desired site due to eventual local failure in DNA repair. This may cause loss of gene function and result in a null phenotype for the desired gene (Cost et al., 2010; Liu et al., 2010; Santiago et al., 2008).

1.12.3 Alternative methods for gene ablation

In models where low frequencies of gene targeting prevent the analysis of the gene of interest, several alternative methods have been applied. The recently-developed technology of small interfering (siRNA) and short hairpin RNA (shRNA) allows for gene ablation in different cell types (Clemens et al., 2000; Fire, 1999). siRNA depends on the delivery of short RNA sequences of 19 complementary bp with 2-nucleotide 3' overhangs. These are transfected into cells and one strand of the siRNA is bound by the multi-subunit ribonucleoprotein complex (RISC). This RISC complex is then targeted to the complementary mRNA, resulting in mRNA degradation by RNAase or RNA-dependent RNA polymerase mechanisms (Harborth et al., 2001). This leads to

down-regulation of target gene expression and subsequently reduction of protein levels (termed as a knock down rather than knockout).

Short hairpin RNA technology allows for more stable, controlled and continuous gene ablation (Cao et al., 2005; Harper and Davidson, 2005; McIntyre and Fanning, 2006; Paddison et al., 2002). In this method, interfering RNA is expressed from a chromosomally-integrated episome which is delivered to the cell by transfection or viral particles. The expressed hairpin RNA (50-70 bp in length and partially double stranded) is cleaved by Dicer to expose a single stranded RNA sequence complementary to the target mRNA. The heteroduplex between the target mRNA and silencing RNA is then degraded. The main advantages of shRNA are that there is no need for repeated RNA delivery to the cell and the possibility of its controlled expression.

Some other methods based on the interfering RNA, such as small internally segmented RNAs (sisiRNAs) and RNA-DNA chimeras have been recently developed (reviewed in (Sibley et al., 2010)). In the sisiRNA method the 22 nucleotide sense sequence of siRNA is segmented into two smaller sequences. These two parts are held together by specific modifications of the nucleic acids. Further, optimisation revealed that sisiRNA has decreased off-target silencing compared to regular RNAi methods (Bramsen et al., 2007). DNA-RNA chimeras were primarily developed to reduce off-target silencing. In this approach, parts of the dsRNA duplex were substituted with deoxyribonucleotides (at their 5’ end). This affects the interaction of RISC with off-target mRNA, thus reducing degradation of non-specific transcripts. Gene silencing with this method proceeds through a mechanism identical with the original siRNA (Ui-Tei et al., 2008).

1.12.4 Disruption of essential genes

Disruption of essential genes is a more problematic challenge. Targeting of these genes is not achievable using standard gene targeting approaches as the cells cannot proliferate in the absence of such genes. Specific methods known as conditional knockout strategies have been developed in order to study the function of essential genes. These include systems, such as expression of switchable transgene (TetOFF), transgene removal by Cre/loxP and FLP/frt mediated recombination or auxin-mediated protein degradation (Gossen and

Bujard, 1992; Gu et al., 1993; Nishimura et al., 2009). The basic principle of conditional gene targeting is to first introduce a transgene encoding the gene of interest whose expression or activity can be shut down on demand. Then the endogenous gene sequence is targeted in the transgene-expressing background. After gene targeting, the essential transgene or activity of the protein it encodes can be inactivated and the null phenotype analysed.

The Tet system is a tetracycline operator based method in which transgene expression is dependent on an inducible transcriptional activator (Baron and Bujard, 2000; Gossen and Bujard, 1992). In the TetOFF variant, the tetracycline controlled transactivator (tTA) regulates expression of the gene that is under transcriptional control of a tetracycline-responsive promoter element (TRE). The tTA is a fusion protein of a tet repressor DNA binding protein and VP16 activation domain. The tetracycline (Tc) or doxycycline (Dox) deactivates the tTA protein which no longer binds to the TRE element and transactivates target gene expression. The main disadvantage of the TetOFF is the extensive timing required for gene shutdown.

In a second system, site-specific bacterial or yeast recombinases are used (Dymecki, 1996; Gu et al., 1993; Marino et al., 2000; Vooijs et al., 1998). The Cre and FLP recombinases recognise and excise DNA sequences flanked by LoxP and Frt sites, respectively. After successful expression of the transgene flanked by these sequences, targeting of the gene of interest is performed. The transgene sequence is removed by transient or inducible expression of the site specific recombinase. The disadvantage of this system is a lack of homogenity of the population after expression of the recombinase and lack of control over its activity. This often results in a mixed population of the cells with or without the transgene at a particular time after transfection or induction of recombinase expression. Additional screening steps may be required to obtain pure clones which may be difficult after deletion of the essential gene.

The auxin degron system allows the rapid depletion of a protein of interest after addition of a plant hormone auxin or its derivatives (Nishimura et al., 2009). The coding seguence of the gene of interest can be fused with an auxin inducible degron (AID) sequence either on an episome or endogenously (single or both alleles). Expression of the fusion protein can be easily confirmed with

AID specific antibodies. After targeting of the genomic sequence that encodes the protein of interest, the transgene product can be then degraded after addition of small heterocyclic acid (indole-3-acetic acid or derivatives). In the presence of auxin the AID tag is poly-ubiqitylated and recognised by SCF complexes which target the fusion protein for proteasomal mediated degradation. A huge advantage of this system is a very rapid response to auxin treatment, which induces protein depletion within minutes. Successful degradation has been confirmed for yeast, chicken and human proteins (Nishimura et al., 2009). The main disadvantage of this system is the relatively big size of the AID tag which may interfere with the essential functions of the protein under study.

1.13 Aims of this study

The functions of the cohesin (Smc1-Smc3) and condensin (Smc2-Smc4) complexes are well described. The cellular roles of Smc5-Smc6 complex and its mechanism of action are not fully understood. Moreover, most of the data on the Smc5-Smc6 complex were derived from work in yeast cells. Therefore, the main aim and focus of this study was to establish the cellular roles and functions of vertebrate Nse2 protein in the cell cycle and in response to DNA damage.

We identified the chicken *Nse2* orthologue and cloned its cDNA. We then generated an Nse2-deficient chicken cell line and analysed the phenotype associated with Nse2 defficiency in DT40 cells. We found that the loss of Nse2 results in DNA repair defects. We also investigated the biochemical properties of Nse2 by its expression in Nse2-deficient cells as different fusion proteins. This allowed us to confirm that chicken Nse2 is a component of a Smc5-Smc6 complex through interaction with Smc5 and that Nse2 is a protein with both cytoplasmic and nuclear localisation. We also found that re-introduction of wild-type but not SUMO ligase dead form of Nse2 in *Nse2*$^{-/-}$ cells rescued the observed phenotype, indicating that the enzymatic activity of Nse2 is essential for its DNA repair functions.

In addition, we attempted to define the functional relationships between Nse2 and its partner Smc5 protein. We carried out epistasis analysis by disruption of *Smc5* in Nse2-deficient cells. Investigation of the phenotype of doubly targeted clones allowed us to dissect the roles of Smc5-Smc6 complex components and suggested that distinct Smc5-Smc6 sub-complexes may exist in vertebrate cells.

Chapter 2 Materials and methods

2.1 Materials

2.1.1 Chemical Reagents

Chemicals used throughout this study were of analytical grade and were purchased from Sigma (Arklow, Ireland), BDH (Hertfordshire, UK), Fisher (Leiceistershire, UK) or GE Healthcare (Bucks, UK). EdU (5-ethynyl-2'-deoxyuridine) and 6-carboxyfluorescein-TEG azide were purchased from Berry & Associates (Dexter, USA). All solutions were prepared using ddH_2O or Milli-Q purified water Millipore (Billerica, USA) and, where appropriate, were autoclaved prior to use. Organic solvents, alcohols and acids were supplied by Sigma (Arklow, Ireland), VWR (Bridgeport, USA) or Fisher (Leiceistershire, UK). Radioisotope (α-^{32}P-dCTP) was supplied by ICN (Asse-Relengen, Belgium); oligodeoxynucleotide primers were purchased from Sigma (Arklow, Ireland). Solutions used for RNA work were treated with 0.1% diethyl pyrocarbonate (DEPC), supplied by Sigma (Arklow, Ireland). RNA was prepared from tissue culture cells using TRIzol (Total RNA Isolation Reagent) obtained from Invitrogen (Carlsbad, USA).

All common reagents and buffers used throughout this study are presented in the Table 2.1 (listed in alphabetical order).

Table 2.1 Common reagents and buffers

Name	Composition	Notes and references
3 X SDS-PAGE Sample Buffer (3xsb)	150mM Tris pH 6.8, 45% sucrose, 6mM K-EDTA pH 7.4, 9% SDS, 0.03% bromophenol blue 10 % β-mercaptoethanol	For denaturation and loading of proteins prior to SDS-PAGE
6 X DNA Loading Dye	20% sucrose, 0.1M EDTA pH 8.0, 1% SDS, 0.25% bromophenol blue, 0.25% xylene cyanol.	For DNA sample loading prior to running agarose gel
Aprotinin	1000 x stock solution	Protease inhibitor

Aqueous Coomassie Blue	0.1% Coomassie, 25 mM Tris, 250 mM glycine	For staining preparative protein gels
Calenoa Solution	Methanol : Acetic acid (3 : 1)	For cell fixation in chromosome spreads preparation
Church Hybe Buffer	0.5M NaPi, 7% SDS	For Southern blot hybridisation
Church Wash Buffer	40mM NaPi, 1% SDS	For Southern blot washes
CLAP	1000 x stock solution of Chymostatin, Leupeptin, Antipain, Pepstatin A	Protease inhibitors, each 1 mg/ml in DMSO
Click Reaction Mix	10 mM ascorbic acid, 0.1 mM 6-carboxyfluoroscein-TEG azide, 2 mM $CuSO_4$ - added in the order indicated	For labeling of S-phase cells
Coomassie Brilliant Blue R	0.5% Coomassie in 35% Methanol, 14% acetic acid	For SDS-PAGE analysis
Cross-Linking Solution	20mM dimethyl pimelimidate dihydrochloride (DMP) in 200mM Hepes pH 8.5	For cross-linking of antibodies or fusion tagged proteins to agarose beads
Cytoskeleton Buffer	137mM NaCl, 5mM KCl, 1.1mM Na_2HPO_4, 0.4mM KH_2PO_4, 2mM $MgCl_2$, 2mM EGTA, 5mM PIPES, 5.5mM glucose, pH 6.1 and filter sterilised	For immunofluorescence microscopy
Destain Solution	30% methanol, 10% acetic acid	To destain Coomassie gels
Detection Buffer	100 mM Tris pH 9.5, 100 mM NaCl	For detection of DIG labeled probes
Fixation Solution	4% methanol, 1% glycerol	To dry Coomassie gels
Giemsa Stain	3% Giemsa in Phosphate Buffer pH 6.8	For staining of chromosome spreads
Glycine Elution Buffer	200 mM Glycine-HCl pH 2.0, 150mM NaCl	For elution of affinity purified antibodies
GST Binding Buffer	50 mM HEPES pH 7.5, 150 mM NaCl, 2 mM EDTA	For binding of GST-tagged proteins
High Stringency Buffer	0.5 x SSC, 0.1% SDS	For membrane washes in non-radioactive Southern blot
HIS-Tag Buffer	8 M Urea, 10 mM Tris, 100 mM sodium phosphate buffer pH 8.0, 0.1% Triton X-100, 10 mM imidazole 5 mM β-mercaptoethanol	For purification of His tagged fusion proteins

Immunoprecipitation Buffer	50 mM HEPES pH 7.3, 150 mM NaCl, 2 mM EDTA, 0.5% NP-40, 10% Glycerol	For immunoprecipitation of endogenous and tagged proteins
LB (Luria-Bertani Medium)	1% tryptone, 0.5% yeast extract, 1% NaCl, pH adjusted to 7.0 with 4M NaOH	To grow bacterial cultures
Low Stringency Buffer	2 x SSC, 0.1% SDS	For membrane washes in non-radioactive Southern blot
Lysis Buffer 1	50 mM Tris pH 7.5, 150 mM NaCl, 1% Triton X-100	For whole cell lysate preparation and analysis by SDS-PAGE
Lysis Buffer 2	10mM Tris pH 7.5, 0.1% Triton X-100	To lyse cells for protein analysis by SDS-PAGE
Macllvane Solution	164 mM Na_2HPO_4, 16 mM citric acid pH 7.0	For washes in sister chromatid exchange preparations
Maleic Acid Washing Buffer	100 mM Maleic acid pH 7.5, 150 mM NaCl, 0.3% Tween 20	For membrane washes in non-radioactive Southern blot
Hot Southern Blot Washing Buffer (NaPi)	1M $Na_2HPO_4 \bullet H_2O$ pH 7.2	1M stock for Southern blot Buffers
Non-Radioactive Southern Blot Blocking Solution	10 % Caseine in Maleic Acid Wash Buffer	For blocking of Southern blot membranes
PBS	Phosphate buffered saline	Made up to 100 x stock solution with tablets (Sigma)
Phosphate Buffer pH 6.8	11.5 mM Na_2HPO_4, 15.7 mM KH_2PO_4 pH 6.8	For chromosome spreads staining
PMSF	Protease inhibitor, 250mM in ethanol	1000 x stock solution
Ponceau S. Solution	0.5% Ponceau S, 5% acetic acid	To stain proteins on the nitrocellulose membrane
Running Buffer	25mM Tris, 250mM glycine, 0.1% SDS	For running SDS-PAGE gels
Semi Dry Transfer Buffer	25 mM Tris pH 8.5, 0.2 M glycine, 20% methanol	For semi dry transfer
SSC	1.5M NaCl, 0.15M sodium citrate, pH adjust to 7.0 with citric acid	10 x stock, for transfer of gels to nylon membrane
Super Broth	0.5% tryptone, 2% yeast extract, 0.5% NaCl, pH adjust to 7.5 with 4M NaOH	To grow bacterial cultures

TAE	40mM Tris-acetate pH8.0, 1mM EDTA	To run agarose gels
Tail Buffer	50mM Tris pH 8.8, 100mM EDTA, 100mM NaCl, 1% SDS	For the preparation of genomic DNA
TBS	20mM Tris pH 7.5, 150mM NaCl	For affinity purification of antibodies
Tfb I	30mM Potassium Acetate, 100mM $RbCl_2$, 10mM $CaCl_2$, 50mM $MnCl_2$, 15% glycerol; pH adjust to 5.8 with 50% HCl, filter sterilise and store at 4^oC.	For the preparation of chemically competent *E. coli*
Tfb II	10mM MOPS, 75mM $CaCl_2$, 10mM $RbCl_2$, 15% glycerol, pH adjust to 6.5 with KOH, filter sterilise and store at 4^oC.	For the preparation of chemically competent *E. coli*
Transfer Buffer	72mM Tris, 58.5mM glycine, 15% methanol, 0.1% SDS	For wet transfer of SDS-PAGE onto nitrocellulose membranes

2.1.2 Molecular biology reagents

All biological reagents employed in DNA digestion and cloning reactions, such as restriction enzymes, DNA polymerase (Klenow Fragment I), DNA ligase, were obtained from New England Biolabs (Ipswich, USA). The DNA polymerases TaKaRa LA Taq, KOD and SigmaTaq used in PCR were purchased from Takara Shizo Co, Ltd. (Osaka, Japan), Novagen (Darmstadt, Germany) and Sigma (Arklow, Ireland), respectively. Shrimp Alkaline Phosphatase (SAP) was from USB (Cleveland, USA). DNA and protein size markers were supplied by New England Biolabs (Ipswich, USA), Fermentas (Glen Burnie, USA) or BioRad (Hercules, USA).

Molecular biology kits used throughout this study are listed in Table 2.2

Table 2.2 Molecular biology kits used

Name	Use	Source
GenElute™ Plasmid Miniprep Kit	Small scale plasmid DNA extraction	Sigma (Arklow, Ireland)
Midi/Maxi Prep Kit (Endotoxin-free)	Large scale plasmid DNA extraction	Qiagen (Crawley, UK)
QIAquick Gel Extraction Kit	Extraction and purification of DNA Fragments from the agarose gel	Qiagen (Crawley, UK)
Superscript First-Strand Synthesis for RT-PCR kit	cDNA synthesis	Invitrogen (Carlsbad, USA)
Megaprime DNA Labelling kit	Radiolabeling of probes used in Southern blot hybridisation	GE Healthcare (Bucks, UK)
SUMOylation Kit	For sumoylation of proteins	ENZO Life Scienes (Exeter, UK)

Four *E. coli* strains were used during the course of the work described in this thesis. The genotypes of these strains are listed in Table 2.3.

Table 2.3 Genotype of E. coli strains used

Strain	Genotype	Use
Top 10	F$^-$ *mcrA*Δ*(mrr-hsdRNS-mcrBC) ϕ80lacZΔM15* Δ*lacX74deoR recA1 araD139* Δ*(ara-leu)7697 galU galK rpsL(Str^R) endA1 nupG*	General cloning
SURE	*endA1 glnV44 thi-1 gyrA96 relA1 lac recB recJ sbcC umuC::Tn5 uvrC e14- Δ(mcrCB-hsdSMR-mrr)171 F'[proAB$^+$ lacI^q lacZΔM15 Tn10]*	Expression of recombinant fusion proteins
BL21(DE3)pLysS	F$^-$ *ompT hsdS*$_B$(r_B^- m_B^-) *gal dcm* (DE3) pLysS (Cam^R)	Expression of recombinant fusion proteins
BL21 pRIL	*E. coli* B F– *ompT hsdS(rB– mB–) dcm+* Tetr *gal λ(DE3) endA* Hte *[argU ileY leuW Camr]*	Expression of recombinant fusion proteins

A number of commercially available cloning and expression plasmids were used during the course of this project, as shown in Table 2.4.

Table 2.4 Commercial plasmids used in this study

Plasmid name	Use	Source
pGEMT-Easy	General cloning	Promega (Southampton, UK)
pBlueScript(SK)		Stratagene (La Jolla, USA)
pEGFP-C1/N1	Expression in mammalian cells	Clontech[1] (Palo Alto, USA)
pcDNA3.1(+)		Invitrogen (Carlsbad, USA)
pCMV-3TAG-2A/B/C	Expression in bacterial cells	Stratagene (La Jolla, CA)
pRSET-A/B/C	Expression in bacterial cells	Invitrogen (Carlsbad, USA)
pGEX4T-1/2/3	Expression in bacterial cells	Amersham (GE Healthcare, Bucks, UK)

Antibodies (Table 2.5) used throughout this study were mainly applied in western blot immunodetection (IB) and immunofluorescence microscopy (IF). Tables 2.5 and 2.6 show working dilutions along with the source of the particular antibodies.

Table 2.5 Primary antibodies used in this study

Antigen	Host	Working dilution for IF	Working dilution for IB	References
EGFP (11 814460 001)	Mouse monoclonal	N/D	1:500	Roche (Mannheim, Germany)
Hutingtin interacting protein 2, anti-human (HIP2, ab 37917)	Goat polyclonal	N/D	1:1000	Abcam (Cambridge, UK)
MCM2 pSer40/41	Rabbit polyclonal	N/D	1:1000	Gift from Prof. Corrado Santocanale
Myc, anti-human (9E10)	Mouse monoclonal	1:2000	1:10,000	Charles River Laboratories, (Wilmington, USA)
Nse2, anti-chicken	Rabbit polyclonal		1:250	This study

[1] recently purchased by Takara Bio Company

(SIE009AP)				
Rad51, anti-human (PC130)	Rabbit polyclonal	1:500	1:200	Novagen (Darmstadt, Germany)
RanGap1, anti-human (N-19)	Goat polyclonal	N/D	1:500	Santa Cruz Biotechnology **(**Santa Cruz, USA)
Scc1, anti-chicken (2110 final bleed)	Rabbit polyclonal	N/D	1:500	Dr. Ciaran Morrison (unpublished)
Septin 6, anti-human (SEPT 6, 1D6)	Mouse monoclonal	N/D	1:1000	Sigma
Set oncogene, anti-human (SET, ab 92872)	Rabbit polyclonal	N/D	1:1000	Abcam (Cambridge, UK)
Smc1, anti-chicken (8232 3rd bleed)	Rabbit polyclonal	N/D	1:250	(Stephan et al., 2011a)
Smc5, anti-chicken (C9057AP)	Rabbit polyclonal	N/D	1:100	(Stephan et al., 2011a)
Smc5, anti-human (Serum EQ)	Rabbit polyclonal	N/D	1:1000	Prof. Alan Lehman (Taylor et al., 2001)
Smc6, anti-human (DR1031)	Rabbit polyclonal	N/D	1:1000	Calbiochem
Smc6, anti-human (Serum Ma)	Rabbit polyclonal	N/D	1:1000	Prof. Alan Lehman (Taylor *et al.*, 2001)
Sortin nexin 3, anti-human (SNX3 C-16)	Goat polyclonal	N/D	1:500	Santa Cruz Biotechnology
SUMO-1, anti-human (FL-101)	Rabbit polyclonal	N/D	1:500	Santa Cruz Biotechnology (Santa Cruz, USA)
β–actin, anti-human (A2066)	Rabbit polyclonal	1:2000	1:10000	Sigma
γ-H2AX, anti-human (JBW301)	Mouse monoclonal	1:1000	1:1000	Upstate[2]
γ-tubulin, anti-human (GTU88)	Mouse monoclonal	1:100	N/D	Sigma

[2] recently purchased by Millipore

Table 2.6 Secondary antibodies used in this study

Antigen	Host	Working dilution for IF	Working dilution for IB	References
Alexa, Texas Red and FITC (fluorescein isothiocyanate) conjugated Affini Pure F(ab')2 fragment, anti-mouse and anti-rabbit IgG (H+L)	Goat poyclonal	1:200	-	Jackson Labs (Bar Harbor, USA)
HRP (horseradish peroxides)-conjugated Affini Pure, anti-mouse and anti-rabbit IgG (H+L) secondary antibodies for ECL	Goat polyclonal	N/D	1:10000	Jackson Labs (Bar Harbor, USA)
Digoxigenin (1.71.256)	Mouse monoclonal	N/D	1:10000	Roche (Mainnheim, Germany)

2.1.3 Tissue culture reagents and cell lines

All sterile plasticware used for tissue culturing was obtained from Sarstedt (Numbrecht, Germany), Corning (Riverfront Plaza, NY) and Sigma. For transient transfection of chicken DT40 cells the Amaxa (Gaithersburg, MD) nucleofector (programme B-23) was used. Transfections for the generation of stable chicken cell lines were carried out with the Gene pulser apparatus from Bio-Rad (Hercules, CA). Cells were frozen down for both -80^{o}C and liquid nitrogen storage in FBS with 10% DMSO. Roswell Park Memorial Institute media (RPMI) 1640 was from Lonza (Cambridge, UK). Different drugs at varying concentrations were used as selection markers in the generation of stable chicken cell lines, as listed in Table 2.7.

Table 2.7 Drugs used for stable cell line selection

Name of the drug	Final concentration
Blasticidin	25 μg/ml
Geneticin (Invitrogen)	2 mg/ml
G418 (Invivogen)	2 mg/ml
Histidinol	1 mg/ml
Hygromycin	1.5 mg/ml
Puromycin	0.5 μg/ml

This study was performed on the chicken DT40 cell line. Specific culturing conditions used are given in the Table 2.8.

Table 2.8 Cell types and growth conditions

Cell Type	Description	Source	Culture Medium	Culture Conditions
Wild-type DT40	Chicken, B-cell lymphoma	Dr. Ciaran Morrison	RMPI-1640, 10% FBS, 1% chicken serum	39.5^{o}C, 5% CO_2

In clonogenic survival assays, semi-solid methylcellulose medium was used, composed of 1.5% methylcellulose (Sigma, Arklow, Ireland), 1 x Dulbecco's Modified Eagle Medium (DMEM)/F-12, L-glutamine(+) (Invitrogen), 15% FCS, 1.5% chicken serum, 1% penicillin/streptomycin and 50 μM ß-mercaptoethanol.

Different drugs that were used for pharmacological treatment of DT40 cells can be found in Table 2.9.

Table 2.9 Drugs used in this study

Drug	Concentration	Application	Source
Colcemid	0.1 μg/ml	Reversible activation of spindle assembly checkpoint (metaphase arrest)	Sigma
Nocodazole	100 μg/ml	Reversible activation of spindle assembly checkpoint	Sigma

		(metaphase arrest)	
Methyl methanesulfonate	0.2 – 1.2 mM	Clonogenic survival assay and DNA damage response	Sigma
Camptothecin	10 – 40 nM	Clonogenic survival assay and DNA damage reponse	Sigma
Cis-platin	0.5 – 2 μg/ml	Clonogenic survival assay and DNA damage response	Hospira (Warwickshire, UK)
Mitomycin C	50 – 500 ng/ml	Clonogenic survival assay, DNA damage response and sister chromatid exchange assay	Sigma
4-nitroquinoline-1-oxide	1 – 12 ng/ml	Clonogenic survival assay and DNA damage response	Sigma
Hydroxyurea	0.1 – 10 mM	Clonogenic survival assay and reversible activation of S-phase checkpoint	Sigma
3,4-Dihydro-5[4-(1-piperindinyl)butoxy]-1(2H)-isoquinoline (DPQ)	10 μM	Clonogenic survival assay – inhibition of PARP-1	Sigma
7-Nitro-1H-indole-2-carboxylic acid (CRT0044876)	100 μM	Clonogenic survival assay – inhibition of APE-1	Sigma

For the treatment of cells with ionising radiation (IR), a ^{137}Cs source at 23.5 Gy/min was used (Mainance Engineering, Hampshire, UK).

2.1.4 Computer programmes

DNA plasmid maps were created using pDRAW32 software (Acaclone, www.acaclone.com). Sequenced DNA samples were viewed using Chromas software (version 2.31, Digital River GmbH, Shannon, Ireland). For bioinformatic analyses ScanProSite (www.expasy.org/tools/scanprosite), BlastN or BlastP (http://www.ncbi.nlm.nih.gov/BLAST), ClustalW

(www.ebi.ac.uk/clustalw), ASTD (http://www.ebi.ac.uk/astd) dbEST (http://www.ncbi.nlm.nih.gov/dbEST/) were used. Microscopy imaging was performed using an Olympus BX-51 microscope driven by OpenLab software (version 5, Improvision, Emeryville, USA). Deconvolved images were saved as Adobe Photoshop images (version 7, San Jose, USA). Analysis of flow cytometry samples was carried out using CELLQuest (version 3.3, Becton Dickinson, Oxford, UK) or BD FACS Diva Software (version 6.1.2, Beckton Dickinson, Oxford, UK). For the quantification of immunoblot signals a FUJI FILM Multi Gauge (v2.2) was used (Dusseldorf, Germany).

2.2 Nucleic acid methods

2.2.1 RNA preparation

The nucleic acid methods and techniques applied in this study were as described (Sambrook and Russell, 2001). RNA was isolated from tissue culture cells using TRIzol (Total RNA Isolation Reagent, Invitrogen, Carlsbad, USA) according to the manufacturer's instructions. Approximately 2 x 10^6 suspension cells were harvested and the RNA pellet was re-suspended in 20 µl of 0.1% DEPC-treated water and incubated at 50^{o}C for 10 minutes for good re-suspension.

2.2.2 Reverse Transcriptase-PCR (RT-PCR)

cDNA synthesis was carried out using the Superscript First-Strand Synthesis for RT-PCR kit from Invitrogen. RNA was prepared as described in section 2.2.1. The first-strand cDNA was generated using oligo dT primers and synthesised according to the manufacturer's instructions. PCRs were carried out as described in section 2.2.3.

2.2.3 Polymerase Chain Reaction (PCR)

Polymerase chain reaction (PCR) was carried out using either KOD, Takara LA Taq or Sigma Taq polymerases depending on the experiment performed. PCR experiments were carried out on a TGradient (Biometra,

Göttingen, Germany). Table 2.10 gives an example of the PCR conditions and programmes used.

Table 2.10 Example of typical PCR reaction conditions

		TaKaRa LA Taq Polymerase	**SigmaTaq Polymerase**	**KOD Polymerase**
Reagent concentrations	buffer (10x)	1x	1x	1x
	Primers	0.2 µM	0.2 µM	0.2 µM
	dNTP's	200 µM	200 µM	200 µM
	Mg^{2+}	2.5 mM	2 mM	2 mM
	Enzyme	0.5 µl (5 U/µl)	0.2 µl (5 U/µl)	0.5 µl (5 U/µl)
PCR steps	'Hot start'	94°C – 1 min	94°C – 1 min	94°C – 2 min
	Denaturation	98°C – 10 sec	94°C – 1 min	94°C – 1 min
	Annealing	58-64°C – 30 sec	58-64°C – 30 sec	58-64°C-30sec
	Extension	68°C – 3 min	72°C – 2 min	72°C – 2 min
	Final extension	72°C – 10 min	72°C – 10 min	72°C – 10 min
No. of cycles	30	30	30	30

2.2.4 Site-directed mutagenesis

Site-directed mutagenesis was performed using the KOD method. To introduce mutations, forward and reverse primers bearing specific sequence alterations were designed. After the PCR reaction, the parental plasmid was degraded by overnight digestion with *DpnI* and analysed by agarose gel electrophoresis. 1/10 of the digested PCR reaction was used to transform competent *E.coli* (as described in Section 2.2.9). Positive bacterial clones were confirmed with digestion and sequencing as described in section 2.2.11. Table 2.11 gives an example of PCR conditions for site-directed mutagenesis.

Table 2.11 PCR conditions of site directed mutagenesis PCR

		KOD
Reagent concentrations	Template	100 ng
	Primers	0.4 µM
	dNTP's	200 µM
	DIG-11-dUTP	70 µM
	Mg^{2+}	2 mM
	Enzyme	0.5 µl (5 U/µl)
PCR steps	'Hot start'	95°C – 2 min
	Denaturation	95°C – 30 sec
	Annealing	55°C – 20 sec
	Extension	68°C – 3 min
	Final extension	72°C – 5 min
No. of cycles		16

2.2.5 Digoxigenin labeling of probes by PCR

Table 2.12 PCR conditions for DIG labeling of probes

		Expand High Fidelity Polymerase
Reagent concentrations	Template	100 ng
	Primers	0.2 µM
	dNTPs	200 µM
	DIG-11-dUTP	70 µM
	Enzyme	0.5 µl (3.5 U/µl)
PCR steps	'Hot start'	95°C – 2 min
	Denaturation	95°C – 30 sec
	Annealing	55°C – 20 sec
	Extension	68°C – 3 min
	Final extension	72°C – 5 min
No. of cycles		16

For labeling of probes with digoxigenin for non-radioactive Southern hybridizations, the PCR DIG Probe Synthesis Kit (Roche, Mannheim, Germany) was used. Table 2.12 shows an example of conditions and programmes used for DIG labeling of probes.

2.2.6 Plasmid DNA preparation

Mini and midi plasmid DNA isolation was carried out by ion-exchange chromatography using HiYield Plasmid Mini kit from RBC Bioscience or GeneElute^{TM} Plasmid MiniPrep Kit (Sigma) and Qiagen Midi Prep kit or Qiagen Endotoxin free MidiPrep kit, respectively. In both procedures, plasmid DNA was prepared according to the manufacturer's instructions. For mini plasmid isolation 2 ml of an overnight *E. coli* culture were used. Bacteria were grown in the presence of selective antibiotics at 37^{o}C with shaking. The DNA was eluted off the column with 30-100 µl of deionised water (ddH_2O). For larger midi plasmid preparations 50 ml of the overnight *E. coli* culture were used. The DNA pellet was re-suspended with 120-200 µl of ddH_2O.

2.2.7 Restriction digestion of DNA

Unless otherwise stated, restriction enzymes used for digestion of DNA (plasmid or genomic) were purchased from New England Biolabs (NEB). The endonucleases were used with the 10 x buffer provided and bovine serum albumin (BSA, 0.1 mg/ml) where required. Digestions were performed at the optimum temperature for 2-16 hours depending on the amount and type of DNA being digested. Where appropriate, the enzyme was inactivated by incubation under the recommended conditions i.e. 65^{o}C for 15 minutes.

2.2.8 Preparation of DNA for cloning

Briefly, each digested plasmid used for cloning was purified with SigmaSpin^{TM} Sequencing Reaction Clean-Up columns (Sigma) to remove restriction endonuclease(s) and traces of buffer. Subsequently prior to ligation, digested plasmid was dephosphorylated on the 5'ends with shrimp alkaline phosphatese (SAP, 1U / pmol of DNA ends). The reaction was carried out in

shrimp alkaline phosphatase buffer at 37°C for 1 hour followed by 15 minutes incubation at 65°C in order to inactivate SAP.

Klenow DNA polymerasae (fragment I) and T4 DNA polymerase were used to blunt both 5' and 3'overhangs generated after restriction digestion. Reactions were carried out in the presence of 10 x buffer and supplemented with BSA (0.1 mg/ml) and dNTPs (100 μM). Usually, 1 μg of DNA was incubated with 5 U of enzyme at 37°C for 5-30 minutes and then heat inactivated at 75°C for 15 minutes.

Ligations were performed using T4 DNA ligase in the buffer provided. Prior to ligation, dephosphorylated plasmid and gel-extracted insert DNA (see section 2.2.10) were analysed by agarose gel electrophoresis. An excess of insert over plasmid was generally used (1:2 to 1:10, depending on the DNA concentration estimated by agarose gel electrophoresis) and the reaction incubated at 4-25°C for 2-24 hours prior to transformation into competent *E. coli* cells.

2.2.9 Preparation of chemically competent *E. coli* and transformation

E. coli cells (see Table 2.3) were grown in 500 ml of LB broth at 37°C with shaking. When culture reached A_{600nm} of 0.5, cells were transferred to ice for 5 minutes and pelleted by centrifugation at 5000 *g* for 15 minutes. The cell pellet was re-suspended in ice cold Tfb I (40 ml per 100 ml culture, see Table 2.1). Thereafter, cells were spun and re-suspended in ice cold Tfb II (4 ml per initial 100 ml culture, see Table 2.1). Subsequently cells were incubated on ice for 15 minutes, snap frozen in liquid nitrogen and stored at -80°C.

For transformations, 25-50 μl of competent *E. coli* cells were mixed with DNA and incubated on ice for 20 minutes. Cells were then transferred to 42°C for 90 seconds and chilled on ice for another 90 seconds. Cells were then mixed with 1 ml of LB broth and gently shaken for 30 minutes at 37°C. For ligations, cells were pelleted by centrifugation at 16 100 *g* for 1 minute and the entire culture plated onto agar plates containing appropriate antibiotics. In the case of pure plasmid DNA transformations only 50 – 100 μl of such culture was plated onto agar plates. Plates were inserted and incubated at 37°C overnight.

2.2.10 Agarose gel electrophoresis and purification of DNA

Generally, 0.7-1.0% agarose gels were prepared using Sigma electrophoresis grade agarose in 1 x TAE buffer containing 0.5 μg/ml ethidium bromide. These gels were run in 1 x TAE buffer in Hoefer HE33 tanks (Mini Horizontal Submarine Unit, Amersham) according to the manufacturer's instructions. DNA on the gel was analysed using a Multi Image Light Cabinet (ChemiImager 5500, Alpha Innotech, Medical Supply Company, Dublin, Ireland) and images were taken with a digital camera. For DNA extraction, bands of interest were excised from the agarose gel with a scalpel blade. DNA was purified using the Qiagen QIAquick Gel Extraction Kit according to the manufacturer's instructions. 20-50 μl of 1 x TE (supplied with kit) or MilliQ water was used to elute bound DNA off the column.

2.2.11 DNA sequencing

DNA samples were sent to either Cogenics (Takeley, UK) or Agowa GmbH (Berlin, Germany) for commercial sequencing. In general, 250 ng of DNA (mini or midi prepped) and 5 – 10 pM primers were used per reaction. Analysed sequences were used to construct correct vector maps with the pDRAW32 (Acaclone, www.acaclone.com) software.

2.2.12 Preparation of genomic DNA from tissue culture cells

Genomic DNA was prepared from chicken DT40 cells to amplify genomic regions of interest or to screen clones for potential targeting events by either ^{32}P (Sonoda et al., 1998) or digoxigenin-based Southern hybridisation (Roche, Mannheim, Germany). Colonies were picked from 96 well plates into 24 well plates and grown for 3-4 days. 1.5 ml of confluent cells was taken for freezing and 1.5 ml for DNA preparation. The cells were pelleted at 160 *g* for 5 minutes and re-suspended in 500 μl of 'Tail' Buffer (see Table 2.1) containing 0.5 mg/ml proteinase K and incubated overnight at 37^{o}C. Next, cell lysates were vigorously shaken for 5 minutes at 37^{o}C, 250 μl of 6 M NaCl was added and the shaking was repeated. Precipitated proteins were removed by centrifugation at 16 100 *g* for 10 minutes. The supernatant was removed and mixed with 1 volume of isopropanol to precipitate the DNA. DNA was spun at 16 100 *g* for 10 minutes,

pellet washed in 70% ethanol and the centrifugation repeated. DNA was air dried for 5-15 minutes and re-suspended in 70 µl of ddH_2O.

2.2.13 Southern Blot and hybridisation of radiolabeled probe

Genomic DNA digestion was performed as described in section 2.2.7. Briefly, each digest consisted of a final volume of 45 µl with the addition of RNase (10 µg/ml), BSA and the appropriate endonuclease was incubated overnight at 37°C. Digested DNA was separated on a 0.7-0.8% agarose gel as previously described in section 2.2.10. DNA was nicked and residual proteins removed by treatment with 0.25 M HCl for 20 minutes and DNA denatured with 0.5 M NaOH/ 1.5 M NaCl for 20 minutes. DNA fragments were transferred by capillary transfer onto a positively charged nylon membrane (GE Healthcare, Bucks, UK) overnight in 2 x SSC (see Table 2.1). The DNA was cross-linked to membrane with UV 300 J/cm^2 using a UV Cross-linker (Hoefer UVC500, GE Healthcare, Bucks, UK). Radiolabeling of probes with α-^{32}P-dCTP was carried out using the Megaprime DNA labeling kit and digoxigenin labeling was performed with Roche PCR DIG Probe Synthesis Kit (Mannheim, Germany).

For radiolabeling, a mixture of primers and DNA probe (10-200 ng) was denatured at 95°C for 5 minutes prior to the addition of dNTPs, radiolabeled α-^{32}P-dCTP and 5 U of DNA polymerase. This mixture was then incubated at 37°C for 30 minutes and purified over a SigmaSpin Post-Reaction Clean-up Column (Sigma) to remove unincorporated radionucleotides. The purified probe was then denatured at 95°C for 5 minutes and added to the Church Hybe pre-hybridised membrane (30 minutes at 65°C). The membrane was then hybridised overnight at 65°C in a hybridisation oven. The next day membrane was washed three times (1 x 5 minutes and 2 x 20 minutes) in Church Wash Buffer (see Table 2.1) at 65°C and then exposed overnight to autoradiography film at -80°C.

For the digoxigenin labeling, probes were amplified by PCR using the DIG PCR Synthesis Kit (Roche, Mannheim, Germany) as described in section 2.2.5. 3-10 µl of the PCR reaction was then denatured in 50 µl of MiliQ water at 95°C for 5 minutes. The membrane (prepared as previously described) was pre-treated with Pre-Hybe Buffer according to the manufacturer's instructions (Roche, Mannheim, Germany). The denatured probe was then added to the pre-

hybridised membrane and incubated overnight at the appropriate hybridization temperature (T_m was calculated according to manufacturer's instructions). The next day, the membrane was washed twice with Low Stringency Buffer (see Table 2.1) for 5 minutes at room temperature, followed by two washes in High Stringency Buffer (see Table 2.1) at 65^{o}C for 15 minutes. The membrane was then blocked with Non-radioactive Southern Blot Blocking Solution (see Table 2.1) for 30 minutes at 25^{o}C and incubated with anti-digoxigenin antibody in the same buffer for 30 minutes at 25^{o}C. Non-specifically bound antibody was removed with two 15 minute washes in Maleic Acid Washing Buffer at 25^{o}C and the membrane incubated with Detection Buffer for 2 minutes at 25^{o}C to bring the membrane to pH required for probe detection (see Table 2.1). The membrane was then transferred into a plastic bag incubated with CSPD substrate for 5 minutes at room temperature. Excess CSPD substrate was removed; the membrane was sealed in a plastic bag and incubated at 37^{o}C for 10 minutes to enhance the signal. The membrane was exposed to film for 2-18 hours depending on the signal strength.

2.3 Protein methods

2.3.1 SDS – Polyacrylamide Gel Electrophoresis (SDS - PAGE)

Equipment used for SDS-PAGE:

- small gels (10x10 cm) – Hoefer mini VE, Amersham
- large gels (14x14 cm) – Hoefer SE 400, Amersham
- wide gels (10x20 cm) – Vertical Maxi 2 Gel Device, Medical Supplies Co. Ltd. (Dublin, Ireland)

Mini and wide gels were generally run in running buffer (see Table 2.1) for 60 to 90 minutes at 25mA or 50mA, respectively. Large gels were normally run for a total of 12-15 hours at 135mA, but this varied depending on gel percentage and protein size being analysed. The final concentration of components used to prepare 8% and 10% polyacrylamide gels are shown in Table 2.13. 30% acrylamide: bisacrylamide (19:1 and 37.5:1) stock was purchased from Severn Biotech Ltd (Worcestershire, UK).

Protein samples were prepared as follow: cells were centrifuged at 160 *g* for 5 minutes, washed in 1 x PBS and pelleted again. The cells were then lysed for 5 - 10 minutes on ice in lysis buffer of choice (supplemented with protease and phosphatase inhibitors) depending on the experiment performed (see Table 2.1). Next, cells were centrifuged at 16 100 *g* for 10 minutes at 4^{o}C to pellet DNA and cell membranes. The protein concentration in the supernatant containing the solubilised proteins was determined by Bradford Protein Assay (see section 2.3.2). In general, 30 – 60 µg of total proteins were loaded onto gels. Prior to electrophoresis or storage at -20^{o}C, samples were boiled at 95^{o}C for 5 minutes in 3 x sample buffer containing ß-mercaptoethanol (see Table 2.1).

Table 2.13 Example of 8% and 10% lower and upper gel mix

	8% gel	**10% gel**
Resolving Gel Mix	375mM Tris pH 8.8	375 mM Tris pH 8.8
	8% acrylamide/ bis (37.5:1)	10% acrylamide/ bis (19:1)
	0.1% SDS	0.1% SDS
	-	1 mM EDTA
	0.07% APS	0.1% APS*
	0.1% TEMED	0.1% TEMED*
Stacking Gel Mix	78mM Tris pH 6.8	125 mM Tris pH 6.8
	5% acrylamide/ bis (37.5:1)	4% acrylamide/ bis (19:1)
	0.1% SDS	0.1% SDS
	-	1 mM EDTA
	0.05% APS	0.1% APS

(*) - See 'Abbreviations' for the full-name

2.3.2 Bradford Protein Assay

For the determination of protein concentration, the Bradford dye-binding protein assay was employed as described (Bradford *et al.*, 1976). Briefly, 1 µl of a protein sample was diluted in 1 ml 1:1 Bradford : MilliQ water solution (Pierce, Rockford, IL). The absorbance at 595 nm was measured with a spectrophotometer (Eppendorf, Hamburg, Germany). The protein concentration

was calculated based on a BSA (bovine serum albumin) standard curve, in which absorbance was plotted *vs.* varying concentrations of the BSA protein.

2.3.3 SDS – PAGE staining

In order to visualise proteins in a gel, they were stained with Coomassie Blue R (see Table 2.1) for 20 minutes at room temperature, with gentle agitation. The gel was destained for the desired length of time with a few changes of the destain solution (see Table 2.1). Destained gels were dried after treatment with a fixation solution (see Table 2.1) using the Hoefer Slab Gel Dryer SE1160 (Amersham) for 90 minutes at 70^{o}C.

2.3.4 Western blotting

Proteins were separated by SDS-PAGE and then transferred to nitrocellulose membrane (GE Healthcare, Bucks, UK). This was carried out using wet or semi-dry transfer systems for 1-2 hours at up to 350 mA (either at 4^{o}C or room temperature, see Table 2.1). Transfer of mini gels was performed using a Hoefer TE 22 Mighty Small Transfer apparatus (GE Healthcare, Bucks, UK), while large gels were transferred using a Hoefer TE 77 Semi Dry Transfer Unit (GE Healthcare, Bucks, UK) according to the manufacturer's instructions. Membrane was then rinsed three times in dH_2O and Ponceau S. solution was used to visualise the quality of protein transfer. To decrease non-specific antibody binding, the membrane was blocked with a 5% milk solution in 1 x PBS-0.05% Tween-20 for 30 minutes on a rocking platform at room temperature. The blocked membrane was then incubated overnight in the primary antibody solution at 4^{o}C at the concentrations shown in Table 2.5. The next day, the membrane was washed three times for 10 minutes in 1 x PBS-0.05% Tween-20 and transferred to the secondary antibody solution (see Table 2.6) in 3% milk for 60 minutes at room temperature. Again, 3 x 10 minute washes in 1 x PBS-0.05% Tween-20 were performed, and the specific proteins detected with ECL detection kit (GE Healthcare or Milipore) and autoradiograph film exposure (Hartenstein, Germany). The exposed film was then fixed and developed by passing it through a developing machine (CP 1000, AGFA, Brentford, UK).

2.3.5 Expression of recombinant proteins in *E. coli*

A single colony of *E. coli* previously transformed with a plasmid of interest (see section 2.2.9) was expanded overnight shaking in 5 ml LB broth (see Table 2.1) containing selective antibiotics at 37^{o}C. The following day the culture was diluted 1:100 and grown at 37^{o}C to an OD_{600} of 0.6. At this stage, a 1 ml control ('uninduced') sample was collected for SDS-PAGE analysis. For optimisation of recombinant protein expression, concentrations of isopropyl-ß-D-thiogalactoside (IPTG (Sigma, 0.1-1 mM)); temperatures (25-37^{o}C) and times (2 – 4 hours) were varied. After induction, 1 ml of cells (the "induced" sample) was collected at different time points to assess protein expression. All collected samples were spun for 1 minute at 16 100 *g* and re-suspended in 3 x sample buffer prior to 5 minutes boiling at 95^{o}C, SDS-PAGE analysis and storage at -20^{o}C.

2.3.6 Purification of GST fusion proteins

Immobilised glutathione (GST-Bind Resin, Novagen) was used for the purification of recombinant GST fusion proteins from bacterial cells. Beads were washed three times in GST Binding Buffer (see Table 2.1), followed by pelleting at 500 *g*. 50 – 500 ml bacterial culture was spun for 5 minutes at 6000 *g* and the pellet re-suspended in 1 – 20 ml of GST Binding Buffer supplemented with the protease inhibitors CLAP and PMSF. N-Lauroylsarcosine was then added to a final concentration of 0.8% and the cell suspension lysed for 10 minutes on ice. The cell lysate was then sonicated three times for 1 - 10 seconds for total of 3 – 30 seconds with 10 seconds pause at 20% amplitude using a Digital Sonifier (Branson, London**,** UK) to solubilise proteins and fragment chromosomal DNA. Triton X-100 was then added to a final concentration of 0.9% and the sample incubated for 5 minutes at 4^{o}C with gentle rocking to reduce non-specific protein interactions. The extract was centrifuged at 16 100 *g* for 15 minutes at 4^{o}C to remove cell debris. The supernatant was diluted 1:1 with GST Binding Buffer to decrease detergent concentrations and mixed with the previously equilibrated beads. In general, 50 µl bed volume of GST resin per 500 µl of lysate was used. Lysate and beads were then incubated on a rotating mixer for 1-2 hours at 4^{o}C to

capture GST fusion proteins. After binding, the beads were washed three times with GST Binding Buffer supplemented with 0.5% Triton X-100. The fusion protein was eluted either by boiling in 3 x sample buffer for 5 minutes or with 20 mM reduced glutathione in Tris-Cl (pH 8.5). For glutathione elutions a total of three elutions were collected for analysis. Eluted proteins were then analysed by SDS-PAGE, together with previously-collected uninduced and induced samples (see Section 2.3.5). Gels were stained by Coomassie Blue R (see Section 2.3.3).

2.3.7 Purification of His-tagged fusion proteins from DT40 cells

For the purification of His-tagged fusion proteins from DT40 cells, Ni Sepharose^{TM} 6 Fast Flow (GE Healthcare) was used. Prior to use, beads were washed twice in His-tag Buffer (see Table 2.1), followed by centrifugation at 500 *g*, according to the manufacturer's instructions. The cell pellet from 50 ml culture of confluent DT40 cells was re-suspended in 1-2 ml of His-tag Buffer supplemented with protease inhibitors (CLAP, PMSF and Aprotonin, for details see Table 2.1) and lysed for 10 minutes on ice. Afterwards, the cell extract was sonicated for 15 seconds with 3 seconds pulse and 10 seconds pause at 20% amplitude to shear genomic DNA. Sonicated extracts were then spun for 10 minutes at 30 000 *g* at 4^{o}C to remove cell debris. The protein concentration was then assessed by Bradford assay as described in section 2.3.2. Equal amounts of total protein were taken from each extract analysed (usually from 2 – 10 mg of total protein). The appropriate volume of supernatant was then transferred to a fresh tube containing 50 – 200 µl bed volume of pre-equilibrated Nickel beads. The binding of His-tagged proteins was performed for 2 hours at 4^{o}C on a rotating mixer. After binding, the beads were washed three times with His-tag Buffer to remove unwanted background proteins and the proteins of interest eluted with 50 – 200 µl of 250 mM imidazole or by boiling in 3 x sample buffer for 5 minutes at 95^{o}C. The purified samples together with input and unbound samples were then analysed by either SDS-PAGE and Coomassie gel staining or immunoblotting.

2.3.8 Preparation of GST-tagged protein as antigen for immunisation

Recombinant protein was purified as described in section 2.3.6. The purified protein was separated by SDS-PAGE and the gel washed with ddH_2O, three times for 10 minutes. The visualised protein band (Coomassie blue R) was excised using a scalpel and resuspended in sterile 1 x PBS. A gel slice in this form was sent for rabbit immunisation (Eurogentec, Seraign, Belgium).

2.3.9 Purification of antibody against immobilized antigen

GST and the GST-fusion protein of interest were purified with glutathione sepharose 4B as described in section 2.3.6, without the elution steps being carried out. The proteins were then cross-linked to sepharose beads. Prior to cross-linking the beads were equilibrated to the required pH by washing three times with 200 mM HEPES pH 8.5, and incubated in cross-linking solution (see Table 2.1) for 30 minutes at room temperature. After the cross-linking reaction, the beads were spun for 2 minutes at 500 *g* and washed once with 200 mM HEPES pH 8.5 to remove the cross-linking reagent. The coupling reaction was terminated by incubation of the resin with 200 mM ethanolamine pH 8.2 for 60 minutes at room temperature. Beads with covalently bound GST and GST-fusion proteins were washed twice with Glycine Elution Buffer (see Table 2.1) to remove non-covalently bound molecules, followed by two washes with 1 x TBS to restore the pH to 7.5. The purification and cross-linking of GST fusion protein was confirmed by SDS-PAGE and Coomassie Blue R staining of the gel. For affinity purification, 1 ml of crude serum raised against the GST-fusion protein was brought to 1 x TBS with 8 ml of ddH_2O and 1 ml of 10 x TBS. The diluted serum was filtered through a 0.2 μm filter and spun at 4^oC for 10 minutes at 30 000 *g* to remove debris. This serum was first incubated with GST protein coupled to beads for 4 h at 4^oC on a rotating mixer to remove GST-specific antibodies. The beads were then spun for 2 minutes at 500 *g* and the supernatant containing antibodies against the GST fusion protein were captured by incubation with GST-fusion protein containing beads for 12 hours at 4^oC on a rotating mixer. After incubation, the beads were pelleted, the supernatant

removed and the resin washed five times with 1 x TBS containing 0.1% Triton X-100, followed by two washes with 0.1 x TBS. To elute specific antibodies, the beads were incubated twice with Glycine Elution Buffer on a rotating mixer, for 5 minutes at room temperature. The collected fractions were analysed by SDS-PAGE and Coomassie Blue R staining of the gel. Both fractions were combined and spun over Amicon Ultra (Millipore, Cork, Ireland) columns with a 3 kDa cut-off membrane to concentrate the antibody solution. Antibodies were aliquotted and stored at -20^{o}C with 0.02% NaN_3. After elution, the beads were regenerated with 100 mM phosphate solution pH 12.0 and extensive washing with 1 x TBS, then stored in the same buffer with 0.02% NaN_3.

2.3.10 Immunoprecipitation

For the immunoprecipitation of proteins from chicken DT40 cells, 5 x 10^7 cells were washed once in 1 x PBS and the pellet re-suspended in 1 ml immunoprecipitation buffer (see Table 2.1) supplemented with protease inhibitors (CLAP, PMSF and Aprotonin). The cells were then sonicated briefly for 15 seconds with a 3 seconds pulse and 10 seconds pause at 20% amplitude to solubilise proteins and shear genomic DNA. The cell lysate was then centrifuged at 16 100 *g* for 10 minutes at 4^{o}C to remove insoluble material. Protein concentration was determined using the Bradford assay and 2 mg of total protein was usually used per immunoprecipitation. The appropriate amount of the cell lysate was mixed with 10 µl of Protein A or G beads and incubated 30 minutes at 4^{o}C on a rotating mixer to remove proteins that unspecifically bound to the beads (pre-clean step). The resin was then spun for 5 minutes at 500 *g* and the pre-cleared cell lysate was mixed with the previously-prepared antibody. Briefly, 25 µl of bed volume of Protein A or G resin was washed three times with immunoprecipitation buffer to remove the storage solution, re-suspended in 1 ml of the same buffer containing 2 µg of antibody and incubated 2 hours or optionally overnight at 4^{o}C. Antibodies coupled to the Protein A or G beads were spun for 5 minutes at 500 *g* and the beads washed three times with immunoprecipitation buffer to remove unbound antibodies. The pre-cleared cell lysate was mixed with prepared antibodies and incubated at 4^{o}C for 2 hours

rotating. After immunoprecipitation beads were washed three times with 1 ml of immunoprecipitation buffer and finally re-suspended in 40 µl of the same buffer with 20 µl of 3 x SB containing ß-mercaptoethanol. Precipitated material was eluted by boiling for 5 minutes at 95^{o}C. Input, unbound and precipitated proteins were separated by SDS-PAGE and analysed by immunoblotting.

2.3.11 *In vitro* SUMOylation assay

For *in vitro* SUMOylation assay, a commercial kit was used (Enzo Lifesciences, Exeter, UK). According to the manufacturer's instructions, 0.5 µg of GST-Nse2 or GST-Nse2.AA (C178A, H180A mutant) was incubated with appropriate volume of MilliQ water, 2 µl of 10 x Reaction Buffer, 1 µl of Mg-ATP, 1 µl of 20 x E1 enzyme (Aos1/Uba2), 1 µl of E2 enzyme (Ubc9) and 1 µl of SUMO-1, -2 or -3 peptide. The positive control reaction was performed with control GST-RG1 protein (GST-RanGap1 derived peptide) and in the absence of GST fusion ligases. In parallel, negative control reactions without the energy mix (Mg-ATP) were prepared. All reactions were incubated for 1 hour at 30^{o}C and stopped by the addition of sample buffer, followed by boiling for 3 minutes at 95^{o}C. Then 5-10 µl of the reaction was analysed by SDS-PAGE and immunoblotting with target or SUMO1/2/3 specific antibodies.

2.3.12 Phosphatase assay

30 µg of clear lysate from DT40 cells was incubated for 30 minutes at 30^{o}C with 400 units (1 µl) of λPPase (New England Biolabs) in 1 x λPPase reaction buffer (New England BioLabs), supplemented with 2 mM $MnCl_2$ in total volume 40 µl. Control samples containing the phosphatase in the presence of the phosphatase inhibitors: 5 mM sodium fluoride and 2 mM sodium orthovanadate or samples without phosphatase addition, were incubated in the same conditions. The phosphatase reaction was terminated by addition of 3 x sample buffer directly into the reaction. Samples were boiled for 3 minutes at 95^{o}C and proteins were separated by SDS-PAGE and transfer to nitrocellulose membrane for immunoblot analysis.

2.4 Cell biology methods

2.4.1 Transient transfections

DT40 cells were transiently transfected by nucleofection using Amaxa nucleofector (Gaithersburg, USA). Briefly, 5 μg of endotoxin-free DNA (see 2.2.6 for plasmid DNA preparation) was mixed with 5 x 10^6 DT40 cells, previously re-suspended in 100 μl of Solution-T. The cells were then nucleofected with Amaxa using programme B-23. 18 to 24 hours post-transfection, cells were harvested and analysed either by immunofluorescence or SDS-PAGE and immunoblotting.

2.4.2 Stable transfections and gene targeting

Electroporation was used to either generate stably expressing DT40 cell lines or for a gene targeting, as previously described (Morrison et al., 2000; Sonoda et al., 1998; Takata et al., 1998). 1 x 10^7 of cells were pelleted for 5 minutes at 160 *g*, washed once and re-suspended in 0.5 ml of 1 x sterile PBS. 20-25 μg of linearised DNA was then added to the cells, transferred to an electroporation cuvette (BioRad, 0.4 cm gap) and incubated on ice for 10 minutes. Electroporation was carried out in BioRad Gene Pulser (Hercules, USA) at conditions of 300 V/600 μF. The electroporated cells were again incubated on ice for 10 minutes and transferred to 20 ml of fresh, pre-warmed medium. After 18 to 24 hours, 20 ml of fresh media was added to the transfected cells. The appropriate selective antibiotics at the concentrations, was added to the culture as shown in Table 2.6 and cells were plated out in 4 x 96 well plates. Plates were incubated at 39.5^{o}C until colonies were visible through the bottom of the plate. Each single colony was then transferred to a well in a 24 well plate containing 3 ml of medium and incubated under non-selective conditions at 39.5^{o}C until confluent.

2.4.3 Immunofluorescence microscopy

Chicken cells were fixed and stained for immunofluorescence microscopy using a range of various antibodies (see Table 2.5). Sections 2.4.3 – 2.4.5

summarise the protocols involved. An Olympus BX51 microscope with 60 x (NA 1.4) or 100 x objective (NA 1.35) and Openlab Software (v. 1.35 Improvision, Emeryville, USA) was used for analysis. Serial Z-sections (0.15 μm) were collected and the images then deconvolved and saved as Abode Photoshop TIFF files.

2.4.4 Paraformaldehyde fixation

Before fixation, DT40 cells were spun at 160 *g* for 5 minutes, re-suspended in 1 x PBS and adhered to poly-L-lysine slides (Menzer Glasser, Fisher Dublin Ireland) by gravity for 15 minutes at room temperature. 4% paraformaldehyde in cytoskeleton buffer (CB) or 1 x PBS for 10 minutes at room temperature was used for cell fixation (see Table 2.1) (Wheatley and Wang, 1998). The cells were then washed three times in 1 x PBS and permeabilised in 0.2% Triton X-100 in cytoskeleton buffer or 1 x PBS. The cells were then washed three times again in 1 x PBS and blocked in 1% BSA for 30 minutes at room temperature or overnight at 4^{o}C. Both primary and secondary antibodies were used at the indicated concentrations in a Table 2.5 in 1% BSA and incubated in a humid chamber at 37^{o}C for 1 hour. Unbound and non-specifically bound antibodies were removed with 3 x 3 minute washes with 1 x PBS. The DNA was stained with DAPI (1 μg/ml) in mounting medium (200 mM DABCO, Sigma, Wicklow, Ireland).

2.4.5 Methanol fixation

Certain antibodies and fluorescent fusion proteins were more readily visualised after methanol fixation. Cells were prepared prior to fixation as described in section 2.4.3. The cells were washed in 1 x PBS and fixed/ permeabilised for 3-10 minutes in pre-chilled 95% methanol at -20^{o}C containing 5 mM EGTA. The cells were then washed three times for 3 minutes in 1 x PBS, blocked in 1 x PBS containing 1% BSA and incubated with antibodies as described in section 2.4.3. DNA was stained with DAPI (1 μg/ml) and mounted with 200 mM DABCO.

2.4.6 Dual paraformaldehyde/ methanol fixation

For visualisation of certain fluorescent fusion proteins, a combined fixation of paraformaldehyde/ methanol fixation was used as previously described (Brock *et al.* 1999). Before fixation, cells were prepared as described in section 2.4.3. Briefly, cells were fixed in 4% paraformaldehyde in HBS (see Table 2.1) for 5 minutes at 4^{o}C followed by 10 minutes at room temperature. Cells were then washed three times for 5 minutes in HBS and post-fixed with pre-chilled 95% methanol 5 mM EGTA at -20^{o}C for 6 minutes. After methanol fixation, cells were washed three times for 5 minutes in HBS. If additional staining with antibodies was required it was performed as described in section 2.4.3. DNA was stained with DAPI (1 μg/ml) and slides mounted with 200 mM DABCO.

2.4.7 Chromosome spreads

To obtain chromosome spreads, cells were blocked in metaphase with 0.1 μg/ml colcemid (see section 2.1.3) for 1 - 3 hours. Harvested cells were hypotonically swollen in 1 ml of 0.9% sodium citrate (pre-warmed to 37^{o}C) for 15 minutes at 37^{o}C and fixed in freshly prepared 5 ml of Calenoa solution. Cells were centrifuged at 160 *g* for 5 minutes and re-suspended in 5 ml of Calenoa solution followed by 30 minutes incubation at room temperature. Cells were spun down again at 160 *g* for 5 minutes and re-suspended in the appropriate volume (usually 100-200 μl) of Calenoa solution. Cells were then applied onto pre-wet (50% ethanol) Superfrost slides (Menzer-Glasser-Fisher, Dublin, Ireland) by dropping them from a height of 20-30 cm. Slides were immediately flame-dried and stained with Giemsa Stain (Merck-Seven Seas, Dublin Ireland) for 20 minutes at room temperature (Table 2.1). The chromosomes were analysed by light microscopy under 100 x lens (Axioskop 2 Plus, Zeiss, Berlin, Germany).

2.4.8 Sister chromatid exchange assay

For the differential staining of sister chromatids cells were grown in the dark with 10 μM BrdU for exactly two cell cycles (20 - 22 hours). For the last eight hours cells were left unchallenged or treated with 100 ng/ml mitomycin C

to induce sister chromatid exchanges. To increase the number of metaphase cells, 0.1 μg/ml colcemid was added 2 hours prior to cell harvesting by centrifugation. Cells were then incubated in pre-warmed 75 mM KCl for 15 minutes at 37°C. After the swelling step, cells were fixed with 5 ml of freshly prepared Calenoa solution and pelleted at 160 *g* for 5 minutes. The cell pellet was re-suspended in 5 ml of Calenoa solution and incubated at room temperature for 30 minutes. Fixed cells were spun again and re-suspended in the appropriate volume of Calenoa solution (usually 100 – 200 μl). Next, the cells were applied to Superfrost slides by dropping them from a height of 20-30 cm. Slides were then dried for 15-30 minutes at room temperature and incubated with 10 μg/ml Hoechst 33258 in Phosphate Buffer pH 6.8 to stain the DNA. After staining cells were washed three times for 3 minutes in Macllvane Solution and mounted with the same buffer. Slides were then irradiated with a UV lamp (366 nm) for 1 hour to degrade BrdU-substituded DNA, and washed once with Macllvane Solution. Prior to staining with Giemsa Stain, slides were incubated in 2 x SSC for 1 hour at 62°C. After 20 minutes staining, the slides were washed with tap water from the back side of the slide and dried at room temperatuure. Sister chromatid exchanges were scored using light microscopy as described in Section 2.4.6.

2.4.9 EdU staining and "click chemistry"

Labeling of S-phase cells was performed with EdU (5-ethynyl-2'-deoxyuridine). Briefly, cells were incubated with 10 μM EdU for 10 – 15 minutes and immediately cytopspun onto poly-L-lysine slides for 5 minutes at 150 *g*. Cells were then fixed with 4% paraformaldehyde in 1 x PBS for 10 minutes and permeabilised with 0.2% Triton X-100 in 1 x PBS for 3 minutes. Three washes for 3 minutes in 1 x PBS were applied after the fixation and permeabilisation steps. Slides were then blocked with 1% BSA to reduce unwanted background. After blocking slides were washed once with 1 x PBS and incubated with Click Reaction Mix (see Table 2.1) to couple incorporated EdU to a green fluorophore. The coupling reaction is based on azide-alkyne specific 1,3-dipolar cycloadditon (Huisgen reaction) catalysed by copper, also known as "click chemistry" (Kolb et al., 2001). After the coupling reaction slides were

washed twice for 15 minutes in 1% BSA 0.5 % Tween 20 in 1 x PBS. DNA was stained with DAPI and slides mounted with 200 mM DABCO.

2.4.10 Clonogenic survival assays

Clonogenic survival assays were performed to determine the sensitivity of cells to different DNA damaging agents as previously described (Takata *et al*., 1998). Prior to IR treatment, serially-diluted cells were plated in 8 ml of semi-solid methylcellulose medium (see section 2.1.3) and incubated for 1 hour at 39.5^{o}C. The plated cells were then irradiated at various doses (2-8 Gy) using a ^{137}Cs source (see section 2.1.3). For UV treatment, cells were exposed to UVC light (5 – 15 J/m^{2}) at density of 2.5 x 10^{6} in 0.5 ml of 1 x PBS. Immediately after radiation, 2.0 ml of pre-warmed, fresh media was added to the cells. Serial dilutions were then prepared and cells plated onto methyl cellulose-containing media. To determine cells' sensitivity to 4-nitroquinoline 1-oxide, camptothecin, cis-platin, hydroxyurea, methyl methanesulfonate and mitomycin C (see table 2.8), cells at a density of 1 x 10^{5} were treated for 2 hours at 39.5^{o}C with different doses of the drugs and plated onto methyl cellulose-containing media from serial dilutions. In general colonies were counted 10 - 14 days after seeding. Cell survival was expressed as a percentage of the survival of untreated cells.

2.4.11 Flow cytometry

For cell cycle analysis, cells were centrifuged at 160 *g* for 5 minutes resuspended in 5 ml of 1 x PBS and fixed by drop wise addition of 10 ml ethanol (pre-chilled to -20^{o}C) and stored at 4^{o}C prior to flow cytometry. Before analysis cells were washed in media (pre-warmed to 37^{o}C) to remove precipitated salt and re-suspended in 1 x PBS supplemented with 100 μg/ml RNase A and 40 μg/ml propidium iodide (PI, Sigma). After 20 minutes' incubation at room temperature, optionally overnight (in the dark), cells were analysed using a FACS Calibur or FACS Canto (Becton Dickinson, San Jose, CA) and Cell Quest (version 3.3, Becton Dickinson) or BD FACS Diva Software (version 6.1.2, Becton Dickinson), respectively.

2.4.12 pDR-GFP – direct repeat recombination assay

pDR-GFP was integrated into DT40 cells (Pierce et al., 1999). The day before the analysis, cells were transiently transfected by Amaxa nucleofection (as described in the section 2.4.1.1) using 5 µg endotoxin-free DNA, Solution T and programme B-23. The DNA used in the transfection was as follows, pRFP-C1 (0.5 µg) + pCBA-SceI (4.5 µg) or pBluescriptII SK (4.5 µg) as a negative control. After overnight incubation (16 hours) cells were harvested by centrifugation, washed once, re-suspended in 1 x PBS and analysed by flow cytometry (see section 2.4.6). The GFP positive cells (recombination positive) were expressed as a fraction of RFP positive cells (transfection positive).

Chapter 3 Cloning and characterisation of chicken *Nse2*

3.1 Introduction

Studies in yeast have established a role for the Nse2 protein in DNA damage response and repair (Andrews et al., 2005; Pebernard et al., 2004; Potts and Yu, 2005; Zhao and Blobel, 2005). In order to study the functions of the vertebrate homologue of Nse2, we decided to clone chicken *Nse2* and assess the biochemical properties of the gene product, as well as to study its cellular localisation. Here we report that, similar to yeast and human Nse2, it forms a complex with the Smc5 protein *in vivo* and shows cell cycle dependent localisation.

3.2 Cloning and analysis of chicken *Nse2*

To identify the chicken *Nse2* orthologue we used human (NSMCE2), mouse (NSMCE2) and yeast (MMS21) Nse2 sequences to search by BLAST the *Gallus gallus* non-redundant protein sequences available in the NCBI database. In several searches, we found an open reading frame (ORF) coding for a hypothetical protein, similar to *Saccharomyces cerevisiae* non-Smc element 2 (*MMS21*, NCBI accession number XP_418440.1). The candidate *Nse2* ORF was then translated and analysed using the ScanProSite software available from the Expasy database. The ScanProSite allows for identification of domains embedded in linear protein sequence by its comparison with previously characterised protein motifs. This analysis revealed the presence of a specific E3 SUMO ligase domain (SP-RING) at the C-terminus of protein encoded by the candidate ORF (Figure 3.1).

Figure 3.1 Linear structure of the hypothetical protein similar to S. cerevisiae homologue of Nse2.

The candidate ORF sequence was analysed with ScanProSite software to identify a conserved protein domains and motifs. The analysis identified a specific E3 SUMO ligase domain at the C-terminus of the ORF (here shown as SP-RING). The numbers indicate amino acid positions in the predicted protein.

A similar domain has been identified in human and fission yeast Nse2, and it has been shown to be essential for its enzymatic activity (Andrews et al., 2005; Potts and Yu, 2005; Zhao and Blobel, 2005). The analysis did not identify any known domains in the N-terminus but recent crystallographic data showed that the N-terminus of *S. cerevisiae* Nse2 is required for its interaction with Smc5 (Duan et al., 2009a). We then compared the sequence of the candidate Nse2 ORF against human, mouse and yeast Nse2. As shown in Figure 3.2A, chicken Nse2 shows significant similarity to mouse and human Nse2, but only a slight homology to the yeast homologues, within the catalytic domain (SP-RING). Sequence values were obtained by BLASTP alignment between Nse2 homologues. These values correspond to the evolutionary conservation of Nse2 between the species analysed. As shown on the phylogenetic tree (Figure 3.2B), the estimated evolutionary time difference separating chicken from human and mouse Nse2 is smaller than the one between the chicken and yeast Nse2 homologues. This indicates that chicken Nse2 is different from human, mouse and yeast but shows a higher similarity to mammalian Nse2 than to its homologues from unicellular organisms. The most conserved amino acid residues were found within the SP-RING domain (residues 147 to 229 in the chicken peptide, Figure 3.2A). Six amino acids within the SP-RING domain (four cysteines and two histidines (C2H4)), have an essential function in zinc coordination and the transfer of the SUMO peptide (Figure 3.2A, residues coloured with red) (Andrews et al., 2005; Duan et al., 2009a; Potts and Yu, 2005).

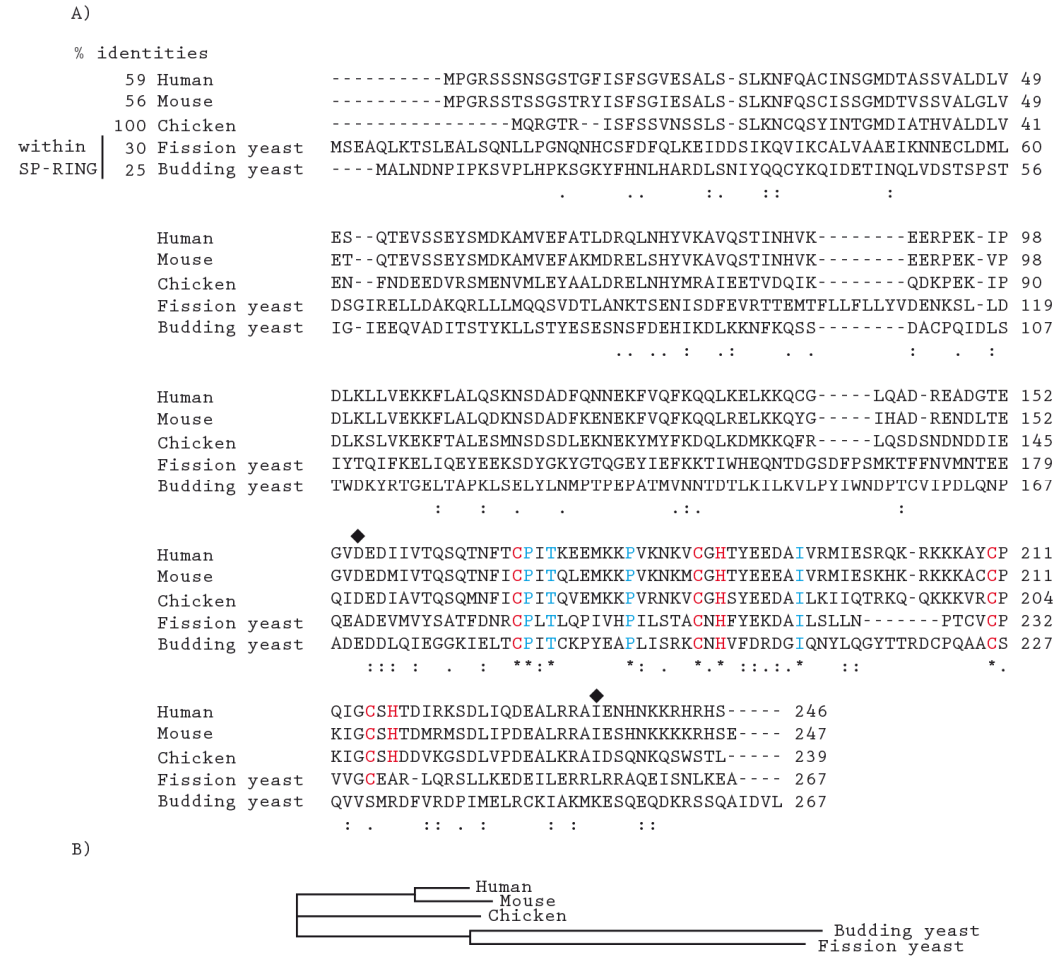

Figure 3.2 Analysis of Nse2 protein sequences.

(A) Alignment of Nse2 protein sequences from human, mouse, chicken, budding and fission yeast. Values for the protein identities between the species were obtained by BLASTP alignment of the chicken and human, mouse or yeast Nse2 and are shown in the first five rows of the alignment. The black diamonds show the beginning and end of the predicted catalytic domain (SP-RING) of chicken Nse2. Amino acid coloured with red and blue are evolutionarily conserved between the analysed species, with the red showing residues essential for catalytic activity of Nse2 (B) The phylogenetic tree shows the evolutionary conservation of Nse2 sequences between the species analysed. The branches joined together indicate that sequences descended from a common ancestor. The edge length corresponds to the estimated evolutionary time between different forms of Nse2.

To confirm that the candidate Nse2 ORF is expressed in chicken cells we identified the mRNA entry associated with it (NCBI accession number XM_418440) and used it to search the expressed sequence tag (EST) database (dbEST, NCBI). As shown in Table 3.1, we found multiple EST clones that cover the entire *Nse2* cDNA sequence. None of the EST sequences that

contained gaps coded for an alternatively spliced form of Nse2, suggesting that these were low quality sequences. The BLAST search against the entire nucleotide collection revealed that there is no similar gene in *G. gallus* genome. These data indicate that there is only a single *Nse2* gene that is expressed as a single spliced form in different chicken tissues.

Table 3.1 Results of chicken EST database screen.

EST accession number	Coverage of candidate *Nse2* cDNA	Tissue
BU317419	100%	Head
BU232236	100%	Heads
BU465927	100%	Ovary
BU358762	100%	Heart
BU110116	100%	Limbs
BU210432	99%	Whole embryo
BU123930	99%	Small intestine
CV853048	98%	Gonad

Additionally, screening of the predicted cDNA sequence with Alternative Splicing and Transcript Diversity software (ASTD, EMBL-EBI) confirmed expression of a single spliced form of the Nse2 candidate ORF. We then used the *Nse2* cDNA sequence to design specific primers for cDNA amplification. Chicken cDNA was obtained using reverse transcription with random hexamer primers of total mRNA isolated from DT40 cells. This cDNA was then used as a template to amplify by PCR (with gene-specific primers) the full-length *Nse2* cDNA, as shown in Figure 3.3. Analysis of the amplified candidate *Nse2* cDNA product by agarose gel electrophoresis revealed a size (720 bp) consistent with the sequence predicted in the NCBI database (Figure 3.6). Subsequent sequencing of the cloned candidate ORF cDNA confirmed this observation.

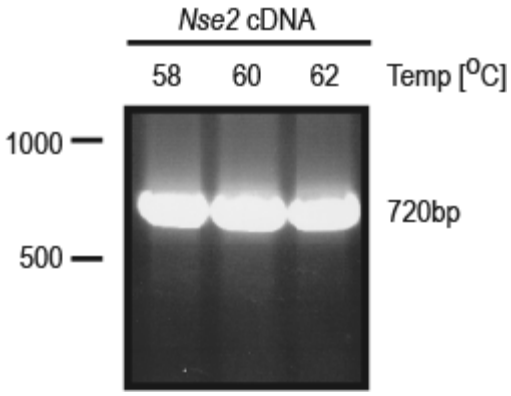

Figure 3.3 Cloning of the chicken Nse2 candidate cDNA.

Reverse transcriptase PCR (RT-PCR) was performed on mRNA isolated from DT40 cells in order to amplify chicken Nse2 cDNA. A temperature gradient was used to find optimal conditions for Nse2 cDNA amplification.

To further validate our observation that the cloned candidate *Nse2* ORF is the chicken homologue of *Nse2*, we compared its gene structure with human *Nse2*. This comparison revealed that both the chicken and human *Nse2* genes consist of six exons, as shown in Table 3.2.

Table 3.2 Analysis of protein coding exon number and length between human Nse2 and potential chicken Nse2 genes.

Human exon	Exon length (bp)	Chicken exon	Exon length (bp)
1	157	I	133
2	107	II	107
3	154	III	154
4	101	IV	104
5	107	V	107
6	118	VI	115
Total	744	Total	720

The chicken *Nse2* gene is transcribed as a 720 bp mRNA which encodes a protein of 240 amino acids with a predicted size of 27 kDa. The human mRNA and protein are a similar size of 744 bp, 248 amino acids and 28 kDa in size. In addition the Kozak sequence was investigated. This is the sequence upstream of the start codon which acts as a signal for the initiation of translation. This

consensus sequence was found to be GCCA/GCC**ATG**G, with the most conserved nucleotide at the position -3 (Kozak, 1986). From the data in Appendix 1 it can be seen that although the sequence does not confirm closely the consensus one, it has conserved an A at the position -3.

We also looked at the genomic region of the human and the candidate of chicken *Nse2* because chromosomal localisation of genes can also be conserved throughout evolution (Lalley et al., 1978). We found two identical genes upstream of the genes of interest; KIAA0196 codes for the membrane protein Strumpellin and SQLE codes for squalene epoxidase. The gene downstream of chicken *Nse2* is a predicted ORF of a protein similar to a G-protein-coupled receptor induced protein GIG2 (LOC428386), whereas the gene downstream of human NSE2 is a Tribbles homologue 1 (TRIB1), also a G-protein-coupled receptor induced protein. The observed similarities between chicken, human, mouse and yeast Nse2 on the protein and gene levels, indicate that we have identified and cloned the chicken orthologue of hNSE2.

3.3 Generation of antisera against chicken Nse2 protein

To characterise and explore the cellular functions of chicken Nse2, rabbit polyclonal antibodies were raised against the protein. An N-terminal glutathione S-transferase (GST) tagged Nse2 fusion protein was used as an antigen to generate antibodies. The chicken *Nse2* cDNA was cloned into pGEX-4T-2. The GST-Nse2 fusion (27 + 27 kDa) was expressed in the BL21 pLysS strains of *E. coli*, giving a fusion protein with a predicted size of 54 kDa. The GST-Nse2 was then purified over glutathione agarose beads (as described in Section 2.3.6). Induction and purification of GST-Nse2 is shown in Figure 3.4.

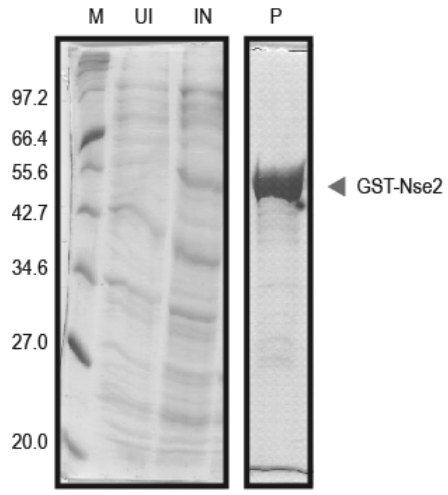

Figure 3.4 Expression and purification of GST-Nse2 fusion protein.

E.coli transformed with pGEX-4T-2-Nse2 plasmid were treated with 0.1mM IPTG to induce expression of the GST-Nse2 protein. After 2 hours induction, cells were lysed and the fusion protein purified over GST resin. Legend: (M) – protein marker, (UI) – uninduced sample, (IN) – induced sample, (P) purified GST-Nse2. Estimated size of GST-Nse2 fusion: 54 kDa.

3.4 Characterisation of anti-chicken Nse2 sera

All three bleeds obtained from two different rabbits were tested in immunoblot experiments using DT40 whole cell extracts. Conditions including bleed dilution factor, membrane types and blocking solutions were varied. This analysis revealed that only the third bleed from rabbit SIE009 recognised a number of Nse2 proteins, such as 3myc-Nse2 (32 kDa) and Nse2-GFP (55 kDa) as well as the original antigen (GST-Nse2, 54 kDa), but failed to detect the endogenous protein (Figure 3.5).

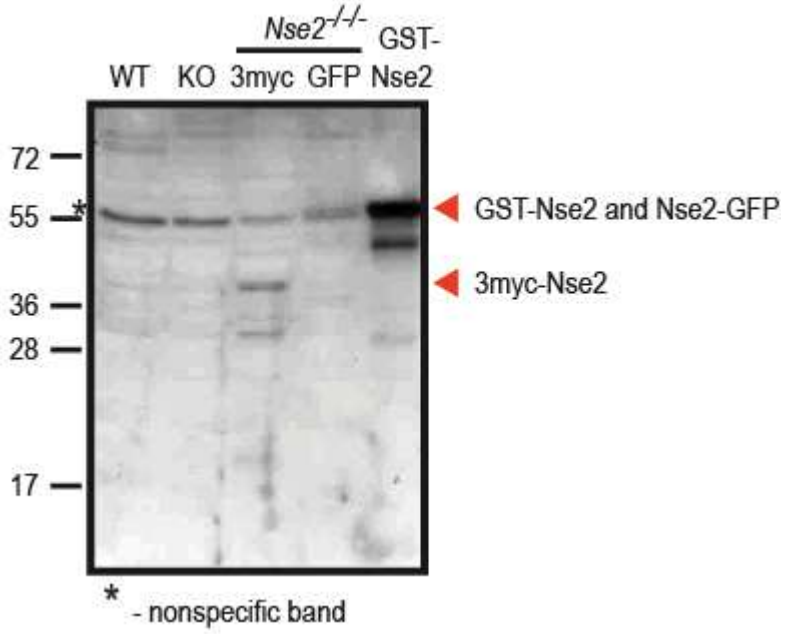

Figure 3.5 Testing of the anti-Nse2 sera.

Proteins from the indicated cell lines were extracted, separated by SDS-PAGE and analysed by immunoblotting with bleed SIE009 (K/O – Nse2$^{-/-}$, 3myc and GFP correspond to 3myc-Nse2 and Nse2-GFP expressing Nse2$^{-/-}$ cells, respectively). Predicted sizes of the recombinant Nse2 proteins are: endogenous (27 kDa), 3myc fusion (32 kDa), GFP fusion (55 kDa) and GST fusion (54 kDa).

The laddering observed in the GST-Nse2 lane probably represents products of degradation that occurred during GST-Nse2 purification. In addition, the SIE009 serum recognised a 55 kDa band in all samples analysed. This is consistent with the reactivity of the pre-immune sera from the same rabbit, which also recognised a similar band but was clean in the blot area where the chicken Nse2 is predicted to migrate (between 20 – 50 kDa, data not shown). The bleeds obtained from the second rabbit (SIE010, mainly the third bleed) were only able to recognise the antigen and free GST protein, leading to the conclusion that SIE010 bleeds contain antibodies against the GST, but not Nse2 protein (data not shown).

In order to increase the sensitivity of the SIE009 third bleed we performed affinity chromatography purification (thereafter SIE009AP, as described in section 2.3.9). The affinity purified anti-chicken Nse2 antibody was able to detect 3myc-Nse2 (32 kDa) and Nse2-GFP (55 kDa) fusions as well as the endogenous form of Nse2 (27 kDa, Figure 3.6). The SIE009AP detects only a

single band in wild-type DT40 cell lysates of the predicted size of 27 kDa, which is consistent with the presence of a single isoform of *Nse2* being expressed in DT40 cells.

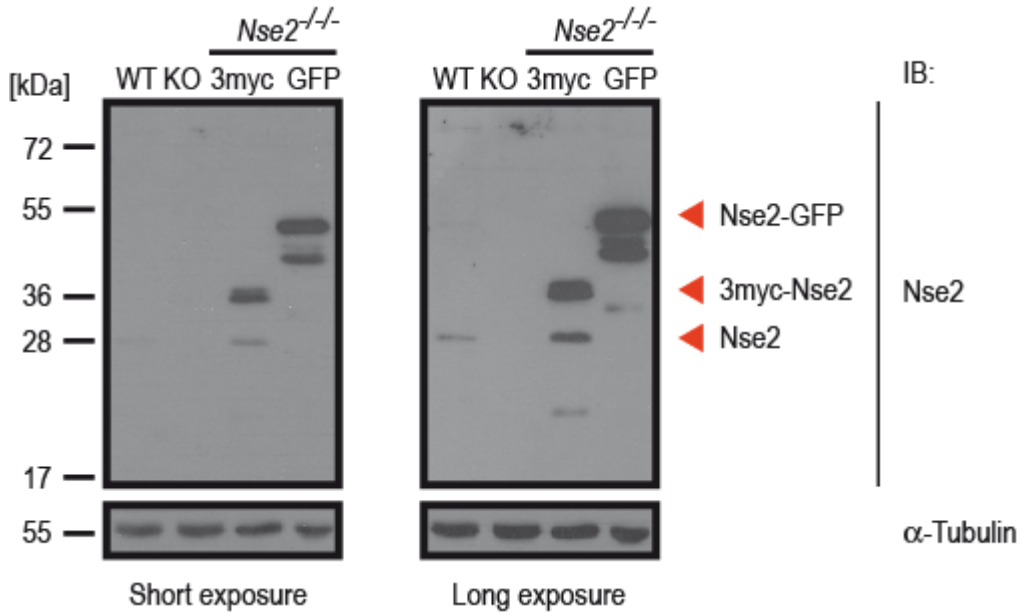

Figure 3.6 Testing of the affinity purified anti-Nse2 sera (SIE009AP).

Proteins from the indicated cell lines were extracted, separated by SDS-PAGE and analysed by immunoblotting with SIE009AP and α-Tubulin antibodies (KO – Nse2$^{-/-/-}$, 3myc and GFP correspond to 3myc-Nse2 and Nse2-GFP expressing Nse2$^{-/-/-}$ cells, respectively) Predicted sizes of the Nse2 are: endogenous (27 kDa), 3myc fusion (32 kDa), GFP fusion (55 kDa) and GST fusion (54 kDa).

Additionally, the SIE009AP antibody did not detect any endogenous protein in the *Nse2*$^{-/-/-}$ cell line (described in Chapter 4), even after prolonged exposure of the membrane or when a high protein concentration was run on a gel (up to 80 µg per lane with long-life ECL, data not shown). Therefore, we conclude that the band observed in the wild-type lane is indeed the endogenous form of the Nse2 protein. We tried to confirm the nature of the wild-type band with different antibodies. We atested a human antibody raised to full length human Nse2 protein (gift from Prof. A. Lehmann, University of Sussex, UK) but it also failed to recognise the endogenous chicken Nse2.

We next tested the SIE009AP antibody in immunofluorescence microscopy experiments using wild-type and Nse2-deficient cells as a negative

control. Different concentrations of SIE009AP antibody and fixation protocols were tested but we could not detect any signal from the endogenous Nse2 in the wild-type cells. This could be due to a low concentration of SIE009AP antibody in the purified fraction (as assayed by SDS-PAGE with BSA standards and Coomasie staining of the gel; data not shown) or an inability of the SIE009AP to detect native Nse2 protein.

3.5 Biochemical studies of myc-tagged Nse2

The myc tag is a well recognised affinity tag and widely used to purify proteins from vertebrate cells or to identify protein interactors by co-immunoprecipitation (Kramer et al., 1997). To study the biochemical properties of the Nse2 protein we generated a 3myc-Nse2 fusion protein. The chicken *Nse2* cDNA was cloned into pCMV-3Tag-2A plasmid. The size of the resultant fusion protein was predicted to be 32 kDa. The 3myc tagged form of Nse2 was then stably expressed in *Nse2*$^{-/-}$ cells (thereafter 3myc-Nse2) and used in immunoprecipitation and rescue experiments (see Figure 4.15 in section 4.3.1) As previously mentioned, Nse2 interacts with Smc5 through an extensive region on its N-terminus (Duan et al., 2009a). To test if the presence of the 3myc tag interferes with Smc5 binding we performed an immunoprecipitation experiment using anti-myc antibody as described in Section 2.3.10. In this experiment wild-type cell extract and appropriate mouse IgG antibody were used as controls. As shown in Figure 3.7, we detected Smc5 within the anti-myc precipitated material (IP lane in the 3myc-Nse2 experiment). We observed a significant depletion of the fusion protein in the unbound fraction, as shown on the Figure 3.7, lanes I and U, in the 3myc-Nse2 experiment. The signal was specific to extracts from 3myc-Nse2 cells and it was absent in wild-type and control immunoprecipitation samples. We conclude from this experiment that 3myc-Nse2 interacts with Smc5 *in vivo* and that this interaction is not impeded by the presence of an N-terminal myc tag in Nse2.

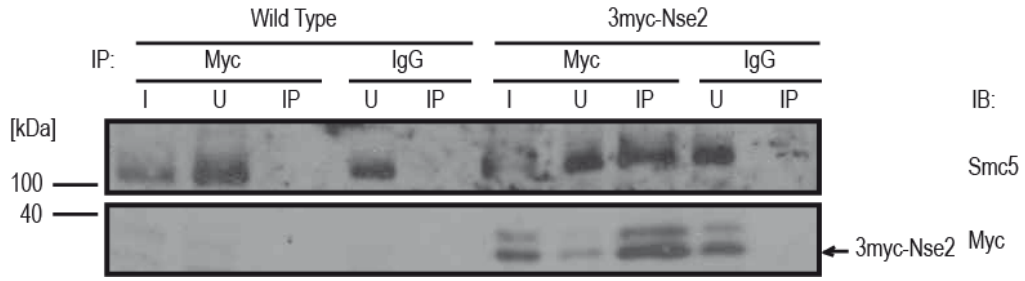

Figure 3.7 Immunoprecipitation of 3myc-Nse2.

The Nse2$^{-/-}$::3myc-Nse2 cells were subjected to immunprecipitation using anti-myc antibody. The lanes are as follows: (I) – input, (U) – unbound fraction, (IP) – immunoprecipitated material. Estimated size of 3myc-Nse2: 32 kDa.

In our immunoprecipitation experiments (Figure 3.7) we found that the anti-myc antibody recognises 3myc-Nse2 as a double band (both with size of just below 40 kDa). Similarly, the SIE009AP antibody detected two different bands in the 3myc-Nse2 cell extract (Figure 3.7 and 3.8, lane 3myc-Nse2). However, the SIE009AP antibody does not recognise a double band of the endogenous Nse2 protein in the wild-type cells even after prolonged exposure (Figure 3.6 and data not shown). We suspect that upper band might be caused by post translational modification (PTM) of the 3myc-Nse2 fusion. This PTM might not be detectable in wild-type cells due to lower levels of the endogenous protein compared to the higher levels of the 3myc-Nse2 (Figure 3.6). The best candidate for PTM of the Nse2 protein would be SUMOylation, as such automodification by the SUMO ligase has been previously reported for Nse2 (Andrews et al., 2005; Potts and Yu, 2005). However, the size difference between the observed bands appears to be less than 10 kDa which would argue against this type of modification (as well as ubiquitination).

To test whether the slower migrating band is a phospho-form, we subjected 3myc-Nse2 extracts to phosphatase assay. Figure 3.8 shows immunoblots after the experiment.

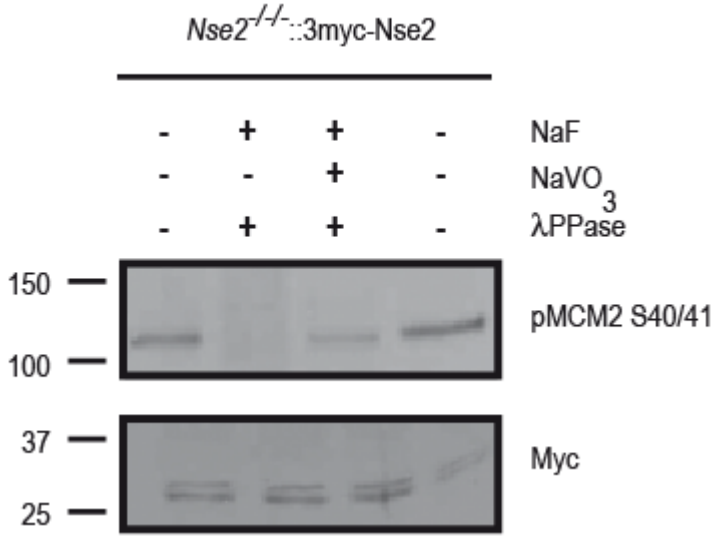

Figure 3.8 Phosphatase assay.

Proteins extracted from Nse2$^{-/-}$::3myc-Nse2 cell line were treated with different reaction cocktails (with or without activity of λPPase) to test the nature of the slower migrating band of 3myc-Nse2 protein . MCM2 phospho-protein was used here as a positive control.

We used MCM2 protein as a positive control in this experiment (Pospiech et al., 2010). The MCM2 protein, which is a part of a replicative helicase complex, is constitutively phosphorylated at S40/41 in a Cdc7-dependent manner. After phosphatase treatment, the phosphorylated MCM2 was no longer present, whereas we could still detect the 3myc-Nse2 double band after treatment with the same cocktail. Therefore we conclude that the observed extra band is not a phospho-form of the 3myc-Nse2 protein.

3.6 Localisation of chicken Nse2

To study the localisation of the Nse2 protein (and by implication the Smc5-Smc6 complex), we tagged the Nse2 protein with the green fluorescent protein (GFP). The *Nse2* cDNA was cloned into pEGFPN1 vector. The Nse2-GFP fusion protein, with a size of approximately 55.5 kDa, was then stably expressed in Nse2-deficient cells (thereafter Nse2-GFP, see Figure 4.15 in section 4.3.1**)**. The clones positive for Nse2-GFP were then used to investigate the cellular localisation of the Nse2-GFP fusion protein. Depending on the clone analysed, between 30 – 90 % of the cells were Nse2-GFP positive.

We found Nse2-GFP in both the cytoplasm and nucleus during interphase (Figure 3.19, G_1 and G_2 panels). Conversely, we did not observe any Nse2-GFP signal co-localising with DAPI-stained DNA in mitotic cells. Therefore, it would appear that localisation of the Nse2-GFP may be cell cycle dependent (Figure 3.9, metaphase and telophase panels).

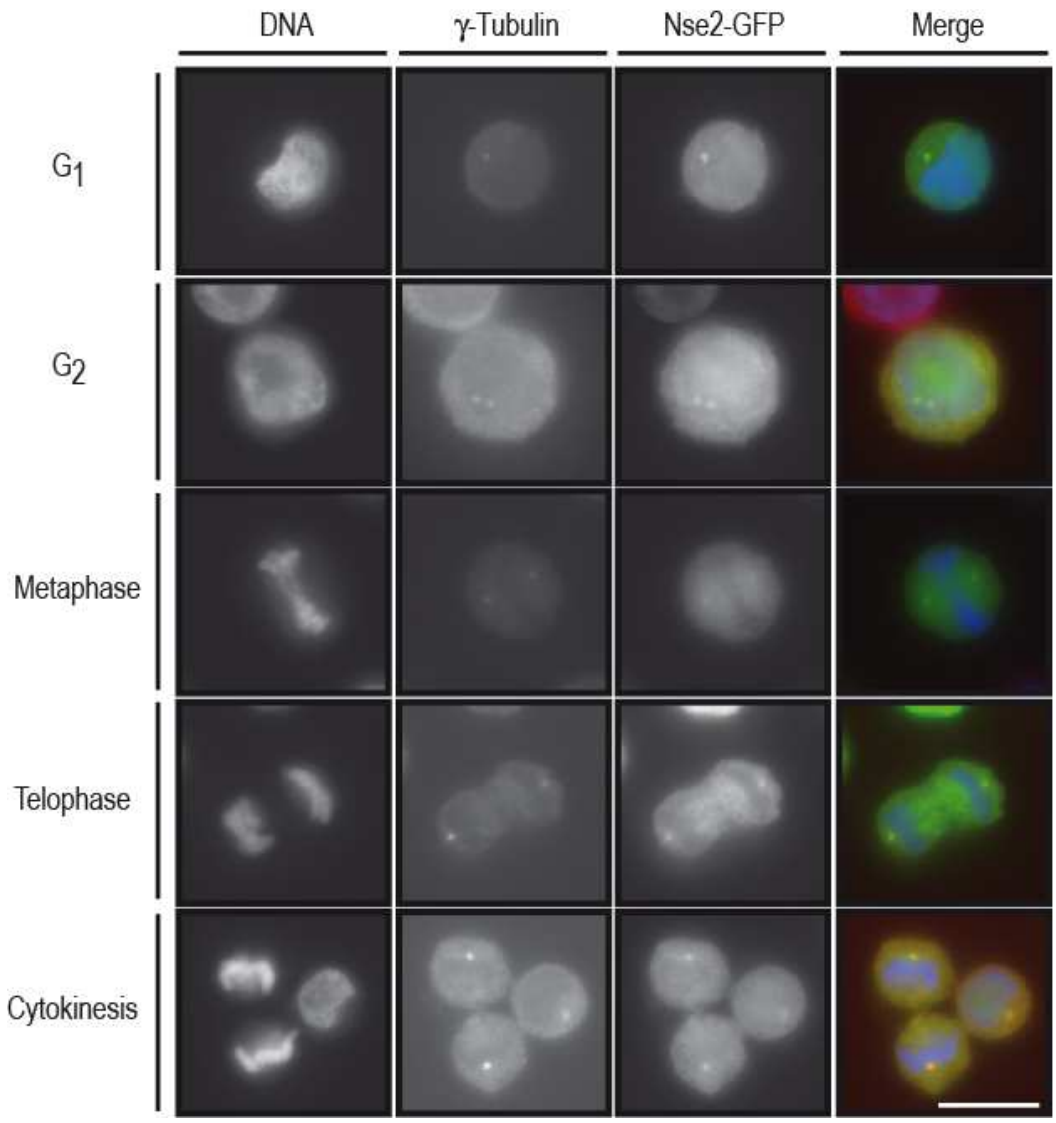

Figure 3.9 Expression of the Nse2-GFP fusion proteins.

The Nse2-GFP expressing cells were fixed with both methanol and paraformaldehyde prior to staining with γ-tubulin antibody (DNA: blue; γ-Tubulin: red; Nse2-GFP: green). Scale bar shows 10μm.

Additionally, in our preliminary analysis of Nse2-GFP expressing cells, we found a relatively large, discrete signal from the fusion protein. There were

either one or two such spots detected per cell (Figure 3.9, all panels). We also found that these foci appear to localise to opposite poles of the cell in mitotic cells (Figure 3.9 metaphase and telophase panels). We speculated that Nse2-GFP may be a component of the centrosome, as we previously detected Smc5-GFP protein localising to centrosomes (Stephan, 2007). To test our hypothesis, we counter stained the Nse2-GFP cells with a centrosome marker (γ-tubulin) and looked for co-localisation with the Nse2-GFP signal. We could confirm the centrosomal localisation of Nse2-GFP fusion protein using this approach, but only after paraformaldehyde or combined methanol/ paraformaldehyde fixation (Figure 3.9). We neither observed Nse2-GFP after only methanol fixation nor 3myc-Nse2 at the centrosome. To eliminate the possibility that Nse2-GFP localisation to centrosomes is a fixation artefact, we decided to analyse Nse2-GFP cells using the live-cell microscopy. We hypothesised that, if Nse2-GFP protein is a *bona fide* centrosomal component, we should be able to detect it in live cells. In this experiment Nse2-GFP cells were split into two batches. One batch was fixed with paraformaldehyde to confirm the observation of Nse2 at centrosomes, and the other batch was analysed by live-cell microscopy (Figure 3.10).

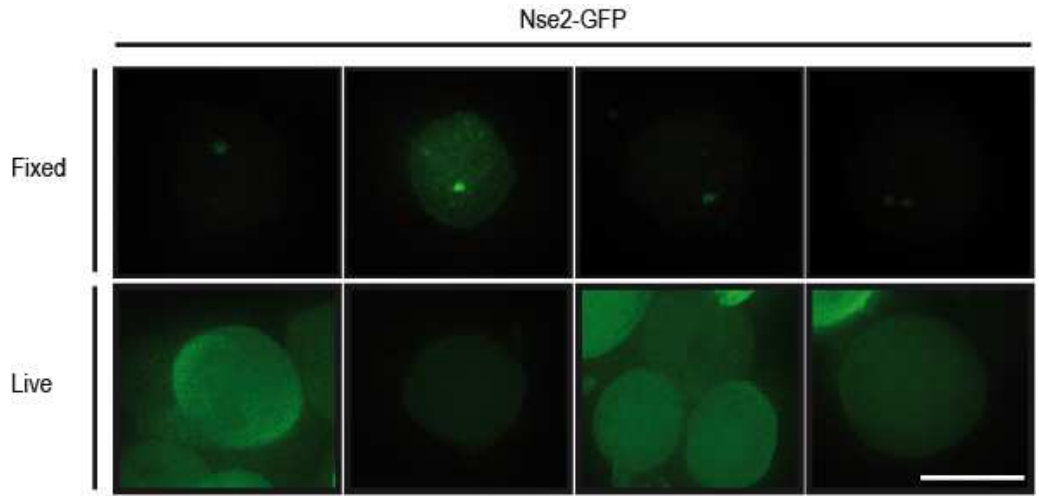

Figure 3.10 Live cell microscopy analysis of Nse2-GFP expressing cells.

The Nse2-GFP cells were either paraformaldehyde fixed or analysed live under a microscope (Nse2-GFP: green). Top panel shows paraformaldehyde fixed cells and bottom panel show stills from live cell imaging. Scale bar shows 10μm.

We could still detect the centrosomal localisation of the Nse2-GFP fusion protein in the fixed cells but never in the live cells. In addition, the live-cell analysis confirmed the cytoplasmic and nuclear localisation of the fusion protein (Figure 3.10). Therefore, we conclude that the Nse2-GFP protein may not be a constitutive component of the centrosome and that the observed localisation may be an artefact of the paraformaldehyde fixation step.

3.7 Discussion

3.7.1 Cloning of chicken *Nse2*

The chicken *Nse2* cDNA was successfully cloned allowing the generation of anti-chicken Nse2 antibodies, and preliminary biochemical and localisation analysis of the Nse2 protein. In addition, we confirmed that the predicted protein from the *G. gallus* non-redundant protein sequences database similar to *S. cerevisiae* MMS21, is indeed a chicken homologue of Nse2. We found that the size and sequence of the chicken *Nse2* cDNA are in agreement with information published in the NCBI database. Comparison of Nse2 protein sequences from different species revealed that chicken Nse2 is significantly similar to vertebrate but not to its unicellular homologues. The highest similarity has been observed in the region of Nse2 catalytic domain, which is required for Nse2 SUMO ligase activity. Despite the fact that the overall Nse2 sequence has changed from yeast to human, the sequence required for Nse2 SUMO ligase activity has been conserved throughout evolution. Additionally, the structure of the chicken *Nse2* gene is very similar to its human homologue, suggesting that the gene itself is also evolutionarily conserved, at least between chicken and human. This analysis confirmed that we have cloned the chicken homologue of Nse2 protein.

3.7.2 Generation of antisera against chicken Nse2

We have generated an anti-chicken Nse2 (SIE009AP) antibody and used it in immunoblotting experiments. The SIE009AP antibody detects the endogenous Nse2 protein as single band in wild-type DT40 cells, showing that there is only one form of Nse2 protein expressed in these cells. This is consistent

with the data from human experiments, in which a single form of Nse2 was detected in HeLa cells (Behlke-Steinert et al., 2009; Potts et al., 2006; Taylor et al., 2008). The observed size of chicken Nse2 (27 kDa) is similar to the mass predicted from its amino acid sequence. Additionally, the SIE009AP antibody does not detect any protein in the Nse2-deficient cells, confirming that indeed it is Nse2 that we are detecting in wild-type DT40 cells. Unfortunately, the SIE009AP is not able to detect Nse2 protein in immunofluorescence microscopy experiments; therefore we concluded that SIE009AP can be used only for immunoblotting.

3.7.3 Biochemical properties of myc-tagged Nse2

The cloned *Nse2* cDNA was used to generate a 3myc fusion protein to analyse chicken Nse2. The fusion protein has been successfully expressed in Nse2-deficient cells. Human Nse2 co-immunoprecipitates with Smc5, Smc6 and Nse1 (Potts and Yu, 2005; Taylor et al., 2008). We found that 3myc-Nse2 co-immunoprecipitated with Smc5, indicating that as in human cells, chicken Nse2 interacts with Smc5 *in vivo*. Furthermore, this confirms that the cDNA we have cloned codes for a component of the Smc5-Smc6 complex. The N-terminal 3myc tag on the Nse2 protein does not interfere with its binding to Smc5, suggesting that the fusion is a functional protein *in vivo.*

In our immunoblot experiments, the anti-myc antibody detects 3myc-Nse2 as a double band. Because it is expressed ectopically from the cDNA sequence it is unlikely that these represent alternative forms of Nse2. Extensive studies in yeast and human models identified post translational modification (PTM) of several components of the Smc5-Smc6 complex; Smc6 phosphorylation and Smc5, Smc6, Nse2, Nse3 and Nse4 SUMOylation (Andrews et al., 2005; Pebernard et al., 2004; Potts and Yu, 2005; Taylor et al., 2008; Taylor et al., 2001; Zhao and Blobel, 2005). The SUMO peptide is highly charged and its addition to a target protein results in an increase of observed molecular mass by 10-20 kDa. We hypothesised that the extra band may be a phospho-form of Nse2. However, phosphatase treatment did not abolish presence of the slower migrating form of 3myc-Nse2. Therefore, we concluded that the extra band is not a phosphorylated form of Nse2. In addition, the SIE009

antibody detects a double band of 3myc-Nse2 but not of the endogenous protein. This raises two possibilities; (1) myc tag is part of the protein being modified and (2) we do not detect modification of endogenous Nse2, because of its low abundance compared to over-expressed 3myc-Nse2. We believe that it is rather unlikely that the myc tag is specifically modified, as no such PTM has been reported in the literature. Therefore, we concluded that the extra band that we detected is a yet unidentified PTM of over-expressed chicken Nse2.

3.7.4 Localisation of chicken Nse2

We expressed an Nse2-GFP fusion in Nse2-deficient cells and used it to study the localisation of Nse2. Experiments in human and yeast cells have shown a nuclear localisation of Nse2 (Potts and Yu, 2007; Zhao and Blobel, 2005). We observed both cytoplasmic and nuclear localisation of the Nse2-GFP. In interphase cells, Nse2-GFP co-localised with the DNA signal but not in mitotic cells, suggesting a cell cycle-dependent localisation of Nse2. We also detected a centrosomal localisation of the Nse2 protein, which has not been previously reported. To confirm our observation we performed a set of experiments which suggest that this localisation of Nse2-GFP may be an artefact of paraformaldehyde fixation. We believe that the relatively abundant Nse2-GFP protein can be detained at the centrosome through pareformaldehyde cross-linking activity. In addition, we have not detected 3myc-Nse2 at the centrosome. However, we cannot rule out the possibility that Nse2 is present at the centrosomes, but that our microscopy experiments performed failed to reveal such localisation. We have observed 9myc-Smc5 and Smc6-GFP localisation at centrosomes, suggesting that Nse2 might be present at this organelle (Stephan, 2007). Recently, the human cohesin complex has been found on the centrosomes (Guan et al., 2008). The Smc5-Smc6 complex co-localises with cohesin at chromosomes and has been reported to be required for cohesin recruitment to double strand breaks (Lindroos et al., 2006; Potts et al., 2006). In addition, both complexes share a similar chromatin loading mechanism which relies on interaction with the Scc2/Scc4 heterodimer (Lindroos et al., 2006; Michaelis et al., 1997). This suggests that, similar to the cohesin complex, Smc5-Smc6 complex may be a component of the centrosome.

Chapter 4 Generation and characterisation of *Nse2* knockout cells

4.1 Chicken *Nse2* is not essential for DT40 cell viability

4.1.1 Introduction

The structural maintenance of chromosomes (Smc) family of proteins is involved in different pathways of DNA metabolism (reviewed in (Hirano, 2002)). They are required for sister chromatid cohesion, chromosome condensation and DNA repair (reviewed in (Losada and Hirano, 2005)). The cohesin (Smc1-Smc3), condensin (Smc2-Smc4), Smc5-Smc6 complex and Rad50 make up the eukaryotic Smc family (reviewed in (Hirano, 2006)). Processes involving the Smc1-Smc3 and Smc2-Smc4 heterodimers, as well as the Rad50 protein are well explored, whereas the functions of the Smc5-Smc6 complex remain less well-defined. The Smc5-Smc6 complex is made up of eight proteins: the core Smc5 and Smc6 and six non-Smc elements (Nse1 - 6) (Duan et al., 2009b; Lehmann et al., 1995; Palecek et al., 2006; Pebernard et al., 2004; Pebernard et al., 2006; Taylor et al., 2008; Zhao and Blobel, 2005). One of these elements, Nse2, is a small 27 kDa protein that interacts directly with the core Smc5 *in vivo* (Andrews et al., 2005; McDonald et al., 2003; Pebernard et al., 2004). Nse1 and Nse2 are the only non-Smc elements of the Smc5-Smc6 complex that possess known enzymatic activities. Nse1 is an ubiquitin ligase with an *in* vitro enzymatic activity confirmed so far and Nse2 is an *in vitro* and *in vivo* functional E3 SUMO ligase (Andrews et al., 2005; Doyle et al., 2010; McDonald et al., 2003; Potts, 2009; Zhao and Blobel, 2005). Nse2 SUMOylates several proteins, including Ku70, Smc5, Smc6, Scc1, as well as the telomere sheltering proteins Trf1 and Trf2 (Andrews et al., 2005; Pebernard et al., 2004; Potts and Yu, 2005; Zhao and Blobel, 2005). Nse2, also known as MMS21, was first identified as an essential protein required for responses to MMS-induced DNA damage (Prakash and Prakash, 1977). A large body of data indicates that this E3 SUMO ligase is essential for proper homologous recombinational repair,

replication fork restart and maintenance of repetitive DNA sequences, such as rDNA and telomeres (reviewed in (Potts, 2009) and (De Piccoli et al., 2009)). The analysis of the recombination intermediates induced by DNA damage in budding and fission yeast revealed that SUMO ligase activity of Nse2 is required for efficient removal of X-shaped DNA molecules that arise at stalled replication forks, probably through recombination (Ampatzidou et al., 2006; Branzei et al., 2006; Chavez et al., 2010b). Recently, Rai et al. showed that Nse2 activity is required to prevent gross chromosomal rearrangements (Rai et al., 2011). All this suggests that Nse2 SUMO ligase plays a crucial role in orchestrating DNA damage responses and the maintenance of genomic integrity. In addition, SUMOylation has recently emerged as an important modification in DNA damage response and repair (reviewed in (Bergink and Jentsch, 2009)). As most of the information gathered about Nse2 comes from the analysis of unicellular organisms, we wondered if the vertebrate homologue possesses similar cellular functions.

To better understand the cellular functions of Nse2 we decided to use a reverse genetics approach**.** We chose a well-established knockout system, namely the chicken DT40 cell line. This hyper-recombinogenic chicken cell line allows high efficiency gene targeting (Buerstedde and Takeda, 1991). We mapped the genomic locus of chicken *Nse2* on chromosome two, we cloned and sequenced the *Nse2* cDNA and confirmed its correspondence with the NCBI database information. We used this knowledge to generate *Nse2*$^{-/-/-}$ knockout clones in chicken DT40 cells to analyse the roles of Nse2 in the cell cycle and in the DNA damage response. In this study, we show that chicken cells lacking Nse2 are viable but hypersensitive to DNA damage and exhibit defects in homologous recombinational repair.

4.1.2 Cloning and mapping of the chicken *Nse2* genomic locus

As described in section 3.2, we have identified and cloned the chicken *Nse2* cDNA and used it to localise its genomic locus. We found that *Nse2* is located on chromosome two (NCBI accession number NC006089 Region 144363623 - 144490094). DT40 cells have a trisomy of chromosome II, therefore there are three copies of *Nse2* in these cells. As mentioned previously,

comparison between the chicken and human *Nse2* genes revealed that they both consist of six exons and are spread over 122.6 kb and 264.6 kb, respectively. The sizes of chicken and human *Nse2* loci were found by alignment of the respect cDNAs and genomic sequences.

4.1.3 Targeting of the chicken *Nse2* locus

As previously mentioned the *Nse2* gene spreads over 122.6 kb. The gene targeting efficiency drops proportional to the size of the targeting region (Capecchi, 1989). Due to this we could not use the traditional approach and disrupt the whole genomic sequence of the *Nse2* gene. The LoxP-Cre recombinase approach to remove the entire *Nse2* gene was not used because of the disadvantages of this system presented in Section 1.12.4 of the Introduction. However, exons IV, V and VI, which code for the catalytic domain of the *Nse2* SUMO ligase (SP-RING) could be easily targeted using a standard knockout strategy as they are spread over only 4.3 kb (Figure 4.1)

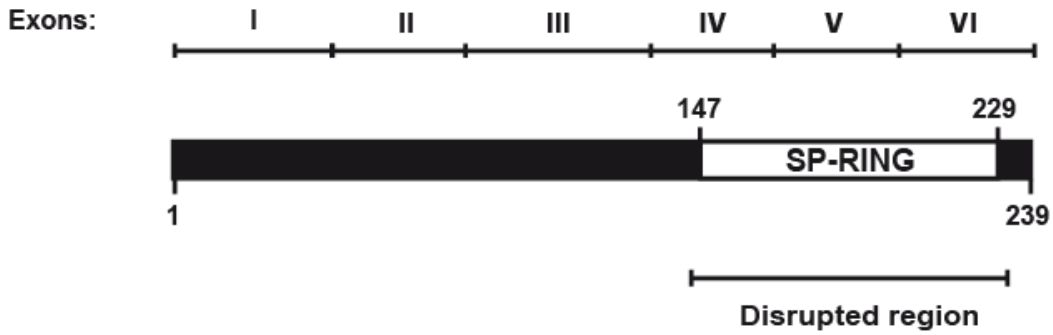

Figure 4.1 Linear structures of the Nse2 gene and protein.
The alignment of the Nse2 exons and protein showing the region to be disrupted. Exons and protein are to scale.

After identification of the genomic sequence encoding the Nse2 SP-RING domain, the targeting strategy was designed (Figure 4.2). Homology arms (5' – 3.0 kb and 3' – 4.5 kb) and probes were chosen to facilitate *Nse2* gene disruption and detection of the desired mutation by Southern blot.

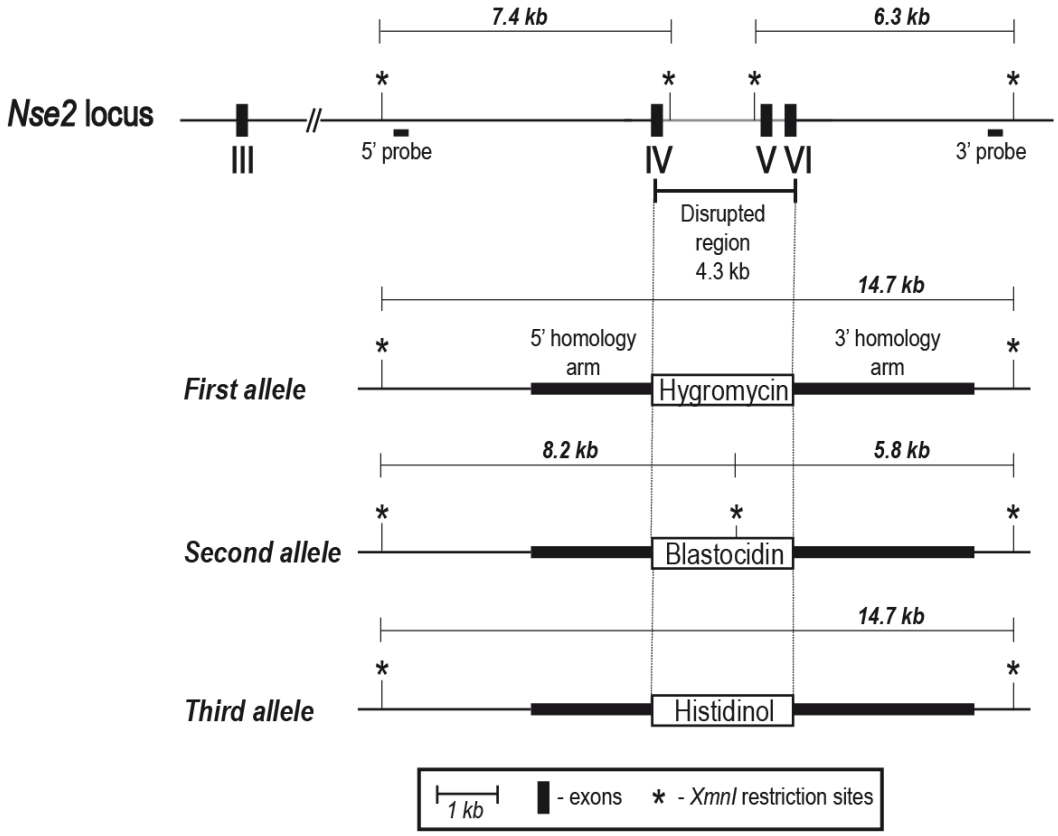

Figure 4.2 Gene targeting strategy.

The Nse2 genomic locus before and after targeting with the targeting vectors. The bold italic numbers show distances between XmnI sites as well as the sizes of bands recognised with either the 5' or 3' probes by Southern blot.

Targeting vectors containing blastocidin, histidinol and hygromycin resistance cassettes were generated in order to disrupt the desired region (Figure 4.2). Before DT40 wild-type cells were transfected with the targeting vectors, the 5' and 3' probes (Figure 4.2) were tested by radioactive Southern blot (as described in Section 2.2.13).

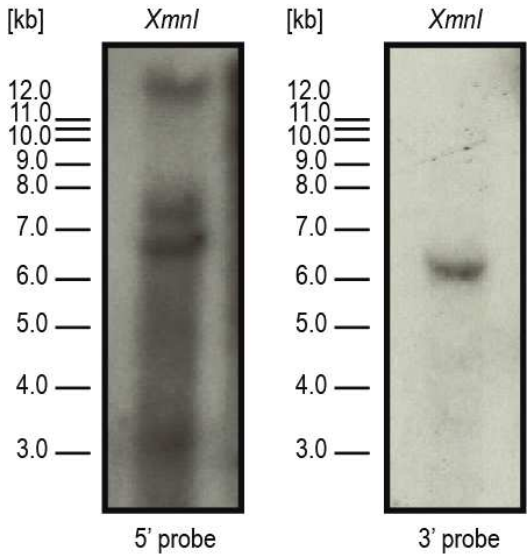

Figure 4.3 Testing of the radiolabelled 5' and 3' probes by Southern blot hybridization.
Genomic DNA was digested with the indicated restriction nucleases and probed with 5' or 3' probes.

We found that both probes recognised the predicted bands after digestion with *XmnI* (Figure 4.3). Moreover the 3' probe had far less background signal than 5' probe which also picks up unspecific bands (Figure 4.3). Therefore the 3' probe was chosen for the screening of targeted clones.

After probe optimisation, wild-type DT40 cells were transfected with each targeting vector using electroporation (as described in section 2.4.3). A total of 160 clones were screened after targeting of the first allele with blastocidin, histidinol and hygromycin vectors. The plasmids showed different targeting frequencies ranging from 18.0% to 27.0% (Table 4.1 and Figure 4.4).

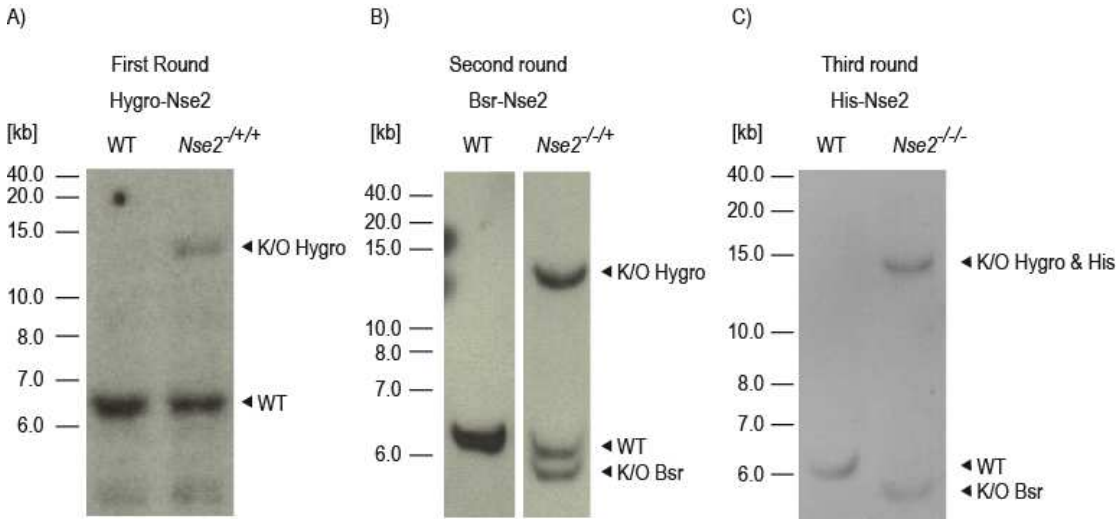

Figure 4.4 Southern blot analysis of representative clones.

Genomic DNA from wild-type and the indicated heterozygotes was isolated and digested with XmnI. The 3'probe was used to detect targeting events at each stage of Nse2 gene targeting A) first allele, B) second allele and C) third Nse2 allele. The 3' probe recognised wild-type bands (6.3 kb) and two targeted bands (K/O indicates the targeted band with 14.7 kb after transfection with Hygromycin- and Histidinol-containing vectors; and 5.8 kb after transfection of Blastocidin). The wild-type band is absent in the $Nse2^{-/-/-}$ cells and is replaced by two targeted bands.

Table 4.1 Targeting frequencies of the targeting vectors used at different stages of the Nse2 knockout generation.

First targeting round			
Targeting construct	**Hygro-Nse2**	**Bsr-Nse2**	**His-Nse2**
No. of clones screened	35	61	70
No. of targeted clones	8	11	19
Targeting efficiency (%)	22.8	18.0	27.0
Second targeting round			
Targeting construct		**Bsr-Nse2**	
No. of clones screened		72	
No. of targeted clones		5	
Targeting efficiency (%)		6.9	
Third targeting round			

Targeting construct	His-Nse2
No. of clones screened	72
No. of targeted clones	5
Targeting efficiency (%)	6.9

Transfection with the hygromycin targeting vector gave the lowest number of viable clones, so it was used to target the first allele (Figure 4.4). One of the hygromycin resistant heterozygotes (22.8% efficiency) was then targeted with the blastocidin vector, yielding double heterozygotes with 6.9% efficiency (Figure 4.4). The histidinol vector, which had the highest targeting frequency, was used last in order to increase the possibility of obtaining a knockout cell line. In the final targeting step, 72 clones were screened and 5 clones were identified as positives (6.9% targeting efficiency) (Figure 4.4). Figure 4.4 shows Southern blot hybridization performed at each stage of *Nse2* gene targeting. Each vector that was successfully integrated into the *Nse2* locus gave the band sizes predicted by the targeting strategy (Figure 4.4).

To confirm the Southern blot results and the disruption of *Nse2* gene, we isolated total mRNA from wild-type and Nse2-targeted cells, and performed reverse transcriptase-polymerase chain reaction (RT-PCR) using two different sets of primers (Figure 4.5). β–actin primers were used as a positive control in this experiment (Figure 4.5). RT-PCR analysis revealed that full length *Nse2* mRNA is present in the wild-type cells but not in the knockout clones tested. We also found that the 5' part of the *Nse2* gene, which has not been disrupted, is still transcribed and its mRNA is detectable in the knockout clones.

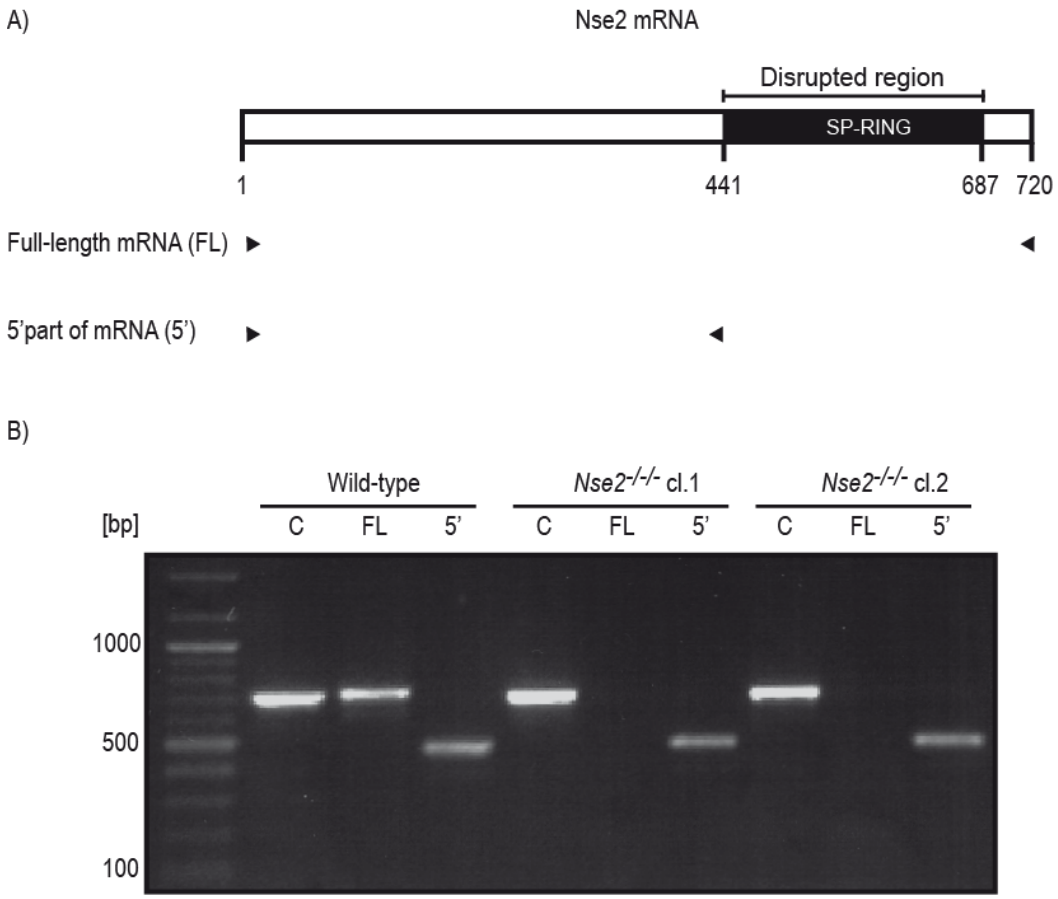

Figure 4.5 Amplification of the Nse2 cDNA from the wild-type and Nse2-targeted cells.
A) Linear representation of Nse2 mRNA showing the disrupted region of Nse2 gene and the position of the primers used to test expression of full-length and truncated forms of Nse2 mRNA. B) Reverse transcriptase-polymerase chain reaction with total mRNA isolated from the wild-type, two Nse2-targeted clones and primers shown in panel A).

To determine whether the generated cell line is indeed a knockout or represents just a deletion of SP-RING domain, we examined Nse2 protein levels in these cells. We have generated an antibody to the full-length chicken Nse2 protein (as described in Section 3.3) and used it in immunoblotting experiments. As shown in Figure 4.6, the full length Nse2 protein is only present in the wild-type cells but not in the *Nse2* knockout cell line.

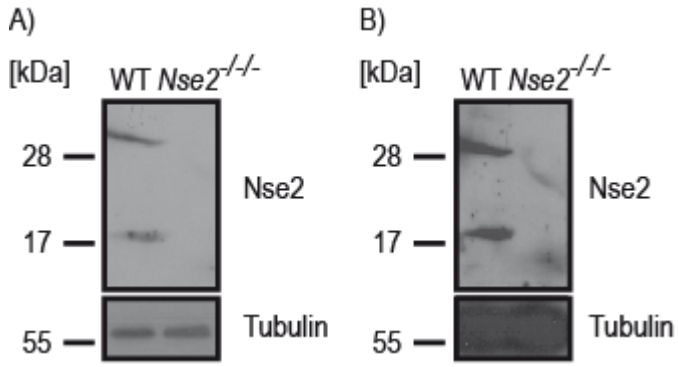

Figure 4.6 Western blot analysis of the Nse2-targeted cell line.

Total proteins from wild-type and Nse2-targeted cells were separated by SDS-PAGE and subjected to immunoblotting with the indicated antibodies A) short exposure and B) prolonged exposure.

We failed to detect the Nse2 protein in the knockout cells even after prolonged exposure (Figure 4.6B). Furthermore, there was no evidence for the explanation of a truncated form of the protein from the remaining 5' region of *Nse2*. Such a gene product would have been predicted to have a molecular weight of 18 kDa. We also detected an extra lower band in the wild-type cells (approximately 17 kDa). We predict that this band may be a degradation product of the-full length Nse2 protein. This suggests that the *Nse2*$^{-/-/-}$ cell line is a full knockout and not a deletion mutant.

Together, analysis of the *Nse2* knockout cells at the DNA, mRNA and protein levels confirm that we have successfully generated an Nse2-SP-RING-deficient DT40 cell line.

4.2 Chicken Nse2 is required for proper mitosis and DNA repair

Deletion of the *Nse2* gene in yeast cells results in non-viable cells (Andrews et al., 2005; McDonald et al., 2003; Pebernard et al., 2004; Zhao and Blobel, 2005). Similar results are observed in mutants of other components of the Smc5-Smc6 complex. *Nse1-4, Smc5* and *Smc6* are essential in *S. pombe* and *S. cerevisiae*, but *Nse5-6* are also required for the viability of budding yeast (Ampatzidou et al., 2006; Andrews et al., 2005; Lehmann et al., 1995; Palecek et

al., 2006; Pebernard et al., 2006; Taylor et al., 2001; Verkade et al., 1999). Hypomorphic alleles of the yeast *Nse2* gene are viable but show growth retardation (Andrews et al., 2005; Zhao and Blobel, 2005). This suggests that essential function of the yeast Nse2 protein is not associated with its enzymatic activity. On the other hand *Nse2* is not essential in *Arabidopsis* or human cells (Potts et al., 2006; Watanabe et al., 2009). Unexpectedly, the chicken *Nse2* knockouts are viable, indicating that *Nse2* is not an essential gene in DT40 cells. To test if the absence of *Nse2* had an impact on cell proliferation, we analysed the proliferation of Nse2-deficient cells. In this assay, an identical number of cells were plated and the accumulative cell number monitored every 24 hours for up to 48 hours. Figure 4.7 shows the growth curve of wild-type and two *Nse2* knockout clones.

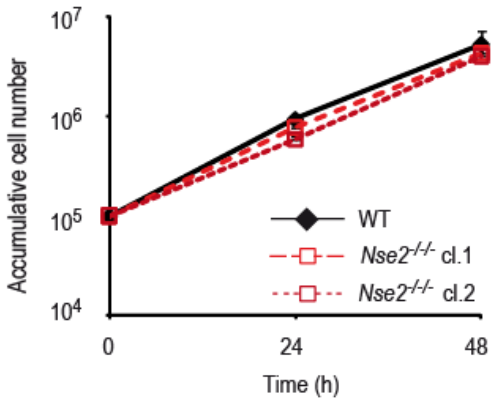

Figure 4.7 Growth curves of the knockout cells.

The same number of cells (10^5 per ml) was seeded and cell number monitored over 48 hours time period. Data points show mean of three independent experiments +/- SD.

This experiment revealed that *Nse2* knockout clones proliferate with kinetics similar to wild-type cells. Therefore, we concluded that *Nse2* is not required for the proliferation of DT40 cells. This suggests that there are fundamental differences between uni- and multi-cellular organisms in their requirement for the Smc5-Smc6 complex.

We then analysed the cell cycle profile of Nse2-deficient cells. Hypomorphic alleles of Smc5-Smc6 complex genes do not show notably affected cell cycle profiles in fission yeast *smc6-X*, *smc6-74* and budding yeast *smc6-9* (Ampatzidou et al., 2006; Irmisch et al., 2009; Outwin et al., 2009; Torres-Rosell

et al., 2005b; Torres-Rosell et al., 2007). Apart from a slight increase in number of dead and mitotic cells, deletion of S*mc5*$^{-}$ in chicken DT40 cells does not result in abnormal cell cycle profiles (Stephan et al., 2011a). Depletion of Nse2 and Smc5 but not Smc6 in HeLa cells significantly increases the number of mitotic cells (Behlke-Steinert et al., 2009). Using flow cytometry, we observed wild-type distribution of cells in different phases of the cell cycle in the absence of *Nse2* (Figure 4.8A).

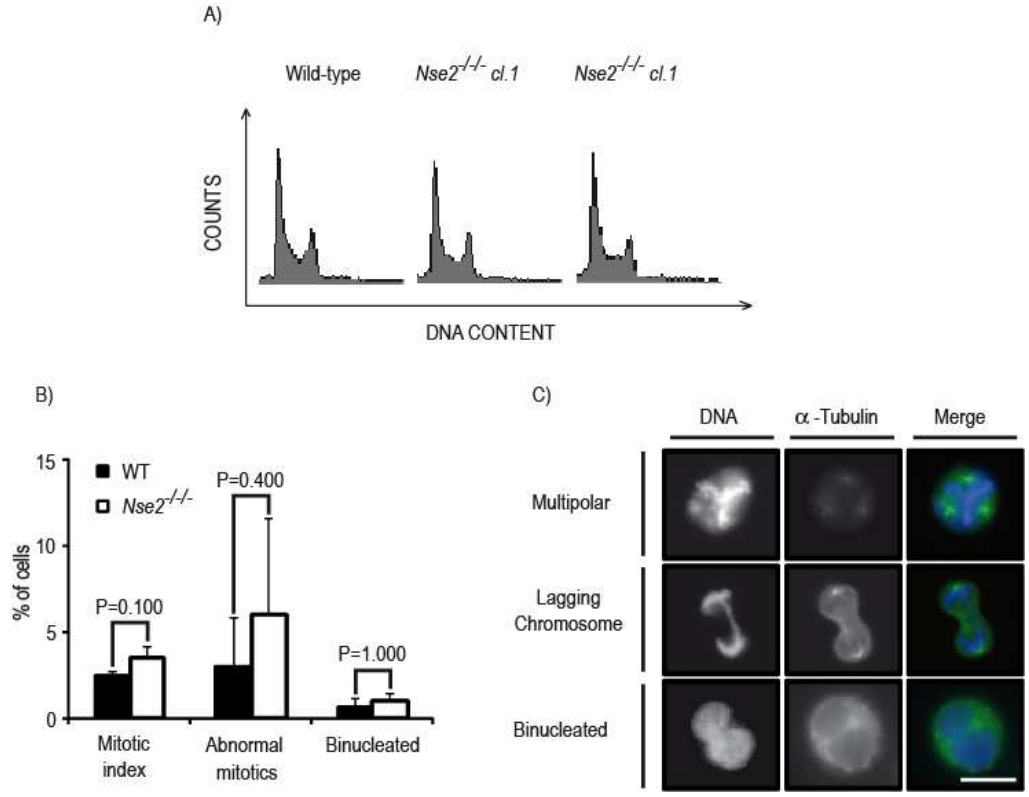

Figure 4.8 Cell cycle analysis.

(A) Cell cycle profiles of clones. (B) Levels of mitotic indices, aberrations and binucleated cells in wild-type and two Nse2$^{-/-}$ clones. Data points represent an average of three experiments +/- SD where at least 100 mitotic cells were scored. (C) Micrographs of mitotic aberrations observed in Nse2$^{-/-}$ mutants. Scale bar shows 10 μm.

Microscopy analysis of the cell cycle revealed increased numbers of mitotic cells in the *Nse2*$^{-/-}$ background (Figure 4.8B). We also detected a higher percentage of cells showing mitotic abnormalities such as multipolarity or lagging chromosomes (anaphase bridges) (Figure 4.8B and C). This is consistent with results from yeast and human cells where Nse2 deficiency is associated with

mitotic abnormalities, including chromosome mis-segregation, 'cut' phenotype or premature chromosome segregation (Behlke-Steinert et al., 2009; Chavez et al., 2010b; Chen et al., 2009; Torres-Rosell et al., 2005a; Torres-Rosell et al., 2007; Verkade et al., 1999). These data together suggest that while Nse2 function is not necessary for normal cell proliferation, but may be required for proper mitotic progression.

4.2.1 Analysis of Smc5-Smc6 complex stability

Nse2 is a component of the high molecular weight Smc5-Smc6 complex (Andrews et al., 2005; McDonald et al., 2003; Pebernard et al., 2004; Potts and Yu, 2005; Sergeant et al., 2005). It interacts with the complex through binding to Smc5 (Duan et al., 2009a). Our group has recently reported the loss of Smc6 and Nse2 upon disruption of *Smc5* (Stephan et al., 2011a).

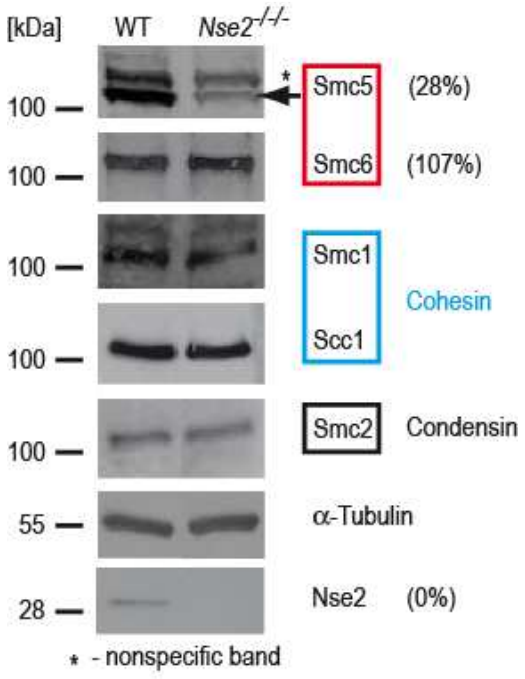

Figure 4.9 Western blot analysis of Smc complexes in Nse2$^{-/-}$ background.

Total proteins from wild-type and Nse2-deficient cells were extracted, separated by SDS-PAGE and analysed by immunoblotting with the indicated antiobodies. Numbers in brackets show the percentage of wild-type levels of each protein in Nse2-deficient cells.

We did not observe down-regulation of cohesin or condensin components in *Smc5*$^{-}$ cells, therefore we concluded that the disruption of *Smc5* specifically affects the Smc5-Smc6 complex (Stephan et al., 2011a). A similar effect was observed after the depletion of Nse2 and Smc6 by siRNA in human cells (Taylor et al., 2008). To test whether loss of Nse2 protein has a similar effect on the stability of the Smc5-Smc6 complex, we analysed the levels of Smc5 and Smc6 in *Nse2*$^{-/-}$ cells by immunoblotting (Figure 4.9).

Consistently, this analysis revealed a significant depletion of Smc5 protein in the absence of *Nse2*, whereas levels of Smc6 protein remain unchanged. In addition, we did not detect any change in the levels of the cohesin (Smc1 and Scc1) or condensin (Smc2) complexes, confirming the destabilisation of only the Smc5-Smc6 complex upon *Nse2* deletion (Figure 4.9). As Nse2 and Smc5 interact directly *in vivo*, we propose that the stability of Smc5, but not Smc6, requires the binding of Nse2.

4.2.2 Cell cycle checkpoint analysis

Yeast *Smc5-Smc6* mutants are proficient in G_2 phase checkpoint activation after MMS and UV treatment but fail to maintain the arrest. These mutants are also proficient in the S phase checkpoint (Ampatzidou et al., 2006; Bermúdez-López et al., 2010; Irmisch et al., 2009; Lee et al., 2007; Sollier et al., 2009). To test the function of chicken Nse2 in cell cycle checkpoint activation, we examined wild-type and Nse2-deficient cells after 12 hours' treatment with hydroxyurea (G_1/S and S phase checkpoints) or nocodazole (spindle assembly checkpoint). Cells were then released from the block and harvested at different time points post-recovery. Using flow cytometry we found that *Nse2* mutants are as proficient as wild-type in activation of HU- and nocodazole-induced cell cycle checkpoints (Figure 4.10).

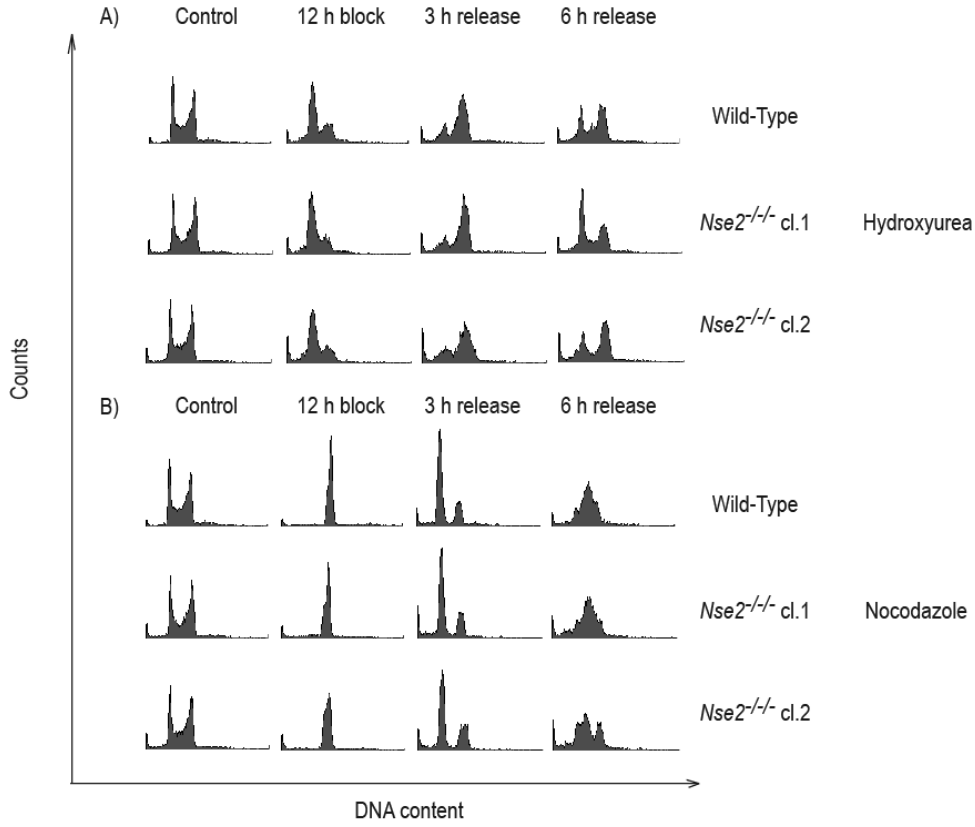

Figure 4.10 Analysis of cell cycle checkpoints.

Wild-type and Nse2-deficient cells were treated with HU (1 mM) and, nocodazole (1 mM) in order to induce G_1/S and spindle assembly checkpoints. After checkpoint induction cells were released from the block and their DNA content was analysed by flow cytometry at the indicated times post-release.

The mutant cell lines were efficiently blocked in either G_1/S phase after indirect inhibition of DNA synthesis or in metaphase after the depolymerisation of microtubules. We also did not observe abnormalities in recovery from S phase and spindle assembly checkpoints and therefore we concluded that Nse2 is not required for HU- and nocodazole-induced cell cycle checkpoint activation and cell cycle progression upon recovery, at least under our experimental conditions. We also tested whether Nse2-deficient cells arrest at the G_2/M border after IR treatment (Figure 4.11).

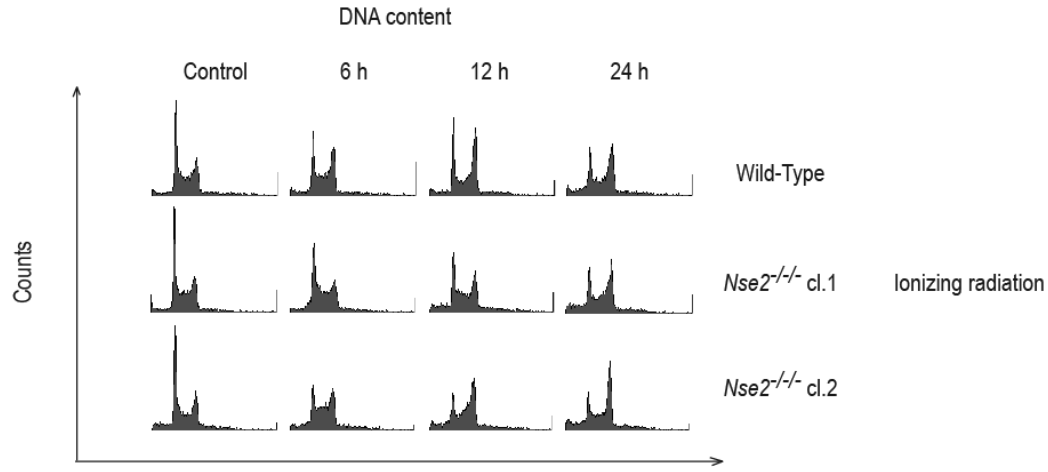

Figure 4.11 Analysis of G_2/M checkpoint activation.

Wild-type and Nse2 deficient cells were treated with IR (2 Gy). Cells were harvested and their DNA content was analysed by flow cytometry at the indicated times post-treatment.

We observed lower levels of G_2/M arrested cells in the *Nse2* mutants compared to wild-type cells at 6 and 12 hours after exposure to IR (Figure 4.11). However similar numbers of G_2/M cells in *Nse2*$^{-/-/-}$ knockouts and wild-type cells were detected at 24 hours post-IR treatment. This suggests that Nse2-deficient cells induced G_2/M arrest but with delayed kinetics compared to wild-type cells. The observed delay in cell cycle progression of Nse2-deficient cells after IR treatment suggests a potential role of Nse2 in the activation of the G_2/M checkpoint.

4.2.3 Role of Nse2 in DNA repair

A function for Nse2 protein in DNA repair was first identified in yeast during a screen for MMS-sensitive mutants (Prakash and Prakash, 1977). It was not clear how Nse2 mediates cellular responses to MMS-induced DNA damage until it was shown to be a part of a high molecular weight DNA repair complex (McDonald et al., 2003; Zhao and Blobel, 2005). Hypomorphic alleles of *Nse2* show increased sensitivity towards cis-platin, HU, IR, MMS and UV, indicating that it has a role in different pathways of the DNA damage response and DNA repair such as post-replicative DNA damage repair (PRR) (Andrews et al., 2005; McDonald et al., 2003; Pebernard et al., 2004; Potts, 2009; Potts and Yu, 2005). X-shaped molecules accumulate in Nse2-deficient cells as a consequence of

defect in DNA repair and these cells progress into mitosis in the presence of unrepaired DNA lesions (Bermúdez-López et al., 2010; Chavez et al.; Chavez et al., 2010b; Chen et al., 2009; Sollier et al., 2009; Zhao and Blobel, 2005).

We next investigated the role of chicken Nse2 in the DNA damage response and DNA repair. To do so, we performed clonogenic survival assays on wild-type and Nse2-deficient cells. The cells were treated with various DNA damaging agents, plated in methylcellulose media and allowed to form colonies (as described in Section 2.4.9). Figure 4.12 shows the sensitivity of Nse2-deficient cells to different types of DNA damage. We found that *Nse2*$^{-/-}$ cells were severely sensitive to MMC (~100 fold), MMS (~100 fold), 4NQO (4-nitroquinoline-1-oxide, ~100 fold) and moderately to UV (~10 fold) (Figure 4.12C, D, E, F). *Nse2* mutants form colonies with wild-type ability after HU and IR treatment (Figure 4.12A and B). RNAi depletion of Nse2 in human cells results in a DNA repair defect after MMS treatment, observed only in G_2 cells (Potts and Yu, 2005).

Yeast mutants of Nse2 are sensitive to IR (*nse2-1*, *nse2-SA*) (Andrews et al., 2005; Pebernard et al., 2004), UV (*mms21-11*, *mms21-Δsl*, *nse2-1*, *nse2-SA*) (Andrews et al., 2005; McDonald et al., 2003; Pebernard et al., 2004; Rai et al., 2011; Zhao and Blobel, 2005), MMS (*mms21-11*, *mms21-Δsl*, *mms21-CH*, *nse2-SA)* (Andrews et al., 2005; Rai et al., 2011; Sollier et al., 2009; Zhao and Blobel, 2005), HU (*mms21-Δsl*, *mms21-H202A*, *mms21-C221A*, *nse2-SA)* (Andrews et al., 2005; Rai et al., 2011) and bleomycin (*mms21-11*, *mms21-Δsl*) (Rai et al., 2011; Zhao and Blobel, 2005). The sensitivity of chicken Nse2-deficient cells towards MMC, MMS, UV and 4NQO is consistent with the reported yeast phenotypes. Surprisingly, our *Nse2* mutants are not sensitive to IR or HU, suggesting differences between the requirements for Nse2 in response to these DNA damaging agents in chicken and yeast. These data show that chicken Nse2 protein is required for robust response to DNA damage agents, such as MMC, MMS, UV and 4-NQO that couse replication fork stalling at the lesions they induce.

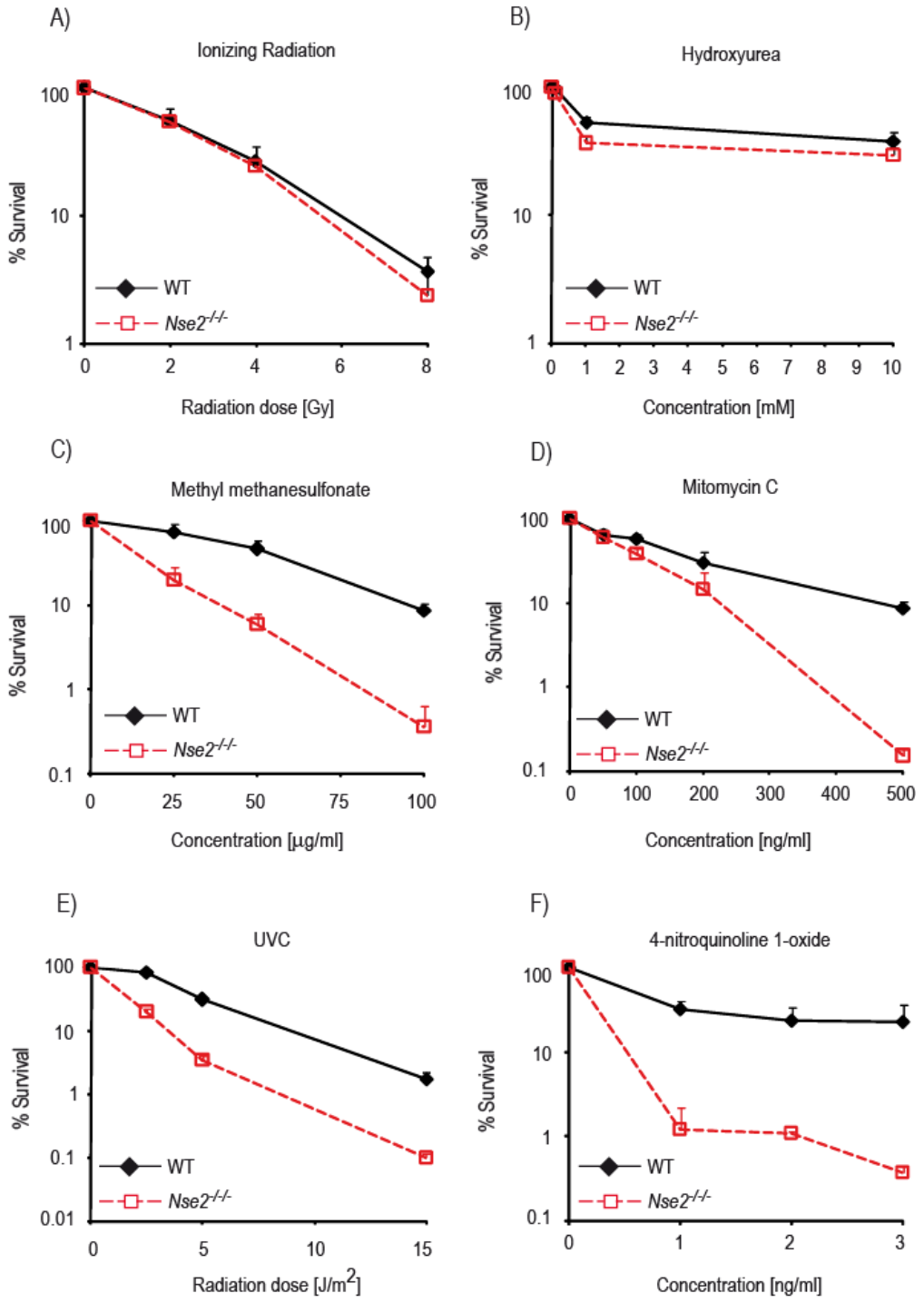

Figure 4.12 Cell survival after induction of DNA damage.

Wild-type and Nse2$^{-/-}$ cells were irradiated or treated with the indicated DNA damaging agents for 2 hours and plated in methylcellulose. Colonies were scored 10-14 days after plating. In the case of IR, cells were exposed to the IR source in the methylcellulose plates. The plots show the mean +/- S.D from three independent experiments normalised to the untreated controls. Plating efficiencies were wild-type, 80%; Nse2$^{-/-}$, 67%.

4.2.4 Role of Nse2 in the maintenance of genomic integrity

Defects in DNA repair may result in loss of essential genetic information. Unrepaired lesions can lead to severe chromosomal rearrangements such as deletions, insertions or translocations (Friedberg, 2003; Harper and Elledge, 2007). Such genome modifications are characteristic of many cancer cells (Friedberg, 2003; Sancar et al., 2004). Gross chromosomal rearrangements were observed in the absence of functional Smc5-Smc6 complex in yeast cells, suggesting that the activity of this complex prevents major chromosomal defects (Hwang et al., 2008). Sister chromatid recombination between two *leu2* repeats located on a single copy plasmid was reduced compared to wild-type cells in *S. cerevisiae smc6-9* and *nse5-1* mutants (De Piccoli et al., 2006). *mms21-Δsl* mutants show an elevated frequency of telomere marker loss (Rai et al., 2011). As the chicken Nse2 protein is required for DNA repair we asked whether it is also involved in the maintenance of genomic stability. To investigate this idea, we compared the integrity of wild-type and *Nse2*$^{-/-/-}$ chromosomes before and after DNA damage.

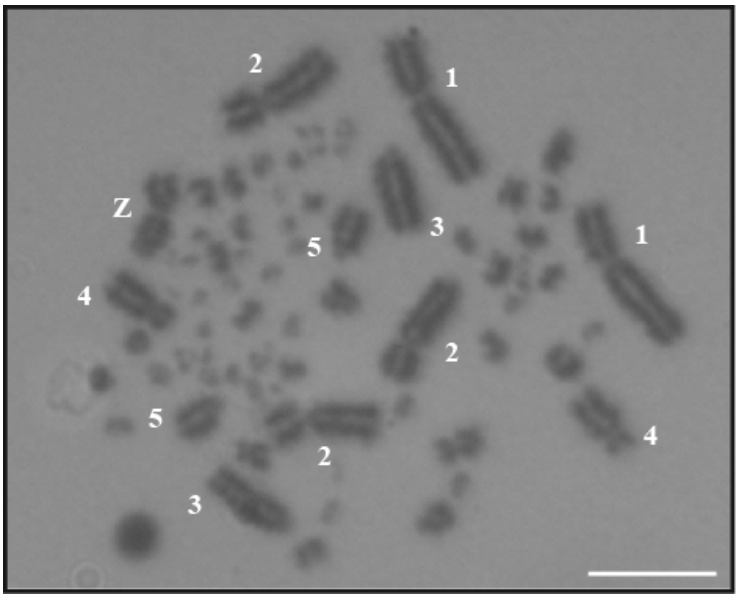

Figure 4.13 Representative chromosome spread of chicken karyotype.

Micrograph of the DT40 cell karyotype. Macrochromosomes 1, 2, 3, 4, 5 and sex chromosome Z are indicated with the corresponding number. Note that there are three copies of chromosome two. Scale bar shows 10 μm.

In this experiment, we analysed the karyotypes of these cell lines. The karyotype of the chicken DT40 cell line consists of 80 chromosomes from which chromosomes 1, 2, 3, 4, 5 and Z (macro-chromosomes) can be easily analysed by microscopy (Figure 4.13).

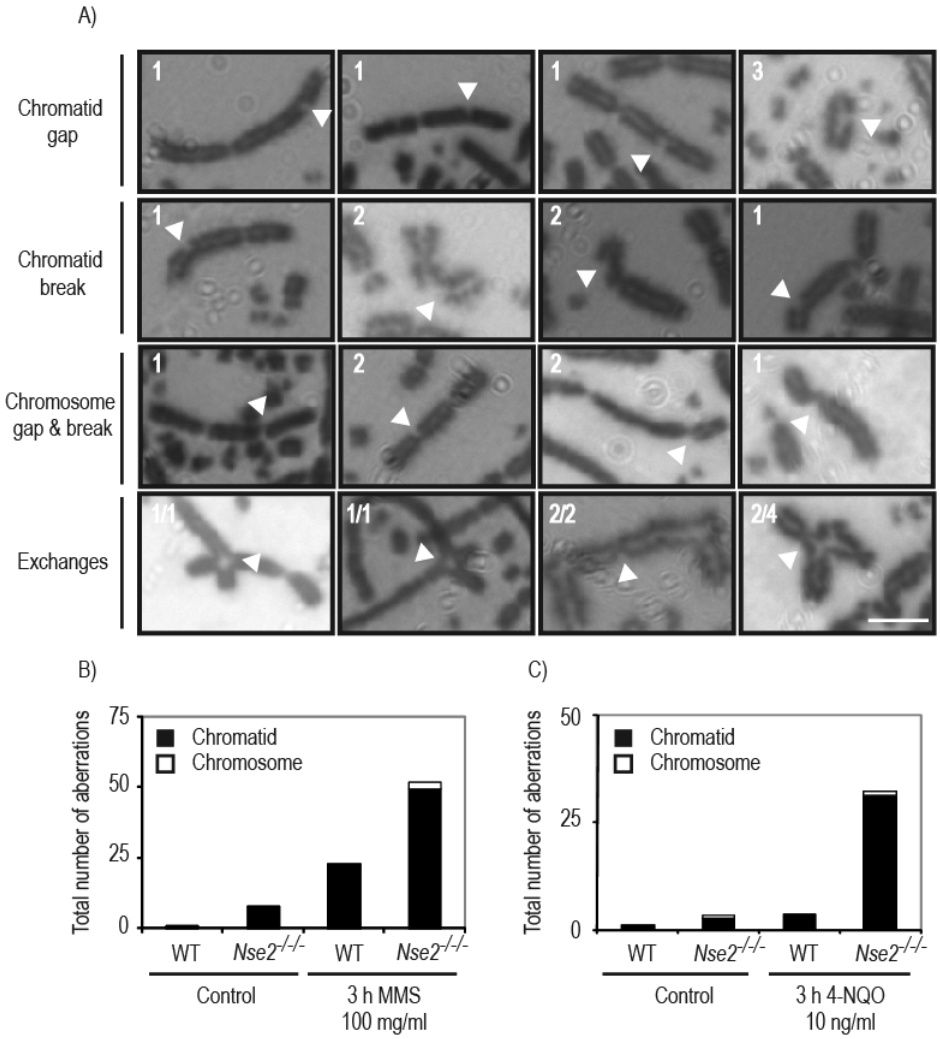

Figure 4.14 Chromosomal aberration assays.

A) Examples of chromosomal aberrations scored. Scoring criteria: gaps were scored as discontinuities and breaks as discontinuities with structural distortions of chromatids or chromosomes; exchanges were scored as chromosome fusions. The numbers in the left top corner of each micrograph indicates which chromosome(s) carries the aberration. Scale bar shows 10 μm. B) and C) Quantification of chromosome aberration in wild-type and Nse2-deficient cell. The indicated cell lines were treated with the indicated DNA damaging agent for 3 hours or left untreated. Cells were then blocked in mitosis and metaphase spreads were prepared. The plots show average of three independent experiments in which at least 50 cells were scored. S.D is not shown for histogram clarity.

Wild type and *Nse2*$^{-/-}$ cells were either treated with a DNA damaging agent or left without drug for 3 hours. For the final 2 hours, the cells were incubated with the microtubule depolymerising agent colcemid to enrich the population of prometaphase cells. Finally, cells were harvested, fixed and chromosome spreads were prepared (as described in Section 2.4.6). Slides were then analysed by microscopy and the integrity of each macro-chromosome assessed. Chromosomal aberrations such as gaps and breaks in the chromatids or chromosomes, as well as chromosome exchanges were scored in this assay. Representative lesions are shown in Figure 4.14A.

The Nse2-deficient cells showed an increased number of spontaneous and MMS-induced chromosomal aberrations compared to wild-type cells (Figure 4.14B). We observed an elevation (approximately 2-fold) of spontaneous and induced DNA lesions in the absence of Nse2. We repeated the same assay using the UV mimetic 4-NQO. As was seen for MMS treatment, Nse2-deficient cells showed sensitivity to this drug in a colony formation assay (Figure 3.11). The analysis of chromosome spreads after treatment with the 4-NQO, revealed an even more dramatic phenotype (Figure 4.14C). The wild-type cells did not show an increase in chromosomal aberrations after treatment with 4-NQO, whereas Nse2-deficient cells showed a 10-fold increase in chromosomal lesions (control: 2.6 aberrations/cell; 4-NQO: 31.3 aberrations/cell). Chromosome aberrations provide direct evidence for the presence of unrepaired DNA, thus the elevated chromosome aberrations in Nse2-deficient cells offer a strong argument in support of a role of Nse2 in DNA repair.

Defects in post-replicative DNA repair will result in increased chromatid aberrations (only damaged sister chromatid is affected), whereas abnormal repair in S phase will produce chromosome-type lesions (due to discontinuity of DNA replication). We detected mainly chromatid lesions in the absence of *Nse2*, which indicates defects in post-replicative repair. As MMS and 4-NQO induce DNA damage that is repaired by BER/HR and NER/HR, respectively, we conclude that Nse2 is required for the maintenance of genomic integrity through its role in post-replicative DNA repair.

4.3 Chicken Nse2 is required to repair MMS-induced DNA damage

4.3.1 Nse2-deficient cells are hypersensitive to alkylating DNA damage

As previously mentioned, the *Nse2* gene was first identified in a yeast screen for mutants defective in repair of MMS-induced DNA damage (Prakash and Prakash, 1977). *Nse2* is required for yeast proliferation and SUMO ligase dead alleles of *Nse2* are viable but hypersensitive to DNA damage, indicating that the essential function of this gene product is not associated with its SUMO activity (Andrews et al., 2005; McDonald et al., 2003; Pebernard et al., 2004). Chicken *Nse2*$^{-/-}$ cells are viable and we observed that Nse2 protein is required for an efficient response to MMS. We next investigated the function of this SUMO ligase in this process.

First we wanted to confirm that the observed MMS sensitivity is specific to the loss of *Nse2*. To test this, we stably transfected the Nse2-deficient cells with a vector that expresses a fusion protein of Nse2 with either a 3myc or GFP tag (N- and C-terminal, respectively). In addition, we also expressed a SUMO ligase-dead form of Nse2 as a 3myc or GFP fusion to test if Nse2 SUMO activity is required for MMS responses.

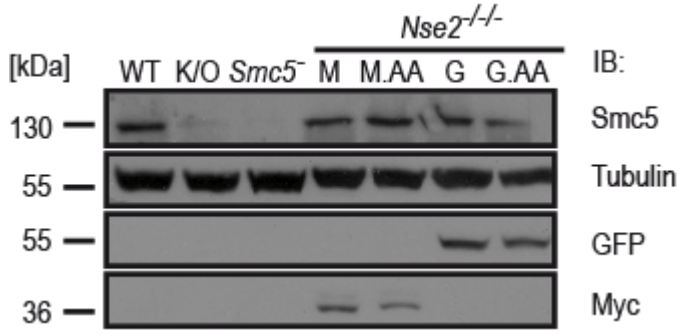

Figure 4.15 Ectopic expression of Nse2 fusion proteins.

Total protein was isolated from the wild-type, Smc5^{-}*, Nse2*$^{-/-}$ *and Nse2*$^{-/-}$ *rescue cell lines expressing wild-type or SUMO ligase dead Nse2, separated by SDS-PAGE; and detected using the indicated antibodies. (K/O – Nse2*$^{-/-}$ *M - Nse2*$^{-/-}$*::3myc-Nse2, M.AA - Nse2*$^{-/-}$*::3myc-Nse2.AA, G - Nse2*$^{-/-}$*::Nse2-GFP, G.AA - Nse2*$^{-/-}$*::Nse2.AA-GFP).*

To generate the SUMO ligase dead form, two point mutations (C178A and H180A) were introduced into the cDNA sequence encoding the catalytic SP-RING domain of the Nse2 protein (thereafter Nse2.AA). We then introduced the wild-type and mutated forms of Nse2 into the *Nse2*$^{-/-/-}$ cells. The ectopic expression of the Nse2 and Nse2.AA fusion proteins was tested by immunoblotting (Figure 4.15).

GFP and myc tagged wild-type or mutated SUMO ligase proteins were expressed ectopically at similar levels but overexpressed compared to endogenous Nse2 (as shown in Figure 3.6). Functionality of the N-terminal 3myc-Nse2 fusion was tested as described in Section 3.5. The GFP protein is relatively large as a tag (approximately 27 kDa) and its presence on the N-terminus of Nse2 could impede binding to Smc5. For that reason we introduced GFP at the C-terminus. However, this could affect activity of the SUMO ligase SP-RING of Nse2. Functionality of the Nse2-GFP fusion was later tested in survival assays as described in this section. As shown in Section 4.2.1 and Figures 4.9/4.15, loss of the *Nse2* gene results in significant depletion of Smc5. Nse2 is an E3 SUMO ligase that binds to Smc5 protein *in vivo*, so we hypothesised that this interaction or Nse2-dependent modification of Smc5 may be necessary for the stability of Smc5. Expression of either wild-type or mutant Nse2 restored levels of Smc5 to wild-type levels (Figure 4.15). Wild-type levels of Smc5 are observed in *Nse2*$^{-/-/-}$::*Nse2* and *Nse2*$^{-/-/-}$::*Nse2.AA* backgrounds, therefore we conclude that binding of Nse2 to its Smc partner, but not Nse2 SUMO ligase activity, is required for Smc5 protein stability.

We also tested if these proteins are able to rescue the viability of *Nse2*$^{-/-/-}$ cells post-MMS treatment. Wild-type, *Nse2*$^{-/-/-}$, *Nse2*$^{-/-/-}$::*Nse2* and *Nse2*$^{-/-/-}$ ::*Nse2.AA* cell lines were analysed by clonogenic survival assay after MMS treatment. As shown in Figure 4.16A and B, reintroduction of the wild-type Nse2 protein within the Nse2-deficient cells restored the sensitivity towards MMS to wild-type levels, whereas expression of the Nse2.AA mutant only partially rescued this phenotype.

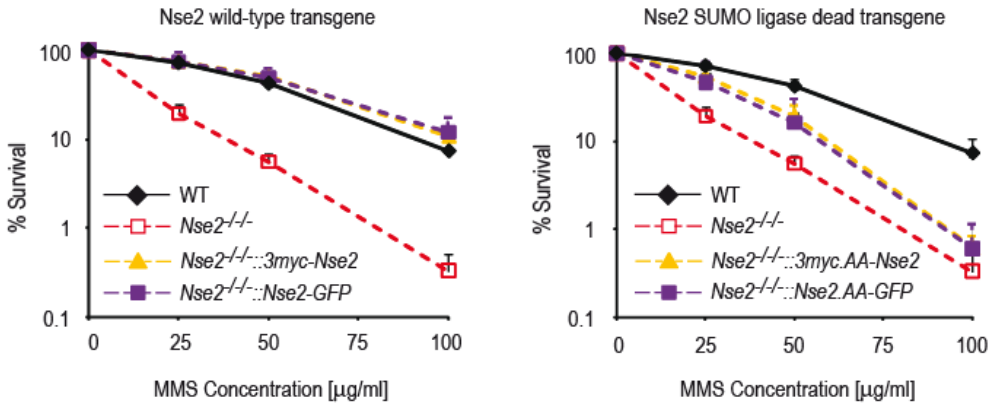

Figure 4.16 Reintroduction of wild-type Nse2 restores MMS sensitivity of Nse2-deficient cells to wild-type cells levels.

The indicated cell lines were treated with different doses of MMS for 2 hours and seeded onto methylcellulose containing dishes. Colonies were scored 10-14 days after seeding. The plots show average of three experiments +/- SD. Plating efficiencies were wild-type, 80%; Nse2$^{-/-/-}$, 67%; Nse2$^{-/-/-}$::3myc-Nse2, 69%; Nse2$^{-/-/-}$::3myc-Nse2.AA, 77%; Nse2$^{-/-/-}$::Nse2-GFP, 71%; Nse2$^{-/-/-}$::Nse2-GFP.AA, 52%.

The rescue of MMS sensitivity upon expression of wild-type Nse2 protein confirms that the observed phenotype is specifically due to loss of the *Nse2* gene and is not the result of additional factors. In addition, partial reversion of MMS phenotype in the Nse2 SUMO dead background suggests that the SUMO activity of chicken Nse2 protein is only required to a limited extent for response to MMS-induced DNA damage. In parallel experiments, we observed that the loss of *Smc5* results in higher sensitivity towards MMS than was detected in *Nse2*$^{-/-/-}$ cells (Stephan et al., 2011a). Therefore, we hypothesise that a major function of chicken Nse2 is to stabilise Smc5 and SUMOylate different cellular targets in response to DNA damage.

The partial ability of the Nse2.AA protein to rescue the MMS sensitivity of Nse2-deficient cells and restore Smc5 stability was rather surprising. To test if the Nse2.AA SUMO ligase dead protein is indeed inactive, we purified the wild-type and Nse2.AA ligases as GST fusion proteins and used them in *in vitro* SUMOylation assays (as described in Section 2.3.11). SUMO ligases are able to automodify themselves and such autosumoylation activity has been reported for Nse2 (Andrews et al., 2005; Potts and Yu, 2005; Zhao and Blobel, 2005). As described in Section 2.3.11, equal amounts of GST-Nse2 and GST-Nse2.AA

ligases (approximately 0.5 μg) were incubated with E1, E2 and SUMO-1 proteins in the presence or absence of an energy mix containing ATP (Figure 4.17A and B).

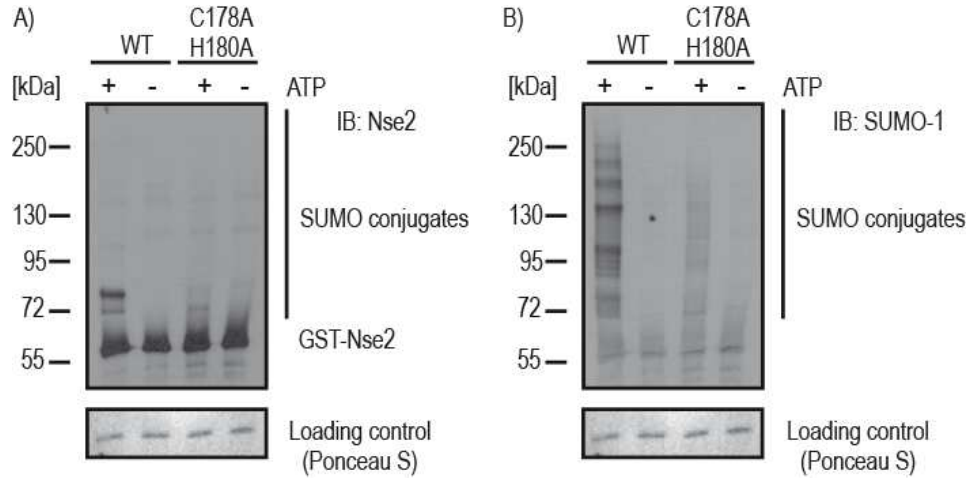

Figure 4.17 Chicken Nse2 is an active SUMO ligase in vitro and its activity depends on intact SP-RING.

Equal amounts of recombinant GST-Nse2 and GST-Nse2.AA proteins were incubated with E1, E2 and SUMO-1 proteins at 30°C for 1 hour. Reactions were terminated by addition of sample buffer and boiling for 5 minutes at 95°C. Reaction mixtures were then separated by SDS-PAGE and analysed by immunoblotting with antibodies to A) anti-cNse2 and B) anti-hSUMO1.

The reaction mixtures were then separated by SDS-PAGE and analysed by immunoblotting with anti-Nse2 and anti-SUMO-1 antibodies. We observed an extensive laddering of SUMO-1 conjugates only when the reaction occurred in the presence of ATP, since its removal abrogated the high molecular weight forms of the Nse2 ligase (Figure 4.17A and B). This analysis revealed that wild-type and SUMO dead Nse2 ligase are SUMOylated in this assay. We found also that the SUMO dead form of the ligase produced less of the SUMO-1 conjugates than the wild-type Nse2 SUMO ligase. To confirm that the observed laddering contains SUMO conjugates, we blotted the same membrane with the anti-SUMO-1 antibody. The Figure 4.17B shows that detectable high molecular weight forms of Nse2 ligase indeed contain the SUMO-1 peptide, therefore they are SUMO-1 conjugates. The detectable SUMO-1 conjugates in the SUMO ligase dead reaction could be the result of residual activity of the mutated Nse2 ligase or activity of the E2 enzyme, which is able to efficiently SUMOylate most

substrates *in vitro* (approximately 90%) (Bernier-Villamor et al., 2002). Therefore, we conclude that the introduced C178A/H180A mutations abrogate the activity of the Nse2 SUMO ligase *in vitro*. These results confirm that chicken Nse2 can be SUMOylated *in vitro* and that an intact SP-RING is required for this activity. In addition this confirms that the SUMO ligase activity of Nse2 is not required for the stability of Smc5, but is essential for some aspects of the DNA damage response and DNA repair after MMS treatment.

4.3.2 Nse2-deficient cells show delayed checkpoint activation upon MMS treament

Activation of the G_2 checkpoint occurs normally after DNA damage, but it is not maintained in the yeast mutants of the Smc5-Smc6 complex (Ampatzidou et al., 2006; Verkade et al., 1999). As described in Section 1.5, the ATR/ATM/Chk1/Chk2 pathway is responsible for activation of G_1, S and G_2 phase checkpoints (Canman and Lim, 1998; Ciccia and Elledge, 2010; Nyberg et al., 2002; Xu et al., 2001; Zhou and Elledge, 2000). Phosphorylation of checkpoint kinase 1 by the ATM/ATR kinases is a crucial event in the activation of this protein (Bartek and Lukas, 2003; Canman and Lim, 1998; Kastan, 2004; Stracker et al., 2009; Zhou and Elledge, 2000). Chk1 S317 and S345 are phosphorylated in response to different types of DNA damage (Stracker et al., 2009). In addition to its functions in cell cycle regulation, Chk1 is required for the stabilisation and integrity of replication forks (Sorensen et al., 2005). It has been shown to keep stalled replication forks in a recombination-competent state, through phosphorylation of different target proteins (Despras et al., 2010; Sorensen et al., 2005).

We asked if chicken Nse2 plays an active role in MMS-induced cell cycle checkpoints. We first monitored phosphorylation of Chk1 kinase on S345 as an output of checkpoint activation. For this purpose, cells were constantly exposed to low and high doses of MMS (25 and 100 µg/ml) and analysed at different time points by immunoblotting for Chk1 S345. Our analysis revealed different kinetics of Chk1 activation in response to MMS-induced DNA damage in Nse2-deficient cells (Figure 4.18A and B).

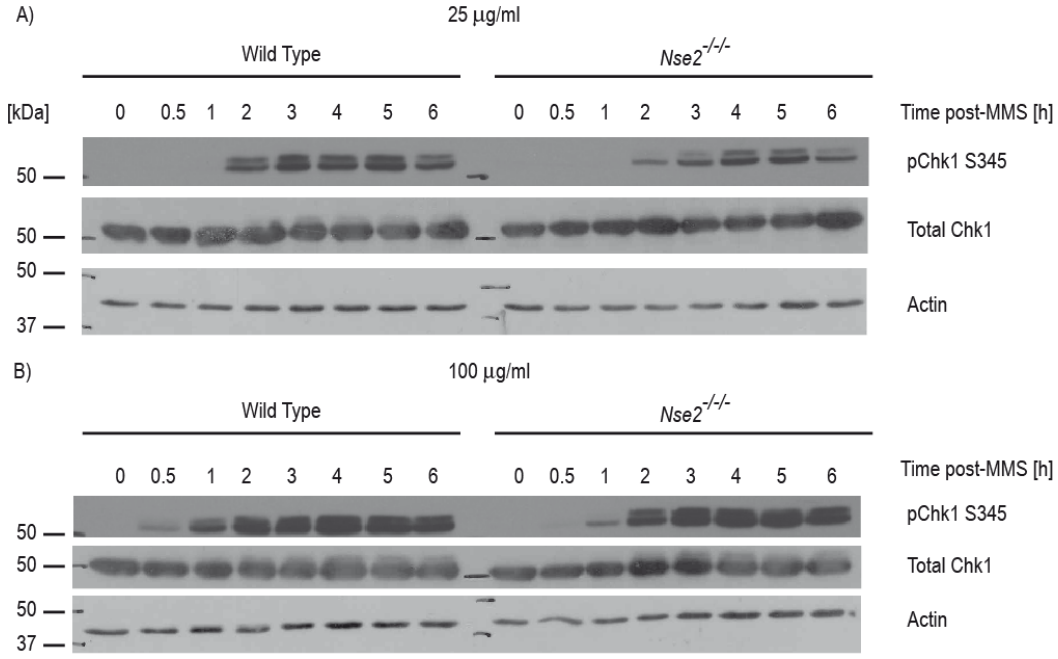

Figure 4.18 Chk1 phosphorylation at S345 after MMS treatment.

Wild-type and Nse2$^{-/-/-}$ cells were chronically exposed to A) 25 µg/ml and B) 100µg/ml of MMS and harvested at different time points post-treatment. Extracted proteins were separated by SDS-PAGE and analysed by immunoblotting with the indicated antibodies.

Wild-type cells fully activate the Chk1 kinase as soon as 2 hours (low dose) and 1 hour (high dose) after MMS exposure. However, the *Nse2* mutants show this level of Chk1 activation only at 4 hours (low dose) and 2 hours (high dose) post-MMS treatment (Figure 4.18A and B). This clearly indicates that the loss of Nse2 protein results in a delay in Chk1 phosphorylation at S345 and by implication, delayed checkpoint activation.

Next we asked whether the absence of *Nse2* has an effect on cell cycle distribution upon MMS treatment. Wild-type and *Nse2*$^{-/-/-}$ cells were treated with different doses of MMS (25 – 100 µg/ml) for 2 hours. After exposure to MMS, cells were washed and released into fresh media. At different time points post-release, cells were harvested and then analysed by flow cytometry. We found that at higher doses of MMS (50 and 100 µg/ml) wild-type and Nse2-deficient cells responded similarly to MMS treatment. Both cell lines blocked strongly in G_1 and most of them died after 24 hours post-treatment (data not shown). At lower doses (25 µg/ml), we observed a difference in response to MMS treatment between wild-type cells and *Nse2* mutants (Figure 4.19).

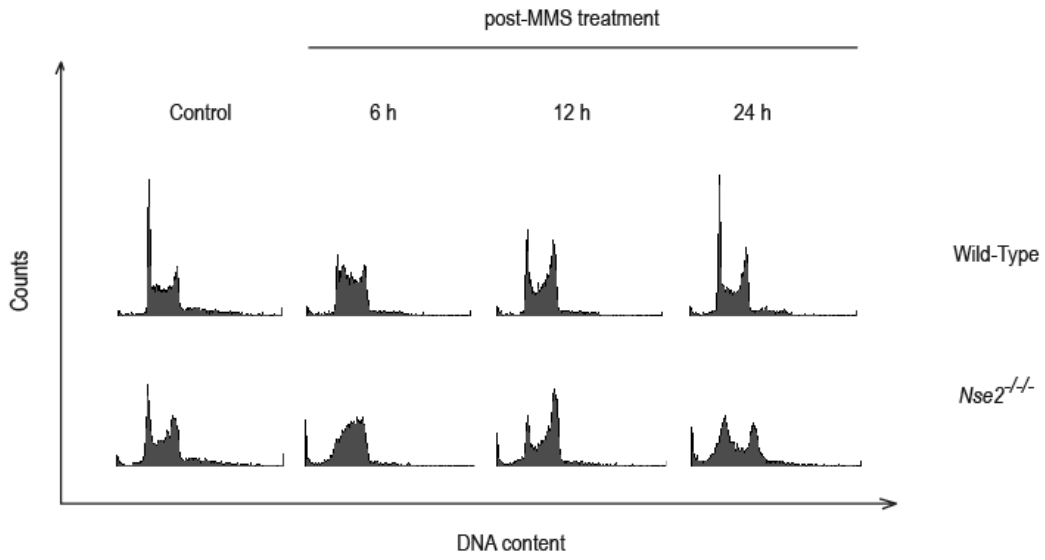

Figure 4.19 Nse2-deficient cells show abnormal cell cycle profiles after treatment with MMS.
Cells were treated with 25 µg/ml of MMS for 2 hours then washed and released into fresh medium. Cells were then harvested at the indicated time points and their DNA content was analysed by flow cytometry. This analysis is representative of three independent experiments.

Both wild-type and *Nse2*$^{-/-/-}$ cells slowed in S phase, probably due to the retardation of replication fork progression by MMS-induced DNA lesions (Figure 3.29, 6 hours time point). Such an MMS-induced replication block effect has been described in human cells after MMS treatment (Groth et al., 2010). Twelve hours post-treatment, most of the wild-type and Nse2-deficient cells finished DNA replication and blocked at the G_2/M border (Figure 4.19, 12 hours time point). Finally the wild-type cells fully recovered from MMS-induced DNA damage after 24 hours, whereas Nse2-deficient cells were not able to return to the cell cycle (Figure 4.19, 24 hours time point). Similar results were obtained in another experiment where S phase cells were additionally stained with BrdU (Figure 4.20).

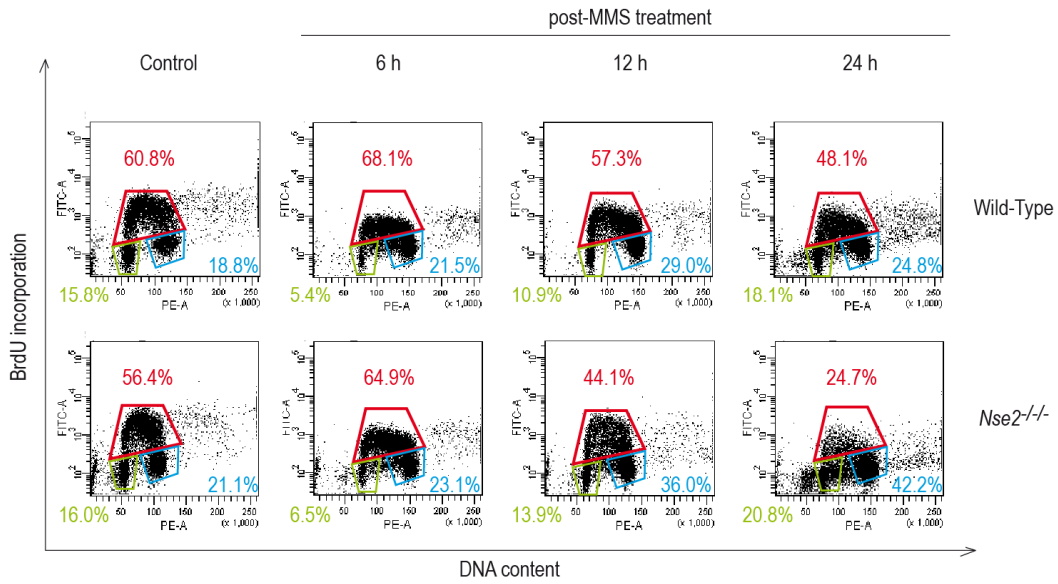

Figure 4.20 Nse2-deficient cells show abnormal cell cycle profiles after treatment with MMS. *Cells were treated with 25 μg/ml of MMS for 2 hours, then washed and released to fresh medium. Cells were then pulsed with BrdU at the indicated time points, harvested and their DNA contents analysed by flow cytometry. This analysis is representative of three independent experiments. The red, blue and green gates show cells in S, G_2 and G_2 phases, respectively.*

Both wild-type and Nse2-deficient cells accumulated in S phase 6 hours post-MMS treatment (Figure 4.20, red gate). However, the *Nse2*$^{-/-/-}$ mutants showed increased number of G_2/M cells at 12 and 24 hour time points compared to wild-type cells (Figure 4.20, blue gate). This was also associated with an elevated numbers of apoptotic cells in *Nse2*$^{-/-/-}$ knockouts at 24 hours time point (Figure 4.20, sub G_1 population).

This analysis suggests that *Nse2*$^{-/-/-}$ cells either do not enter, or fail to complete, mitosis due to unrepaired or incompletely replicated DNA (Figure 4.19 and 4.20). This is consistent with the delay observed in checkpoint activation in the absence of *Nse2* (Figure 4.18). Without a robust checkpoint response in the absence of Nse2, more DNA damage could be converted into more toxic types of DNA lesions, such as stalled replication forks or DSB (Beranek, 1990; Groth et al., 2010) (see also Section 4.3.3). Elevated numbers of such lesions and defect in their repair (as shown in Sections 4.2.3 and 4.2.4) could trigger cell death at the G_2/M border. It is also possible that cells with unrepaired or incompletely replicated DNA could evade the G_2 checkpoint and enter mitosis, where they would fail to finish division and die due to mitotic catastrophe. This indeed

happens in yeast mutants of the Smc5-Smc6 complex (Ampatzidou et al., 2006; Chen et al., 2009; McDonald et al., 2003; Pebernard et al., 2004; Pebernard et al., 2008a). We conclude that to some extent, a defect in MMS-induced checkpoint activation is responsible for the increased sensitivity of *Nse2* mutants to this DNA damaging agent.

4.3.3 Loss of *Nse2* results in slow repair of MMS-induced DNA damage

Phosphorylation of H2AX histone (termed γ-H2AX) by different kinases is a well established marker for DNA repair (Sedelnikova et al., 2003). This modification is detected after exposure to IR, UV, HU and MMS but it is not always associated with DSB and may represent DNA repair foci (Marti et al., 2006; Petermann et al., 2010; Stucki et al., 2005). MMS treatment can induce γ-H2AX by at least two different mechanisms. Single strand breaks produced by BER during removal of N^7-methylguaine and N^3-methyladenine can be converted to DSB in S phase if encountered by the replication machinery (Groth et al., 2010). In the second mechanism, N^3-methyladenine induce replication fork stalling what can lead to formation of DSBs through their eventual collapse (Beranek, 1990; Groth et al., 2010).

In order to test whether Nse2-deficient cells fail to enter or complete mitosis because of unrepaired DNA damage, we followed the formation and resolution of γ-H2AX foci as a marker of ongoing DNA damage signalling and repair (Figure 4.21A and B). At various times (Figure 4.21A and B) cells were harvested by cytospin and stained for γ-H2AX. The γ-H2AX foci were then analysed by microscopy. Each cell containing six or more γ-H2AX foci was scored as positive (Figure 4.21A). We observed similar levels of spontaneous DNA damage in wild-type and *Nse2* mutants (Figure 4.21A and B, 0 hour time point). Both cell lines induced phosphorylation of histone H2AX after MMS treatment with the same kinetics (Figure 4.21B, 1 hour and 6 hour time points), suggesting that events upstream of H2AX phosphorylation operate normally in the *Nse2* background. The highest number of γ-H2AX positive cells was detected

6 hours post-MMS treatment in both cell lines analysed. MMS-induced γ-H2AX foci formation is slower than that induced after exposure to IR.

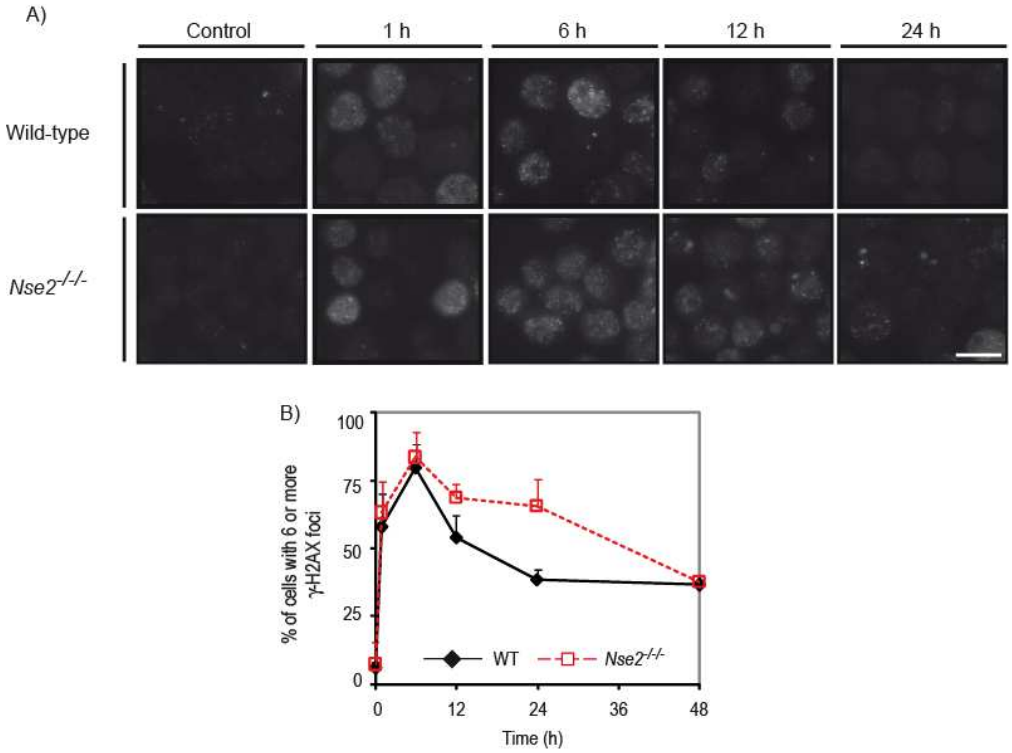

Figure 4.21 Quantification of γ-H2AX foci after MMS treatment in wild-type and Nse2-deficient cells.

A) Micrographs of the wild-type and Nse2-deficient cells. Cells were pulsed with 100 μg/ml of MMS for 15 minutes and immediately released to fresh media, then harvested by cytospinning at the indicated time points and stained for γ-H2AX. B) Quantification of γ-H2AX foci in wild-type and Nse2-deficient cells. The plot shows average of three independent experiments +/- S.D where at least 300 cells were scored per time point. Scale bar shows 10 μm.

This is consistent with the notion that only actively replicating cells will induce γ-H2AX as a result of impeded replication forks. Wild-type cells start to repair DNA damage as soon as 12 hours post-treatment and remove most of it by 48 hours (Figure 4.20B, 12 – 48 hour time points). This was observed as a decrease in number of the γ-H2AX positive cells (Figure 4.21A and B). On the other hand, resolution of γ-H2AX foci was significantly retarded in the *Nse2* background. Nse2-deficient cells needed approximately 36 hours more to resolve γ-H2AX foci to wild-type like levels. This confirms that, in the absence of *Nse2*, DNA

repair is defective. At 24 hours, approximately 60% of the *Nse2*$^{-/-}$ population still had unrepaired DNA damage, compared to 30% in wild-type cells.

Flow cytometry analysis of MMS treated cells showed that cells enter mitosis 12 to 24 hours after MMS treatment (Figure 4.19 and 4.30). Nse2-deficient cells show an elevated number of γ-H2AX foci for as long as 24 hours post-MMS pulse (Figure 4.21). Therefore *Nse2*$^{-/-}$ cells have more unrepaired DNA at the time of the G_2/M transition than do to wild-type cells. This suggests that Nse2-deficient cells may die due to unrepaired DNA during G_2 or mitosis, probably through activation of G_2 checkpoint or mitotic catastrophe.

4.3.4 Chicken Nse2 is not required for replication fork restart and base excision repair

Methyl methanesulfonate (MMS) produces two major DNA methyl adducts, N^3-methyladenine, which is believed to stall replication forks and N^7-methylguanine which is removed by the base excision repair pathway (11% and 82% of all MMS adducts, respectively) (Beranek, 1990). The remaining 7% of DNA methyl adducts are nitrogen and oxygen modification of carboxyl, amino and phosphate residues (Beranek, 1990). To test whether Nse2 is involved in the repair of either N^3-methyladenine or N^7-methylguanine, we performed two sets of experiments.

In the first set we decided to apply a chemical genetic approach in which epistasis between *Nse2* and BER pathways was analysed. BER was chemically inhibited (30 minutes pre-treatment) before induction of DNA damage with MMS for 2 hours. Wild-type and *Nse2*$^{-/-}$ cells were then plated onto methylcellulose-containing dishes and their ability to form colonies was scored 10 – 14 days after treatment with MMS and base excision repair pathway inhibition. The inhibitors used in this study blocked BER at different stages. The APE-1 inhibitor CRT0044876 (7-Nitroindole-2-carboxylic acid) abolishes hydrolysis of apurinic/apyrymidinic (AP) sites and production of SSB intermediates (Madhusudan et al., 2005). PARP-1 inhibition by the small molecule DPQ (3,4-Dihydro-5[4-(1-piperindinyl)butoxy]-1(2H)-isoquinoline)

interferes with detection and further processing of single strand break intermediates (more details can be found in Section 1.6.1) (Suto et al., 1991).

We hypothesised that if Nse2 protein is involved in base excision repair, inhibition of this pathway should not exacerbate the MMS phenotype. Otherwise, inhibition of BER should result in further sensitisation of Nse2-deficient cells to MMS-induced DNA damage. We found that combined treatment with BER inhibitors and MMS had a synergistic effect on the lethality of wild-type and *Nse2*$^{-/-}$ cells, with a stronger impact in *Nse2* (~100 fold increase) than wild-type (~10 fold decrease) background, at the highest dose (Figure 4.22A and B).

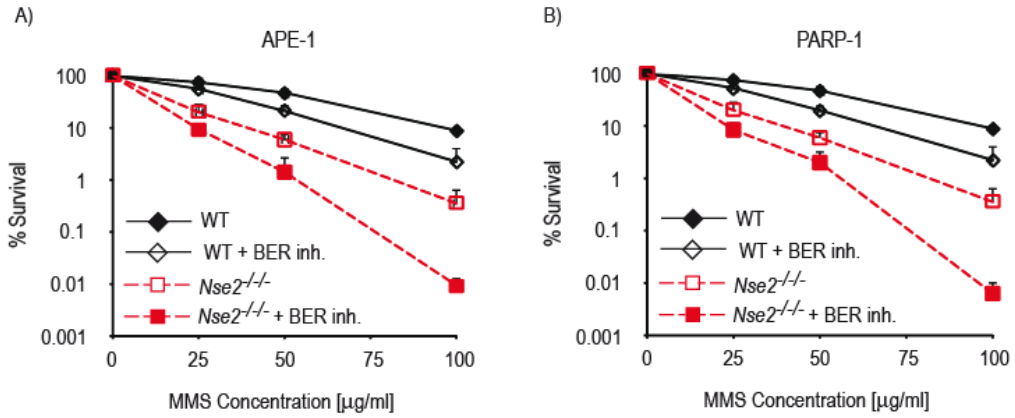

Figure 4.22 Clonogenic survival assay after BER inhibition.

Wild-type and Nse2-deficient cells were pre-treated for 30 minutes with two different base excision repair inhibitors A) 100 µM CRT004876 (an inhibitor of APE-1 endonuclease) and B) 10 µM DPQ (an PARP-1 inhibitor) and with the indicated doses of MMS for the next 2 hours. Cells were then plated and colonies scored after 10 – 14 days. The plots show the mean of relative survival from three independent experiments +/- S.D. Plating efficiencies were wild-type 80%; wild-type + CRT004876, 90%; wild-type + DPQ, 90%; Nse2$^{-/-/-}$, 67%; Nse2$^{-/-/-}$ + CRT004876, 63%; Nse2$^{-/-/-}$ + DPQ, 72%.

There was no difference observed between the effects caused by inhibition of APE-1 and PARP-1 (Figure 4.22A and B). This strongly suggests that base excision repair is still active in the absence of Nse2 protein. This indicates that Nse2-deficient cells rely more on BER activity after MMS treatment than wild-type cells.

In parallel, we also analysed Smc5-deficient cells with the same approach. Surprisingly, we found that inhibition of BER in these cells does not

exacerbate the MMS sensitivity phenotype of *Smc5* mutants but actually results in a moderate rescue of *Smc5*$^{-}$ cells sensitivity (Figure 4.23A and B). Yeast double mutants of *Smc6* and BER genes show marked sensitivity to MMS treatment (Lee et al., 2007). *smc6mag1* (*Mag1* – DNA glycosylase) and *smc6nth1* (*Nth1* – 3' AP lyase) mutants show higher sensitivity towards MMS, whereas mutants of *smc6apn2* (*Apn2* – 5' AP lyase) show severe growth defects (Lee et al., 2007). These observations confirm a genetic interaction between the Smc5-Smc6 complex and BER. We conclude that Smc5, but not Nse2 plays an active role in the removal of N^7-methylguanine adducts through BER.

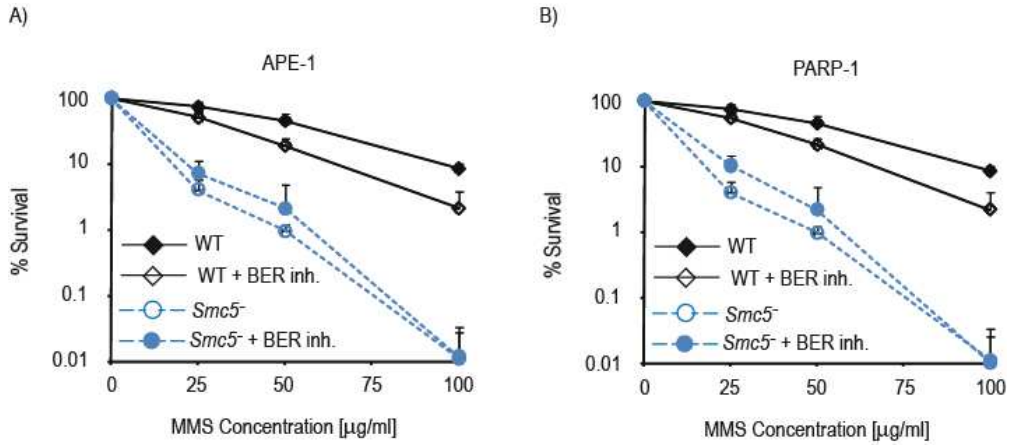

Figure 4.23 Clonogenic survival assay after BER inhibition.

Wild-type and Smc5-deficient cells were pre-treated for 30 minutes with the base excision repair inhibitors (A) 100 µM CRT004876 and (B) 10 µM DPQ and with the indicated doses of MMS for next 2 hours. Cells were then plated and colonies scored after 10 – 14 days. The plots show mean of relative survival from three independent experiments +/- S.D. Plating efficiencies were wild-type 80%; wild-type + CRT004876, 90; wild-type + DPQ, 90%; Smc5^{-}*, 48%; Smc5*$^{-}$ *+ CRT004876, 63; Smc5*$^{-}$ *+ DPQ, 79%.*

As previously mentioned, MMS-induced DNA damage can also lead to replication fork stalling (Beranek, 1990; Groth et al., 2010). In yeast, the Smc5-Smc6 complex is involved in restart of replication forks after HU treatment (Ampatzidou et al., 2006; Irmisch et al., 2009). To test whether Nse2 is required for replication fork restart after MMS treatment, we designed a fluorescent replication assay. In this assay, the formation of replication foci was specifically

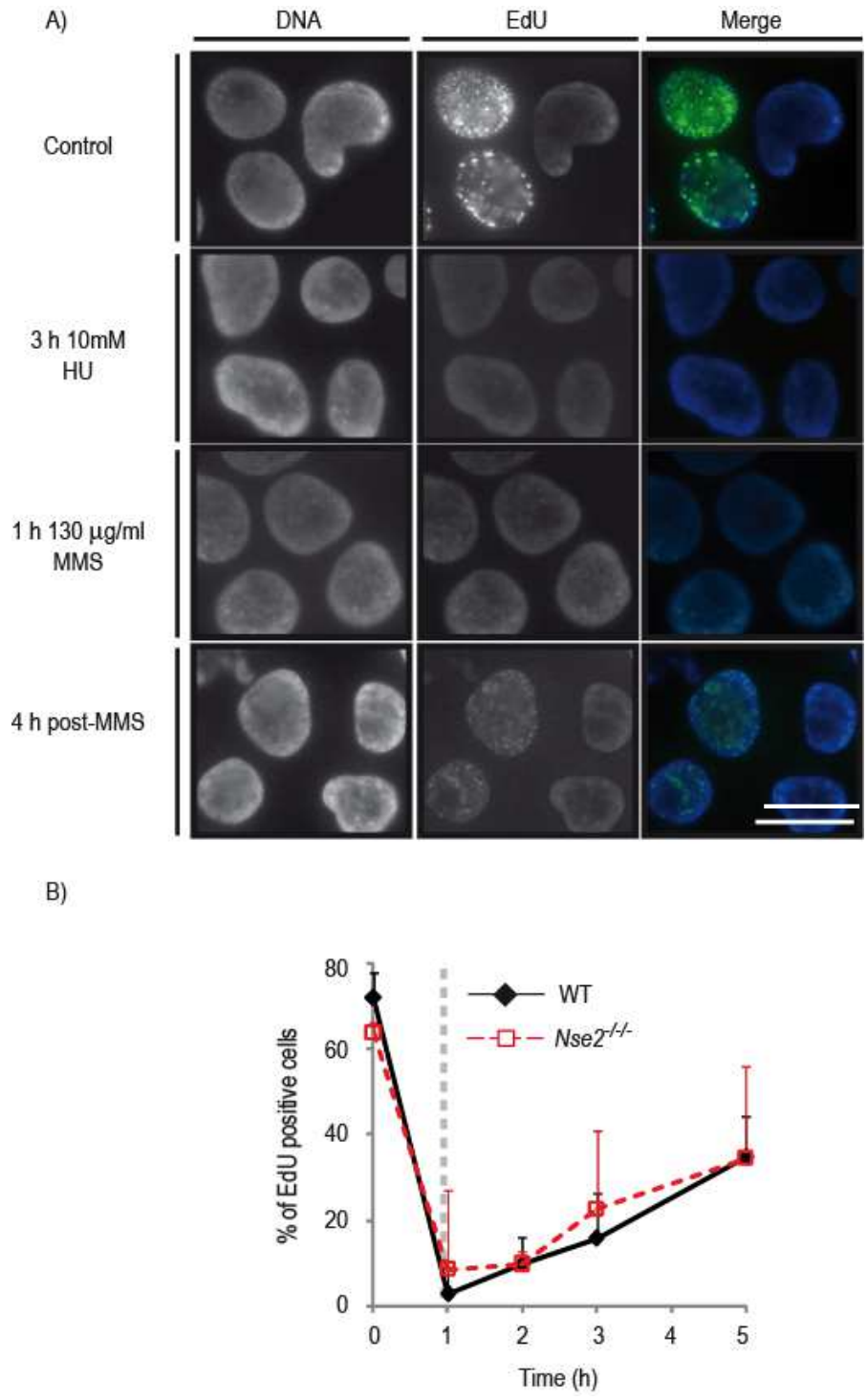

Figure 4.24 DNA synthesis restart after release form MMS treatment.

A) Micrographs of wild-type cells showing cells stained with EdU to label replication foci before and after addition of HU and MMS, as well as after release from MMS treatment. B) Quantification of EdU positive wild-type and Nse2 deficient cells before and 1 hour after MMS treatment (130 µg/ml). Dashed gray line shows time of MMS removal. Data points represent mean +/- S.D of three independent experiments in which at least 300 cells were scored. Scale bar shows 10 µm.

monitored by incorporation of the thymidine analogue 5'-ethynyl-2'-deoxyuridine (EdU) into DNA during DNA synthesis (Figure 4.24A). To visualise replication foci, the EdU was then coupled to a green fluorophore 6-carboxyfluorescein (as described in Section 2.4.8). To stall the replication forks, cells were treated with high doses of MMS (130 μg/ml) for 1 hour. This dose was found experimentally to inhibit formation of replication foci and it is similar to the doses needed to stall the same process in human cells (Groth et al., 2010). DNA synthesis was then restarted by releasing cells to fresh media without drug. At different times post-release, cells were spun onto slides and replication foci stained (Figure 4.24A). Hydroxyurea, a known inhibitor of DNA synthesis, was used as a positive control in this experiment (Figure 4.24A, middle panel). Untreated control cells show many bright and distinct replication foci within the nucleus (Figure 4.24A, top panel). We could efficiently abolish replication foci formation by treatment with either HU or MMS (Figure 4.24A, middle panels). After release from the MMS-induced DNA synthesis block, we could again detect these foci, indicating that replication was restarted or reinitiated in these cells (Figure 4.24A, bottom panel).

Next, wild-type and Nse2-deficient cells were analysed in the same experiment. Cells with more than 3 replication foci were scored as positives and expressed as a fraction of total cell number screened. We could detect between 65-70% (around 50-60% is detected by flow cytometry) of cells as actively replicating before MMS addition in both wild-type and Nse2-deficient cells (Figure 4.24B). After one hour MMS treatment (dashed gray line indicates time of drug removal) most of the wild-type and *Nse2*$^{-/-}$ cells stopped DNA synthesis (Figure 4.24B, 1 hour time point). During the time course of the experiment, wild-type and Nse2-deficient cells showed a constant increase of the number undergoing DNA synthesis after removal of MMS (Figure 4.24B). We did not observe a difference in DNA synthesis restart or re-initiation in both cell lines after treatment with MMS. Therefore this indicates that chicken Nse2 protein may not play a role in restart of MMS-stalled replication forks in DT40 cells.

4.3.5 Nse2-deficient cells show defects in homologous recombinational repair

The Smc5-Smc6 and Nse2 protein complex have been implicated in homologous recombinational (HR) repair. In fission yeast, double mutants of *smc6-X* and *rhp51*^{Rad51} show similar sensitivity towards IR as the single *rhp51*^{Rad51} mutant (Lehmann et al., 1995). A similar observation was made in budding yeast mutants of *smc5-31rad52Δ0, smc5-33rad52Δ0* and chicken *Smc5*$^{-}$ *Rad54*$^{-/-}$ (Cost and Cozzarelli, 2006; Stephan et al., 2011a). siRNA experiments in human cells revealed increased levels of break-induced recombination and elevated frequencies of sister chromatid exchanges upon depletion of Nse2 and Smc5 (Potts et al., 2006). This suggests that the roles of the Smc5-Smc6 complex in recombinational repair are evolutionarily conserved.

A large body of evidence, from analysis of the recombination intermediates by two dimensional gel electrophoresis in yeast Smc5-Smc6 mutants, indicates that Nse2 is required for efficient resolution of HR intermediates, suggesting that Smc5-Smc6 is involved in later stages of HR (Ampatzidou et al., 2006; Bermúdez-López et al., 2010; Branzei et al., 2006; Choi et al., 2010). We and others observed an intact mobilisation of early recombination factors, such as Rad51 and Rad52 in mutants of the Smc5-Smc6 complex (Ampatzidou et al., 2006; Irmisch et al., 2009; Stephan et al., 2011a; Torres-Rosell et al., 2007). From our previous analysis, we know that chicken Smc5 is required for efficient HR, possibly through regulation of the cohesin complex (Stephan et al., 2011a). A similar observation was made in human cells where Nse2 and Smc5 are required for cohesin recruitment to *I-SceI* induced DSB (Potts et al., 2006). These data suggest that the Smc5-Smc6 complex is involved in both early and late stages of homologous recombination.

We asked whether chicken Nse2 is also required for efficient homologous recombination. Because disruption of *Nse2* results in severe depletion of Smc5 and both proteins are components of the same complex, we hypothesised that Nse2-deficient cells will show similar defects in homologous recombinational repair as *Smc5*$^{-}$ mutants. To test this hypothesis we tested the HR status of *Nse2*$^{-/-/-}$ cells. In the first experiment we compared the gene targeting efficiency between wild-type and Nse2-deficient cells at three different loci: *ATM*

(Morrison et al., 2000), *Centrin2* (Tiago Dantas 2011) and *Ovalbumin* (Buerstedde and Takeda, 1991). In the same assay, HR mutants such as *Rad52* and *Rad54* show reduced targeting frequencies at the *Ovalbumin* locus (Bezzubova et al., 1997; Yamaguchi-Iwai et al., 1998a). For that purpose wild-type and *Nse2*$^{-/-}$ cells were transfected with these vectors and the clones obtained screened for targeting events by Southern blotting (Figure 4.25A and B).

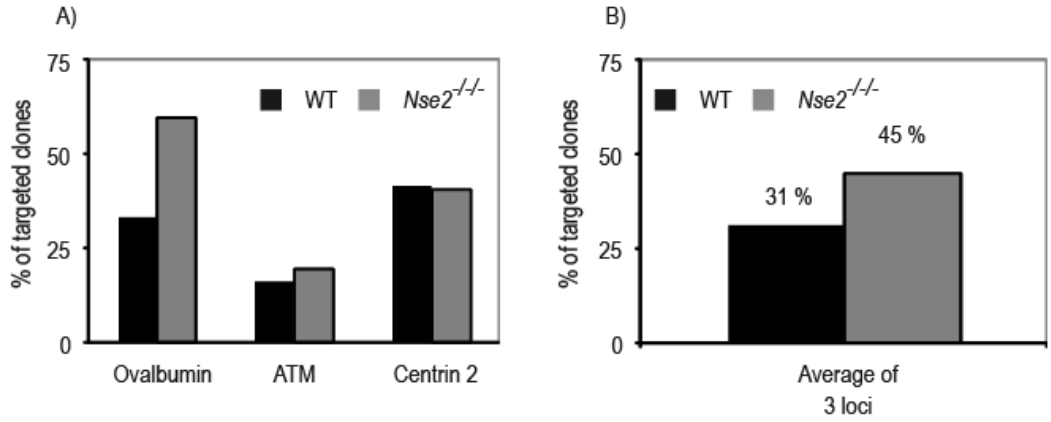

Figure 4.25 Gene gargeting efficiencies.

A) Wild-type and Nse2 deficient cells were transfected by electroporation with the indicated vectors. An equal number of single clones (55 for each cell line per vector) was collected and screened for targeting events by Southern blotting. Results represent a single experiment for each targeting vector. B) Mean of targeting efficiencies from three targeting vectors showed in A).

We observed a notable increase in targeting efficiencies at the *Ovalbumin* locus, and wild-type like levels at the *Centrin 2* and *ATM* loci (Figure 4.25A). Combining these observations, the mean efficiencies were approximately 50% increased in the *Nse2* background. Potts et al. have also observed increased targeting efficiencies in the absence of Nse2 protein in human cells (Potts et al., 2006). Our data are consistent with a regulatory role of Nse2 in the HR pathway.

In the second HR assay we measured the ability of cells to perform sister chromatid exchanges (SCE). These can be visualized by the incorporation of 5-bromo-2'-deoxyuridine during DNA synthesis. SCE formation is still not fully understood but it is well established that these reflect a DNA repair process (Sonoda et al., 1999; Wolff et al., 1974). Elevated levels of SCEs are detected in cells lacking the BLM (Bloom syndrome) helicase, PARP-1 and XRCC1

proteins (Thompson et al., 1990; Wang et al., 2000; Wang et al., 1997). The exposure of cells to DNA damage in S phase is an essential requirement for SCE formation, indicating a connection between SCEs and DNA replication (Wolff et al., 1974). Homologous recombination has been proposed as one of the mechanisms driving the formation of SCEs, as HR mutants show markedly reduced levels of SCEs (Kato, 1974; Kuzminov, 1996; Sonoda et al., 1999; Yamaguchi-Iwai et al., 1998b).

We induced SCE in wild-type and Nse2-deficient cells with the DNA cross-linker Mitomycin C (MMC) (Sonoda et al., 1999). We then scored and compared the levels of sister chromatid exchanges in these cell lines (Figure 4.26A and B). We observed a 50% increase in both spontaneous and MMC induced sister chromatid exchange frequencies in the *Nse2* background. This is consistent with the gene targeting assay results, where increased HR activity was observed.

In a similar experiment in human cells, reduced levels of spontaneous SCEs were observed after depletion of the Nse2 protein by siRNA (Potts et al., 2006). This discrepancy may be a result of differences between chicken and human functions of Nse2 protein as well as an effect of residual amount of Nse2 protein left after RNAi mediated depletion. Increased gene targeting and intersister chromatid recombination indicate that chicken Nse2 negatively regulates HR activity.

To further investigate the roles of Nse2 in the HR pathway, we decided to use a well-established assay in which recombination between two direct repeats is measured (Pierce et al., 1999). In this experiment, two fragments of GFP sequence (termed SceGFP and iGFP) were stably integrated into the genomes of wild-type and Nse2-deficient cells (Figure 4.27A). Separately, these sequences do not code for functional GFP protein. Expression of functional GFP can be induced by recombination between the SceGFP and iGFP sequences. This is achieved by the expression of *ISce-I* restriction endonuclease which cuts the SceGFP sequence and initiates recombinational repair (Figure 4.27A). Wild-type, *Rad54*$^{-/-}$ and *Nse2*$^{-/-/-}$ cells were transfected with *I-SceI* endonuclease to induce recombination between the direct repeats. In addition, cells were co-transfected with an RFP-expressing vector to ensure normalisation for

transfection efficiency between the cell lines analysed (Stephan et al., 2011a). HR-defective *Rad54*$^{-/-}$ mutants were used as a negative control in this experiment (Sonoda et al., 1999; Stephan et al., 2011a; Yamaguchi-Iwai et al., 1998b). The *Rad54*$^{-/-}$ mutants, as expected, showed severely reduced levels of recombination (Figure 4.26B, 3.25% GFP positive cells). Surprisingly, we observed more than a 50% decrease in break induced-recombination between direct repeats in the *Nse2*

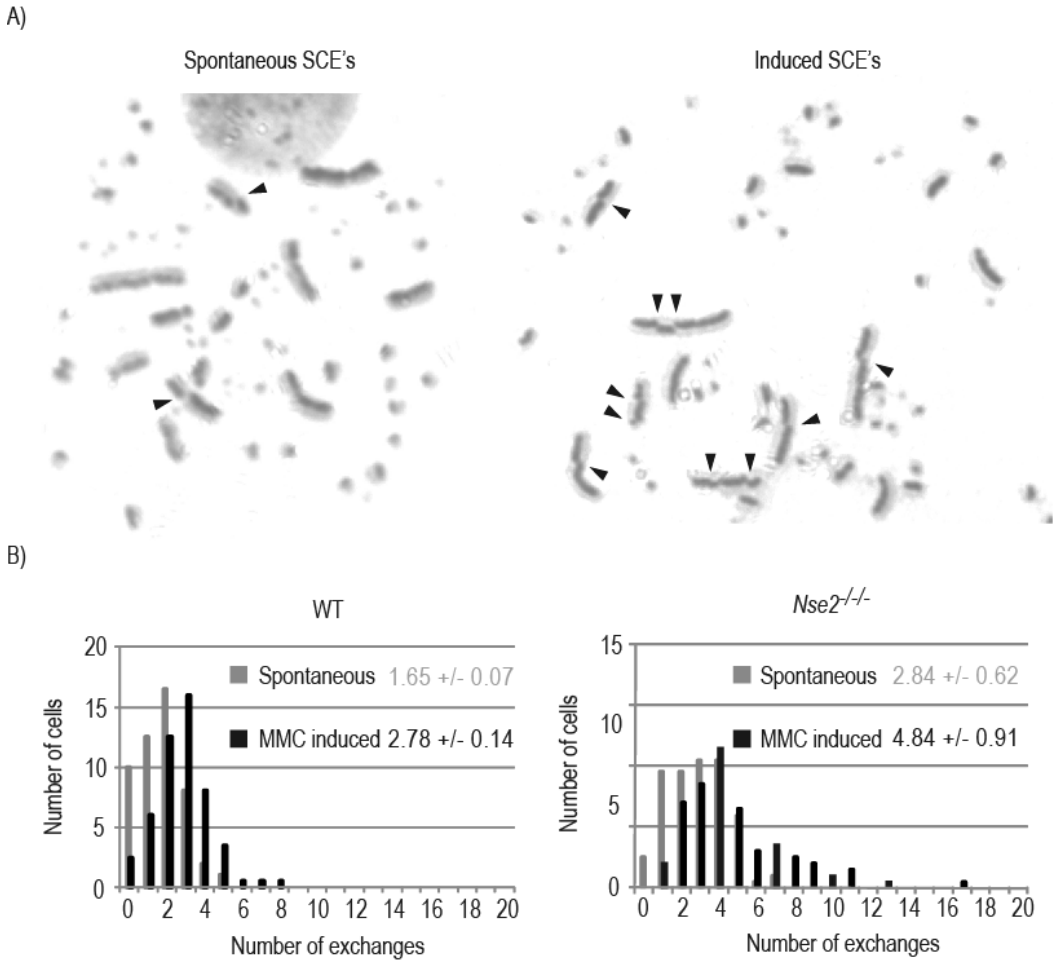

Figure 4.26 Nse2 cells show increased level of sister chromatid exchanges.

A) Micrograph of spontaneous and MMC-induced sister chromatid exchanges in wild-type cells. Arrowheads show sister chromatid exchanges. B) Quantification of sister chromatid exchange frequencies in wild-type and Nse2-deficient cells scored in macrochromosomes. The histograms show mean of the indicated sister chromatid exchanges per cell from two independent experiments in which at least at least 100 cells were scored. The values represents mean of sister chromatid exchanges per cell from the same experiments +/- S.D.

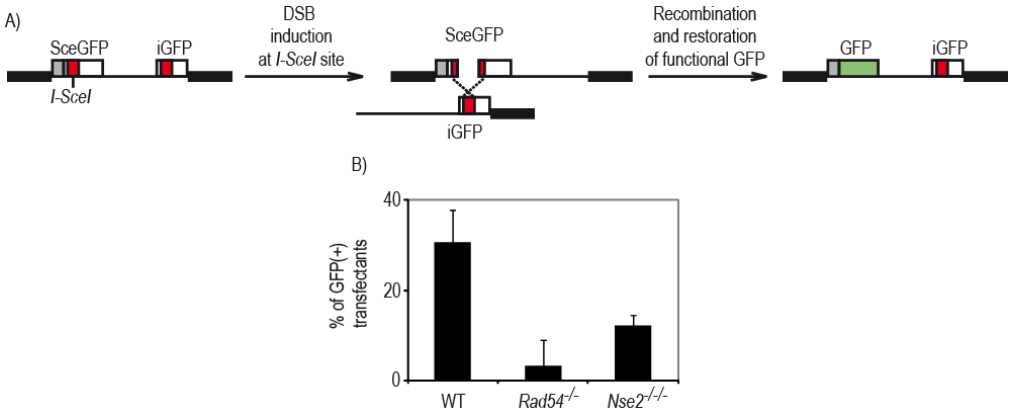

Figure 4.27 Recombination assay between direct repeats.

(A) Graphical representation of pDR-GFP assay. (B) Wild-type, Rad54$^{-/-}$ and Nse2 deficient cells bearing the pDR-GFP plasmid were transfected with I-SceI endonuclease to induce recombination between SceGFP and iGFP repeats. The GFP positive cells were scored by flow cytometry and expressed as % of positive transfectants. Plot shows mean of three independent experiments +/- S.D.

mutants compared to wild-type cells (Figure 4.27B, 12% and 30.6% of GFP positive cells in *Nse2*$^{-/-/-}$ and wild-type cells, respectively). The pDR-GFP assay showed results that differ from the gene targeting and sister chromatid exchange assay findings, with a decreased activity of HR in the *Nse2* background. This may reflect varying activity and role of Nse2 protein in different HR pathways. Therefore, we conclude that chicken Nse2 protein is required for the regulation of different subpathways of homologous recombination.

4.3.6 Loss of *Nse2* has no effect on sister chromatid cohesion

Cohesin recruitment to DSB is essential for proper DSB repair through the establishment of local cohesion around the DNA damage site (Bauerschmidt et al., 2010; Ellermeier and Smith, 2005; Kim et al., 2002). In human cells, cohesin recruitment to DSBs is dependent on the Smc5 and Nse2 proteins (Potts et al., 2006). However, cohesin recruitment to DSB is not observed in budding and fission yeast (Outwin et al., 2009; Ström et al., 2004). In addition, yeast and chicken mutants of the Smc1-Smc3 cohesin complex show increased sensitivity to DNA damaging agents (Birkenbihl and Subramani, 1992; Sonoda et al., 2001).

We also found that the loss of *Smc5* in chicken cells results in increased inter-sister chromatid distances before and after DNA damage (Stephan et al., 2011a).

We wanted to check if the observed HR defects in *Nse2*$^{-/-}$ cells might be a result of mis-regulation of cohesion. For this purpose, we applied an assay in which the distances between chromosomally-integrated TetO arrays visualised as spots with a TetR-GFP fusion protein, were measured in metaphase cells (Figure 4.28A) (Dodson and Morrison, 2009a).

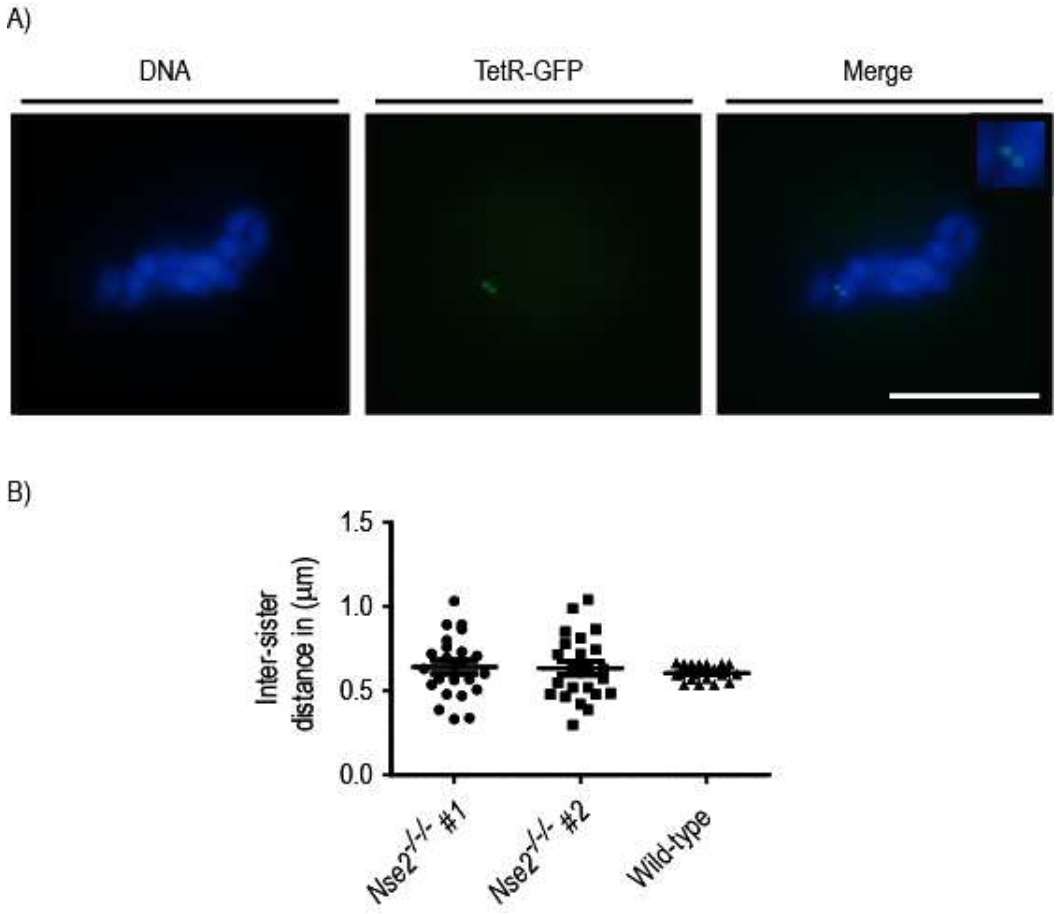

Figure 4.28 Inter-sister chromatid distances.

A) Micrographs showing expression of TetR-GFP protein and two separate signals from each sister chromatids (DNA is stained with blue, TetR-GFP with green). B) The distances between two GFP signals were measured in untreated metaphase cells. The plots show mean of two experiments in which at least 20 cells were scored. Scale bar shows 10 µm.

These distances are an indication of inter-sister chromatid separation (Dodson and Morrison, 2009a). We successfully used this assay in our laboratory to detect differences before and after induction of DNA damage in *ATM*$^{-/-}$ cells (Dodson

and Morrison, 2009a). We subjected the wild-type and Nse2-deficient cells to this analysis and observed normal sister chromatid separation in the *Nse2* background, suggesting that Nse2 is not required for genome-wide sister chromatid cohesion (Figure 4.28B).

4.4 Discussion

4.4.1 Chicken *Nse2* is not essential for DT40 viability

Our analysis of the Nse2-deficient DT40 cells demonstrates that Nse2 is not required for vertebrate cell viability. We have generated multiple clones that lack Nse2 which proliferated with kinetics similar to wild-type cells. This was unexpected as the deletion of budding and fission yeast Smc5-Smc6 complex proteins results in non-viable cells (Harvey et al., 2004; Lehmann et al., 1995; McDonald et al., 2003; Onoda et al., 2004; Pebernard et al., 2004; Pebernard et al., 2006; Sergeant et al., 2005; Zhao and Blobel, 2005). However, Smc5-Smc6 proteins are not essential for the viability of *Arabidopsis* (*Smc5* and *Smc6*), chicken (*Smc5*) and human cells (*Nse2* and *Smc5*) (Potts et al., 2006; Potts and Yu, 2005; Stephan et al., 2011a; Watanabe et al., 2009). This indicates that there are significant differences in the requirement for Smc5-Smc6 complex between lower and higher eukaryotes.

Even though the Nse2-deficient cells are viable, its loss clearly destabilises the Smc5-Smc6 complex. We observed a depletion of the Nse2-interacting partner Smc5 upon *Nse2* disruption. Conversely, the loss of *Smc5* in DT40 cells results in depletion of Nse2 and Smc6 but such down-regulation of Smc6 was not detected in Nse2-deficient cells (Stephan et al., 2011a). Taylor and Lehmann used an RNAi-based approach to study the cellular roles of the human Smc5-Smc6 complex and found that depletion of its various components (Smc5, Nse1, Nse2, Nse3, Nse4a) leads to destabilisation of the complex (Taylor et al., 2008). Re-introduction of the wild-type or SUMO ligase dead form of Nse2 in Nse2-deficient DT40 cells restored levels of Smc5. This indicates that the stability of Smc5 is not dependent on the SUMO ligase activity of Nse2 but rather on the interaction between Nse2 and Smc5. Therefore, we concluded that direct interactions between the Smc5/Smc6 and Nse2/Smc5 are essential for their

stability. We propose that the SUMO ligase-independent function of Nse2 is to bind to Smc5 and stabilise the Smc5-Smc6 complex, thus allowing it for proper DNA damage response and repair.

Hypomorphs of fission yeast *smc6-X, smc6-74, smc6-9, smc6-1* and budding yeast *smc5-31, smc5-33, mms21-11* show nuclear fragmentation and chromosome mis-segregation (Bermúdez-López et al., 2010; Cost and Cozzarelli, 2006; Lehmann et al., 1995; Verkade et al., 1999; Zhao and Blobel, 2005). Microscopy analysis of Nse2- and Smc5-deficient cells revealed a similar phenotype with increased levels of abnormal mitotic (anaphase bridges and mulitpolar cells) and elevated mitotic indices (Stephan et al., 2011a). In yeast, this is caused by the presence of unrepaired or incompletely replicated DNA, a direct effect of defective DNA repair and maintenance of the G_2/M checkpoint (Ampatzidou et al., 2006; Cost and Cozzarelli, 2006; Harvey et al., 2004; Verkade et al., 1999). Recently, a highly-extended delay in metaphase and premature separation of sister chromatids were reported in HeLa cells after RNAi-mediated depletion of Smc5 and Nse2 (Behlke-Steinert et al., 2009). We have not analysed this phenotype in detail but these data suggest that similar defects may be responsible for the observed mitotic aberrations in our mutants. These consistencies between yeast, chicken and human cells indicate that, even though Nse2-deficient DT40 cells are viable, the core functions of Smc5-Smc6 complex are conserved throughout evolution.

4.4.2 The cellular functions of Nse2 in cell cycle checkpoints and DNA repair

Analysis of the Nse2-deficient cells by flow cytometry showed wild-type cell cycle distribution. Minor defects in cell cycle progression were observed upon disruption of Smc5-Smc6 genes in yeast and chicken cells, suggesting that the chicken Smc5-Smc6 complex has no role during progression of the undisturbed cell cycle (Ampatzidou et al., 2006; Bermúdez-López et al., 2010; Lehmann et al., 1995; McDonald et al., 2003; Stephan et al., 2011a; Zhao and Blobel, 2005). We observed wild-type-like cell cycle profiles upon HU- and nocodazole-induced cell cycle arrest and release, suggesting that Nse2 is not

involved in the activation of the G_1/S and SAC checkpoints. However, we observed a slight delay in G_2/M checkpoint activation after IR treatment and a strong delay in Chk1 S345 phosphorylation post-MMS treatment. Yeast mutants of the Smc5-Smc6 complex, such as *smc6-74*, *smc6-dn*, *smc5-31*, *smc5-33* and *nse1,* activate the G_2/M checkpoint with wild-type kinetics after MMS and UV treatment but fail to maintain it (Ampatzidou et al., 2006; Cost and Cozzarelli, 2006; Harvey et al., 2004). We did not analyse the activation of factors upstream of Chk1, such as ATM, ATR, DNA-PK or the MRN complex, thus we cannot conclude if this is due to defects in DNA damage sensing or signalling. However, hyperactivation of ATM/ATR was observed in HeLa cells upon RNAi-mediated Nse2 depletion (Potts and Yu, 2005). The defects in cell cycle checkpoints we detected are consistent with observations in yeast where failure in G_2/M checkpoint maintenance in the absence of functional Smc5-Smc6 complex leads to nuclear fragmentation and abnormal chromosome segregation. This indicates that chicken Smc5-Smc6 complex is required for efficient response to DNA damage.

Yeast hypomorphs, such as *smc5-31*, *smc5-33* (Cost and Cozzarelli, 2006) and *smc6-X, smc6-74* (Ampatzidou et al., 2006; Lehmann et al., 1995; Verkade et al., 1999) are sensitive to MMS, HU and IR, UV, respectively. In addition, mutants of Nse2 (*nse2-1*, *nse2-SA*) (Andrews et al., 2005; McDonald et al., 2003) and Nse6 (*nse6Δ*) (Pebernard et al., 2006) are hypersensitive to IR. Moreover, mutants of Nse1 (*nse1-1*) (Pebernard et al., 2008a), Nse2 (*nse2-SA*) (Andrews et al., 2005), Nse3 (*nse3-1*) (Pebernard et al., 2004), Nse4 (*nse4-4*^{ts}) (Hu et al., 2005) and Nse6 (*nse6Δ*) (Pebernard et al., 2006) show sensitivity to HU, MMS and UV, and Nse1 (*nse1-1*) (Pebernard et al., 2008a), Nse3 (*nse3-1*) (Pebernard et al., 2004), whereas Nse6 (*nse6Δ*) (Pebernard et al., 2006) are also sensitive to camptothecin.

The survival of chicken Nse2-deficient cells after DNA damage correlates with checkpoint defects. We observed hypersensitivity of *Nse2* mutants to MMS but not to IR and HU, suggesting that, at least to some extent, the survival of Nse2-deficient cells after MMS is caused by abnormal checkpoint activation. Disruption of *Smc5* in DT40 cells is associated with MMS and IR sensitivity (Stephan et al., 2011a). This is rather surprising as both proteins are components

of the same DNA repair complex. In addition, *Nse2* mutants are hypersensitive to 4-NQO, MMC and UVC. We also found that Nse2-deficient cells have elevated frequencies of chromatid gaps and breaks after treatment with MMS and 4-NQO. Chromatin type lesions are formed when DNA damage is not removed by the post-replicative DNA repair. These data suggest that Nse2 is may be required for efficient DNA damage response and repair in both S and G_2 phases.

4.4.3 Nse2 is required for efficient repair of MMS-induced DNA damage

Nse2 was first identified in a screen for MMS sensitive mutants in *S. cerevisiae* (Prakash and Prakash, 1977). The MMS sensitivity of Nse2-deficient DT40 cells is consistent with the data from yeast and human cells (Pebernard et al., 2004; Potts and Yu, 2005; Zhao and Blobel, 2005). Expression of wild-type Nse2 cDNA in *Nse2*$^{-/-}$ cells restored their MMS sensitivity to wild-type levels, whereas reintroduction of the SUMO ligase dead form of Nse2 results in only partial rescue of this phenotype. This clearly demonstrates that even though the SUMO ligase activity of Nse2 is not required for stability of Smc5, it is required for efficient DNA repair after MMS treatment. Nse2 is essential in yeast but not its SUMO ligase activity; however, SUMO ligase activity is necessary for efficient DNA repair in these cells (Andrews et al., 2005; Pebernard et al., 2004; Zhao and Blobel, 2005). Chicken and human Nse2 are not required for cell viability but similarly to yeast, Nse2 is necessary for efficient DNA repair in these cells (Potts and Yu, 2005). This suggests that only the enzymatic functions of Nse2 may be evolutionarily conserved.

Flow cytometry analysis of *Nse2* mutants pulsed with MMS showed that in the absence of Nse2, cells do not re-enter G_1 phase after a G_2/M block. A similar phenotype has been observed in *mms21ΔC* and *smc6-9* after MMS treatment (Bermúdez-López et al., 2010). Analysis of γ-H2AX foci resolution after MMS treatment revealed that Nse2-deficient cells suffer from unrepaired DNA damage. γ-H2AX foci resolution in these cells was slower compared to wild-type cells. These data, together with the defect seen in MMS-induced checkpoint activation and increased levels of chromosomal aberrations, suggest

that *Nse2* mutants enter mitosis in the presence of unrepaired DNA. In budding yeast, Bermúdez-López et al. suggested that the unrepaired DNA represents sister chromatid junctions (SCJs) (Bermúdez-López et al., 2010), whereas other groups proposed that these represent cohesin-mediated sister chromatid linkages (Outwin et al., 2009). We have not analysed this defect in detail, therefore we cannot rule out that both mechanisms are the cause of the observed phenotype in our mutants.

MMS-induced DNA damage is repaired through base excision repair or through HR if replication forks collapse at the sites of methylated DNA (Beranek, 1990; Groth et al., 2010). Deletion of BER factors in yeast mutants of the Smc5-Smc6 complex, such as *Mag1, Nth1* and *Apn2,* results in increased sensitivity towards MMS, suggesting that BER is active in *smc6-74* cells and therefore removing a subset of the DNA methylated bases (Lee et al., 2007). Inhibition of BER in Nse2-deficient cells results in an effect similar to that observed in yeast. Deactivation of PARP-1 or APE-1 by small molecule inhibitors increased the sensitivity of $Nse2^{-/-/-}$ mutants to MMS, indicating that Nse2 is not involved in BER. Surprisingly, $Smc5^{-}$ cells after inhibition of BER showed slightly increased survival to that without APE-1 and PARP-1 inhibitors. Loss of the BER activity in Smc5-deficient cell may be responsible for increased MMS sensitivity compared to $Nse2^{-/-/-}$ mutants, where BER is functional. We also know that Nse2 is still present in Smc5-deficient cells, further confirming that Smc5 but not Nse2, is required for efficient BER. As MMS-induced DNA damage causes replication fork stalling beside BER activation, this indicates that Nse2-deficient cells possibly die due to impaired replication fork restart.

Bermúdez-López et al. detected significantly slower DNA replication and an increased number of unreplicated DNA gaps in *smc6-9* and *mm21ΔC* mutants after MMS treatment compared to wild-type (Bermúdez-López et al., 2010). Studies from the Murray and Sjögren labs showed that the Smc5-Smc6 complex is present at the stalled replication forks and that it is required for their efficient restart (Ampatzidou et al., 2006; Lindroos et al., 2006). We observed a wild-type rate of DNA synthesis in Nse2-deficient cells after MMS-induced DNA replication arrest, but our microscopy assay may not be sensitive enough to detect small differences in replication velocities. We also may not detect any

defects as they may be masked by the robust firing of the alternative replication origins. Recently, such an effect was described in human cells where alternative origin firing was detected after HU-induced cell cycle arrest (Petermann et al., 2010). A more sensitive assay, such as DNA fibre analysis should be performed to test if chicken Nse2 is necessary for efficient DNA replication and fork restart in the presence of MMS-induced DNA damage. Data gathered here indicate that Nse2 is required for efficient DNA repair after MMS treatment.

4.4.4 Nse2 plays a role in HR but not in sister chromatid cohesion

The Smc5-Smc6 complex and Nse2 protein have been implicated in DNA repair through homologous recombination. Deletion of HR genes, such as *Rad51* and *Rad54* in *Smc5, Smc6* and *Nse2* mutants does not increase sensitivity towards DNA damaging agents, showing that these genes are epistatic in response to DNA damage (Ampatzidou et al., 2006; Lehmann et al., 1995; McDonald et al., 2003; Stephan et al., 2011a; Torres-Rosell et al., 2007; Zhao and Blobel, 2005). Depletion of Smc5 and Nse2 in human and yeast cells disregulates HR, possibly through compromised recruitment of Smc1-Smc3 complex to the DSB (De Piccoli et al., 2006; Potts, 2009). Recently, severe loss of chromosome cohesion was reported in human cells after RNAi-mediated depletion of Smc5 and Nse2 (Behlke-Steinert et al., 2009). We also observed a loss of sister chromatid cohesion in Smc5-deficient DT40 cells, suggesting an active role of vertebrate Smc5-Smc6 complex in the regulation of sister chromatid cohesion (Stephan et al., 2011a). In addition, yeast and human Smc5-Smc6 complexes are dispensable for efficient non-homologous end joining (De Piccoli et al., 2006; Potts, 2009). Disruption of the NHEJ gene, *Ku70* in chicken *Smc5*$^{-}$ cells increased their sensitivity towards IR, further confirming a HR role of the vertebrate Smc5-Smc6 complex (Stephan et al., 2011a). We did not observe spontaneous loss of sister chromatid cohesion in *Nse2*$^{-/-}$ knockouts, suggesting that chicken Nse2 does not play an active role in this process, at least under our experimental conditions. This is consistent with the lack of sensitivity of Nse2-deficient cells to IR-induced DSB.

We also analysed homologous recombination activities in *Nse2*$^{-/-}$ background. Nse2-deficient cells are proficient at gene targeting and show slightly increased gene targeting at two of three loci investigated (*Ovalbumin* and *ATM* but not in *Cetn2*), thus suggesting that Nse2 plays a negative regulatory role in HR. Wild-type like frequencies were observed in Smc5-deficient cells, suggesting a separable role of Nse2 and Smc5 in this process (Stephan et al., 2011a). We cannot explain why we observe a different effect at these loci but this may be associated with their chromosomal localisation or differences in targeting vectors per se. Conversely, a break induced recombination assay revealed reduced HR activities in Nse2- and Smc5-deficient cells (Stephan et al., 2011a). In this assay, the GFP signal can be restored by intra-chromatid, unequal sister chromatid HR or single strand annealing processes but not through equal sister chromatid HR or NHEJ (Moynahan et al., 2001). Potts et al. in an identical assay observed the opposite effect after RNAi-mediated depletion of Nse2 and Smc5 in human cells and showed that in the absence of Nse2, sister chromatid HR is blocked and DSB is repaired through gene targeting or intra-chromatid recombination (Potts et al., 2006). The same group reported a decrease in sister chromatid recombination, as measured by SCE frequencies, in the absence of Nse2 and Smc5 (Potts et al., 2006). In the same assay, chicken *Nse2*$^{-/-}$ and *Smc5*$^{-}$ cells showed increased SCE frequencies (Stephan et al., 2011a).

We have no explanation as to why a HR mechanism driving increased sister chromatid recombination observed in SCE and gene targeting assays would not positively affect break induced recombination between the sisters. It is possible that the observed discrepancies may be a result of residual levels of Smc5 and Nse2 proteins remaining after knockdown by RNAi. In addition we may be looking at species specific differences between chicken and human systems. It is also possible that the nature of these HR events support slightly different outcomes in these experiments. Gene targeting occurs mainly in S phase and requires active replication machinery to happen (Wong and Capecchi, 1986). Similarly, there is a link between SCE formation and DNA synthesis, indicating that these are formed only when the replication machinery encounters a DNA lesion (Wolff et al., 1974). Possibly, the establishment of Nse2-dependent HR structures in DT40 cells might be restricted only to the S phase of the cell cycle,

since its loss increases the levels of gene targeting and SCEs but not repair of double strand breaks induced by *I-SceI*, which may be repaired through a different mechanism.

In conclusion, we report here that Nse2 protein is required for efficient DNA repair, possibly through the regulation of homologous recombination.

Chapter 5 Generation and characterisation of *Nse2*$^{-/-/-}$*Smc5*$^{-}$ cells

5.1 Genetic dissection of the Smc5-Smc6 complex

5.1.1 Generation of *Nse2*$^{-/-/-}$*Smc5*$^{-}$ knockout cells

Our analysis of the Smc5-Smc6 complex by characterisation of Nse2-deficient cells (this study) and *Smc5* knockouts (Stephan et al., 2011a) revealed distinct phenotypes (Table 5.1). We observed different responses of Nse2- and Smc5-deficient cells towards IR and MMS. Chromosomal aberrations are increased after IR in *Smc5*$^{-}$ cells but not in *Nse2*$^{-/-/-}$ cells. Conversely, *Nse2*$^{-/-/-}$ but not Smc5-deficient cells show elevated chromosomal aberrations after MMS. Loss of Smc5 results in depletion of Smc6 and Nse2, whereas disruption of *Nse2* leads only to loss of Smc5 but not Smc6.

Fission yeast *smc6.T2nse2.SA* double mutants show slower growth kinetics and budding yeast *smc6-9mms21-sp* demonstrate increased sensitivity towards UV-induced DNA damage than either of single mutants (Andrews et al., 2005; Chavez et al., 2010b). Hazbun et al. have identified two different Smc5-Smc6 complexes and recently, two complexes, Nse2-Smc5-Smc6 in interphase and Nse2-Smc5 in mitotic cells, were detected by gel filtration in human cells (Behlke-Steinert et al., 2009; Hazbun et al., 2003). *In vitro* studies with recombinant Smc5 protein showed its preferential binding to single stranded DNA, independently of its Smc partner Smc6 (Roy et al., 2011). These data suggest that components of the Smc5-Smc6 complex may have separable functions. Taking these observations into consideration, we hypothesised that the differences observed between Nse2- and Smc5-deficient cells are due to (1) some non-overlapping functions of Nse2 and Smc5 proteins, (2) defective regulation of Smc5-Smc6 the in absence of Nse2 SUMO ligase, (3) or that different Smc5- and Nse2- containing subcomplexes exist that have distinct functions. As shown in Table 5.1, chromosomal aberrations seem to be specifically Nse2-dependent and IR sensitivity is only observed in the absence of Smc5 supporting the first hypothesis.

Table 5.1 Comparison of Smc5*$^{-}$ *and Nse2*$^{-/-}$ *phenotypes

	Smc5*$^{-}$ cells	***Nse2*$^{-/-}$ cells****
Viability	Viable	Viable
Growth rate	Wild-type	Wild-type
Mitotic index/aberrations	Higher than wild-type	Higher than wild-type
Destabilisation of Smc5-Smc6 complex	Depletion of Smc6 and Nse2 proteins	Depletion of Smc5 protein
Checkpoint proficiency:		
S	WT	WT
G_2/M	WT	Delayed
Spindle assembly checkpoint	WT	WT
MMS induced Chk1 S345 phosphorylation	N/D	Delayed
IR sensitivity	↑↑	↑
MMS sensitivity	↑↑↑	↑↑
Chromosomal aberrations	Increased after IR but not MMS	Increased after MMS and 4-NQO
Sister chromatid cohesion	↑	WT
Targeting assay frequencies	Wild-type	Slightly increased
Sister chromatid exchange frequencies	~2.5-fold increase	1.5-fold increase
Direct repeat recombination	↓↓	↓↓
Base excision repair	-	+
Phenotype rescue by transgene expression:		
MMS sensitivity	N/D	Rescued
Direct repeat recombination	Rescued	N/D

*** - (Stephan et al., 2011a), ** - this study**

Smc5 mutants showed more severe phenotypes than the *Nse2*$^{-/-}$ cells in most of the experiments. Assuming that an Smc5-Smc6 heterodimer is still formed within the *Nse2* mutants (but not in *Smc5* background) and if this Smc5-

Smc6 complex lacks Nse2-mediated SUMOylation, the more severe phenotypes support the idea that the observed phenotypic differences between Nse2- and Smc5-deficient cells are due to mis-regulation of the Smc5-Smc6 complex. To investigate this notion, we disrupted the *Smc5* gene in *Nse2* background. We hypothesised that if Smc5 and Nse2 proteins have separate functions, the loss of Smc5 protein in the Nse2-deficient cells would result in a phenotype stronger that that observed in *Smc5*$^{-}$ cells.

The targeting strategy and vectors for *Smc5* disruption were as described (Stephan et al., 2011a). *Nse2*$^{-/-/-}$ cells were transfected with an *Smc5* targeting vector to disrupt *Smc5* (Stephan et al., 2011a). We successfully targeted *Smc5* in the *Nse2*$^{-/-/-}$ background and obtained several viable clones (Figure 5.1).

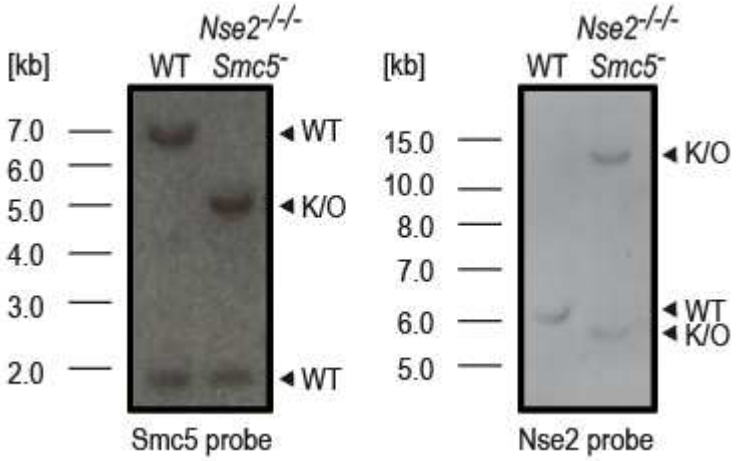

Figure 5.1 Southern blot analysis of the Nse2*$^{-/-/-}$*Smc5*$^{-}$ *mutants.

Genomic DNA was isolated from wild-type and Nse2$^{-/-/-}$*Smc5*$^{-}$ *cells and digested with EcoRI (Smc5 probe), XmnI (Nse2 probe) and analysed by Southern blotting with the indicated probes.*

As expected, the *Smc5* probe detects replacement of the wild-type band (6.9 kb) with a targeted band of 4.9 kb (Figure 5.1). We also looked at the *Nse2* locus with the *Nse2* probe. The 6.3 kb wild-type band was absent in the double mutant and it had been replaced by two 14.7 kb (double intensity) and 5.8 kb (single intensity) mutant bands, showing that we have targeted *Smc5* in the Nse2-deficient cells (Figure 5.1).

Next, we isolated total mRNA from the *Nse2*$^{-/-/-}$*Smc5*$^{-}$ cells and tested whether the mRNA of *Nse2* and *Smc5* genes was still present in these cells (Figure 5.2). Reverse transcriptase PCR revealed that there is no *Nse2* and *Smc5*

mRNA present in the double knockout cells. The Smc5 and Nse2 deficient cells were used here as negative controls.

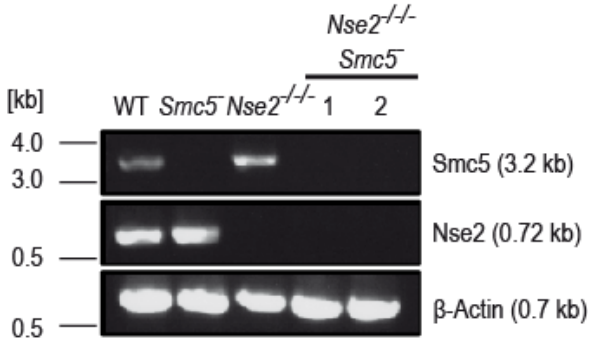

Figure 5.2 Analysis of Smc5 and Nse2 mRNA expression in Nse2$^{-/-}$Smc5^{-} cells.

Reverse transcriptase-polymerase chain reaction with total mRNA isolated from the wild-type, Smc5^{-}-, Nse2$^{-/-}$-, and two Nse2$^{-/-}$Smc5^{-}-targeted clones and the indicated gene specific primers.

We then investigated the levels of Smc5 and Nse2 proteins to confirm their absence in these cells (Figure 5.3). Immunoblotting revealed depletion of Smc5 and Nse2 proteins in the double knockout background.

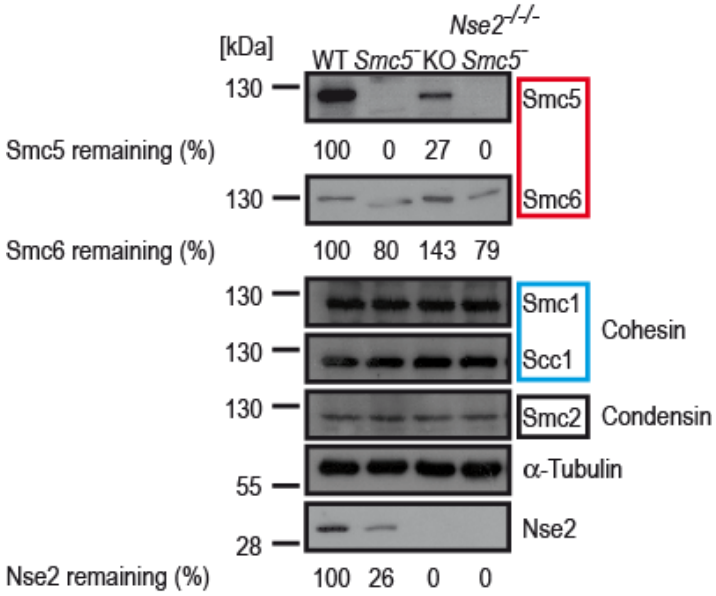

Figure 5.3 Immunoblot analysis of Smc complexes Nse2$^{-/-}$Smc5^{-}.

Proteins from wild-type, Nse2-, Smc5-deficient and Nse2$^{-/-}$Smc5^{-} cells were extracted, separated by SDS-PAGE and analysed by immunoblotting with the indicated antibodies.

Our previous analysis had shown that loss of the Smc5 results in depletion of Smc6 and Nse2, whereas disruption of Nse2 proteins leads to reduction of only Smc5 protein (Stephan et al., 2011a). We found that the loss of *Nse2* and *Smc5*

results in depletion of Smc6 to levels similar to those observed in Smc5-deficient cells. The levels of cohesin and condensin complexes did not change upon disruption of *Nse2* and *Smc5*, indicating that only Smc5-Smc6, but not other Smc complexes, is destabilised in the absence of Nse2 and Smc5. The lack of *Nse2* and *Smc5* mRNAs and respective proteins in the *Nse2*$^{-/-/-}$*Smc5*$^{-}$ cells further confirms that the Smc5-Smc6 complex is not essential for chicken cell viability.

5.1.2 *Nse2*$^{-/-/-}$*Smc5*$^{-}$ cells show growth retardation and mitotic aberrations

The proliferative properties of *Nse2*$^{-/-/-}$*Smc5*$^{-}$ cells were analysed by measuring the growth kinetics and mitotic indices (Figure 5.4). The double knockouts proliferated with much slower kinetics than wild-type cells or either single knockout, indicating a defect in cell proliferation. Similar growth retardation was observed in yeast double mutants of *smc6.T2nse2.SA* (Andrews et al., 2005). The *Nse2*$^{-/-/-}$*Smc5*$^{-}$ cells showed a similarly increased mitotic index and number of abnormal mitotic cells as *Nse2*$^{-/-/-}$ and *Smc5*$^{-}$ mutants. We also observed an increased population of binucleated cells in the double mutant. This may be a factor contributing to observed growth retardation. Loss of either *Nse2* or *Smc5* does not result in significant decrease in growth rate but loss of *Smc5* and *Nse2* does. These data suggest that Smc5 and Nse2 may have different functions in cell cycle progression.

5.1.3 *Smc5* and *Nse2* are not epistatic in response to DNA damage

To investigate the relationship between *Smc5* and *Nse2*, we subjected our Smc5-Smc6 complex mutants to epistasis experiments. If these genes have separate functions in DNA damage response and repair, one would expect an exacerbation of the phenotype observed for the individual mutants in the doubly-targeted clones. Our analysis of single *Smc5*$^{-}$, *Nse2*$^{-/-/-}$ and double *Nse2*$^{-/-/-}$*Smc5*$^{-}$ clones

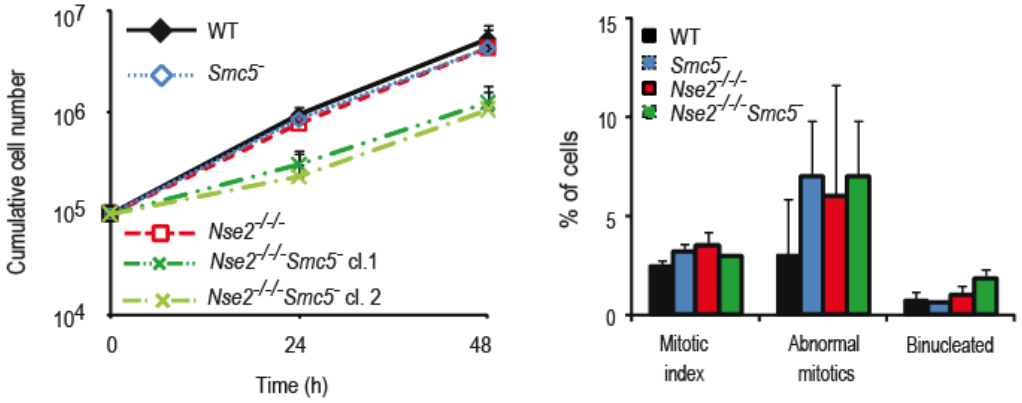

Figure 5.4 Proliferative properties of Smc5-Smc6 complex mutants.

A) Growth curve – equal number of cells (10^5 per ml) was seeded and cell number monitored over 48 hours time period. Data points show mean of three independent experiments +/- S.D. B) Quantification of mitotic indices and aberrations. Histogram shows mean of three independent experiments +/- S.D in which at least 100 mitotic cells were scored.

revealed an increased sensitivity of *Nse2*$^{-/-/-}$*Smc5*$^{-}$ cells towards cis-platin, MMS and IR, compared to either single mutant (Figure 5.5A, B and C). *Nse2*$^{-/-/-}$*Smc5*$^{-}$ mutants are severely sensitive to cis-platin treatment and only moderately to IR and MMS, compared to Smc5- and Nse2-deficient cells (Figure 5.5A, B and C). Increased cell death of the double mutants to IR treatment was rather surprising as the *Nse2*$^{-/-}$ cells are not sensitive to this DNA damaging agent (Figure 5.5B).

Overall, the *Nse2* mutants were consistently the least, and double knockouts the most, sensitive to DNA damage of the four cell lines we analysed. We did not observe any elevated sensitivity of Smc5-Smc6 complex mutants towards the topoisomerase I toxin camptothecin (Figure 5.5D). Higher concentrations of camptothecin were also used in other experiments but we did not observe any difference in responses between Smc5-Smc6 complex mutants and wild-type cells. Camptothecin induces SSB which are converted to DSB by the replication machinery and these are specifically repaired by HR (Fiorani and Bjornsti, 2000; Hsiang et al., 1989). We expected that our Smc5-Smc6 complex mutants would be sensitive towards this drug as such sensitivity is observed in fission yeast *nse6Δ, nse1ΔRING, nse1-C197A* and *nse1-C199A* mutants (Pebernard et al., 2008a; Pebernard et al., 2006). It is possible that our mutants are not hypersesnsitive towards camptothecin under the particular experimental conditions we used (two hours treatment). Decrease in cell survival of the *Nse2*$^{-/-}$

$^{/-}$*Smc5*$^{-}$ mutants indicate that *Smc5* and *Nse2* are not epistatic in DNA repair after cis-platin, IR and MMS treatment. These data suggest that in addition to common roles the Smc5 and Nse2 may have non-overlapping functions.

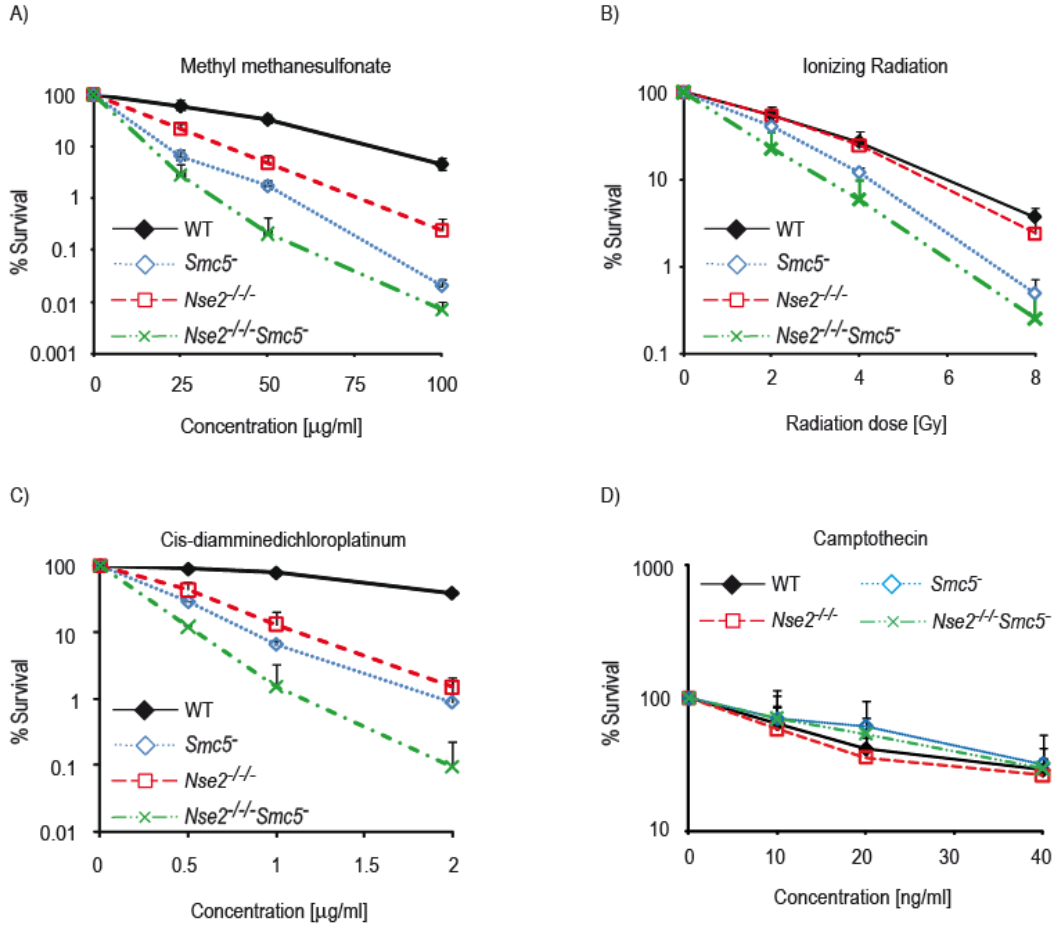

Figure 5.5 Epistasis analysis of the Smc5-Smc6 complex.

Wild-type, Smc5^{-}*, Nse2*$^{-/-}$ *and Nse2*$^{-/-}$ *Smc5*$^{-}$ *cells were treated with the indicated DNA damaging agents for 2 hours and plated in methylcellulose media. Colonies were scored after 10-14 days after plating. In the case of IR cells were exposed to IR source (*^{137}*Cs) on the methylcellulose plates. The plots show mean of relative survival from three independent experiments +/- S.D. Plating efficiencies were wild-type, 80%; Nse2*$^{-/-}$*, 67%; Smc5*$^{-}$*, 46%; Nse2*$^{-/-}$*Smc5*$^{-}$*, 20%.*

5.1.4 Nse2, but not Smc5, is required to minimise chromosomal aberrations

We then compared the levels of chromosomal aberrations between the mutants generated. Karyotypes were analysed by microscopy after exposure to MMS. *Nse2* mutants had the highest levels of spontaneous and MMS-induced chromosomal lesions (Figure 5.6).

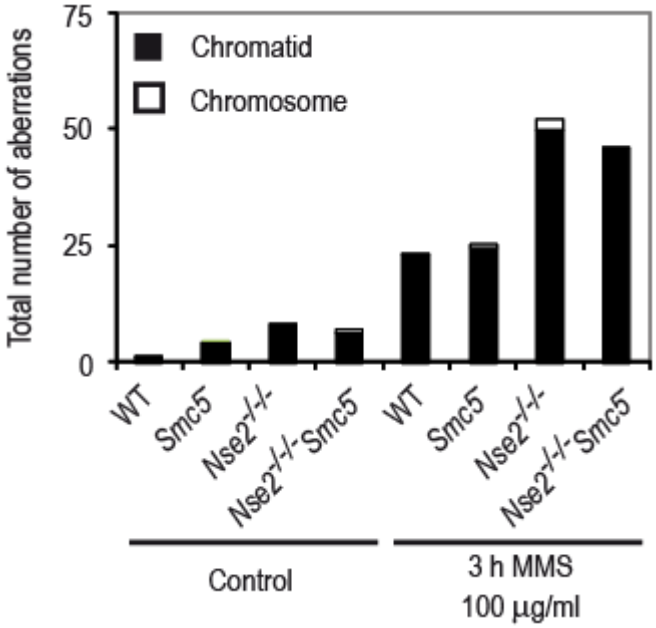

Figure 5.6 Nse2 but not Smc5 is required to prevent chromosomal aberrations post-MMS treatment.

Wild-type, Smc5^{-}*, Nse2*$^{-/-}$ *and Nse2*$^{-/-}$ *Smc5*$^{-}$ *cells were treated with the DNA damaging agent for 3 hours or left untreated. Cells were then blocked in mitosis and metaphase spreads were prepared. The plots show average of three experiments in which at least 50 cells were scored. S.D is not shown for histogram clarity.*

Double knockouts of *Nse2* and *Smc5* showed similar levels of aberrations as Nse2-deficient cellsm and the *Smc5* mutants, as previously described, showed a wild-type like phenotype (Stephan et al., 2011a). The elevated levels of chromosomal aberrations after MMS observed in Nse2-deficient compared to *Smc5*$^{-}$ mutants do not agree with their survival rates after MMS treatment. Nse2-deficient cells may die through different mechanisms, than *Smc5*$^{-}$ mutants, which may include formation of chromosomal aberrations and this phenotype may be dominant over *Smc5*, as observed in *Nse2*$^{-/-}$*Smc5*$^{-}$ cells. Our analysis suggests

that Nse2 but not Smc5, is the component of the Smc5-Smc6 complex required for maintenance of genome integrity. This is another argument that favours the idea of separable roles of Smc5 and Nse2 in response to DNA damage.

5.1.5 Roles of Smc5-Smc6 complex in replication fork restart

We then tested if the *Smc5* deficient cells and double knockout show a replication restart defect using the same assay as described for *Nse2*$^{-/-/-}$ cells in Section 4.3.4. We observed wild-type like kinetics of DNA synthesis restart after release from MMS block in Nse2- and Smc5-deficient cells but not in the double mutants (Figure 5.7). *Nse2*$^{-/-/-}$*Smc5*$^{-}$ cells showed a decreased number of replication foci positive cells post-MMS removal (Figure 5.7). This decrease was detected at all time points analysed with just 20% of EdU positive cells 4 hours post-release in *Nse2*$^{-/-/-}$*Smc5*$^{-}$ compared to 34% in wild-type cells (Figure 5.7).

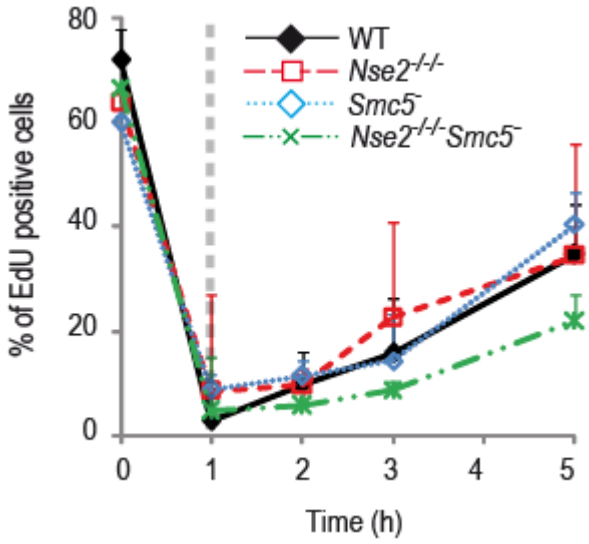

Figure 5.7 Analysis of replication foci in cells treated with MMS.

Quantification of EdU positive cells before and after 1 hour MMS block (130 μg/ml). Data points show mean of three experiments +/- S.D in which at least 300 cells were scored.

This may be due to their slower proliferation of *Nse2*$^{-/-/-}$*Smc5*$^{-}$; however, it is unlikely as they show wild-type levels of EdU incorporation before MMS treatment. The loss of *Nse2* or *Smc5* does not affect the rate of DNA synthesis after MMS treatment, but deletion of both genes does. This suggests that Nse2 and Smc5 may be involved in DNA synthesis restart after MMS treatment and it

is consistent with observations in both yeast where Smc5-Smc6 complex is required for the restart of the collapsed replication forks (Ampatzidou et al., 2006; Branzei et al., 2006).

5.1.6 Roles of Smc5 and Nse2 in HR

Our observation that Smc5 and Nse2 have non-overlapping functions in the cellular responses to DNA damage, led us to hypothesise that the loss of both proteins will result in further deregulation of homologous recombination. To test this, we analysed sister chromatid exchange frequencies in these mutant cell lines. We found that all knockouts had increased levels of spontaneous and MMC-induced sister chromatid exchanges compared to wild-type cells (Figure 5.8).

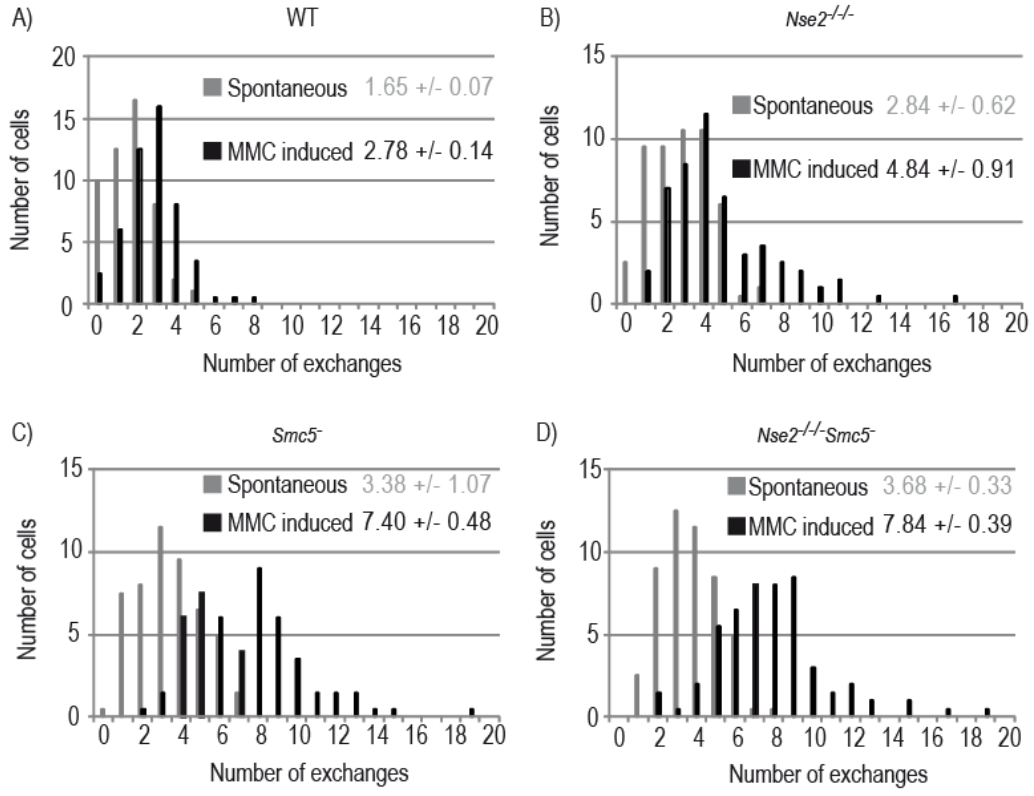

Figure 5.8 Analysis of sister chromatid exchange levels in Smc5-Smc6 mutants.

Sister chromatid exchange frequencies in wild-type A) Nse2- B), Smc5-deficient C) and Nse2$^{-/-}$ *Smc5*$^{-}$*double mutants scored in macrochromosomes. The histograms show mean of the indicated sister chromatid exchanges per cell from two independent experiments in which at least at least 100 cells were scored. The values represents mean of sister chromatid exchanges per cell from the same experiments +/- S.D.*

Nse2-deficient cells showed 1.7-fold increase in sponataneous and MMC-induced sister chromatid exchanges compared to wild-type cells. *Smc5*$^{-}$ mutants showed 2.0-fold and 2.6-fold increase in spontaneous and induced SCEs over wild-type cells, respectively. *Nse2*$^{-/-}$*Smc5*$^{-}$ demonstrated SCE levels slightly above the level observed in *Smc5*$^{-}$ cells, suggesting that *Smc5* and *Nse2* genes are epistatic in their HR functions.

5.2 Conclusions

5.2.1 Smc5-Smc6 complex is not essential for DT40 cell viability

Several viable clones of *Nse2*$^{-/-}$*Smc5*$^{-}$ cells were obtained confirming that the chicken Smc5-Smc6 complex is not essential for proliferation of DT40 cells. However, strong growth retardation was observed in these mutants compared to wild-type or Nse2- and Smc5-deficient cells. Disruption of Nse2 SUMO ligase activity in yeast *smc6* cells also resulted in slower proliferation, suggesting that separation of Nse2 and Smc5-Smc6 heterodimer functions may be evolutionarily conserved (Andrews et al., 2005; Chavez et al., 2010b). *Nse2*$^{-/-}$*Smc5*$^{-}$ cells showed mitotic indices and levels of abnormal mitotic similar to single mutants. The loss of Smc5 in Nse2-deficient cells did not further destabilise the Smc5-Smc6 or other Smc complexes. Therefore, we conclude that Smc5 and Nse2 may have separable functions in cell cycle progression.

5.2.2 *Smc5* and *Nse2* are not epistatic in response to DNA damage and homologous recombination

Fission yeast *smc6.T2nse2.SA* mutants demonstrate increased sensitivity towards UV-induced DNA damage compared to either single mutant (Andrews et al., 2005). Deletion of *Smc5* in *Nse2*$^{-/-}$ DT40 cells results in a similar effect, with a stronger sensitivity towards cis-platin, IR and MMS, compared to single mutants. This indicates that *Smc5* and *Nse2* are required for efficient DNA repair but are not epistatic in response to DNA damage.

Hypomorphic alleles of *S. cerevisiae smc6-9* and *nse5-1* show more frequent gross chromosomal rearrangements (De Piccoli et al., 2006). Loss of SUMO ligase activity in *S. cerevisiae mms21Δsl* allele results in elevated

telomere marker loss and elevated chromosomal instability (Rai et al., 2011). In *S. cerevisiae* temperature-sensitive mutants *smc5-31* and *smc5-35* show severe loss of heterozygosity at the *MET15* locus compared to wild-type cells (Cost and Cozzarelli, 2006). We observed increased levels of chromosome aberrations after MMS treatment in *Nse2*$^{-/-/-}$ and *Nse2*$^{-/-/-}$*Smc5*$^{-}$ but not *Smc5*$^{-}$ mutants. Smc5-deficient cells are more sensitive to MMS-induced DNA damage compared to *Nse2*$^{-/-/-}$ mutants but still they showed wild-type levels of chromosomal aberrations. As mentioned in Section 5.1.4, Nse2- and Smc5-deficient cells may die through different mechanisms. Loss of Nse2 is associated with delayed activation of Chk1 after MMS treatment, which possibly allows a subset of cells to evade checkpoint and enter mitosis with unrepaired DNA damage. We did not analyse Chk1 activation in Smc5-deficient cells so we cannot dismiss the possibility that *Smc5*$^{-}$ mutants activate this checkpoint properly. If this is indeed the case it would explain wild-type levels of chromosomal aberrations. On the other hand, these two experiments measure different responses (short and long term), which may account for the observed differences between *Nse2*$^{-/-/-}$ and *Smc5*$^{-}$ mutants. These data suggest that Nse2 but not Smc5 is required for maintenance of genomic integrity through preventing formation of chromosomal aberrations.

In human cells RNAi-mediated depletion of Nse2 or Smc5 leads to decreased camptothecin-induced sister chromatid exchange frequencies (Potts et al., 2006). In addition, loss of the Smc5-Smc6 complex function results in dysregulation of homologous recombination in yeast, chicken, *Arabidopsis* and human cells (De Piccoli et al., 2006; Lehmann et al., 1995; Potts et al., 2006; Stephan et al., 2011a; Watanabe et al., 2009). *Nse2*$^{-/-/-}$*Smc5*$^{-}$ cells showed increased sister chromatid exchange frequencies compared to wild-type and Nse2-deficient cells but not *Smc5*$^{-}$ mutants. The frequencies of SCE correlate with levels of Smc5 protein in these mutants. Smc5 protein is partially depleted in Nse2-deficient cells which show slightly elevated SCE levels. In the complete absence of Smc5 in *Smc5*$^{-}$ mutants SCE levels are further increased but are identical compared to *Nse2*$^{-/-/-}$*Smc5*$^{-}$ cells. Since depletion of Smc5 in Nse2-deficient cells did not increase SCE frequencies significantly above these observed in *Smc5*$^{-}$ mutants, we concluded that it may be the loss of Smc5 but not

Nse2 that results in the formation of SCE in our mutants. This suggests that *Smc5* and *Nse2* may be epistatic in their homologous recombination functions.

Chapter 6 Conclusion and future perspectives

6.1 Conclusions

We have identified and cloned the chicken homologue of Nse2 and showed that it is an active E3 SUMO ligase *in vitro.* Cell survival assays revealed that Nse2 is required for efficient DNA repair after exposure to various DNA damaging agents. Our analysis suggests that the binding of Nse2 to Smc5 but not Nse2 SUMO ligase activity stabilises Smc5-Smc6 complex, thus allowing it for efficient DNA repair. However, the catalytic activity of Nse2 is required for efficient DNA repair, suggesting that SUMOylation of the Smc5-Smc6 complex or other cellular targets by Nse2 may be important in this process. Smc5-Smc6 localisation to distinct chromatin domains, such as DSBs and stalled replication forks may be dependent on Nse2-mediated Smc5-Smc6 complex SUMOylation.

We also established a role for Nse2 in cell cycle checkpoint activation and in the maintenance of genome integrity. In addition, expression of an Nse2-GFP fusion protein revealed its cytoplasmic and nuclear localisation which is in agreement with the current literature and the functions of Smc5-Smc6 complex. We also showed that the Nse2 is required for the proper regulation of homologous recombination but not for sister chromatid cohesion. Our analysis of Nse2-deficient, Smc5-deficient and $Nse2^{-/-}Smc5^{-}$ mutants suggests that Nse2 and Smc5 have separable functions or that they are components of distinct complexes. Little is known about how the Smc5-Smc6 complex mediates DNA repair and future studies will be necessary to determine the mechanism of Nse2-Smc5-Smc6 action.

6.2 Overall conclusions

In conclusion, this study highlights the function of Nse2 and Smc5-Smc6 complex in regulation of several cellular processes, such as cell cycle and cell cycle checkpoints, DNA repair and homologous recombination. In general, it revealed a number of interesting discoveries on the different cellular roles of Nse2 and the Smc5-Smc6 complex. These proteins coordinate these cellular

processes, probably through regulation of higher-order chromatin structure, modification and recruitment of DNA repair factors to sites of DNA damage.

6.3 Model

Data gathered in this thesis, along with other published data, provide evidence that the Smc5-Smc6 complex is involved in DNA repair (reviewed in (Stephan et al., 2011a)). However, a mechanism for Smc5-Smc6 complex action still remains elusive, mainly because of the gap in understanding how Smc5-Smc6 interacts with DNA. In this section we describe a potential mechanism of Smc5-Smc6 action based on the current literature and our own observations.

We propose that Smc5-Smc6 has multiple DNA substrates (referred to here after as SSSSS (Structure-Specific Smc5-Smc6 DNA Substrates), examples of which are shown in Figure 6.1.

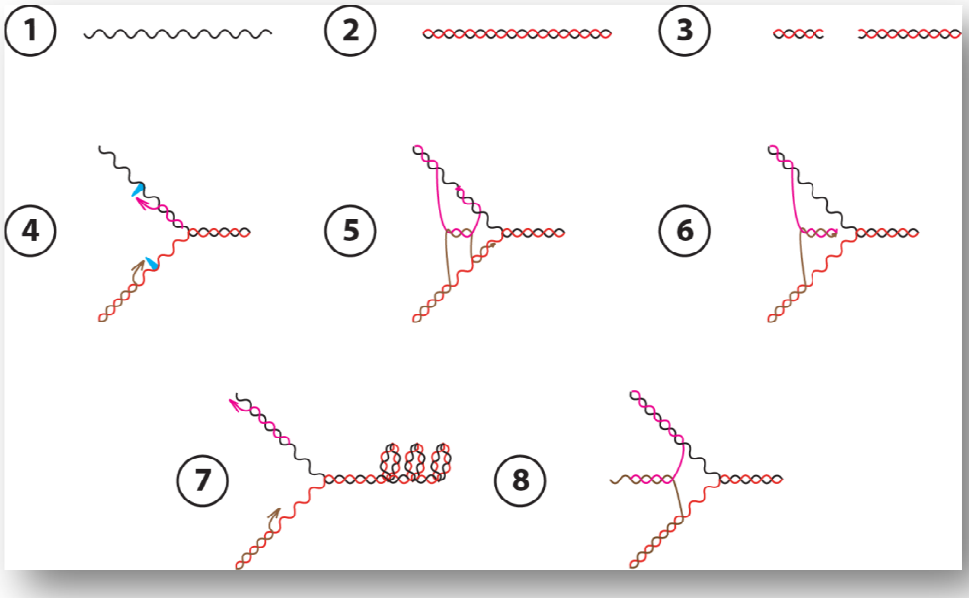

Figure 6.1 Potential DNA structures bound by Smc5-Smc6 complex.

Cartoon representation of potential DNA substrates of Smc5-Smc6 complex. (1) ssDNA, (2) dsDNA, (3) DSB, (4) stalled replication fork (lagging and leading strand), (5) Holliday junctions, (6) template switch intermediate, (7) supercoiled DNA, (8) reversed fork 'chicken foot'. Blue triangles represent replication for- stalling DNA lesions.

Such SSSSSs require processing via Smc5-Smc6 for their efficient resolution. The pathway controlled by Smc5-Smc6 is essential in response to DNA damage,

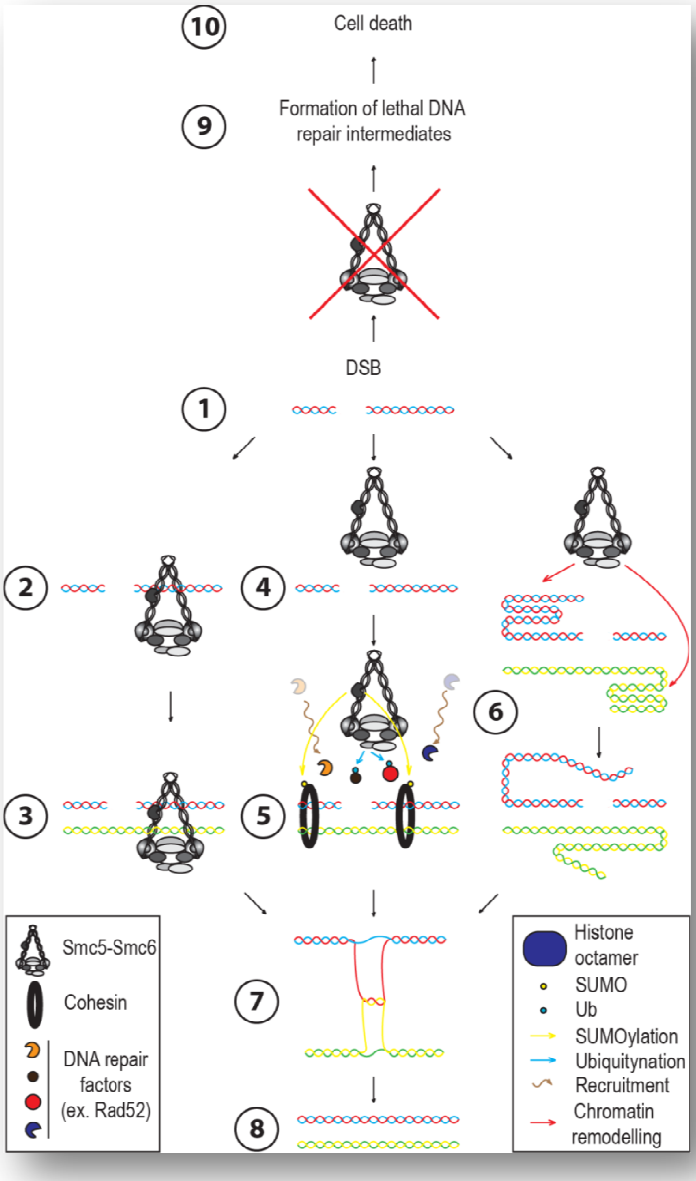

Figure 6.2 Model of Smc5-Smc6 action.

Cartoon representation of Smc5-Smc6 mechanism of action. Structure-specific Smc5-Smc6 DNA substrates, such as DSBs are processed by the Smc5-Smc6 complex for efficient DNA repair. When DSBs are formed (1) the Smc5-Smc6 complex may repair DNA through different mechanisms. The Smc5-Smc6 complex could bind in proximity of DSB (2) and facilitate its repair through establishment of sister chromatid cohesion (3). Alternatively, the Smc5-Smc6 could be recruited to DNA damage site (4) and act as a protein interaction platform to recruit DNA repair factors (5). Additionally, Nse1- and Nse2-dependent protein modification could regulate the precise timing of recruitment and activities of these DNA repair factors (5). In the third mechanism, the Smc5-Smc6 complex could act on global chromatin conformation in order to facilitate efficient DNA repair (6). In the presence of Smc5-Smc6 DNA repair occurs normally (7) and (8) but when its functions are compromised, illegitimate DNA repair intermediates are formed (9) leading to cell death (10).

Depending on spatial and temporal circumstances and the SSSSS itself, Smc5-Smc6 may be engaged in distinct mechanisms of DNA lesion processing. The Smc5-Smc6 may act on SSSSSs such as DSB (Figure 6.2 (1)) by binding to it directly (Figure 6.2 (2)) and facilitating efficient DNA repair through for example increase in the local sister chromatid cohesion (Figure 6.2 (3)). Alternatively, after localisation of the Smc5-Smc6 complex to DNA lesion (Figure 6.2 (4)), it may help to recruit DNA repair factors and regulate their activities through post-translational modification mediated by Nse1 and Nse2 E3 ligases (Figure 6.2 (5)). Moreover, the Smc5-Smc6 complex similarly to cohesin and condensin proteins may act on global chromatin conformation (chromatin remodeler) to facilitate efficient DNA repair (Figure 6.2 (6)). Using these activities, the Smc5-Smc6 complex ensures formation and resolution of essential DNA repair intermediates leading to cell survival (Figure 6.2 (7) and (8)). In the absence of functional Smc5-Smc6 complex, DNA repair intermediates that are formed (Figure 6.2 (9)) may not be properly processed, leading to failure in DNA repair and consequently to cell death (Figure 6.2 (10)). These three modes of action are not exclusive and all of them may exist mutually. Using these activities the Smc5-Smc6 complex facilitates the formation of specific DNA repair/ replication intermediates, which unfortunately, have not been identified yet. Nevertheless, Smc5-Smc6 specific intermediates seem to be primary substrates for different DNA repair pathways and only these are efficiently processed to sustain proper DNA repair and replication.

6.3.1 Direct interaction model

There is a good deal of biochemical data supporting the direct interaction model, including chromosome mapping of Smc5-Smc6 localisation which revealed that the complex is enriched at stalled replication forks and double strand breaks (De Piccoli et al., 2006; Lindroos et al., 2006; Potts et al., 2006). Roy and coworkers showed that Smc5 binds preferentially to ssDNA in an ATP-dependent manner (Roy et al., 2011). Smc5-Smc6 also helps to release DNA tension during replication, suggesting that it may bind to supercoiled DNA (Kegel et al., 2011). Even though it is hard to predict what other DNA structures

are bound by Smc5-Smc6 *in vivo* in the presence of Nse1-6, these data indicate that Smc5-Smc6 complex interacts with and regulates different DNA structures.

In yeast, Smc5-Smc6-deficient cells accumulate X-shaped molecules after DNA damage (Ampatzidou et al., 2006; Bermúdez-López et al., 2010; Branzei et al., 2006), suggesting that these may be misprocessed SSSSSs. In agreement with this deletion of MphI/FANCM helicase, required for processing of DNA damage, rescues sensitivity of Smc5-Smc6 mutants to MMS and HU in yeast (Chavez et al., 2010a). Moreover, overexpression of BRCT repeat containing protein Brc1, required for efficient DNA repair in S phase through Smc5-Smc6 independent recombination pathway, rescues sensitivity of Smc5-Smc6 mutants in yeast to MMS and HU (Lee et al., 2007; Sheedy et al., 2005). We and others envisage that in the absence of Smc5-Smc6 complex, SSSSSs, such as DSB, when not bound by Smc5-Smc6 are transformed to lethal DNA repair/ replication intermediates.

6.3.2 Smc5-Smc6 as protein interaction/ regulation platform

The structure of the Smc5-Smc6 complex is a potential protein interaction platform. Several interactions with DNA repair proteins have been demonstrated and these include direct interactions with MphI/FANCM (Chen et al., 2009), Srs2 (Chiolo et al., 2005), RTT107 (Ohouo et al., 2010), Ku70 (Zhao and Blobel, 2005), Rad60/Esc2 (Boddy et al., 2003) or genetic interactions with Sgs1 (Sollier et al., 2009), Rad51 (Chen et al., 2009) and Rad52 (Torres-Rosell et al., 2005b) and Ku70 (Stephan et al., 2011a). Smc5-Smc6 bound to SSSSSs or its presence at these sites could regulate the precise timing and localisation of its interactors leading to efficient DNA repair and replication. Additionally, Smc5-Smc6 complex contains two enzymatically active subunits: E3 ubiquitin ligase Nse1 (Doyle et al., 2010) and E3 SUMO ligase Nse2 (Andrews et al., 2005; McDonald et al., 2003; Potts and Yu, 2005; Zhao and Blobel, 2005). SUMOylation of the Nse2 substrates could recruit and regulate activity of DNA repair factors as supported by Smc5-Smc6-dependent cohesin recruitment to DSB in human cells (Potts et al., 2006). In addition, Nse2 SUMOylates Ku70 in budding yeast (Zhao and Blobel, 2005), suggesting that it may regulate or prevent NHEJ. However,

the biological significance of this modification is not understood. On the other hand, Nse1-dependent ubiquitination may also add another level of protein regulation at the DNA damage site. Unfortunately, no Nse1 substrates have been identified to date. Interestingly, SUMOylation and ubiquitination compete for the same sites within target proteins, suggesting that Smc5-Smc6 complex may act as a molecular ubiquitin/ SUMO switch. Smc5-Smc6 may control cellular processes through a fine tuned balance between Nse2- and Nse1-dependent protein modifications. This balance could be changed in response to the stressful conditions, where Nse1-dependent protein modification increase and Nse2-mediated SUMOylation decrease or vice versa.

As mentioned earlier, RNAi-mediated depletion of Smc5 and Nse2 results in reduced cohesin recruitment to DSB (Potts et al., 2006). However, cohesin localisation to DSB has not been shown to be dependent on SUMOylation (Potts et al., 2006). Additionally, after RNAi-mediated Nse2 knockdown, reduced SUMOylation of telomere sheltering proteins and telomere shortening was observed (Potts and Yu, 2007). Similarly, in budding yeast Nse2-and Smc5-deficiency is associated with increased telomere shortening and accumulation of X-shaped molecules at this repetitive DNA region (Chavez et al., 2010b; Zhao and Blobel, 2005). In support of this model, chromatin association of Rad52 when replication forks are stably stalled after HU treatment is compromised in Smc5-Smc6 mutant *smc6* (Irmisch et al., 2009). All these observations suggest that the Smc5-Smc6 complex may interact or regulate many DNA maintenance proteins and in its absence abnormal DNA intermediates are formed leading to cell death.

6.3.3 Chromatin remodeling activities of the Smc5-Smc6 complex

Finally, Smc5-Smc6 may act on global chromatin conformation, such as cohesin and condensin complexes. Loss of Smc5-Smc6 results in lethal chromosome segregation defects, dysregulation of sister chromatid cohesion (reviewed in (Stephan et al., 2011b)), and abnormal chromatin structure, including sister chromatid linkages, both DNA (Torres-Rosell et al., 2005b) and

protein (Outwin et al., 2009) mediated. In addition, Smc5-Smc6 is involved in the removal of chromatin intertwinings during DNA replication and its deficiency results in replication defects of longer chromosomes (Kegel et al., 2011). Moreover, mobility of the DSB required for its efficient repair in budding yeast is decreased in the absence of functional Smc5-Smc6 (Torres-Rosell et al., 2007). All these data suggest that Smc5-Smc6 is a potential chromatin remodeler that changes chromatin conformation allowing for distinct DNA mechanisms to happen.

6.3.4 Model testing

To test the potential Smc5-Smc6 activities, *in vitro* DNA binding experiments with purified Smc5-Smc6 complex or its individual components could be performed. Different DNA substrates, such as ssDNA, dsDNA and more complicated structures, including replication forks and Holliday junctions could be used to study how Smc5-Smc6 proteins interact with DNA. However, this approach could be extremely challenging in terms of the *in vitro* reconstitution of functional Smc5-Smc6 complex and may not reflect the *in vivo* activities of the complex. To test *in vivo* interactions of the Smc5-Smc6 complex with DNA, crosslink of the complex to DNA and subsequent analysis by Southern blotting could be performed, as described for cohesin complex (Haering et al., 2008).

To test the idea if Smc5-Smc6 acts as protein interaction and recruitment platform, a large scale immunoprecipitation of Smc5-Smc6 combined with mass spectrometry could be pefrormed to identify interactors of the complex before and after DNA damage. Additionally, to test the hypothesis of the Smc5-Smc6 Ub/ SUMO switch activity, a comparison of the phenotypes associated with Nse1- and Nse2-deficiency should be made. Such analysis may allow understanding of SUMO and ubiquitin ligase activities of the Smc5-Smc6 complex. In addition, double mutant of *Nse1* and *Nse2* could be performed to study the potential interactions between ubiquitination and SUMOylation mediated by Smc5-Smc6 complex. Moreover, mapping of potential common substrates of Nse1 and Nse2 could be also performed to confirm this hypothesis.

To test for Smc5-Smc6 in chromatin remodeling activities, analysis of the proteins associated with mitotic chromosomes from Smc5-Smc6-deficient cells could be performed. Such analysis is currently underway in collaboration with Bill Earnshaw laboratory. Differences in chromosome proteins isolated from wild-type and Smc5-Smc6-deficient cells may allow understanding of the Smc5-Smc6 cellular functions in establishment of normal chromatin structure, as recently demonstrated using proteomic studies of isolated mitotic chromosomes from condensin-deficient cells (Ohta et al., 2010). Additionally, analysis of chromatin properties, such as topology, compactness etc could shed light onto Smc5-Smc6 complex activities as a chromatin remodeler.

REFERENCES

Al-Minawi, A.Z., Lee, Y.F., Hakansson, D., Johansson, F., Lundin, C., Saleh-Gohari, N., Schultz, N., Jenssen, D., Bryant, H.E., Meuth, M., *et al.* (2009). The ERCC1/XPF endonuclease is required for completion of homologous recombination at DNA replication forks stalled by inter-strand cross-links. Nucleic Acids Res *37*, 6400-6413.

Alexeev, A., Mazin, A., and Kowalczykowski, S.C. (2003). Rad54 protein possesses chromatin-remodeling activity stimulated by the Rad51-ssDNA nucleoprotein filament. Nat Struct Biol *10*, 182-186.

Amon, A. (2001). Together until separin do us part. Nat Cell Biol *3*, E12-E14.

Ampatzidou, E., Irmisch, A., O'Connell, M.J., and Murray, J.M. (2006). Smc5/6 Is Required for Repair at Collapsed Replication Forks. Mol Cell Biol *26*, 9387-9401.

Andersen, S.L., Bergstralh, D.T., Kohl, K.P., LaRocque, J.R., Moore, C.B., and Sekelsky, J. (2009). Drosophila MUS312 and the Vertebrate Ortholog BTBD12 Interact with DNA Structure-Specific Endonucleases in DNA Repair and Recombination. Mol Cell *35*, 128-135.

Anderson, D.E., Losada, A., Erickson, H.P., and Hirano, T. (2002). Condensin and cohesin display different arm conformations with characteristic hinge angles. J Cell Biol *156*, 419-424.

Anderson, D.E., Trujillo, K.M., Sung, P., and Erickson, H.P. (2001). Structure of the Rad50·Mre11 DNA Repair Complex fromSaccharomyces cerevisiae by Electron Microscopy. J Bio Chem *276*, 37027-37033.

Andersson, B.S., Sadeghi, T., Siciliano, M.J., Legerski, R., and Murray, D. (1996). Nucleotide excision repair genes as determinants of cellular sensitivity to cyclophosphamide analogs. Cancer Chemother Pharmacol *38*, 406-416.

Andrews, E.A., Palecek, J., Sergeant, J., Taylor, E., Lehmann, A.R., and Watts, F.Z. (2005). Nse2, a Component of the Smc5-6 Complex, Is a SUMO Ligase Required for the Response to DNA Damage. Mol Cell Biol *25*, 185-196.

Arumugam, P., Gruber, S., Tanaka, K., Haering, C.H., Mechtler, K., and Nasmyth, K. (2003). ATP Hydrolysis Is Required for Cohesin's Association with Chromosomes. Curr Biol *13*, 1941-1953.

Avery, O.T., McLeod, C.M., and McCarty, M. (1944). Studies on the chemical nature of the substances inducing transformation of Pneumococcal types: inductionof transformation by a deoxyrybonucleic acid fraction isolated from Pneumococcus type III. J Exp Med *79*.

Avis, J., and Clarke, P. (1996). Ran, a GTPase involved in nuclear processes: its regulators and effectors. J Cell Sci *109*, 2423-2427.

Baba, T.W., Giroir, B.P., and Humphries, E.H. (1985). Cell lines derived from avian lymphomas exhibit two distinct phenotypes. Virology *144*, 139-151.

Baba, T.W., and Humphries, E.H. (1984). Differential response to avian leukosis virus infection exhibited by two chicken lines. Virology *135*, 181-188.

Banin, S., Moyal, L., Shieh, S.-Y., Taya, Y., Anderson, C.W., Chessa, L., Smorodinsky, N.I., Prives, C., Reiss, Y., Shiloh, Y., *et al.* (1998). Enhanced Phosphorylation of p53 by ATM in Response to DNA Damage. Science *281*, 1674-1677.

Baron, U., and Bujard, H. (2000). Tet repressor-based system for regulated gene expression in eukaryotic cells: principles and advances. Methods Enzymol *327*, 401-421.

Bartek, J., Bartkova, J., and Lukas, J. (1997). The retinoblastoma protein pathway in cell cycle control and cancer. Exp Cell Res *237*, 1.

Bartek, J., Lukas, C., and Lukas, J. (2004). Checking on DNA damage in S phase. Nat Rev Mol Cell Bio *5*, 792.

Bartek, J., and Lukas, J. (2003). Chk1 and Chk2 kinases in checkpoint control and cancer. Cancer Cell *3*, 421.

Bauerschmidt, C., Arrichiello, C., Burdak-Rothkamm, S., Woodcock, M., Hill, M.A., Stevens, D.L., and Rothkamm, K. (2010). Cohesin promotes the repair of ionizing radiation-induced DNA double-strand breaks in replicated chromatin. Nucleic Acids Res *38*, 477-487.

Bauerschmidt, C., Woodcock, M., Stevens, D.L., Hill, M.A., Rothkamm, K., and Helleday, T. (2011). Cohesin phosphorylation and mobility of SMC1 at ionizing radiation-induced DNA double-strand breaks in human cells. Exp Cell Res *317*, 330-337.

Bayer, P., Arndt, A., Metzger, S., Mahajan, R., Melchior, F., Jaenicke, R., and Becker, J. (1998). Structure determination of the small ubiquitin-related modifier SUMO-1. J Mol Bio *280*, 275-286.

Bedell, M.A., Largaespada, D.A., Jenkins, N.A., and Copeland, N.G. (1997). Mouse models of human disease. Part II: recent progress and future directions. Genes Dev *11*, 11-43.

Behlke-Steinert, S., Touat-Todeschini, L., A. Skoufias, D., and L. Margolis, R. (2009). SMC5 and MMS21 are required for chromosome cohesion and mitotic progression. Cell Cycle *8*, 2211-2218.

Bell, S.P., and Dutta, A. (2002). DNA replication in eukaryotic cells. Annu Rev Biochem *71*, 333-374.

Beranek, D.T. (1990). Distribution of methyl and ethyl adducts following alkylation with monofunctional alkylating agents. Mutat Res *231*, 11-30.

Bergink, S., and Jentsch, S. (2009). Principles of ubiquitin and SUMO modifications in DNA repair. Nature *458*, 461-467.

Bergoglio, V., and Magnaldo, T. (2006). Nucleotide excision repair and related human diseases. Genome Dyn *1*, 35-52.

Bermúdez-López, M., Ceschia, A., de Piccoli, G., Colomina, N., Pasero, P., Aragón, L., and Torres-Rosell, J. (2010). The Smc5/6 complex is required for dissolution of DNA-mediated sister chromatid linkages. Nucleic Acids Res *38*, 6502-6512.

Bernier-Villamor, V., Sampson, D.A., Matunis, M.J., and Lima, C.D. (2002). Structural Basis for E2-Mediated SUMO Conjugation Revealed by a Complex between Ubiquitin-Conjugating Enzyme Ubc9 and RanGAP1. Cell *108*, 345-356.

Beucher, A., Birraux, J., Tchouandong, L., Barton, O., Shibata, A., Conrad, S., Goodarzi, A.A., Krempler, A., Jeggo, P.A., and Lobrich, M. (2009a). ATM and Artemis promote homologous recombination of radiation-induced DNA double-strand breaks in G2. EMBO J *28*, 3413-3427.

Beucher, A., Birraux, J., Tchouandong, L., Barton, O., Shibata, A., Conrad, S., Goodarzi, A.A., Krempler, A., Jeggo, P.A., and Lobrich, M. (2009b). ATM and Artemis promote homologous recombination of radiation-induced DNA double-strand breaks in G2. EMBO J *28*, 3413-3427.

Bezzubova, O., Silbergleit, A., Yamaguchi-Iwai, Y., Takeda, S., and Buerstedde, J.M. (1997). Reduced X-ray resistance and homologous recombination frequencies in a RAD54-/- mutant of the chicken DT40 cell line. Cell *89*, 185-193.

Bhagwat, N., Olsen, A.L., Wang, A.T., Hanada, K., Stuckert, P., Kanaar, R., D'Andrea, A., Niedernhofer, L.J., and McHugh, P.J. (2009). XPF-ERCC1 Participates in the Fanconi Anemia Pathway of Cross-Link Repair. Mol Cell Biol *29*, 6427-6437.

Birkenbihl, R.P., and Subramani, S. (1992). Cloning and characterization of rad21 an essential gene of Schizosaccharomyces pombe involved in DNA double-strand-break repair. Nucleic Acids Res *20*, 6605-6611.

Biton, S., Barzilai, A., and Shiloh, Y. (2008). The neurological phenotype of ataxia-telangiectasia: solving a persistent puzzle. DNA repair (Amst) *7*, 1028-1038.

Blackwell, L.J., Bjornson, K.P., and Modrich, P. (1998). DNA-dependent Activation of the hMutSα ATPase. J Bio Chem *273*, 32049-32054.

Blat, Y., and Kleckner, N. (1999). Cohesins Bind to Preferential Sites along Yeast Chromosome III, with Differential Regulation along Arms versus the Centric Region. Cell *98*, 249-259.

Boddy, M.N., Shanahan, P., McDonald, W.H., Lopez-Girona, A., Noguchi, E., Yates, I.J., and Russell, P. (2003). Replication checkpoint kinase Cds1 regulates recombinational repair protein Rad60. Mol Cell Biol *23*, 5939-5946.

Bolderson, E., Tomimatsu, N., Richard, D.J., Boucher, D., Kumar, R., Pandita, T.K., Burma, S., and Khanna, K.K. (2010). Phosphorylation of Exo1 modulates homologous recombination repair of DNA double-strand breaks. Nucleic Acids Res *38*, 1821-1831.

Bramsen, J.B., Laursen, M.B., Damgaard, C.K., Lena, S.W., Babu, B.R., Wengel, J., and Kjems, J. (2007). Improved silencing properties using small internally segmented interfering RNAs. Nucleic Acids Res *35*, 5886-5897.

Branzei, D., Sollier, J., Liberi, G., Zhao, X., Maeda, D., Seki, M., Enomoto, T., Ohta, K., and Foiani, M. (2006). Ubc9- and mms21-mediated sumoylation counteracts recombinogenic events at damaged replication forks. Cell *127*, 509-522.

Brown, T.A. (2002). Genomes 2 (Gerland Science).

Buerstedde, J.M., and Takeda, S. (1991). Increased ratio of targeted to random integration after transfection of chicken B cell lines. Cell *67*, 179-188.

Bugreev, D.V., Yu, X., Egelman, E.H., and Mazin, A.V. (2007). Novel pro- and anti-recombination activities of the Bloom's syndrome helicase. Genes Dev *21*, 3085-3094.

Bunz, F., Dutriaux, A., Lengauer, C., Waldman, T., Zhou, S., Brown, J.P., Sedivy, J.M., Kinzler, K.W., and Vogelstein, B. (1998). Requirement for p53 and p21 to sustain G2 arrest after DNA damage. Science *282*, 1497-1501.

Busino, L., Donzelli, M., Chiesa, M., Guardavaccaro, D., Ganoth, D., Dorrello, N.V., Hershko, A., Pagano, M., and Draetta, G.F. (2003a). Degradation of Cdc25A by beta-TrCP during S phase and in response to DNA damage. Nature *426*, 87-91.

Busino, L., Donzelli, M., Chiesa, M., Guardavaccaro, D., Ganoth, D., Valerio Dorrello, N., Hershko, A., Pagano, M., and Draetta, G.F. (2003b). Degradation of Cdc25A by [beta]-TrCP during S phase and in response to DNA damage. Nature *426*, 87-91.

Cabello, O.A., Eliseeva, E., He, W., Youssoufian, H., Plon, S.E., Brinkley, B.R., and Belmont, J.W. (2001). Cell Cycle-dependent Expression and Nucleolar Localization of hCAP-H. Molecular biology of the cell *12*, 3527-3537.

Caldecott, K.W. (2008). Single-strand break repair and genetic disease. Nat Rev Genet *9*, 619-631.

Canman, C.E. (2003). Checkpoint mediators: relaying signals from DNA strand breaks. Curr Biol *13*, R488-490.

Canman, C.E., and Kastan, M.B. (1998). Small contribution of G1 checkpoint control manipulation to modulation of p53-mediated apoptosis. Oncogene *16*, 957-966.

Canman, C.E., and Lim, D.S. (1998). The role of ATM in DNA damage responses and cancer. Oncogene *17*, 3301-3308.

Canman, C.E., Lim, D.S., Cimprich, K.A., Taya, Y., Tamai, K., Sakaguchi, K., Appella, E., Kastan, M.B., and Siliciano, J.D. (1998). Activation of the ATM kinase by ionizing radiation and phosphorylation of p53. Science *281*, 1677-1679.

Cao, W., Hunter, R., Strnatka, D., McQueen, C.A., and Erickson, R.P. (2005). DNA constructs designed to produce short hairpin, interfering RNAs in transgenic mice sometimes show early lethality and an interferon response. J Appl Genet *46*, 217-225.

Capasso, H., Palermo, C., Wan, S., Rao, H., John, U.P., O'Connell, M.J., and Walworth, N.C. (2002). Phosphorylation activates Chk1 and is required for checkpoint-mediated cell cycle arrest. J Cell Sci *115*, 4555-4564.

Capecchi, M. (1989). Altering the genome by homologous recombination. Science *244*, 1288-1292.

Chan, T.A., Hermeking, H., Lengauer, C., Kinzler, K.W., and Vogelstein, B. (1999). 14-3-3[sigma] is required to prevent mitotic catastrophe after DNA damage. Nature *401*, 616-620.

Chavez, A., Agrawal, V., and Johnson, F.B. (2010a). Homologous recombination-dependent rescue of deficiency in the structural maintenance of chromosomes (SMC) 5/6 complex. J Bio Chem.

Chavez, A., George, V., Agrawal, V., and Johnson, F.B. (2010b). Sumoylation and the Structural Maintenance of Chromosomes (Smc) 5/6 Complex Slow Senescence through Recombination Intermediate Resolution. J Biol Chem *285*, 11922-11930.

Chehab, N.H., Malikzay, A., Stavridi, E.S., and Halazonetis, T.D. (1999). Phosphorylation of Ser-20 mediates stabilization of human p53 in response to DNA damage. PNAS *96*, 13777-13782.

Chen, Y.-H., Choi, K., Szakal, B., Arenz, J., Duan, X., Ye, H., Branzei, D., and Zhao, X. (2009). Interplay between the Smc5/6 complex and the Mph1 helicase in recombinational repair. PNAS *106*, 21252-21257.

Cheng, S., Van Houten, B., Gamper, H.B., Sancar, A., and Hearst, J.E. (1988). Use of psoralen-modified oligonucleotides to trap three-stranded RecA-DNA complexes and repair of these cross-linked complexes by ABC excinuclease. J Bio Chem *263*, 15110-15117.

Chiolo, I., Carotenuto, W., Maffioletti, G., Petrini, J.H., Foiani, M., and Liberi, G. (2005). Srs2 and Sgs1 DNA helicases associate with Mre11 in different subcomplexes following checkpoint activation and CDK1-mediated Srs2 phosphorylation. Mol Cell Biol *25*, 5738-5751.

Chiu, A., Revenkova, E., and Jessberger, R. (2004). DNA Interaction and Dimerization of Eukaryotic SMC Hinge Domains. J Biol Chem *279*, 26233-26242.

Choi, K., Szakal, B., Chen, Y.-H., Branzei, D., and Zhao, X. (2010). The Smc5/6 Complex and Esc2 Influence Multiple Replication-associated Recombination Processes in Saccharomyces cerevisiae. Molecular biology of the cell *21*, 2306-2314.

Chou, D.M., Adamson, B., Dephoure, N.E., Tan, X., Nottke, A.C., Hurov, K.E., Gygi, S.P., Colaiácovo, M.P., and Elledge, S.J. (2010). A chromatin localization screen reveals poly (ADP ribose)-regulated recruitment of the repressive polycomb and NuRD complexes to sites of DNA damage. PNAS *107*, 18475-18480.

Chu, W.K., and Hickson, I.D. (2009). RecQ helicases: multifunctional genome caretakers. Nat Rev Cancer *9*, 644-654.

Chung, C.D., Liao, J., Liu, B., Rao, X., Jay, P., Berta, P., and Shuai, K. (1997). Specific Inhibition of Stat3 Signal Transduction by PIAS3. Science *278*, 1803-1805.

Ciccia, A., and Elledge, S.J. (2010). The DNA Damage Response: Making It Safe to Play with Knives. Mol Cell *40*, 179-204.

Ciccia, A., McDonald, N., and West, S.C. (2008). Structural and Functional Relationships of the XPF/MUS81 Family of Proteins. Annu Rev Biochem *77*, 259-287.

Cimprich, K.A., and Cortez, D. (2008). ATR: an essential regulator of genome integrity. Nat Rev Mol Cell Biol *9*, 616-627.

Ciosk, R., Shirayama, M., Shevchenko, A., Tanaka, T., Toth, A., Shevchenko, A., and Nasmyth, K. (2000). Cohesin's Binding to Chromosomes Depends on a Separate Complex Consisting of Scc2 and Scc4 Proteins. Mol Cell *5*, 243-254.

Cipak, L., and Jantova, S. (2010). PARP-1 inhibitors: a novel genetically specific agents for cancer therapy. Neoplasma *57*, 401-405.

Clemens, J.C., Worby, C.A., Simonson-Leff, N., Muda, M., Maehama, T., Hemmings, B.A., and Dixon, J.E. (2000). Use of double-stranded RNA interference in Drosophila cell lines to dissect signal transduction pathways. PNAS *97*, 6499-6503.

Clingen, P.H., De Silva, I.U., McHugh, P.J., Ghadessy, F.J., Tilby, M.J., Thurston, D.E., and Hartley, J.A. (2005). The XPF-ERCC1 endonuclease and homologous recombination contribute to the repair of minor groove DNA interstrand crosslinks in mammalian cells produced by the pyrrolo[2,1-c][1,4]benzodiazepine dimer SJG-136. Nucleic Acids Res *33*, 3283-3291.

Cortez, D., Wang, Y., Qin, J., and Elledge, S.J. (1999). Requirement of ATM-dependent phosphorylation of brca1 in the DNA damage response to double-strand breaks. Science *286*, 1162-1166.

Cost, G.J., and Cozzarelli, N.R. (2006). Smc5p Promotes Faithful Chromosome Transmission and DNA Repair in Saccharomyces cerevisiae. Genetics *172*, 2185-2200.

Cost, G.J., Freyvert, Y., Vafiadis, A., Santiago, Y., Miller, J.C., Rebar, E., Collingwood, T.N., Snowden, A., and Gregory, P.D. (2010). BAK and BAX deletion using zinc-finger nucleases yields apoptosis-resistant CHO cells. Biotechnol Bioeng *105*, 330-340.

Costanzo, V., Shechter, D., Lupardus, P.J., Cimprich, K.A., Gottesman, M., and Gautier, J. (2003). An ATR- and Cdc7-Dependent DNA Damage Checkpoint that Inhibits Initiation of DNA Replication. Mol Cell *11*, 203-213.

Dai, Y., Vaught, T.D., Boone, J., Chen, S.-H., Phelps, C.J., Ball, S., Monahan, J.A., Jobst, P.M., McCreath, K.J., Lamborn, A.E., *et al.* (2002). Targeted disruption of the [alpha]1,3-galactosyltransferase gene in cloned pigs. Nat Biotech *20*, 251-255.

De Piccoli, G., Cortes-Ledesma, F., Ira, G., Torres-Rosell, J., Uhle, S., Farmer, S., Hwang, J.-Y., Machin, F., Ceschia, A., McAleenan, A., *et al.* (2006). Smc5-Smc6 mediate DNA double-strand-break repair by promoting sister-chromatid recombination. Nat Cell Biol *8*, 1032-1034.

De Piccoli, G., Torres-Rosell, J., and Aragon, L. (2009). The unnamed complex: what do we know about Smc5-Smc6? Chromosome Res *17*, 251-263.

De Silva, I.U., McHugh, P.J., Clingen, P.H., and Hartley, J.A. (2000). Defining the Roles of Nucleotide Excision Repair and Recombination in the Repair of DNA Interstrand Cross-Links in Mammalian Cells. Mol Cell Biol *20*, 7980-7990.

Demple, B., Herman, T., and Chen, D.S. (1991). Cloning and expression of APE, the cDNA encoding the major human apurinic endonuclease: definition of a family of DNA repair enzymes. PNAS *88*, 11450-11454.

Dervyn, E., Noirot-Gros, M.-F., Mervelet, P., McGovern, S., Ehrlich, S.D., Polard, P., and Noirot, P. (2004). The bacterial condensin/cohesin-like protein complex acts in DNA repair and regulation of gene expression. Mol Micro *51*, 1629-1640.

Despras, E., Daboussi, F., Hyrien, O., Marheineke, K., and Kannouche, P.L. (2010). ATR/Chk1 pathway is essential for resumption of DNA synthesis and cell survival in UV-irradiated XP variant cells. Human Mol Gen *19*, 1690-1701.

Dodson, H., and Morrison, C.G. (2009a). Increased sister chromatid cohesion and DNA damage response factor localization at an enzyme-induced DNA double-strand break in vertebrate cells. Nucleic Acids Res *37*, 6054-6063.

Dodson, H., and Morrison, C.G. (2009b). Increased sister chromatid cohesion and DNA damage response factor localization at an enzyme-induced DNA double-strand break in vertebrate cells. Nucleic Acids Research *37*, 6054-6063.

Dou, H., Huang, C., Singh, M., Carpenter, P.B., and Yeh, E.T.H. (2010). Regulation of DNA Repair through DeSUMOylation and SUMOylation of Replication Protein A Complex. Mol Cell *39*, 333-345.

Doyle, J.M., Gao, J., Wang, J., Yang, M., and Potts, P.R. (2010). MAGE-RING protein complexes comprise a family of E3 ubiquitin ligases. Mol Cell *39*, 963-974.

Duan, X., Sarangi, P., Liu, X., Rangi, G.K., Zhao, X., and Ye, H. (2009a). Structural and Functional Insights into the Roles of the Mms21 Subunit of the Smc5/6 Complex. Mol Cell *35*, 657-668.

Duan, X., Yang, Y., Chen, Y.-H., Arenz, J., Rangi, G.K., Zhao, X., and Ye, H. (2009b). Architecture of the Smc5/6 Complex of Saccharomyces cerevisiae Reveals a Unique Interaction between the Nse5-6 Subcomplex and the Hinge Regions of Smc5 and Smc6. J Biol Chem *284*, 8507-8515.

Duckett, D.R., Drummond, J.T., Murchie, A.I., Reardon, J.T., Sancar, A., Lilley, D.M., and Modrich, P. (1996). Human MutSalpha recognizes damaged DNA base pairs containing O6-methylguanine, O4-methylthymine, or the cisplatin-d(GpG) adduct. PNAS *93*, 6443-6447.

Dymecki, S.M. (1996). Flp recombinase promotes site-specific DNA recombination in embryonic stem cells and transgenic mice. PNAS *93*, 6191-6196.

Dzantiev, L., Constantin, N., Genschel, J., Iyer, R.R., Burgers, P.M., and Modrich, P. (2004). A Defined Human System That Supports Bidirectional Mismatch-Provoked Excision. Mol Cell *15*, 31-41.

Elchuri, S., Oberley, T.D., Qi, W., Eisenstein, R.S., Jackson Roberts, L., Van Remmen, H., Epstein, C.J., and Huang, T.T. (2005). CuZnSOD deficiency leads to persistent and widespread oxidative damage and hepatocarcinogenesis later in life. Oncogene *24*, 367-380.

Ellermeier, C., and Smith, G.R. (2005). Cohesins are required for meiotic DNA breakage and recombination in Schizosaccharomyces pombe. PNAS *102*, 10952-10957.

Esashi, F., Christ, N., Gannon, J., Liu, Y., Hunt, T., Jasin, M., and West, S.C. (2005). CDK-dependent phosphorylation of BRCA2 as a regulatory mechanism for recombinational repair. Nature *434*, 598-604.

Fackenthal, J.D., and Olopade, O.I. (2007). Breast cancer risk associated with BRCA1 and BRCA2 in diverse populations. Nat Rev Cancer *7*, 937-948.

Falck, J., Mailand, N., Syljuasen, R.G., Bartek, J., and Lukas, J. (2001). The ATM-Chk2-Cdc25A checkpoint pathway guards against radioresistant DNA synthesis. Nature *410*, 842-847.

Falnes, P.O., Johansen, R.F., and Seeberg, E. (2002). AlkB-mediated oxidative demethylation reverses DNA damage in Escherichia coli. Nature *419*, 178-182.

Fekairi, S., Scaglione, S., Chahwan, C., Taylor, E.R., Tissier, A., Coulon, S., Dong, M.-Q., Ruse, C., Yates Iii, J.R., Russell, P., *et al.* (2009). Human SLX4 Is a Holliday Junction Resolvase Subunit that Binds Multiple DNA Repair/Recombination Endonucleases. Cell *138*, 78-89.

Fiorani, P., and Bjornsti, M.-A. (2000). Mechanisms of DNA Topoisomerase I-Induced Cell Killing in the Yeast: Saccharomyces cerevisiae. Ann N Y Acad Sci *922*, 65-75.

Fire, A. (1999). RNA-triggered gene silencing. Trends Genet *15*, 358-363.

Fishman-Lobell, J., and Haber, J.E. (1992). Removal of nonhomologous DNA ends in double-strand break recombination: the role of the yeast ultraviolet repair gene RAD1. Science *258*, 480-484.

Flejter, W.L., McDaniel, L.D., Johns, D., Friedberg, E.C., and Schultz, R.A. (1992). Correction of xeroderma pigmentosum complementation group D mutant cell phenotypes by chromosome and gene transfer: involvement of the human ERCC2 DNA repair gene. PNAS *89*, 261-265.

Fousteri, M.I., and Lehmann, A.R. (2000). A novel SMC protein complex in Schizosaccharomyces pombe contains the Rad18 DNA repair protein. EMBO J *19*, 1691-1702.

Freeman, L., Aragon-Alcaide, L., and Strunnikov, A. (2000). The Condensin Complex Governs Chromosome Condensation and Mitotic Transmission of Rdna. J Cell Biol *149*, 811-824.

Friedberg, E.C. (2003). DNA damage and repair. Nature *421*, 436.

Frosina, G., Fortini, P., Rossi, O., Carrozzino, F., Raspaglio, G., Cox, L.S., Lane, D.P., Abbondandolo, A., and Dogliotti, E. (1996). Two Pathways for Base Excision Repair in Mammalian Cells. J Biol Chem *271*, 9573-9578.

Galanty, Y., Belotserkovskaya, R., Coates, J., Polo, S., Miller, K.M., and Jackson, S.P. (2009). Mammalian SUMO E3-ligases PIAS1 and PIAS4 promote responses to DNA double-strand breaks. Nature *462*, 935-939.

Gartenberg, M.R., and Merkenschlager, M. (2008). Condensin goes with the family but not with the flow. Genome Biol *9*, 236.

Genschel, J., and Modrich, P. (2003). Mechanism of 5'-Directed Excision in Human Mismatch Repair. Mol Cell *12*, 1077-1086.

Genschel, J., and Modrich, P. (2009). Functions of MutLα, Replication Protein A (RPA), and HMGB1 in 5′-Directed Mismatch Repair. J Biol Chem *284*, 21536-21544.

Geurts, A.M., Cost, G.J., Freyvert, Y., Zeitler, B., Miller, J.C., Choi, V.M., Jenkins, S.S., Wood, A., Cui, X., Meng, X., *et al.* (2009). Knockout Rats via Embryo Microinjection of Zinc-Finger Nucleases. Science *325*, 433.

Glickman, B.W. (1982). Methylation-instructed mismatch correction as a postreplication error avoidance mechanism in Escherichia coli. Basic Life Sci *20*, 65-87.

Gossen, M., and Bujard, H. (1992). Tight control of gene expression in mammalian cells by tetracycline-responsive promoters. PNAS *89*, 5547-5551.

Gradia, S., Subramanian, D., Wilson, T., Acharya, S., Makhov, A., Griffith, J., and Fishel, R. (1999). hMSH2-hMSH6 Forms a Hydrolysis-Independent Sliding Clamp on Mismatched DNA. Mol Cell *3*, 255-261.

Groth, P., Ausländer, S., Majumder, M.M., Schultz, N., Johansson, F., Petermann, E., and Helleday, T. (2010). Methylated DNA Causes a Physical Block to Replication Forks Independently of Damage Signalling, O6-Methylguanine or DNA Single-Strand Breaks and Results in DNA Damage. J Mol Biol *402*, 70-82.

Gu, H., Zou, Y.-R., and Rajewsky, K. (1993). Independent control of immunoglobulin switch recombination at individual switch regions evidenced through Cre-loxP-mediated gene targeting. Cell *73*, 1155-1164.

Guan, J., Ekwurtzel, E., Kvist, U., and Yuan, L. (2008). Cohesin protein SMC1 is a centrosomal protein. Biochem Biophys Res Commun *372*, 761-764.

Guillou, E., Ibarra, A., Coulon, V., Casado-Vela, J., Rico, D., Casal, I., Schwob, E., Losada, A., and Méndez, J. (2010). Cohesin organizes chromatin loops at DNA replication factories. Genes Dev *24*, 2812-2822.

Haering, C.H., Farcas, A.M., Arumugam, P., Metson, J., and Nasmyth, K. (2008). The cohesin ring concatenates sister DNA molecules. Nature *454*, 297-301.

Haince, J.-F., Kozlov, S., Dawson, V.L., Dawson, T.M., Hendzel, M.J., Lavin, M.F., and Poirier, G.G. (2007). Ataxia Telangiectasia Mutated (ATM) Signaling Network Is Modulated by a Novel Poly(ADP-ribose)-dependent Pathway in the Early Response to DNA-damaging Agents. J Biol Chem *282*, 16441-16453.

Haince, J.-F., McDonald, D., Rodrigue, A., Déry, U., Masson, J.-Y., Hendzel, M.J., and Poirier, G.G. (2008). PARP1-dependent Kinetics of Recruitment of MRE11 and NBS1 Proteins to Multiple DNA Damage Sites. J Biol Chem *283*, 1197-1208.

Hanada, K., Budzowska, M., Modesti, M., Maas, A., Wyman, C., Essers, J., and Kanaar, R. (2006). The structure-specific endonuclease Mus81-Eme1 promotes conversion of interstrand DNA crosslinks into double-strands breaks. EMBO J *25*, 4921-4932.

Harborth, J., Elbashir, S.M., Bechert, K., Tuschl, T., and Weber, K. (2001). Identification of essential genes in cultured mammalian cells using small interfering RNAs. J Cell Sci *114*, 4557-4565.

Hardeland, U., Steinacher, R., Jiricny, J., and Schar, P. (2002). Modification of the human thymine-DNA glycosylase by ubiquitin-like proteins facilitates enzymatic turnover. EMBO J *21*, 1456-1464.

Hardwick, K.G., and Murray, A.W. (1995). Mad1p, a phosphoprotein component of the spindle assembly checkpoint in budding yeast. J Cell Biol *131*, 709-720.

Hardwick, K.G., Weiss, E., Luca, F.C., Winey, M., and Murray, A.W. (1996). Activation of the Budding Yeast Spindle Assembly Checkpoint Without Mitotic Spindle Disruption. Science *273*, 953-956.

Harper, J.W., and Elledge, S.J. (2007). The DNA Damage Response: Ten Years After. Mol Cell *28*, 739-745.

Harper, S.Q., and Davidson, B.L. (2005). Plasmid-based RNA interference: construction of small-hairpin RNA expression vectors. Methods Mol Biol *309*, 219-235.

Hartwell, L.H., and Weinert, T.A. (1989). Checkpoints: controls that ensure the order of cell cycle events. Science *246*, 629-634.

Harvey, S.H., Sheedy, D.M., Cuddihy, A.R., and O'Connell, M.J. (2004). Coordination of DNA damage responses via the Smc5/Smc6 complex. Mol Cell Biol *24*, 662-674.

Hays, S.L., Firmenich, A.A., Massey, P., Banerjee, R., and Berg, P. (1998). Studies of the interaction between Rad52 protein and the yeast single-stranded DNA binding protein RPA. Mol Cell Biol *18*, 4400-4406.

Hazbun, T.R., Malmstrom, L., Anderson, S., Graczyk, B.J., Fox, B., Riffle, M., Sundin, B.A., Aranda, J.D., McDonald, W.H., Chiu, C.H., *et al.* (2003). Assigning function to yeast proteins by integration of technologies. Mol Cell *12*, 1353-1365.

Hearst, J.E., Isaacs, S.T., Kanne, D., Rapoport, H., and Straub, K. (1984). The reaction of the psoralens with deoxyribonucleic acid. Q Rev Biophys *17*, 1-44.

Hershey, A.D., and Chase, M. (1952). Independent functions of viral protein and nucleic acid in growth of bacteriophage. J Gen Physiol *36*, 39-56.

Heyer, W.-D. (2004). Recombination: Holliday Junction Resolution and Crossover Formation. Curr Biol *14*, R56-R58.

Hinz, J.M. (2010). Role of homologous recombination in DNA interstrand crosslink repair. Environ Mol Mutagen *51*, 582-603.

Hirano, M., and Hirano, T. (2002). Hinge-mediated dimerization of SMC protein is essential for its dynamic interaction with DNA. EMBO J *21*, 5733-5744.

Hirano, M., and Hirano, T. (2004). Positive and negative regulation of SMC-DNA interactions by ATP and accessory proteins. EMBO J *23*, 2664-2673.

Hirano, M., Hirano, T., Anderson, D.E., and Erickson, H.P. (2001). Bimodal activation of SMC ATPase by intra- and inter-molecular interactions. EMBO J *20*, 3238-3250.

Hirano, T. (2002). The ABCs of SMC proteins: two-armed ATPases for chromosome condensation, cohesion, and repair. Genes Dev *16*, 399-414.

Hirano, T. (2005). SMC proteins and chromosome mechanics: from bacteria to humans. Philos Trans R Soc Lond B Biol Sci *360*, 507-514.

Hirano, T. (2006). At the heart of the chromosome: SMC proteins in action. Nat Rev Mol Cell Biol *7*, 311-322.

Hirano, T., Kobayashi, R., and Hirano, M. (1997). Condensins, Chromosome Condensation Protein Complexes Containing XCAP-C, XCAP-E and a Xenopus Homolog of the Drosophila Barren Protein. Cell *89*, 511-521.

Ho, T.V., and Schärer, O.D. (2010). Translesion DNA synthesis polymerases in DNA interstrand crosslink repair. Environ Mol Mutagen *51*, 552-566.

Hochegger, H., Dejsuphong, D., Fukushima, T., Morrison, C., Sonoda, E., Schreiber, V., Zhao, G.Y., Saberi, A., Masutani, M., Adachi, N., *et al.* (2006). Parp-1 protects homologous recombination from interference by Ku and Ligase IV in vertebrate cells. EMBO J *25*, 1305-1314.

Hoege, C., Pfander, B., Moldovan, G.-L., Pyrowolakis, G., and Jentsch, S. (2002). RAD6-dependent DNA repair is linked to modification of PCNA by ubiquitin and SUMO. Nature *419*, 135-141.

Hollingsworth, N.M., and Brill, S.J. (2004). The Mus81 solution to resolution: generating meiotic crossovers without Holliday junctions. Genes Dev *18*, 117-125.

Hornig, N.C.D., and Uhlmann, F. (2004). Preferential cleavage of chromatin-bound cohesin after targeted phosphorylation by Polo-like kinase. EMBO J *23*, 3144-3153.

Hsiang, Y.-H., Liu, L.F., Wall, M.E., Wani, M.C., Nicholas, A.W., Manikumar, G., Kirschenbaum, S., Silber, R., and Potmesil, M. (1989). DNA Topoisomerase I-mediated DNA Cleavage and Cytotoxicity of Camptothecin Analogues. Cancer Res *49*, 4385-4389.

Hu, B., Liao, C., Millson, S.H., Mollapour, M., Prodromou, C., Pearl, L.H., Piper, P.W., and Panaretou, B. (2005). Qri2/Nse4, a component of the essential Smc5/6 DNA repair complex. Mol Microbiol *55*, 1735-1750.

Hubscher, U. (2009). DNA replication fork proteins. Methods Mol Biol *521*, 19-33.

Hudson, D.F., Morrison, C., Ruchaud, S., and Earnshaw, W.C. (2002). Reverse genetics of essential genes in tissue-culture cells: 'dead cells talking'. Trends Cell Biol *12*, 281-287.

Huen, M.S.Y., and Chen, J. (2010). Assembly of checkpoint and repair machineries at DNA damage sites. Trends Biochem Sci *35*, 101-108.

Huen, M.S.Y., Grant, R., Manke, I., Minn, K., Yu, X., Yaffe, M.B., and Chen, J. (2007). RNF8 Transduces the DNA-Damage Signal via Histone Ubiquitylation and Checkpoint Protein Assembly. Cell *131*, 901-914.

Hwang, J.Y., Smith, S., Ceschia, A., Torres-Rosell, J., Aragon, L., and Myung, K. (2008). Smc5-Smc6 complex suppresses gross chromosomal rearrangements mediated by break-induced replications. DNA repair (Amst) *7*, 1426-1436.

Iaccarino, I., Marra, G., Dufner, P., and Jiricny, J. (2000). Mutation in the Magnesium Binding Site of hMSH6 Disables the hMutSα Sliding Clamp from Translocating along DNA. J Biol Chem *275*, 2080-2086.

Iacopetta, B., Grieu, F., and Amanuel, B. (2010). Microsatellite instability in colorectal cancer. Asia Pac J Clin Oncol *6*, 260-269.

Ip, S.C.Y., Rass, U., Blanco, M.G., Flynn, H.R., Skehel, J.M., and West, S.C. (2008). Identification of Holliday junction resolvases from humans and yeast. Nature *456*, 357-361.

Ira, G., Malkova, A., Liberi, G., Foiani, M., and Haber, J.E. (2003). Srs2 and Sgs1-Top3 suppress crossovers during double-strand break repair in yeast. Cell *115*, 401-411.

Irmisch, A., Ampatzidou, E., Mizuno, K.i., O'Connell, M.J., and Murray, J.M. (2009). Smc5/6 maintains stalled replication forks in a recombination-competent conformation. EMBO J *28*, 144-155.

Jackson, P.K. (2001a). A new RING for SUMO: wrestling transcriptional responses into nuclear bodies with PIAS family E3 SUMO ligases. Genes Dev *15*, 3053-3058.

Jackson, P.K. (2001b). A new RING for SUMO: wrestling transcriptional responses into nuclear bodies with PIAS family E3 SUMO ligases. Genes & Development *15*, 3053-3058.

Jackson, S.P., and Bartek, J. (2009). The DNA-damage response in human biology and disease. Nature *461*, 1071-1078.

Jazayeri, A., Balestrini, A., Garner, E., Haber, J.E., and Costanzo, V. (2008). Mre11-Rad50-Nbs1-dependent processing of DNA breaks generates oligonucleotides that stimulate ATM activity. EMBO J *27*, 1953-1962.

Jin, J., Shirogane, T., Xu, L., Nalepa, G., Qin, J., Elledge, S.J., and Harper, J.W. (2003). SCFβ-TRCP links Chk1 signaling to degradation of the Cdc25A protein phosphatase. Genes Dev *17*, 3062-3074.

Johnson, E.S. (2004). Protein modification by SUMO. Ann Rev Biochem *73*, 355-382.

Johnson, E.S., and Blobel, G. (1997). Ubc9p Is the Conjugating Enzyme for the Ubiquitin-like Protein Smt3p. J Biol Chem *272*, 26799-26802.

Johnson, E.S., and Gupta, A.A. (2001). An E3-like Factor that Promotes SUMO Conjugation to the Yeast Septins. Cell *106*, 735-744.

Jones, B.K., and Yeung, A.T. (1990). DNA base composition determines the specificity of UvrABC endonuclease incision of a psoralen cross-link. J Biol Chem *265*, 3489-3496.

Jones, C.J., and Wood, R.D. (1993). Preferential binding of the xeroderma pigmentosum group A complementing protein to damaged DNA. Biochemistry *32*, 12096-12104.

Kagey, M.H., Melhuish, T.A., and Wotton, D. (2003). The Polycomb Protein Pc2 Is a SUMO E3. Cell *113*, 127-137.

Kahyo, T., Nishida, T., and Yasuda, H. (2001). Involvement of PIAS1 in the Sumoylation of Tumor Suppressor p53. Mol Cell *8*, 713-718.

Kamitani, T., Kito, K., Nguyen, H.P., Fukuda-Kamitani, T., and Yeh, E.T.H. (1998). Characterization of a Second Member of the Sentrin Family of Ubiquitin-like Proteins. J Biol Chem *273*, 11349-11353.

Kanne, D., Rapoport, H., and Hearst, J.E. (1984). 8-Methoxypsoralen-nucleic acid photoreaction. Effect of methyl substitution on pyrone vs. furan photoaddition. J Med Chem *27*, 531-534.

Kannouche, P., and Stary, A. (2003). Xeroderma pigmentosium variant and error-prone DNA polymerases. Biochimie *85*, 1123.

Kastan, M.B., Bartek, J. (2004). Cell-cycle checkpoints and cancer. Nature *432*, 316.

Kastan, M.B., Zhan, Q., El-Deiry, W.S., Carrier, F., Jacks, T., Walsh, W.V., Plunkett, B.S., Vogelstein, B., and Fornace, A.J. (1992). A mammalian cell cycle checkpoint pathway utilizing p53 and GADD45 is defective in ataxia-telangiectasia. Cell *71*, 587-597.

Kato, H. (1974). Possible role of DNA synthesis in formation of sister chromatid exchanges. Nature *252*, 739-741.

Kegel, A., Betts-Lindroos, H., Kanno, T., Jeppsson, K., Strom, L., Katou, Y., Itoh, T., Shirahige, K., and Sjogren, C. (2011). Chromosome length influences replication-induced topological stress. Nature *471*, 392-396.

Kerzendorfer, C., and O'Driscoll, M. (2009). Human DNA damage response and repair deficiency syndromes: linking genomic instability and cell cycle checkpoint proficiency. DNA repair (Amst) *8*, 1139-1152.

Kim, J.-S., Krasieva, T.B., LaMorte, V., Taylor, A.M.R., and Yokomori, K. (2002). Specific Recruitment of Human Cohesin to Laser-induced DNA Damage. J Biol Chem *277*, 45149-45153.

Kim, S., Humphries, E.H., Tjoelker, L., Carlson, L., and Thompson, C.B. (1990). Ongoing diversification of the rearranged immunoglobulin light-chain gene in a bursal lymphoma cell line. Mol Cell Biol *10*, 3224-3231.

Kimura, K., Hirano, M., Kobayashi, R., and Hirano, T. (1998). Phosphorylation and Activation of 13S Condensin by Cdc2 in Vitro. Science *282*, 487-490.

Kimura, K., and Hirano, T. (1997). ATP-Dependent Positive Supercoiling of DNA by 13S Condensin: A Biochemical Implication for Chromosome Condensation. Cell *90*, 625-634.

Kirsh, O., Seeler, J.-S., Pichler, A., Gast, A., Muller, S., Miska, E., Mathieu, M., Harel-Bellan, A., Kouzarides, T., Melchior, F., *et al.* (2002). The SUMO E3 ligase RanBP2 promotes modification of the HDAC4 deacetylase. EMBO J *21*, 2682-2691.

Kitagawa, R., Bakkenist, C.J., McKinnon, P.J., and Kastan, M.B. (2004). Phosphorylation of SMC1 is a critical downstream event in the ATM–NBS1–BRCA1 pathway. Genes Dev *18*, 1423-1438.

Kolas, N.K., Chapman, J.R., Nakada, S., Ylanko, J., Chahwan, R., Sweeney, F.D., Panier, S., Mendez, M., Wildenhain, J., Thomson, T.M., *et al.* (2007). Orchestration of the DNA-Damage Response by the RNF8 Ubiquitin Ligase. Science *318*, 1637-1640.

Kolb, H.C., Finn, M.G., and Sharpless, K.B. (2001). Click Chemistry: Diverse Chemical Function from a Few Good Reactions. Angew Chem Int Ed Engl *40*, 2004-2021.

Kolodner, R. (1996). Biochemistry and genetics of eukaryotic mismatch repair. Genes Dev *10*, 1433-1442.

Kotaja, N., Karvonen, U., Janne, O.A., and Palvimo, J.J. (2002). PIAS Proteins Modulate Transcription Factors by Functioning as SUMO-1 Ligases. Mol Cell Biol *22*, 5222-5234.

Kozak, M. (1986). Point mutations define a sequence flanking the AUG initiator codon that modulates translation by eukaryotic ribosomes. Cell *44*, 283-292.

Kragh, P., Nielsen, A., Li, J., Du, Y., Lin, L., Schmidt, M., Bøgh, I., Holm, I., Jakobsen, J., Johansen, M., *et al.* (2009). Hemizygous minipigs produced by random gene insertion and handmade cloning express the Alzheimer's disease-causing dominant mutation APPsw. Trans Res *18*, 545-558.

Kramer, A., Keitel, T., Winkler, K., Stocklein, W., Hohne, W., and Schneider-Mergener, J. (1997). Molecular basis for the binding promiscuity of an anti-p24 (HIV-1) monoclonal antibody. Cell *91*, 799-809.

Kregel, K.C., and Zhang, H.J. (2007). An integrated view of oxidative stress in aging: basic mechanisms, functional effects, and pathological considerations. Am J Physiol Regul Integr Comp Physiol *292*, R18-36.

Kunkel, T.A., and Bebenek, K. (2000). DNA REPLICATION FIDELITY1. Ann Rev Biochem *69*, 497-529.

Kuzminov, A. (1996). Unraveling the late stages of recombinational repair: metabolism of DNA junctions in Escherichia coli. BioEssays *18*, 757-765.

La Spada, A.R. (1997). Trinucleotide repeat instability: genetic features and molecular mechanisms. Brain Pathol *7*, 943-963.

Lai, L., Tao, T., Macháty, Z., Kühholzer, B., Sun, Q.-Y., Park, K.-W., Day, B.N., and Prather, R.S. (2001). Feasibility of Producing Porcine Nuclear Transfer Embryos by Using G2/M-Stage Fetal Fibroblasts as Donors. Biol Reprod *65*, 1558-1564.

Lalley, P.A., Minna, J.D., and Francke, U. (1978). Conservation of autosomal gene synteny groups in mouse and man. Nature *274*, 160-163.

Lee, H.-S., Park, J.-H., Kim, S.-J., Kwon, S.-J., and Kwon, J. (2010). A cooperative activation loop among SWI/SNF, [gamma]-H2AX and H3 acetylation for DNA double-strand break repair. EMBO J *29*, 1434-1445.

Lee, J.H., and Paull, T.T. (2005). ATM activation by DNA double-strand breaks through the Mre11-Rad50-Nbs1 complex. Science *308*, 551-554.

Lee, K.M., Nizza, S., Hayes, T., Bass, K.L., Irmisch, A., Murray, J.M., and O'Connell, M.J. (2007). Brc1-mediated rescue of Smc5/6 deficiency: requirement for multiple nucleases and a novel Rad18 function. Genetics *175*, 1585-1595.

Lehmann, A., Walicka, M., Griffiths, D., Murray, J., Watts, F., McCready, S., and Carr, A. (1995). The rad18 gene of Schizosaccharomyces pombe defines a new subgroup of the SMC superfamily involved in DNA repair. Mol Cell Biol *15*, 7067-7080.

Levine, S.S., King, I.F.G., and Kingston, R.E. (2004). Division of labor in Polycomb group repression. Trends Biochem Sci *29*, 478-485.

Lewis, E.B. (1978). A gene complex controlling segmentation in Drosophila. Nature *276*, 565-570.

Li, G.M., and Modrich, P. (1995). Restoration of mismatch repair to nuclear extracts of H6 colorectal tumor cells by a heterodimer of human MutL homologs. PNAS *92*, 1950-1954.

Li, X., Li, J., Harrington, J., Lieber, M.R., and Burgers, P.M.J. (1995a). Lagging Strand DNA Synthesis at the Eukaryotic Replication Fork Involves Binding and Stimulation of FEN-1 by Proliferating Cell Nuclear Antigen. J Biol Chem *270*, 22109-22112.

Li, Y., Huang, T.T., Carlson, E.J., Melov, S., Ursell, P.C., Olson, J.L., Noble, L.J., Yoshimura, M.P., Berger, C., Chan, P.H., *et al.* (1995b). Dilated cardiomyopathy and neonatal lethality in mutant mice lacking manganese superoxide dismutase. Nat Genet *11*, 376-381.

Lieb, J.D., Albrecht, M.R., Chuang, P.-T., and Meyer, B.J. (1998). MIX-1: An Essential Component of the C. elegans Mitotic Machinery Executes X Chromosome Dosage Compensation. Cell *92*, 265-277.

Lieb, J.D., de Solorzano, C.O., Rodriguez, E.G., Jones, A., Angelo, M., Lockett, S., and Meyer, B.J. (2000). The Caenorhabditis elegans Dosage Compensation Machinery Is Recruited to X Chromosome DNA Attached to an Autosome. Genetics *156*, 1603-1621.

Limbo, O., Porter-Goff, M.E., Rhind, N., and Russell, P. (2011). Mre11 nuclease activity and Ctp1 regulate Chk1 activation by Rad3ATR and Tel1ATM checkpoint kinases at double-strand breaks. Mol Cell Biol *31*, 573-583.

Lindahl, T. (1982). DNA Repair Enzymes. Ann Rev Biochem *51*, 61-87.

Lindahl, T. (1997). Facts and Artifacts of Ancient DNA. Cell *90*, 1-3.

Lindahl, T., and Barnes, D.E. (2000). Repair of Endogenous DNA Damage. Cold Spring Harb Symp Quant Biol *65*, 127-134.

Lindahl, T., Satoh, M.S., and Dianov, G. (1995). Enzymes Acting at Strand Interruptions in DNA. Philos Trans R Soc Lond B Biol Sci *347*, 57-62.

Lindahl, T., Sedgwick, B., Sekiguchi, M., and Nakabeppu, Y. (1988). Regulation and Expression of the Adaptive Response to Alkylating Agents. Ann Rev Biochem *57*, 133-157.

Lindroos, H.B., Strom, L., Itoh, T., Katou, Y., Shirahige, K., and Sjogren, C. (2006). Chromosomal association of the Smc5/6 complex reveals that it functions in differently regulated pathways. Mol Cell *22*, 755-767.

Liu, P.-Q., Chan, E.M., Cost, G.J., Zhang, L., Wang, J., Miller, J.C., Guschin, D.Y., Reik, A., Holmes, M.C., Mott, J.E., *et al.* (2010). Generation of a triple-gene knockout mammalian cell line using engineered zinc-finger nucleases. Biotechnol Bioeng *106*, 97-105.

Lois, L.M., Lima, C.D., and Chua, N.-H. (2003). Small Ubiquitin-Like Modifier Modulates Abscisic Acid Signaling in Arabidopsis. Plant Cell *15*, 1347-1359.

Losada, A., Hirano, M., and Hirano, T. (1998). Identification of Xenopus SMC protein complexes required for sister chromatid cohesion. Genes Dev *12*, 1986-1997.

Losada, A., and Hirano, T. (2005). Dynamic molecular linkers of the genome: the first decade of SMC proteins. Genes Dev *19*, 1269-1287.

Losada, A., Yokochi, T., Kobayashi, R., and Hirano, T. (2000). Identification and Characterization of Sa/Scc3p Subunits in the Xenopus and Human Cohesin Complexes. J Cell Biol *150*, 405-416.

Lowe, S.W., Ruley, H.E., Jacks, T., and Housman, D.E. (1993). p53-dependent apoptosis modulates the cytotoxicity of anticancer agents. Cell *74*, 957-967.

Lu, Y., Wang, Z., Ge, L., Chen, N., and Liu, H. (2009). The RZZ complex and the spindle assembly checkpoint. Cell Struct Funct *34*, 31-45.

Lupo, R., Breiling, A., Bianchi, M.E., and Orlando, V. (2001). Drosophila Chromosome Condensation Proteins Topoisomerase II and Barren Colocalize with Polycomb and Maintain Fab-7 PRE Silencing. Mol Cell *7*, 127-136.

Lynch, H.T., Riley, B.D., Weissman, S.M., Coronel, S.M., Kinarsky, Y., Lynch, J.F., Shaw, T.G., and Rubinstein, W.S. (2004). Hereditary nonpolyposis colorectal carcinoma (HNPCC) and

HNPCC-like families: Problems in diagnosis, surveillance, and management. Cancer *100*, 53-64.

Madhusudan, S., Smart, F., Shrimpton, P., Parsons, J.L., Gardiner, L., Houlbrook, S., Talbot, D.C., Hammonds, T., Freemont, P.A., Sternberg, M.J., *et al.* (2005). Isolation of a small molecule inhibitor of DNA base excision repair. Nucleic Acids Res *33*, 4711-4724.

Mahaney, B.L., Meek, K., and Lees-miller, S.P. (2009). Repair of ionizing radiation-induced DNA double-strand breaks by non-homologous end-joining. Biochem J *417*, 639-650.

Mailand, N., Falck, J., Lukas, C., Syljuasen, R.G., Welcker, M., Bartek, J., and Lukas, J. (2000). Rapid destruction of human Cdc25A in response to DNA damage. Science *288*, 1425-1429.

Maillard, O., Solyom, S., and Naegeli, H. (2007). An aromatic sensor with aversion to damaged strands confers versatility to DNA repair. PLoS Biol *5*, e79.

Marino, S., Vooijs, M., van der Gulden, H., Jonkers, J., and Berns, A. (2000). Induction of medulloblastomas in p53-null mutant mice by somatic inactivation of Rb in the external granular layer cells of the cerebellum. Genes Dev *14*, 994-1004.

Marti, T.M., Hefner, E., Feeney, L., Natale, V., and Cleaver, J.E. (2006). H2AX phosphorylation within the G1 phase after UV irradiation depends on nucleotide excision repair and not DNA double-strand breaks. PNAS *103*, 9891-9896.

Mashimo, T., Takizawa, A., Voigt, B., Yoshimi, K., Hiai, H., Kuramoto, T., and Serikawa, T. (2010). Generation of knockout rats with X-linked severe combined immunodeficiency (X-SCID) using zinc-finger nucleases. PLoS One *5*, e8870.

Matsuda, T., Saijo, M., Kuraoka, I., Kobayashi, T., Nakatsu, Y., Nagai, A., Enjoji, T., Masutani, C., Sugasawa, K., Hanaoka, F., *et al.* (1995). DNA repair protein XPA binds replication protein A (RPA). J Biol Chem *270*, 4152-4157.

Matsumoto, Y., and Kim, K. (1995). Excision of deoxyribose phosphate residues by DNA polymerase beta during DNA repair. Science *269*, 699-702.

Matunis, M.J., Coutavas, E., and Blobel, G. (1996). A novel ubiquitin-like modification modulates the partitioning of the Ran-GTPase-activating protein RanGAP1 between the cytosol and the nuclear pore complex. J Cell Biol *135*, 1457-1470.

Matunis, M.J., Wu, J., and Blobel, G. (1998). SUMO-1 Modification and Its Role in Targeting the Ran GTPase-activating Protein, RanGAP1, to the Nuclear Pore Complex. J Cell Biol *140*, 499-509.

Maya, R., Balass, M., Kim, S.-T., Shkedy, D., Leal, J.-F.M., Shifman, O., Moas, M., Buschmann, T., Ronai, Z.e., Shiloh, Y., *et al.* (2001). ATM-dependent phosphorylation of Mdm2 on serine 395: role in p53 activation by DNA damage. Genes Dev *15*, 1067-1077.

McCabe, K.M., Hemphill, A., Akkari, Y., Jakobs, P.M., Pauw, D., Olson, S.B., Moses, R.E., and Grompe, M. (2008). ERCC1 is required for FANCD2 focus formation. Mol Genet Metab *95*, 66-73.

McDonald, W.H., Pavlova, Y., Yates, J.R., and Boddy, M.N. (2003). Novel Essential DNA Repair Proteins Nse1 and Nse2 Are Subunits of the Fission Yeast Smc5-Smc6 Complex. J Biol Chem *278*, 45460-45467.

McIntyre, G.J., and Fanning, G.C. (2006). Design and cloning strategies for constructing shRNA expression vectors. BMC Biotechnol *6*, 1.

Meek, K., Dang, V., and Lees-Miller, S.P. (2008). Chapter 2 DNA-PK: The Means to Justify the Ends? In Adv Immunol, W.A. Frederick, ed. (Academic Press), pp. 33-58.

Mehta, G.D., Agarwal, M.P., and Ghosh, S.K. (2010). Centromere identity: a challenge to be faced. Mol Genet Genomics *284*, 75-94.

Michaelis, C., Ciosk, R., and Nasmyth, K. (1997). Cohesins: Chromosomal Proteins that Prevent Premature Separation of Sister Chromatids. Cell *91*, 35-45.

Mimitou, E.P., and Symington, L.S. (2008). Sae2, Exo1 and Sgs1 collaborate in DNA double-strand break processing. Nature *455*, 770-774.

Minty, A., Dumont, X., Kaghad, M., and Caput, D. (2000). Covalent Modification of p73α by SUMO-1. J Biol Chem *275*, 36316-36323.

Misteli, T., and Soutoglou, E. (2009). The emerging role of nuclear architecture in DNA repair and genome maintenance. Nat Rev Mol Cell Biol *10*, 243-254.

Moggs, J.G., Yarema, K.J., Essigmann, J.M., and Wood, R.D. (1996). Analysis of Incision Sites Produced by Human Cell Extracts and Purified Proteins during Nucleotide Excision Repair of a 1,3-Intrastrand d(GpTpG)-Cisplatin Adduct. J Biol Chem *271*, 7177-7186.

Moilanen, A.-M., Karvonen, U., Poukka, H., Yan, W., Toppari, J., Jänne, O.A., and Palvimo, J.J. (1999). A Testis-specific Androgen Receptor Coregulator That Belongs to a Novel Family of Nuclear Proteins. J Biol Chem *274*, 3700-3704.

Moldovan, G.L., Pfander, B., and Jentsch, S. (2006). PCNA controls establishment of sister chromatid cohesion during S phase. Mol Cell *23*, 723-732.

Moldovan, G.L., Pfander, B., and Jentsch, S. (2007). PCNA, the maestro of the replication fork. Cell *129*, 665-679.

Morgan, D.O. (1995). Principles of CDK regulation. Nature *374*, 131-134.

Morgan, D.O. (1997). Cyclin-dependent kinases: engines, clocks, and microprocessors. Ann Rev Cell Dev Biol *13*, 261-291.

Morris, J.R., Boutell, C., Keppler, M., Densham, R., Weekes, D., Alamshah, A., Butler, L., Galanty, Y., Pangon, L., Kiuchi, T., *et al.* (2009). The SUMO modification pathway is involved in the BRCA1 response to genotoxic stress. Nature *462*, 886-890.

Morrison, C., Sonoda, E., Takao, N., Shinohara, A., Yamamoto, K., and Takeda, S. (2000). The controlling role of ATM in homologous recombinational repair of DNA damage. Embo J *19*, 463-471.

Morrison, C., and Takeda, S. (2000). Genetic analysis of homologous DNA recombination in vertebrate somatic cells. Int J Biochem Cell Biol *32*, 817-831.

Moyer, S.E., Lewis, P.W., and Botchan, M.R. (2006). Isolation of the Cdc45/Mcm2-7/GINS (CMG) complex, a candidate for the eukaryotic DNA replication fork helicase. PNAS *103*, 10236-10241.

Moynahan, M.E., Pierce, A.J., and Jasin, M. (2001). BRCA2 is required for homology-directed repair of chromosomal breaks. Mol Cell *7*, 263-272.

Mozlin, A.M., Fung, C.W., and Symington, L.S. (2008). Role of the Saccharomyces cerevisiae Rad51 paralogs in sister chromatid recombination. Genetics *178*, 113-126.

Muñoz, I.M., Hain, K., Déclais, A.-C., Gardiner, M., Toh, G.W., Sanchez-Pulido, L., Heuckmann, J.M., Toth, R., Macartney, T., Eppink, B., *et al.* (2009). Coordination of Structure-Specific Nucleases by Human SLX4/BTBD12 Is Required for DNA Repair. Mol Cell *35*, 116-127.

Murray, A.W. (2004). Recycling the cell cycle: cyclins revisited Cell *116*, 221.

Naegeli, H. (1995). Mechanisms of DNA damage recognition in mammalian nucleotide excision repair. FASEB J *9*, 1043-1050.

Nezi, L., and Musacchio, A. (2009). Sister chromatid tension and the spindle assembly checkpoint. Curr Opin Cell Biol *21*, 785-795.

Niedernhofer, L.J., Essers, J., Weeda, G., Beverloo, B., de Wit, J., Muijtjens, M., Odijk, H., Hoeijmakers, J.H.J., and Kanaar, R. (2001). The structure-specific endonuclease Ercc1–Xpf is required for targeted gene replacement in embryonic stem cells. EMBO J *20*, 6540-6549.

Niedernhofer, L.J., Odijk, H., Budzowska, M., van Drunen, E., Maas, A., Theil, A.F., de Wit, J., Jaspers, N.G.J., Beverloo, H.B., Hoeijmakers, J.H.J., *et al.* (2004). The Structure-Specific Endonuclease Ercc1-Xpf Is Required To Resolve DNA Interstrand Cross-Link-Induced Double-Strand Breaks. Mol Cell Biol *24*, 5776-5787.

Niida, H., and Nakanishi, M. (2006). DNA damage checkpoints in mammals. Mutagenesis *21*, 3-9.

Nimonkar, A.V., Sica, R.A., and Kowalczykowski, S.C. (2009). Rad52 promotes second-end DNA capture in double-stranded break repair to form complement-stabilized joint molecules. PNAS *106*, 3077-3082.

Nishimura, K., Fukagawa, T., Takisawa, H., Kakimoto, T., and Kanemaki, M. (2009). An auxin-based degron system for the rapid depletion of proteins in nonplant cells. Nat Meth *6*, 917-922.

Nurse, P. (2002). Cyclin pependent kinases and cell cycle control (Nobel lecture). Chem Bio Chem *3*, 596-603.

Nyberg, K.A., Michelson, R.J., Putnam, C.W., and Weinert, T.A. (2002). TOWARD MAINTAINING THE GENOME: DNA Damage and Replication Checkpoints. Ann Rev Genet *36*, 617-656.

O'Driscoll, M., and Jeggo, P.A. (2008). The role of the DNA damage response pathways in brain development and microcephaly: insight from human disorders. DNA repair (Amst) *7*, 1039-1050.

Ohouo, P.Y., Bastos de Oliveira, F.M., Almeida, B.S., and Smolka, M.B. (2010). DNA damage signaling recruits the Rtt107-Slx4 scaffolds via Dpb11 to mediate replication stress response. Mol Cell *39*, 300-306.

Ohta, S., Bukowski-Wills, J.C., Sanchez-Pulido, L., Alves Fde, L., Wood, L., Chen, Z.A., Platani, M., Fischer, L., Hudson, D.F., Ponting, C.P., *et al.* (2010). The protein composition of mitotic chromosomes determined using multiclassifier combinatorial proteomics. Cell *142*, 810-821.

Olson, E., Nievera, C.J., Lee, A.Y., Chen, L., and Wu, X. (2007). The Mre11-Rad50-Nbs1 complex acts both upstream and downstream of ataxia telangiectasia mutated and Rad3-related protein (ATR) to regulate the S-phase checkpoint following UV treatment. J Biol Chem *282*, 22939-22952.

Onoda, F., Takeda, M., Seki, M., Maeda, D., Tajima, J., Ui, A., Yagi, H., and Enomoto, T. (2004). SMC6 is required for MMS-induced interchromosomal and sister chromatid recombinations in Saccharomyces cerevisiae. DNA repair (Amst) *3*, 429-439.

Osborn, A.J., Elledge, S.J., and Zou, L. (2002). Checking on the fork: the DNA-replication stress-response pathway. Trends Cell Biol *12*, 509-516.

Outwin, E.A., Irmisch, A., Murray, J.M., and O'Connell, M.J. (2009). Smc5-Smc6-Dependent Removal of Cohesin from Mitotic Chromosomes. Mol Cell Biol *29*, 4363-4375.

Paddison, P.J., Caudy, A.A., Bernstein, E., Hannon, G.J., and Conklin, D.S. (2002). Short hairpin RNAs (shRNAs) induce sequence-specific silencing in mammalian cells. Genes Dev *16*, 948-958.

Palecek, J., Vidot, S., Feng, M., Doherty, A.J., and Lehmann, A.R. (2006). The Smc5-Smc6 DNA Repair Complex: Bridging of the Smc5-Smc6 heads by the Kleisin, Nse4, and non-Kleisin subunits. J Biol Chem *281*, 36952-36959.

Paull, T.T. (2001). New Glimpses of an Old Machine. Cell *107*, 563-565.

Paull, T.T., and Lee, J.H. (2005). The Mre11/Rad50/Nbs1 complex and its role as a DNA double-strand break sensor for ATM. Cell Cycle *4*, 737-740.

Pebernard, S., McDonald, W.H., Pavlova, Y., Yates, J.R., III, and Boddy, M.N. (2004). Nse1, Nse2, and a Novel Subunit of the Smc5-Smc6 Complex, Nse3, Play a Crucial Role in Meiosis. Molecular biology of the cell *15*, 4866-4876.

Pebernard, S., Perry, J.J., Tainer, J.A., and Boddy, M.N. (2008a). Nse1 RING-like domain supports functions of the Smc5-Smc6 holocomplex in genome stability. Molecular biology of the cell *19*, 4099-4109.

Pebernard, S., Perry, J.J.P., Tainer, J.A., and Boddy, M.N. (2008b). Nse1 RING-like Domain Supports Functions of the Smc5-Smc6 Holocomplex in Genome Stability. Mol Biol Cell *19*, 4099-4109.

Pebernard, S., Schaffer, L., Campbell, D., Head, S.R., and Boddy, M.N. (2008c). Localization of Smc5/6 to centromeres and telomeres requires heterochromatin and SUMO, respectively. EMBO J *27*, 3011-3023.

Pebernard, S., Wohlschlegel, J., McDonald, W.H., Yates, J.R., III, and Boddy, M.N. (2006). The Nse5-Nse6 Dimer Mediates DNA Repair Roles of the Smc5-Smc6 Complex. Mol Cell Biol *26*, 1617-1630.

Petermann, E., Orta, M.L., Issaeva, N., Schultz, N., and Helleday, T. (2010). Hydroxyurea-stalled replication forks become progressively inactivated and require two different RAD51-mediated pathways for restart and repair. Mol Cell *37*, 492-502.

Pfander, B., Moldovan, G.L., Sacher, M., Hoege, C., and Jentsch, S. (2005). SUMO-modified PCNA recruits Srs2 to prevent recombination during S phase. Nature *436*, 428-433.

Pichler, A., Gast, A., Seeler, J.S., Dejean, A., and Melchior, F. (2002). The Nucleoporin RanBP2 Has SUMO1 E3 Ligase Activity. Cell *108*, 109-120.

Pierce, A.J., Johnson, R.D., Thompson, L.H., and Jasin, M. (1999). XRCC3 promotes homology-directed repair of DNA damage in mammalian cells. Genes Dev *13*, 2633-2638.

Pilch, D.R., Sedelnikova, O.A., Redon, C., Celeste, A., Nussenzweig, A., and Bonner, W.M. (2003). Characteristics of gamma-H2AX foci at DNA double-strand breaks sites. Biochem Cell Biol *81*, 123-129.

Pospiech, H., Grosse, F., and Pisani, F.M. (2010). The initiation step of eukaryotic DNA replication. Subcell Biochem *50*, 79-104.

Potts, P.R. (2009). The Yin and Yang of the MMS21-SMC5/6 SUMO ligase complex in homologous recombination. DNA repair *8*, 499-506.

Potts, P.R., Porteus, M.H., and Yu, H. (2006). Human SMC5/6 complex promotes sister chromatid homologous recombination by recruiting the SMC1/3 cohesin complex to double-strand breaks. EMBO J *25*, 3377–3388.

Potts, P.R., and Yu, H. (2005). Human MMS21/NSE2 Is a SUMO Ligase Required for DNA Repair. Mol Cell Biol *25*, 7021-7032.

Potts, P.R., and Yu, H. (2007). The SMC5/6 complex maintains telomere length in ALT cancer cells through SUMOylation of telomere-binding proteins. Nat Struct Mol Biol *14*, 581-590.

Prakash, L., and Prakash, S. (1977). Isolation and characterization of MMS-sensitive mutants of Saccharomyces cerevisiae. Genetics *86*, 33-55.

Przewloka, M.R., and Glover, D.M. (2009). The kinetochore and the centromere: a working long distance relationship. Annu Rev Genet *43*, 439-465.

Rahn, J.J., Adair, G.M., and Nairn, R.S. (2010). Multiple roles of ERCC1-XPF in mammalian interstrand crosslink repair. Environ Mol Mutagen *51*, 567-581.

Rai, R., Varma, S.P.M.V., Shinde, N., Ghosh, S., Kumaran, S.P., Skariah, G., and Laloraya, S. (2011). SUMO-Ligase activity of Mms21 is required for maintenance of chromosome integrity during the unperturbed mitotic cell division cycle in Saccharomyces cerevisiae. J Biol Chem.

Rajasekhar, V.K., and Begemann, M. (2007). Concise review: roles of polycomb group proteins in development and disease: a stem cell perspective. Stem Cells *25*, 2498-2510.

Raleigh, J.M., and O'Connell, M.J. (2000). The G(2) DNA damage checkpoint targets both Wee1 and Cdc25. J Cell Sci *113 (Pt 10)*, 1727-1736.

Ramaswamy, M., and Yeung, A.T. (1994). Sequence-specific interactions of UvrABC endonuclease with psoralen interstrand cross-links. J Biol Chem *269*, 485-492.

Rapp, A., Greulich, K.O. (2004). After double-strand break induction by UV-A, homologous recombination and nonhomologous end joining cooperate at the same DSB if both systems are available. J Cell Sci *117*, 4935.

Rastogi, R.P., Richa, Kumar, A., Tyagi, M.B., and Sinha, R.P. (2010). Molecular mechanisms of ultraviolet radiation-induced DNA damage and repair. J Nucleic Acids *2010*, 592980.

Rémy, S., Tesson, L., Ménoret, S., Usal, C., Scharenberg, A., and Anegon, I. (2010). Zinc-finger nucleases: a powerful tool for genetic engineering of animals. Trans Res *19*, 363-371.

Rivera, T., and Losada, A. (2006). Shugoshin and PP2A, shared duties at the centromere. BioEssays *28*, 775-779.

Robert, T., Dervins, D., Fabre, F., and Gangloff, S. (2006). Mrc1 and Srs2 are major actors in the regulation of spontaneous crossover. EMBO J *25*, 2837-2846.

Robins, P., and Lindahl, T. (1996). DNA Ligase IV from HeLa Cell Nuclei. J Biol Chem *271*, 24257-24261.

Rogakou, E.P., Pilch, D.R., Orr, A.H., Ivanova, V.S., and Bonner, W.M. (1998). DNA double-stranded breaks induce histone H2AX phosphorylation on serine 139. J Biol Chem *273*, 5858-5868.

Rogers, C.S., Stoltz, D.A., Meyerholz, D.K., Ostedgaard, L.S., Rokhlina, T., Taft, P.J., Rogan, M.P., Pezzulo, A.A., Karp, P.H., Itani, O.A., *et al.* (2008). Disruption of the CFTR Gene Produces a Model of Cystic Fibrosis in Newborn Pigs. Science *321*, 1837-1841.

Roy, M.A., Siddiqui, N., and D'Amours, D. (2011). Dynamic and selective DNA-binding activity of Smc5, a core component of the Smc5-Smc6 complex. Cell Cycle *10*.

Rudner, A.D., and Murray, A.W. (2000). Phosphorylation by Cdc28 activates the Cdc20-dependent activity of the anaphase-promoting complex. J Cell Biol *149*, 1377-1390.

Sachdev, S., Bruhn, L., Sieber, H., Pichler, A., Melchior, F., and Grosschedl, R. (2001). PIASy, a nuclear matrix–associated SUMO E3 ligase, represses LEF1 activity by sequestration into nuclear bodies. Genes Dev *15*, 3088-3103.

Saitoh, H., and Hinchey, J. (2000). Functional Heterogeneity of Small Ubiquitin-related Protein Modifiers SUMO-1 versus SUMO-2/3. J Biol Chem *275*, 6252-6258.

Saitoh, H., Pu, R., Cavenagh, M., and Dasso, M. (1997). RanBP2 associates with Ubc9p and a modified form of RanGAP1. PNAS *94*, 3736-3741.

Sambrook, J., and Russell, D.C. (2001). Molecular Cloning: A Laboratory Manual (Cold Spring Harbour Laboratory Press).

Sancar, A., Lindsey-Bolts, L.A., Unsal-Kacmaz, K., and Linn, S. (2004). Molecular mechanisms of mammalian DNA repair and DNA damage checkpoints. Ann Rev Biochem *73*, 38.

Sanchez, I., and Dynlacht, B.D. (2005). New insights into cyclins, CDKs, and cell cycle control. Semin Cell Dev Biol *16*, 311-321.

Santiago, Y., Chan, E., Liu, P.-Q., Orlando, S., Zhang, L., Urnov, F.D., Holmes, M.C., Guschin, D., Waite, A., Miller, J.C., *et al.* (2008). Targeted gene knockout in mammalian cells by using engineered zinc-finger nucleases. PNAS *105*, 5809-5814.

Saparbaev, M., Prakash, L., and Prakash, S. (1996). Requirement of mismatch repair genes MSH2 and MSH3 in the RAD1-RAD10 pathway of mitotic recombination in Saccharomyces cerevisiae. Genetics *142*, 727-736.

Scherly, D., Nouspikel, T., Corlet, J., Ucla, C., Bairoch, A., and Clarkson, S.G. (1993). Complementation of the DNA repair defect in xeroderma pigmentosum group G cells by a human cDNA related to yeast RAD2. Nature *363*, 182-185.

Schleiffer, A., Kaitna, S., Maurer-Stroh, S., Glotzer, M., Nasmyth, K., and Eisenhaber, F. (2003). Kleisins: A Superfamily of Bacterial and Eukaryotic SMC Protein Partners. Mol Cell *11*, 571-575.

Schreiber, V., Amé, J.-C., Dollé, P., Schultz, I., Rinaldi, B., Fraulob, V., Ménissier-de Murcia, J., and de Murcia, G. (2002). Poly(ADP-ribose) Polymerase-2 (PARP-2) Is Required for Efficient Base Excision DNA Repair in Association with PARP-1 and XRCC1. J Biol Chem *277*, 23028-23036.

Schreiber, V., Dantzer, F., Ame, J.-C., and de Murcia, G. (2006). Poly(ADP-ribose): novel functions for an old molecule. Nat Rev Mol Cell Biol *7*, 517-528.

Schultz, P., Fribourg, S., Poterszman, A., Mallouh, V., Moras, D., and Egly, J.M. (2000). Molecular structure of human TFIIH. Cell *102*, 599-607.

Sedelnikova, O.A., Pilch, D.R., Redon, C., and Bonner, W.M. (2003). Histone H2AX in DNA damage and repair. Cancer Biol Ther *2*, 233-235.

Sedgwick, B. (2004). Repairing DNA-methylation damage. Nat Rev Mol Cell Biol *5*, 148-157.

Seeberg, E., Eide, L., and Bjørås, M. (1995). The base excision repair pathway. Trends Biochem Sci *20*, 391-397.

Sergeant, J., Taylor, E., Palecek, J., Fousteri, M., Andrews, E.A., Sweeney, S., Shinagawa, H., Watts, F.Z., and Lehmann, A.R. (2005). Composition and architecture of the Schizosaccharomyces pombe Rad18 (Smc5-6) complex. Mol Cell Biol *25*, 172-184.

Sheedy, D.M., Dimitrova, D., Rankin, J.K., Bass, K.L., Lee, K.M., Tapia-Alveal, C., Harvey, S.H., Murray, J.M., and O'Connell, M.J. (2005). Brc1-Mediated DNA Repair and Damage Tolerance. Genetics *171*, 457-468.

Sherr, C.J., and McCormick, F. (2002). The RB and p53 pathways in cancer. Cancer Cell *2*, 103-112.

Shuai, K. (2000). Modulation of STAT signaling by STAT-interacting proteins. Oncogene *19*, 2638-2644.

Sibley, C.R., Seow, Y., and Wood, M.J. (2010). Novel RNA-based strategies for therapeutic gene silencing. Mol Ther *18*, 466-476.

Skibbens, R.V. (2009). Establishment of Sister Chromatid Cohesion. Curr Biol *19*, R1126-R1132.

Sladek, F.M., Munn, M.M., Rupp, W.D., and Howard-Flanders, P. (1989). In vitro repair of psoralen-DNA cross-links by RecA, UvrABC, and the 5'-exonuclease of DNA polymerase I. J Biol Chem *264*, 6755-6765.

Sobol, R.W., Horton, J.K., Kuhn, R., Gu, H., Singhal, R.K., Prasad, R., Rajewsky, K., and Wilson, S.H. (1996). Requirement of mammalian DNA polymerase-[beta] in base-excision repair. Nature *379*, 183-186.

Sollier, J., Driscoll, R., Castellucci, F., Foiani, M., Jackson, S.P., and Branzei, D. (2009). The Saccharomyces cerevisiae Esc2 and Smc5-6 Proteins Promote Sister Chromatid Junction-mediated Intra-S Repair. Molecular biology of the cell *20*, 1671-1682.

Sonoda, E., Matsusaka, T., Morrison, C., Vagnarelli, P., Hoshi, O., Ushiki, T., Nojima, K., Fukagawa, T., Waizenegger, I.C., Peters, J.M., *et al.* (2001). Scc1/Rad21/Mcd1 is required for sister chromatid cohesion and kinetochore function in vertebrate cells. Dev Cell *1*, 759-770.

Sonoda, E., Sasaki, M.S., Buerstedde, J.M., Bezzubova, O., Shinohara, A., Ogawa, H., Takata, M., Yamaguchi-Iwai, Y., and Takeda, S. (1998). Rad51-deficient vertebrate cells accumulate chromosomal breaks prior to cell death. Embo J *17*, 598-608.

Sonoda, E., Sasaki, M.S., Morrison, C., Yamaguchi-Iwai, Y., Takata, M., and Takeda, S. (1999). Sister chromatid exchanges are mediated by homologous recombination in vertebrate cells. Mol Cell Biol *19*, 5166-5169.

Sorensen, C.S., Hansen, L.T., Dziegielewski, J., Syljuasen, R.G., Lundin, C., Bartek, J., and Helleday, T. (2005). The cell-cycle checkpoint kinase Chk1 is required for mammalian homologous recombination repair. Nat Cell Biol *7*, 195-201.

Spry, M., Scott, T., Pierce, H., and D'Orazio, J.A. (2007). DNA repair pathways and hereditary cancer susceptibility syndromes. Front Biosci *12*, 4191-4207.

Starr, D.A., Saffery, R., Li, Z., Simpson, A.E., Choo, K.H., Yen, T.J., and Goldberg, M.L. (2000). HZwint-1, a novel human kinetochore component that interacts with HZW10. J Cell Sci *113 (Pt 11)*, 1939-1950.

Stead, K., Aguilar, C., Hartman, T., Drexel, M., Meluh, P., and Guacci, V. (2003). Pds5p regulates the maintenance of sister chromatid cohesion and is sumoylated to promote the dissolution of cohesion. J Cell Biol *163*, 729-741.

Stelter, P., and Ulrich, H.D. (2003). Control of spontaneous and damage-induced mutagenesis by SUMO and ubiquitin conjugation. Nature *425*, 188-191.

Stephan, A.K. (2007). Genetic and biochemical analysis of the role of chicken Smc5 in the maintenance of genome stability. In School of Natural Sciences (Galway, National University of Ireland Galway).

Stephan, A.K., Kliszczak, M., Dodson, H., Cooley, C., and Morrison, C.G. (2011a). Roles of vertebrate smc5 in sister chromatid cohesion and homologous recombinational repair. Mol Cell Biol *31*, 1369-1381.

Stephan, A.K., Kliszczak, M., and Morrison, C.G. (2011b). The Nse2/Mms21 SUMO ligase of the Smc5/6 complex in the maintenance of genome stability. FEBS Lett.

Stewart, G.S., Wang, B., Bignell, C.R., Taylor, A.M., and Elledge, S.J. (2003). MDC1 is a mediator of the mammalian DNA damage checkpoint. Nature *421*, 961-966.

Stojic, L., Brun, R., and Jiricny, J. (2004a). Mismatch repair and DNA damage signalling. DNA repair *3*, 1091-1101.

Stojic, L., Mojas, N., Cejka, P., di Pietro, M., Ferrari, S., Marra, G., and Jiricny, J. (2004b). Mismatch repair-dependent G2 checkpoint induced by low doses of SN1 type methylating agents requires the ATR kinase. Genes Dev *18*, 1331-1344.

Stracker, T.H., Usui, T., and Petrini, J.H.J. (2009). Taking the time to make important decisions: The checkpoint effector kinases Chk1 and Chk2 and the DNA damage response. DNA repair *8*, 1047-1054.

Ström, L., Lindroos, H.B., Shirahige, K., and Sjögren, C. (2004). Postreplicative Recruitment of Cohesin to Double-Strand Breaks Is Required for DNA Repair. Mol Cell *16*, 1003-1015.

Strunnikov, A.V., Hogan, E., and Koshland, D. (1995). SMC2, a Saccharomyces cerevisiae gene essential for chromosome segregation and condensation, defines a subgroup within the SMC family. Genes Dev *9*, 587-599.

Stucki, M., Clapperton, J.A., Mohammad, D., Yaffe, M.B., Smerdon, S.J., and Jackson, S.P. (2005). MDC1 directly binds phosphorylated histone H2AX to regulate cellular responses to DNA double-strand breaks. Cell *123*, 1213-1226.

Sullivan, M., and Morgan, D.O. (2007). Finishing mitosis, one step at a time. Nat Rev Mol Cell Biol *8*, 894-903.

Sumara, I., Vorlaufer, E., Gieffers, C., Peters, B.H., and Peters, J.-M. (2000). Characterization of Vertebrate Cohesin Complexes and Their Regulation in Prophase. J Cell Biol *151*, 749-762.

Sumara, I., Vorlaufer, E., Stukenberg, P.T., Kelm, O., Redemann, N., Nigg, E.A., and Peters, J.-M. (2002). The Dissociation of Cohesin from Chromosomes in Prophase Is Regulated by Polo-like Kinase. Mol Cell *9*, 515-525.

Suto, M.J., Turner, W.R., Arundel-Suto, C.M., Werbel, L.M., and Sebolt-Leopold, J.S. (1991). Dihydroisoquinolinones: the design and synthesis of a new series of potent inhibitors of poly(ADP-ribose) polymerase. Anticancer Drug Des *6*, 107-117.

Svendsen, J.M., Smogorzewska, A., Sowa, M.E., O'Connell, B.C., Gygi, S.P., Elledge, S.J., and Harper, J.W. (2009). Mammalian BTBD12/SLX4 Assembles A Holliday Junction Resolvase and Is Required for DNA Repair. Cell *138*, 63-77.

Symington, L.S. (2002). Role of RAD52 Epistasis Group Genes in Homologous Recombination and Double-Strand Break Repair. Microbiol Mol Biol Rev *66*, 630-670.

Takahashi, Y., Kahyo, T., Toh-e, A., Yasuda, H., and Kikuchi, Y. (2001). Yeast Ull1/Siz1 Is a Novel SUMO1/Smt3 Ligase for Septin Components and Functions as an Adaptor between Conjugating Enzyme and Substrates. J Biol Chem *276*, 48973-48977.

Takahashi, Y., Toh-e, A., and Kikuchi, Y. (2003). Comparative Analysis of Yeast PIAS-Type SUMO Ligases In Vivo and In Vitro. J Biochem *133*, 415-422.

Takata, M., Sasaki, M.S., Sonoda, E., Morrison, C., Hashimoto, M., Utsumi, H., Yamaguchi-Iwai, Y., Shinohara, A., and Takeda, S. (1998). Homologous recombination and non-homologous end-joining pathways of DNA double-strand break repair have overlapping roles in the maintenance of chromosomal integrity in vertebrate cells. Embo J *17*, 5497-5508.

Tanaka, K., Miura, N., Satokata, I., Miyamoto, I., Yoshida, M.C., Satoh, Y., Kondo, S., Yasui, A., Okayama, H., and Okada, Y. (1990). Analysis of a human DNA excision repair gene involved in group A xeroderma pigmentosum and containing a zinc-finger domain. Nature *348*, 73-76.

Tatham, M.H., Jaffray, E., Vaughan, O.A., Desterro, J.M.P., Botting, C.H., Naismith, J.H., and Hay, R.T. (2001). Polymeric Chains of SUMO-2 and SUMO-3 Are Conjugated to Protein Substrates by SAE1/SAE2 and Ubc9. J Biol Chem *276*, 35368-35374.

Tatham, M.H., Kim, S., Yu, B., Jaffray, E., Song, J., Zheng, J., Rodriguez, M.S., Hay, R.T., and Chen, Y. (2003). Role of an N-Terminal Site of Ubc9 in SUMO-1, -2, and -3 Binding and Conjugation†. Biochemistry *42*, 9959-9969.

Taylor, E.M., Copsey, A.C., Hudson, J.J.R., Vidot, S., and Lehmann, A.R. (2008). Identification of the Proteins, Including MAGEG1, That Make Up the Human SMC5-6 Protein Complex. Mol Cell Biol *28*, 1197-1206.

Taylor, E.M., Moghraby, J.S., Lees, J.H., Smit, B., Moens, P.B., and Lehmann, A.R. (2001). Characterization of a Novel Human SMC Heterodimer Homologous to the Schizosaccharomyces pombe Rad18/Spr18 Complex. Molecular biology of the cell *12*, 1583-1594.

Thomas, K.R., and Capecchi, M.R. (1986). Introduction of homologous DNA sequences into mammalian cells induces mutations in the cognate gene. Nature *324*, 34-38.

Thompson, L.H., Brookman, K.W., Jones, N.J., Allen, S.A., and Carrano, A.V. (1990). Molecular cloning of the human XRCC1 gene, which corrects defective DNA strand break repair and sister chromatid exchange. Mol Cell Biol *10*, 6160-6171.

Tibbetts, R.S., Cortez, D., Brumbaugh, K.M., Scully, R., Livingston, D., Elledge, S.J., and Abraham, R.T. (2000). Functional interactions between BRCA1 and the checkpoint kinase ATR during genotoxic stress. Genes Dev *14*, 2989-3002.

Tomonaga, T., Nagao, K., Kawasaki, Y., Furuya, K., Murakami, A., Morishita, J., Yuasa, T., Sutani, T., Kearsey, S.E., Uhlmann, F., *et al.* (2000). Characterization of fission yeast cohesin: essential anaphase proteolysis of Rad21 phosphorylated in the S phase. Genes Dev *14*, 2757-2770.

Torres-Rosell, J., Machin, F., and Aragon, L. (2005a). Smc5-Smc6 complex preserves nucleolar integrity in S. cerevisiae. Cell Cycle *4*, 868-872.

Torres-Rosell, J., Machin, F., Farmer, S., Jarmuz, A., Eydmann, T., Dalgaard, J.Z., and Aragon, L. (2005b). SMC5 and SMC6 genes are required for the segregation of repetitive chromosome regions. Nat Cell Biol *7*, 412-419.

Torres-Rosell, J., Sunjevaric, I., De Piccoli, G., Sacher, M., Eckert-Boulet, N., Reid, R., Jentsch, S., Rothstein, R., Aragon, L., and Lisby, M. (2007). The Smc5-Smc6 complex and SUMO modification of Rad52 regulates recombinational repair at the ribosomal gene locus. Nat Cell Biol *9*, 923-931.

Tóth, A., Ciosk, R., Uhlmann, F., Galova, M., Schleiffer, A., and Nasmyth, K. (1999). Yeast Cohesin complex requires a conserved protein, Eco1p(Ctf7), to establish cohesion between sister chromatids during DNA replication. Genes Dev *13*, 320-333.

Trewick, S.C., Henshaw, T.F., Hausinger, R.P., Lindahl, T., and Sedgwick, B. (2002). Oxidative demethylation by Escherichia coli AlkB directly reverts DNA base damage. Nature *419*, 174-178.

Ui-Tei, K., Naito, Y., Zenno, S., Nishi, K., Yamato, K., Takahashi, F., Juni, A., and Saigo, K. (2008). Functional dissection of siRNA sequence by systematic DNA substitution: modified siRNA with a DNA seed arm is a powerful tool for mammalian gene silencing with significantly reduced off-target effect. Nucleic Acids Res *36*, 2136-2151.

Vallee, R.B., Varma, D., and Dujardin, D.L. (2006). ZW10 function in mitotic checkpoint control, dynein targeting and membrane trafficking: is dynein the unifying theme? Cell Cycle *5*, 2447-2451.

van Attikum, H., Fritsch, O., Hohn, B., and Gasser, S.M. (2004). Recruitment of the INO80 Complex by H2A Phosphorylation Links ATP-Dependent Chromatin Remodeling with DNA Double-Strand Break Repair. Cell *119*, 777-788.

Van Houten, B., Gamper, H., Holbrook, S.R., Hearst, J.E., and Sancar, A. (1986). Action mechanism of ABC excision nuclease on a DNA substrate containing a psoralen crosslink at a defined position. PNAS *83*, 8077-8081.

Vanoli, F., Fumasoni, M., Szakal, B., Maloisel, L., and Branzei, D. (2010). Replication and recombination factors contributing to recombination-dependent bypass of DNA lesions by template switch. PLoS Genet *6*, e1001205.

Verkade, H.M., Bugg, S.J., Lindsay, H.D., Carr, A.M., and O'Connell, M.J. (1999). Rad18 Is Required for DNA Repair and Checkpoint Responses in Fission Yeast. Molecular biology of the cell *10*, 2905-2918.

Vogelstein, B., Lane, D., and Levine, A.J. (2000). Surfing the p53 network. Nature *408*, 307-310.

Vooijs, M., van der Valk, M., te Riele, H., and Berns, A. (1998). Flp-mediated tissue-specific inactivation of the retinoblastoma tumor suppressor gene in the mouse. Oncogene *17*, 1-12.

Wahl, G.M., and Carr, A.M. (2001). The evolution of diverse biological responses to DNA damage: insights from yeast and p53. Nat Cell Biol *3*, E277-E286.

Waizenegger, I.C., Hauf, S., Meinke, A., and Peters, J.-M. (2000). Two Distinct Pathways Remove Mammalian Cohesin from Chromosome Arms in Prophase and from Centromeres in Anaphase. Cell *103*, 399-410.

Wang, B., and Elledge, S.J. (2007). Ubc13/Rnf8 ubiquitin ligases control foci formation of the Rap80/Abraxas/Brca1/Brcc36 complex in response to DNA damage. PNAS *104*, 20759-20763.

Wang, M., Wu, W., Wu, W., Rosidi, B., Zhang, L., Wang, H., and Iliakis, G. (2006). PARP-1 and Ku compete for repair of DNA double strand breaks by distinct NHEJ pathways. Nucleic Acids Res *34*, 6170-6182.

Wang, W., Seki, M., Narita, Y., Sonoda, E., Takeda, S., Yamada, K., Masuko, T., Katada, T., and Enomoto, T. (2000). Possible association of BLM in decreasing DNA double strand breaks during DNA replication. EMBO J *19*, 3428-3435.

Wang, Z.-Q., Stingl, L., Morrison, C., Jantsch, M., Los, M., Schulze-Osthoff, K., and Wagner, E.F. (1997). PARP is important for genomic stability but dispensable in apoptosis. Genes Dev *11*, 2347-2358.

Warren, W.D., Steffensen, S., Lin, E., Coelho, P., Loupart, M.L., Cobbe, N., Lee, J.Y., McKay, M.J., Orr-Weaver, T., Heck, M.M.S., *et al.* (2000). The Drosophila RAD21 cohesin persists at the centromere region in mitosis. Curr Biol *10*, 1463-1466.

Watanabe, K., Pacher, M., Dukowic, S., Schubert, V., Puchta, H., and Schubert, I. (2009). The Structural Maintenance of Chromosomes 5/6 Complex Promotes Sister Chromatid Alignment and Homologous Recombination after DNA Damage in Arabidopsis thaliana. Plant Cell *21*, 2688-2699.

Watanabe, M., Umeyama, K., Matsunari, H., Takayanagi, S., Haruyama, E., Nakano, K., Fujiwara, T., Ikezawa, Y., Nakauchi, H., and Nagashima, H. (2010). Knockout of exogenous EGFP gene in porcine somatic cells using zinc-finger nucleases. Biochem and Biophys Res Commun *402*, 14-18.

Watrin, E., and Peters, J.-M. (2009). The cohesin complex is required for the DNA damage-induced G2/M checkpoint in mammalian cells. EMBO J *28*, 2625-2635.

Watson, J.D., Crick, F. H. C. (1953). Molecular structure of nucleic acids: a structure for deoxyribose nucleic acid. Nature *171*, 737.

Weeda, G., van Ham, R.C., Masurel, R., Westerveld, A., Odijk, H., de Wit, J., Bootsma, D., van der Eb, A.J., and Hoeijmakers, J.H. (1990a). Molecular cloning and biological characterization of the human excision repair gene ERCC-3. Mol Cell Biol *10*, 2570-2581.

Weeda, G., van Ham, R.C.A., Vermeulen, W., Bootsma, D., van der Eb, A.J., and Hoeijmakers, J.H.J. (1990b). A presumed DNA helicase encoded by ERCC-3 is involved in the human repair disorders xeroderma pigmentosum and Cockayne's syndrome. Cell *62*, 777-791.

West, S.C. (2003). Molecular views of recombination proteins and their control. Nat Rev Mol Cell Biol *4*, 435-445.

Williams, R.S., and Tainer, J.A. (2007). Learning our ABCs: Rad50 directs MRN repair functions via adenylate kinase activity from the conserved ATP binding cassette. Mol Cell *25*, 789-791.

Wold, M.S. (1997). REPLICATION PROTEIN A:A Heterotrimeric, Single-Stranded DNA-Binding Protein Required for Eukaryotic DNA Metabolism. Annual Review of Biochemistry *66*, 61-92.

Wolff, S., Bodycote, J., and Painter, R.B. (1974). Sister chromatid exchanges induced in chinese hamster cells by UV irradiation of different stages of the cell cycle: The necessity for cells to pass through S. Mutat Res *25*, 73-81.

Wong, E.A., and Capecchi, M.R. (1986). Analysis of homologous recombination in cultured mammalian cells in transient expression and stable transformation assays. Somat Cell Mol Genet *12*, 63-72.

Wood, R.D. (1996). DNA Repair in Eukaryotes. Ann Rev Biochem *65*, 135-167.

Wu, L., and Hickson, I.D. (2003). The Bloom's syndrome helicase suppresses crossing over during homologous recombination. Nature *426*, 870-874.

Xhemalce, B., Seeler, J.S., Thon, G., Dejean, A., and Arcangioli, B. (2004). Role of the fission yeast SUMO E3 ligase Pli1p in centromere and telomere maintenance. EMBO J *23*, 3844-3853.

Xu, B., Kim, S.-t., and Kastan, M.B. (2001). Involvement of Brca1 in S-Phase and G2-Phase Checkpoints after Ionizing Irradiation. Mol Cell Biol *21*, 3445-3450.

Xu, B., O'Donnell, A.H., Kim, S.T., and Kastan, M.B. (2002). Phosphorylation of serine 1387 in Brca1 is specifically required for the Atm-mediated S-phase checkpoint after ionizing irradiation. Cancer Res *62*, 4588-4591.

Yamada, K., Ariyoshi, M., and Morikawa, K. (2004). Three-dimensional structural views of branch migration and resolution in DNA homologous recombination. Curr Opin Struct Biol *14*, 130-137.

Yamaguchi-Iwai, Y., Sonoda, E., Buerstedde, J.-M., Bezzubova, O., Morrison, C., Takata, M., Shinohara, A., and Takeda, S. (1998a). Homologous Recombination, but Not DNA Repair, Is Reduced in Vertebrate Cells Deficient in RAD52. Mol Cell Biol *18*, 6430-6435.

Yamaguchi-Iwai, Y., Sonoda, E., Buerstedde, J.M., Bezzubova, O., Morrison, C., Takata, M., Shinohara, A., and Takeda, S. (1998b). Homologous recombination, but not DNA repair, is reduced in vertebrate cells deficient in RAD52. Mol Cell Biol *18*, 6430-6435.

Yan, T., Schupp, J.E., Hwang, H.-s., Wagner, M.W., Berry, S.E., Strickfaden, S., Veigl, M.L., Sedwick, W.D., Boothman, D.A., and Kinsella, T.J. (2001). Loss of DNA Mismatch Repair Imparts Defective cdc2 Signaling and G2 Arrest Responses without Altering Survival after Ionizing Radiation. Cancer Res *61*, 8290-8297.

Yang, S.H., and Sharrocks, A.D. (2010). The SUMO E3 ligase activity of Pc2 is coordinated through a SUMO interaction motif. Mol Cell Biol *30*, 2193-2205.

Yazdi, P.T., Wang, Y., Zhao, S., Patel, N., Lee, E.Y., and Qin, J. (2002). SMC1 is a downstream effector in the ATM/NBS1 branch of the human S-phase checkpoint. Genes Dev *16*, 571-582.

Yeh, E.T.H., Gong, L., and Kamitani, T. (2000). Ubiquitin-like proteins: new wines in new bottles. Gene *248*, 1-14.

You, Z., and Bailis, J.M. (2010). DNA damage and decisions: CtIP coordinates DNA repair and cell cycle checkpoints. Trends Cell Biol *20*, 402-409.

Yun, M.H., and Hiom, K. (2009). CtIP-BRCA1 modulates the choice of DNA double-strand-break repair pathway throughout the cell cycle. Nature *459*, 460-463.

Zhao, X., and Blobel, G. (2005). A SUMO ligase is part of a nuclear multiprotein complex that affects DNA repair and chromosomal organization. PNAS *102*, 4777-4782.

Zhou, B.-B.S., and Elledge, S.J. (2000). The DNA damage response: putting checkpoints in perspective. Nature *408*, 433.

Zhu, Z., Chung, W.H., Shim, E.Y., Lee, S.E., and Ira, G. (2008). Sgs1 helicase and two nucleases Dna2 and Exo1 resect DNA double-strand break ends. Cell *134*, 981-994.

Zimmerman, R., and Cerutti, P. (1984). Active oxygen acts as a promoter of transformation in mouse embryo C3H/10T1/2/C18 fibroblasts. PNAS *81*, 2085-2087.

APPENDIX 1

Full length chicken *Nse2* cDNA sequence with the ATG and STOP codon underlined and indicated in red, 5' and 3' UTR in blue, conserved Kozak sequence shown in green.

```
   1 caccccgccc cgctgcctct gtcgggcctg ggcggcgggg acgagagtaa caattccaag
  61 atgcagaggg gtacaagaat ctcattcagc tctgtgaatt cctctctttc atctctgaaa
 121 aactgccagt cttacataaa tactggaatg gatattgcta ctcacgttgc ccttgacctg
 181 gtggaaaatt tcaatgatga agaggatgtt agaagtatgg agaatgtcat gttagagtat
 241 gctgcattgg acagagagct taatcattac atgagagcaa ttgaagaaac ggtagatcag
 301 ataaaacaag acaaaccaga aaagatacca gatctaaaat cactagtaaa agaaaaattt
 361 actgcattgg agagcatgaa cagtgactcg gatttggaaa aaaatgagaa atatatgtat
 421 tttaaggatc aacttaaaga catgaaaaaa caatttcgtc ttcaatcaga tagtaatgat
 481 aatgacgaca tcgaacaaat cgatgaagat atagctgtga ctcagagtca gatgaacttc
 541 atttgtccca ttacacaggt ggaaatgaag aagccagttc gaaacaaagt ctgtggacat
 601 tcctatgaag aagatgccat tctaaaaatc atccagactc gaaagcagca gaagaagaaa
 661 gtccgctgcc ctaaaattgg ctgtagccat gatgatgtaa aaggatcaga tctcgtgcca
 721 gatgaagcac ttaaaagagc gattgacagt cagaataaac aaagctggtc aacgctgtag
 781 aagtcggctg gatgtgccgt tgccacaaag aaaatttgtt attagaggtc ttgtgagata
 841 agctgccgat tgtgagcagg ttgtgtaacg gattgttatt taaagtgttt catttatagg
 901 cagagttgaa ggtctccgct gtaactgaaa acatttttc atctgtcaaa tatgaggaat
 961 tccaggttag ttagtttttt ttccccttgt tagttttttt ccccttcttg aaattctaaa
1021 tgttgcgttt gttaaataaa atgtggcttt cagccttcaa cttcccc
```

APPENDIX 2

Table I Oligonucleotides used for PCR-based cloning

Primer name	Sequence (5'-3')	Use
Nse2-FW	ATG CAG AGG GGT ACA AGAATC	For cloning of Nse2 cDNA
Nse2-RV	CTA CAG CGT TGA CCA GGT TTG	For cloning of Nse2 cDNA
Nse2 - 5' arm FW (*SalI*)	GTC GAC GGT CTG TGG TTT ATA ACA TCG	For cloning of 5' homology arm
Nse2 – 5' arm RV (*EcoRI*)	GAA TTC GAC TCT GAG TCA CAG CTA TAT C	For cloning of 5' homology arm
Nse2 - 3' arm FW (*NotI*)	GCG GCC GC GTC AGA ATA AAC AAA GCT GG	For cloning of 3' homology arm
Nse2 – 3' arm RV (*SacII*)	CCG CGG GGA GCA GCC AGC GGC AAT GGG	For cloning of 3' homology arm
Nse2 – 5' probe FW	GGC CCT GCA AGC ACT GAG CAG GC	For cloning of 5' probe

Nse2 – 5' probe RV	CCG GGT TTT CCT TGC AAA TGA AAA CC	For cloning of 5' probe
Nse2 – 3' probe FW	GTG GAG ACA GAT AAC TCT GTG AGC	For cloning of 3' probe
Nse2 – 3' probe RV	CCT CAG AAT GAA AAA TAA CAA AGC AGG	For cloning of 3' probe
Nse2 (N) FW (*BamHI*)	GGA TCC ATG CAG AGG GGT ACA AGA ATC	For cloning of full-length Nse2 into pGEX-4T2 (antigen)
Nse2 (N) RV (*NotI*)	GCG GCC GC CTA CAG CGT TGA CCA GCT TTG	For cloning of full-length Nse2 into pGEX-4T2 (antigen)
Nse2 (N) FW (*BamHI*)	GGA TCC ATG CAG AGG GGT ACA AGA ATC	For cloning of full-length Nse2 into pCMV-3tag-2A (3myc fusion)
Nse2 (N) RV (*EcoRI*)	GAT ATC CTA CAG CGT TGA CCA GCT TTG	For cloning of full-length Nse2 into pCMV-3tag-2A (3myc fusion)
Nse2 (C) FW (*XhoI*)	CTC GAG CGA TGC AGA GGG GTA CAA GAA TC	For cloning of full-length Nse2 into pEGFP-N1 (GFP fusion)
Nse2 (C) RV (*SacII*)	CCG CGG AGC AGC GTT GAC CAG CTT TG	For cloning of full-length Nse2 into pEGFP-N1 (GFP fusion)
Nse2 (C178A, H180A) FW (*NarI*)	GAA ATG AAG AAG CCA GTT CGA AAC AAA GTC *GCC GGC GCC* TCC TAT GAA GAA GAT GCC ATT CTA AAA ATC	For site directed mutagenesis of Nse2 (C178A, H180A)
Nse2 (C178A, H180A) RV	GAT TTT TAG AAT GGC ATC TTC TTC ATA GGA *GGC GCC GGC* GAC TTT GTT	For site directed mutagenesis of Nse2

(*NarI*)	TCG AAC TGG TTT CTT CAT TTC	(C178A, H180A)

FW – forward primer, RV – reverse primer, DNA sequences in red show cleavage site for the indicated restriction nucleases, underlined italic sequence show the desired mutation of *Nse2* cDNA sequence.

APPENDIX 3

Poster, seminar presentations and publications arising from thesis work

1. Poster presentation

Kliszczak M, Stephan AK and Morrison CM. *Genetic dissection of the Smc5-Smc6 complex.* (A poster presented at the DNA replication and recombination meeting in Keystone, USA, March 2011)

2. Seminar presentations

Kliszczak M, Stephan AK and Morrison CM. *Involvement of the Smc5-Smc6 complex in sister chromatid cohesion and homologous recombinational repair in vertebrate cells.* (A seminar presented at the annual meeting of the Genome Stability Network, Cambridge, UK, 2009).

Kliszczak M, Stephan AK and Morrison CM. *Genetic dissection of the Smc5-Smc6 complex.* (A seminar presented at the annual meeting of the Irish Association for the Cancer Research, Galway, Ireland, 2010).

3. Publications

Stephan, A.K., Kliszczak, M., Dodson, H., Cooley, C., and Morrison, C.G. (2011). *Roles of vertebrate smc5 in sister chromatid cohesion and homologous recombinational repair.* Mol Cell Biol *31*, 1369-1381.

Stephan, A.K., Kliszczak, M., and Morrison, C.G. (2011). *The Nse2/Mms21 SUMO ligase of the Smc5/6 complex in the maintenance of genome stability.* FEBS Lett. *585*, 2907-13.

Kliszczak, M., Stephan, A.K., and Morrison C.G. (2011). *Distint functions of Nse2 and Smc5 in DNA repair revealed by gene targeting. Submitted to EMBO J on 21.06.2011.*